Regulation of the immune checkpoint PD-L1 by microRNAs

Daniel Yee

PhD

University of York

Biology

September 2018

Abstract

MicroRNAs are evolutionary conserved non-coding RNAs that control more than 60% of human protein-coding genes at the posttranscriptional level. MicroRNAs can either mediate translational repression or mRNA degradation by complementary base-pairing to the 3'-UTR of mRNA. MicroRNAs have critical roles in the regulation of immune responses and inflammation. The expression of PD-L1 protein is found on some normal and cancer cells and contributes to suppression of T cell activity by acting as a brake on the immune response. Previously, it has been shown that posttranscriptional mechanisms regulate PD-L1 levels in cancer, it remains unknown whether such regulatory networks operate also in non-transformed cells.

Here, I tested the hypothesis that expression and function of PD-L1 in stromal, vascular and cancer cells is posttranscriptionally regulated by inflammatory-driven microRNAs. I demonstrate that PD-L1 expression in human dermal lymphatic endothelial cells (HDLECs) can be induced with the treatment of pro-inflammatory cytokines IFN-γ and TNF-α. The microRNA landscape in HDLECs was activated by IFN-γ and TNF-α treatment including some microRNAs that have predicted binding sites on PD-L1. A highly upregulated microRNA was microRNA-155 (miR-155), a multifunctional microRNA that regulates haematopoiesis, normal immune function and mediates the inflammatory response. I determined that miR-155 can bind to the 3'-UTR of PD-L1 on two functional binding sites, and that the kinetics of PD-L1 induction is fine-tuned by inflammation-induced miR-155 in HDLECs and dermal fibroblasts. Interestingly, I found that miR-155 can also silence PD-L1 expression in renal, breast but only in a subset of lung cancer cell lines. These findings reveal that inflammatory activation induce PD-L1 expression on several different cell types presumably to avoid prolonged immune-mediated tissue damage. However, miR-155 can act in a cell type-specific manner to temporally release PD-L1 immunosuppression to regulate the balance between immune tolerance and autoimmunity.

Table of Contents

List of Tables

List of Figures

Acknowledgements

I have spent the past four years working towards completion of the doctoral degree and I can say that I have thoroughly enjoyed the challenge; the hands-on research combining microRNAs and immunology, the connections that I have made and the skills that have shaped me into a better person. I am so glad I came to University of York to pursue my PhD. With that being said, I would like to express my sincere gratitude to my supervisor Dr. Dimitris Lagos who has always been there to guide and train me throughout my journey and has selflessly looked out for my needs. To my co-supervisor Prof. Mark Coles for consistently opening my eyes to the bigger picture and giving me an insight into industry. Thank you for giving me this opportunity to work with you on this project. To my Thesis Advisory Panel, Prof. Ian Hitchcock and Dr. Marika Kullberg, I thank them for their support, discussion and approval of my work. I thank the BBSRC for funding this research and to Dr. Clare Green for managing the doctoral programme for four years.

To past and present companions of the Lagos lab who have motivated, helped and befriended me throughout the degree: Dr. Matthew Warner, Dr. James Hewitson, Dr. German (Johnny) Leonov, Dr. Mia Shandell, Dr. Nidhi Dey, Shoumit Dey, Miles Evans, Sophie Hawkins, Samantha Lawrence, Manon Janet-Maître and Alexander Taylor. Matt, James, Johnny, Mia and Shoumit, thank you for patiently teaching me everything I know in the lab and answering all my questions. Thank you also to Shoumit, Nidhi, Miles, Sophie and Sammy for being such awesome people and for all the fun and experiences we have had. Thank you to (Dr.) Cecilia Pennica who has kept me smiling throughout the four years of our doctoral programme.

Thank you to members of Centre of Immunology and Infection (now York Biomedical Research Institute), and Department of Biology, in particular to Dr. Nathalie Signoret for her help with Jurkat cell culture, Dr. Katrina Reilly for her assistance with flow cytometry and confocal microscopy. To Technology Facility for their invaluable support with small RNA sequencing, flow cytometry and luciferase assays. To our collaborators at Barts Cancer Institute for their expertise with 3'-UTR luciferase assays and lung cancer cell lines.

My sincere appreciation to my friends and family: Mum and Dad for their unconditional love, telling me that I have done my best and checking that I am eating well. To my brothers, Louis and Philip for all their continued support in my life and whom I look up to.

Finally to Grace who I am indebted for her compassion, love and companionship, even after hearing every failed experiment that happened that day. 加油!

Declaration

I declare that this thesis is a presentation of original work and I am the sole author. This work has not previously been presented for an award at this, or any other, University. All sources are acknowledged as References.

Some sections in the literature review in Chapter 1 have been published prior to the submission of the thesis for examination: **Yee et al. (2017). microRNAs in the Lymphatic Endothelium: Master Regulators of Lineage Plasticity and Inflammation**. *Frontiers in Immunology*.

Results in Chapter 3 have been published prior to the submission of the thesis for examination: **Yee et al. (2017). MicroRNA-155 induction via TNF-α and IFN-γ suppresses expression of programmed death ligand-1 (PD-L1) in human primary cells**. *Journal of Biological Chemistry*.

1. Introduction

1.1 Immune checkpoints

1.1.1 Overview on T cells

T cells regulate the initialisation and maintenance of immune responses, homeostasis and immunological memory in response to pathogens, tumours and allergens (Kumar et al. 2018). T cells are found in almost every organ and tissue, originating from bone marrow progenitors which are matured and selected in the thymus to maintain self-tolerance. The ability of the immune system to recognise self-antigen as a non-threat is defined as self-tolerance. In a pathological context, T cells can also contribute towards inflammatory and autoimmune diseases when self-tolerance breaks down. On the other hand, cancer cells manipulate self-tolerance to evade the immune system. Naïve T cells in the periphery interact with antigen-presenting cells (APCs) and become activated upon recognition of antigen and co-stimulatory ligands (Kumar et al. 2018; van den Broek et al. 2018). Different subsets of T cells have been characterised due to the surface expression of either $CD4^+$ or $CD8^+$ glycoproteins, which assist in the recognition of antigen (Golubovskaya & Wu 2016). $CD4^+$ T cells have a number of essential roles in the immune system: to facilitate B cells through the production of antibodies, support the functional responses of $CD8^+$ T cells, regulate the strength of immune responses and help generate immunological memory (Zhu et al. 2010). Differentiation of naïve $CD4^+$ T cells into T helper (Th) cells determines the effector function of $CD4^+$ T cells, which is regulated by a network of transcription factors such as signal transducer and activator of transcription (STAT) proteins. There are a diverse number of Th lineages: Th1, Th2, Th9, Th17, Th22, regulatory T cells (T reg) and T follicular helper cells, and differentiation of T cells can be determined by the surrounding cytokine environment (Golubovskaya & Wu 2016). For example, Th1 cell differentiation requires interleukin-12 (IL-12) and interferon-gamma (IFN-γ), whereas Th2 cells require IL-4 and IL-2 (Zhu et al. 2010). Each lineage can differ by factors including the pattern of cytokine production and antigen specificity but remain highly heterogeneous, plastic and can be reprogrammed to a different lineage (Zhu et al. 2010). On the other hand, $CD8^+$ T cells (also called cytotoxic T lymphocytes or CTLs) become primed by APCs into cytotoxic effector cells that eliminate intracellular pathogens, infected cells and cancer cells (Zhang & Bevan 2011). $CD8^+$ T cells release the cytokines IFN-γ and tumour necrosis factor-alpha (TNF-α) and cytotoxic granules that enable the $CD8^+$ to kill target cells. In addition, activation of $CD8^+$ T cells induces the formation of memory cells that protect against further pathogenic infections.

1.1.2 T cell activation

The T cell receptor (TCR) on T cells initiates detection of antigen that is presented by damaged or infected cells. The amplitude and quality of response by T cells is tightly regulated by a series of immune checkpoints that consist of co-stimulatory and co-inhibitory ligand-receptor interactions (Pardoll 2012). Immune regulation is required to limit damage to healthy tissues (Sun et al. 2018). Failure to maintain self-tolerance can lead to chronic inflammation and autoimmunity. T cell activation stems from the concept that two or three signals must be delivered to determine whether a T cell proliferates, differentiates and produces cytokines. In the absence of these specific signals, T cells fail to develop the necessary effector functions (anergy) or become deleted. The first required signal is mediated by the TCR upon recognition of antigen on the surface of APCs. The second signal is in the form of co-stimulatory signals that enhance TCR signalling and a third signal is delivered by inflammatory cytokines. The increasing number of factors reported to fine-tune T cell responses have evolved the original concept greatly.

Peptide antigens are presented through major histocompatibility complex (MHC) molecules that consist of three α-chains and a beta-2 microglobulin. CD4 and CD8 co-receptors facilitate the discrimination of antigen peptides that are bound to MHC class II molecules or MHC class I molecules, respectively.

$CD8^+$ T cells recognise peptides presented by MHC class I molecules, which are expressed on the surface of all nucleated cells and present endogenously synthesised peptides (Rock et al. 2016). Typically, normal and abnormal proteins are degraded by the proteasome into peptide fragments. To a large extent, the majority of fragments are destroyed by cytosolic peptidases. The few that survive are delivered to the endoplasmic reticulum (ER) through transporter associated with antigen processing (TAP) molecules. A peptide-loading complex is formed by TAP and includes chaperones TAP-associated glycoprotein (tapasin), calreticulin and ERp57 that mediate the binding between peptides and MHC class I molecules (Rock et al. 2016). Tapasin holds empty MHC class I molecules to promote binding. The repertoire of peptides undergoes further shaping and maturation to facilitate stability and specificity before surface presentation. Peptides can be trimmed by ER aminopeptidases (ERAP1 and ERAP2) or remodelled by a tapasin homology TAP-binding protein-related (TAPBPR) (Rock et al. 2016). A different type of MHC class I presentation is through cross-presentation of antigen. APCs such as dendritic cells (DCs) and phagocytes are important for immune surveillance and can acquire exogenous peptide-MHC class I antigens from infected or tumour cells and present these antigens to $CD8^+$ T cells in lymphoid organs.

$CD4^+$ T cells recognise peptides expressed by MHC class II molecules, which are generally restricted to antigen-presenting cells such as DCs, B cells, monocytes, macrophages but can be expressed on other cells following inflammatory signals (Rock et al. 2016). Peptide fragments tend to be larger and can extend out from the peptide-binding groove of MHC class II. Peptides are derived from extracellular proteins such as those from pathogens and from self-proteins that are degraded in the endosomal pathway. MHC class II molecules assemble in the ER with the invariant chain polypeptide, which designates these molecules to a specific endosomal MHC class II-containing compartment (MIIC). The invariant chain blocks the groove of MHC class II to prevent binding of peptides suitable for MHC class I presentation. Endosomal proteases cathepsin S and L degrade the invariant chain to a fragment known as class II-associated invariant chain peptide (CLIP), a prerequisite for loading of peptides (Rock et al. 2016). The high affinity human leukocyte antigen DM (HLA-DM) binds to the MHC class II molecules, releasing the low-affinity CLIP and allows peptides to bind to the groove of MHC class II. Peptide-MHC class II is then transported to the plasma membrane for presentation.

The α- and β-chain of the TCR directly recognise the antigen and associate with CD3 co-receptors that contain immunoreceptor tyrosine-based activation motifs (ITAMs), which are important for TCR signal transduction (Malissen et al. 2014). The close proximity of CD4 or CD8 to the TCR enables lymphocyte-specific protein tyrosine kinase (Lck) to phosphorylate the ITAMs on the cytoplasmic tail of CD3 (Smith-Garvin et al. 2009). This leads to the recruitment and activation of zeta-chain-associated protein kinase 70 (ZAP70), which binds to the ζ-chains and phosphorylates the transmembrane protein linker of activated T cells (LAT). The LAT signalosome constitutes a multi-protein complex that is responsible for most of the responses that result from TCR engagement (Malissen et al. 2014). The complex includes LAT, the cytosolic adaptor Src homology 2 domain-containing leukocyte phosphoprotein of 76 kDa (SLP-76), Vav1, IL-2-inducible T cell kinase (ITK) and phospholipase C (PLCγ1) that contribute to downstream signalling leading to T cell proliferation and differentiation.

Co-stimulatory signals enhance T cell activation and one of the most important receptors is CD28. B7 family members CD80 (B7.1) and CD86 (B7.2) on APCs bind to CD28 and initiate downstream signalling through phosphoinositide 3-kinase (PI3K) to Akt (Smith-Garvin et al. 2009). Activation of Akt leads to the phosphorylation of several proteins associated with cell survival, cellular metabolism, proliferation and cytokine production including nuclear factor kappa-light-chain-enhancer of activated B cells (NF-κB), nuclear factor of activated T cells (NFAT) and IL-2. CD28 promotes the expression of other key co-stimulatory molecules in the CD28 and tumour necrosis factor receptor (TNFR) families

such as inducible T cell co-stimulator (ICOS; CD278), OX40 (CD134) and 4-1BB (CD137) that aid in sustaining the immune response (Smith-Garvin et al. 2009). Furthermore, cytokines can strengthen the activation of $CD8^+$ T cells especially pro-inflammatory cytokines IL-12 and IFN-α, which facilitate the increase in a larger $CD8^+$ T cell population.

Activation of T cells drives the expression of co-inhibitory receptors that negatively regulate TCR signalling. The receptor-ligand immune checkpoints of inhibitory pathways are most druggable using antagonist antibodies (Pardoll 2012). The first few immune checkpoint inhibitory receptors to be targeted for immunotherapy were cytotoxic T lymphocyte antigen-4 (CTLA-4), and programmed cell death protein 1 (*PDCD1, human chromosome 2*; PD-1; CD279) of which the focus of this thesis is based on. Other co-inhibitory targets from the immunoglobulin superfamily now being investigated are B7-H3, LAG-3, TIGIT, TIM3 and VISTA of which our understanding is relatively premature in the identities of associated ligands or receptors (Wei et al. 2018). Some of these molecules are restricted to expression on Th1 T cells and NK cells that regulate T cell activity through non-redundant inhibitory mechanisms. In addition, there is a similar number of known co-stimulatory molecules (ICOS, OX40, GITR, 4-1BB, CD40, CD27), many of which are from the TNFR superfamily (Wei et al. 2018). Together, this shows the complexity of the regulatory mechanisms located at the immune checkpoint that maintain immune responses and protect the host from autoimmunity.

1.1.3 The PD-1/PD-L1 immune checkpoint

PD-1 was discovered in a murine T cell hybridoma where activation of PD-1 correlated with cell death (Ishida et al. 1992). The Pdcd1 locus located on chromosome 2 encodes PD-1, a 288 amino acid type I transmembrane glycoprotein which is part of the immunoglobulin gene superfamily (Agata et al. 1996). Furthermore, PD-1 is heavily glycosylated with a molecular weight of 50-55 kDa. $PD\text{-}1^{-/-}$ deficient mice develop arthritis and lupus-like glomerulonephritis between 6 to 14 months of age (Nishimura et al. 1999) and fatal autoimmune cardiomyopathy (Nishimura et al. 2001). PD-1 expression is best characterised in T cells, with expression also observed on B cells, monocytes, DCs and natural killer (NK) cells (Keir et al. 2008). PD-1 exists as a monomeric receptor as it lacks a membrane-proximal cysteine residue necessary for homodimerisation (Zhang et al. 2004).

PD-1 has two ligands, PD-L1 (*CD274, human chromosome 9*; B7-H1) and PD-L2 (*PDCD1LG2, human chromosome 9*; CD273; B7-DC) (Freeman et al. 2000; Latchman et al. 2001). The two PD-1 ligands differ in their expression and binding affinity. PD-L1 is expressed on T cells, B cells, DCs, macrophages and on various non-haematopoietic cell types including vascular endothelial cells and tumour cells (Sun et al. 2018). PD-L2

expression is restricted to DCs, macrophages and B cells (Sun et al. 2018). The binding affinity of PD-L2 to PD-1 is three- to four-fold stronger compared to PD-L1 due to a three-fold smaller dissociation rate for PD-L2 binding (Butte et al. 2007; Cheng et al. 2013). However, there are 5-fold fewer PD-1/PD-L2 than PD-1/PD-L1 complexes due to lower expression of PD-L2 at steady state (Cheng et al. 2013). PD-L1 is a 290 amino acid type I transmembrane protein encoded by the CD274 gene (Keir et al. 2008) (Figure 1.1). CD274 contains seven exons, the first is a non-coding 5'-UTR followed by three exons that contain the signal sequence (exon 2), extracellular domains IgV-like domain (exon 3) and IgC-like domain (exon 4). The next two exons contain the transmembrane domain (exon 5) and cytoplasmic domain (exon 6). The last exon contains the remaining part of the cytoplasmic domain and the 3'-UTR (Keir et al. 2008).

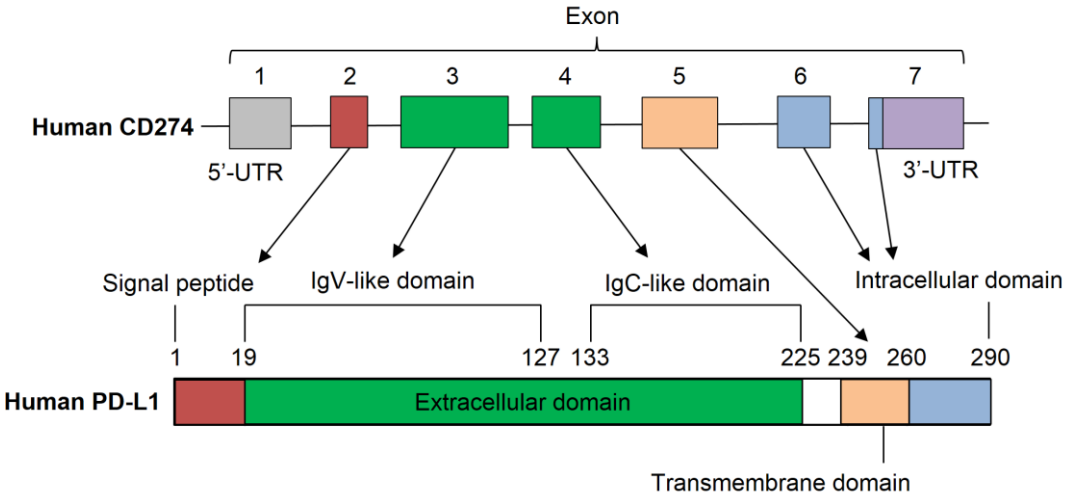

Figure 1.1. **Domain structure of CD274/PD-L1**. Human CD274 gene (located on chromosome 9) contains seven exons flanked by a 5'-UTR and 3'-UTR that encode for PD-L1, a 290 amino acid glycoprotein consisting of IgV-like (variable) and IgC-like (constant) domains in the extracellular domain and ending with a short intracellular domain (30 amino acids).

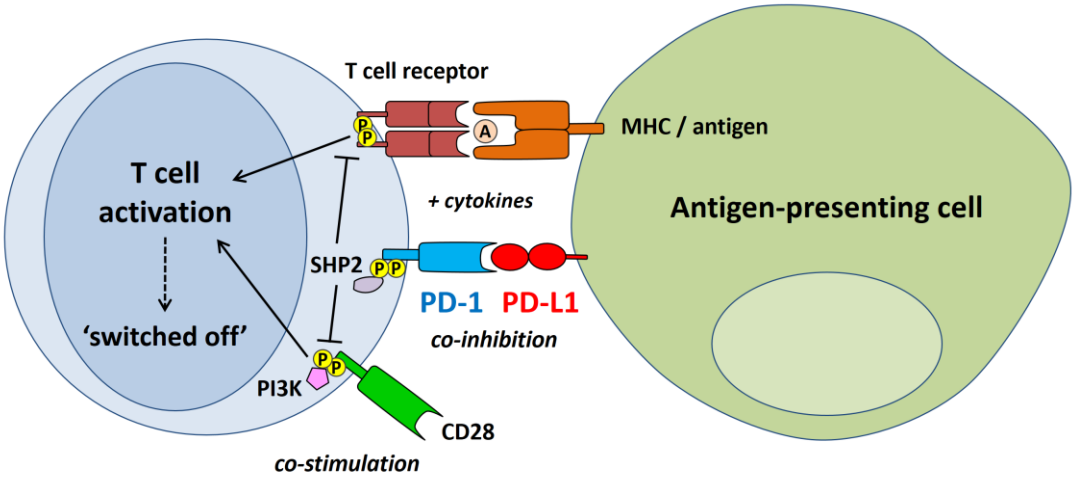

Figure 1.2. **The PD-1/PD-L1 immune checkpoint pathway**. The T cell receptor (TCR) recognises antigens that are presented through major histocompatibility (MHC) molecules on antigen presenting cells (APCs). This results in a signalling cascade initiated at the TCR that effectively activates the T cell, accompanied by a combination of co-stimulatory molecules and activating cytokines that determine the intensity of T cell activation. The inhibitory receptor PD-1 is induced upon T cell activation. Upon engagement of PD-1 by its ligand PD-L1 consequently leads to phosphorylation of tyrosine residues found on the immunoreceptor tyrosine-based switch motif (ITSM) on the tail of PD-1. This leads to the recruitment of Src homology phosphatase 2 (SHP2) to the ITSM which inhibits downstream TCR signalling and CD28-mediated PI3K activation, resulting in the downmodulation of T cell activation and function.

Engagement of PD-1 by PD-L1 on the surface of T cells inhibits T cell activation and function by downregulation of TCR signalling and CD28-mediated activation of PI3K/Akt (Sun et al. 2018) (Figure 1.2). The cytoplasmic domain of PD-1 contains two tyrosine phosphorylation sites located in an immunoreceptor tyrosine-based inhibitory motif (ITIM) and an immunoreceptor tyrosine-based switch motif (ITSM) (Keir et al. 2008). PD-1 is phosphorylated on two tyrosine residues (Y224 and Y248) of the cytoplasmic domain by Src family tyrosine kinases Lck and to a lesser effect by Csk, and results in the recruitment of Src homology phosphatase 2 (SHP2) and SHP1 to the ITSM (Chemnitz et al. 2004; Sheppard et al. 2004; Hui et al. 2017). SHP2 directly binds phosphorylated PD-1 with a 29-fold selectivity over SHP1 and may negatively regulate Lck tyrosine phosphorylation of PD-1 in a slow dissociating manner (Hui et al. 2017). Recruitment of SHP2 to PD-1 was reported to dephosphorylate proximal signalling kinases of the TCR pathway including ZAP70, Vav1, PLCγ1, and CD3ζ, and protein kinase C (PKCθ) (Sheppard et al. 2004; Yokosuka et al. 2012). Another study found that CD28-mediated activation of PI3K/Akt was

affected by PD-1 signalling from the cytoplasmic tail (Parry et al. 2005). By comparing the effect of PD-1 on TCR and CD28 phosphorylation, Hui *et al.* demonstrated that CD28 was the most sensitive target of PD-1/SHP2 (Hui et al. 2017). PD-1 strongly co-localised with CD28 in plasma membrane micro-clusters in $CD8^+$ T cells (Hui et al. 2017). Dephosphorylation did occur with TCR signalling components, CD3ζ, ZAP70, LAT and SLP-76 to a minor extent when there were high PD-L1 levels. Kamphorst *et al.* showed that CD28 signalling was necessary to restore $PD\text{-}1^+$ $CD8^+$ T cell responses during PD-1 blockade in a mouse model of life-long chronic lymphocytic choriomeningitis virus (LCMV) infection (Kamphorst et al. 2017). A recent study has suggested that anti-PD-1 blockade in mice deficient of SHP-2 showed no significant improvement of anti-tumoural $CD8^+$ T cell responses compared to control counterparts, suggesting alternative molecular factors involved in PD-1 signalling (Rota et al. 2018).

CD80 was identified as an additional binding partner of PD-L1 by surface plasmon resonance in both mouse and human studies (Butte et al. 2007; Butte et al. 2008). CD80 is typically known as a ligand for CD28 and CTLA-4 on the T cell surface. Binding affinity between PD-L1 on T cells and CD80 on APCs in both murine and human models was 1.7 μM and 1.4 μM, respectively, compared to the affinity of PD-L1 for PD-1, 0.5 μM and 0.77 μM, respectively (Butte et al. 2007; Butte et al. 2008). The binding site of PD-L1 for PD-1 partially overlaps with CD80. Typically, CD80 is expressed on B cells, DCs and macrophages. Potentially, PD-L1 could signal through CD80, which acts as the receptor. *In vivo* models of T-cell activation and tolerance showed that PD-L1 may transmit co-inhibitory signals to CD80 on T cells and regulate T cell proliferation and apoptosis (Park et al. 2010; Deng et al. 2015).

Some evidence has shown that the cytoplasmic tail of PD-L1 and not PD-L2 may play a role in signalling although there is a lack of canonical signalling motifs in the 30 amino acid sequence. Azuma *et al.* identified that PD-L1 on cancer cells can induce apoptotic resistance against T cell-mediated killing in *in vivo* but not *in vitro*, although the underlying mechanism remains to be defined (Azuma et al. 2008). Furthermore, PD-L1 has been implicated in angiogenesis, where deletion of PD-L1 in murine endothelial cells (MS1) resulted in increased vascular endothelial growth factor receptor 2 (VEGFR2) and proliferation suggesting PDL1 has negative regulatory effects on angiogenesis (Jin et al. 2011). Moreover, deletion of CD80 also increased VEGFR2 expression and cell proliferation suggesting that the inhibitory effect was related to PD-L1 ligation with CD80 in either an autocrine or paracrine manner.

Regarding PD-1 intrinsic signalling, Kleffel et al. demonstrated in melanoma subpopulations that PD-1 promoted tumourigenesis independently of adaptive immunity (Kleffel et al. 2015). PD-1 overexpression modulated downstream effectors of mammalian target of rapamycin (mTOR) signalling such as increased phosphorylation of S6. Inhibition of mTOR but not PI3K reversed PD-1-dependent S6 phosphorylation suggesting PD-1 signals through a PI3K/AKT-independent pathway. In addition, mutation of the ITSM or ITIM abrogated PD-1 mediated tumour growth.

1.1.4 PD-1/PD-L1 in chronic infection and cancer

The level of PD-1 expression and the extent of ligand engagement regulate the threshold for T cell activation and cytokine production (Sharpe et al. 2007). In a disease context, the PD-1/PD-L1 immune checkpoint can often become manipulated or hijacked such that there is either too little or too much regulation of the immune response. During chronic infection or cancer, suppression of T cell activation can lead to T cell 'exhaustion' (or anergy) which is characterised by a loss of IL-2 production, reduced proliferative capacity, reduced cytotoxic capacity and impaired production of pro-inflammatory cytokines such as IFN-γ (Dyck & Mills 2017). Thus, the PD-1/PD-L1 pathway can contribute to a lack of viral control during chronic viral infection (Sharpe et al. 2007).

In the presence of persisting infection using a LCMV mice model, virus-specific $CD8^+$ T cells become exhausted and dysfunctional after more than 60 days of infection (Barber et al. 2006). Exhausted $CD8^+$ T cells displayed high expression of PD-1 and infected cells upregulated PD-L1. Blockade of the PD-L1 reinvigorated function of exhausted $PD\text{-}1^+$ $CD8^+$ T cells to produce IFN-γ and TNF-α and enhanced the clearance of chronic viral infection (Barber et al. 2006). Moreover, LCMV infection affects the differentiation of $CD8^+$ T cells through suppression of PI3K, Akt and mTOR signalling (Staron et al. 2014). Consequently, this led to elevated forkhead box protein O1 (FOXO1) activity which maintained PD-1 expression in exhausted $CD8^+$ T cells. Murine endothelial cells strongly upregulated PD-L1 after LCMV infection which inhibited virus-specific CD8 T cell killing of infected endothelial cells (Mueller et al. 2010; Frebel et al. 2012). Absence of PD-L1 expression on endothelial cells and PD-1 expression on T cells can lead to systemic vascular leakage and fatality during early systemic LCMV infection. Deficiency of PD-1 in $CD8^+$ T cells of PD-1 knockout mice showed an increase in death of infected vascular endothelial cells via perforin-mediated cell lysis that led to the formation of pulmonary oedema (Frebel et al. 2012).

Anti-tumour immunity presents a significant barrier to tumour formation and progression in humans. Immune escape is a hallmark of cancer which enables cancer cells to limit the

extent of immunological killing (Hanahan & Weinberg 2011). Tumour cells of the lung, ovary, colon and skin can hijack the PD-1/PD-L1 pathway to promote tumour antigen-specific T cell apoptosis (Dong et al. 2002). In a study of 150 melanocytic lesions from benign nevi to metastatic melanoma, 57 (38%) were PD-L1$^+$ (Taube et al. 2012). Human PD-L1$^+$ melanocytic lesions correlated with 98% presence of tumour-infiltrating lymphocytes (TILs) compared to 28% in PD-L1$^-$ melanocytic lesions (defined as <5% PD-L1$^+$) (Taube et al. 2012). This high correlation was observed with detection of IFN-γ at the boundary of TILs and PD-L1$^+$ tumour cells (Taube et al. 2012). This suggests that TILs drive the expression of PD-L1 on tumour cells through production of IFN-γ, a mechanism referred to as adaptive immune resistance (Pardoll 2012).

1.1.4.1 Immune checkpoint blockade in cancer

Immune checkpoints have been much the focus of clinical developments due to the ability to reactivate anti-tumour immunity. The first development of an immune checkpoint inhibitor targeted the interaction of CTLA-4 binding to CD28, thereby preventing or sequestering the co-stimulation of T cells (Pardoll 2012). This is in contrast to PD-1 since CTLA-4 affects the early activation of T cell proliferation in lymph nodes (LNs) whereas PD-1 is induced upon activation of T cells and affects the long-term immune response in peripheral tissues. In addition, the expression of CTLA-4 is restricted to professional APCs or immune cells. The primary effect of CTLA-4 inhibition affected the Th and T reg subset of CD4$^+$ T cells such that there was a downregulation of Th cell activity and enhancement of T reg immunosuppressive activity (Pardoll 2012). The first approved anti-CTLA-4 blockade was ipilimumab, which has been demonstrated to prolong survival in patients with advanced melanoma (Buchbinder & Desai 2016). This first development of an immune checkpoint blockade agent paved the way for future clinical developments such as targeting of PD-1/PD-L1.

The PD-1/PD-L1 immune checkpoint can be blocked by antibodies against PD-1 (anti-PD-1) or PD-L1 (anti-PD-L1) to remove the brakes on anti-tumour T cell responses. The first clinical trial showed that anti-PD-1 (nivolumab) blockade in patients with advanced melanoma had positive signs of anti-tumour activity and safety (Brahmer et al. 2010). Since then, the development of anti-PD-1 and anti-PD-L1 treatment has revolutionised cancer immunotherapy by improving the outcome of patient survival. Anti-PD-1/PD-L1 checkpoint inhibitors have expanded to treat cancers from melanoma to non-small cell lung cancer (NSCLC), renal clear carcinoma, head and neck squamous-cell carcinoma, urothelial carcinoma, Merkel cell carcinoma, Hodgkin lymphoma, microsatellite instability (MSI) colorectal cancer, hepatocellular carcinoma and gastric cancer (Sun et al. 2018). So far, five checkpoint inhibitors have been approved of which two are anti-PD-1 (nivolumab and

pembrolizumab) and three are anti-PD-L1 (atezolizumab, avelumab and durvalumab) (Sun et al. 2018).

Observed toxicities from anti-PD-1 agents can include fatigue, low-grade pneumonitis (lung inflammation) and hyperthyroidism (Linardou & Gogas 2016). Anti-PD-L1 inhibitors are associated with few reports of severe toxicities (Linardou & Gogas 2016). A Phase 3 study using untreated patients with metastatic melanoma found that the number of adverse events were higher in patients with anti-CTLA-4 blockade (ipilimumab, 27.3%) than patients in the anti-PD-1 (nivolumab, 16.3%) (Larkin et al. 2015). The combination of PD-1 and CTLA-4 blockade improved the length of progression-free survival but with increased number of adverse events (55.0%).

1.1.4.2 Factors affecting the response to PD-1/PD-L1 checkpoint blockade

Approved PD-1/PD-L1 blockade therapy appears to only benefit a fraction of patients and there is a large amount of heterogeneity in clinical responses (Sun et al. 2018). The overall response rate to anti-PD-1/PD-L1 immunotherapy ranges between 13.3% in hepatocellular carcinoma to 39.6% in microsatellite instability high (MSI-H) and mismatch repair deficient (dMMR) solid tumours (Sun et al. 2018). Blockade of anti-PD-1 can inhibit ligand engagement from PD-L1, PD-L2 and CD80. Tumour responses with anti-PD-1/PD-L1 are mediated by tumour antigen-specific T cells that have been previously blocked by PD-1/PD-L1 interaction (Pardoll 2012). Responses to PD-1/PD-L1 therapy are mainly influenced by factors including: PD-L1 expression, presence of the T cell infiltrate within the tumour and the general immune status of patients (e.g. absolute lymphocyte count, T cell exhaustion) (Blank et al. 2016; Sun et al. 2018). Furthermore, lack of tumour cell recognition or immunogenicity from defects in antigen presentation machinery arising from tumour-associated mutations or neoantigens, and defects in the IFN-γ receptor pathway on tumour cells can act as resistance to blockade therapy (Sun et al. 2018). A genetic screen *in vivo* identified that the loss of multiple genes can sensitise tumours to immunotherapy (Manguso et al. 2017). Loss of tyrosine-protein phosphatase non-receptor type 2 (PTPN2) sensitises tumour cells to IFN-γ-mediated growth suppression in the presence of T cell-mediated immunity. Overall, analysis of clinical trial data has revealed three patient subpopulations: (1) responders to initial therapy which can be maintained, (2) failure to respond due to innate resistance, and (3) responders to initial therapy but later develop disease progression due to acquired resistance (Jenkins et al. 2018). The PD-1/PD-L1 pathway can affect the generation of T cell response, the effector function and the formation of effector memory T cells. Moreover, the effect of other additional immune checkpoints should not be ignored.

Tumours can be classed by PD-L1 expression and presence of TILs (mainly T cell infiltrate): (1) PD-L1$^+$ TIL$^+$, (2) PD-L1$^-$ TIL$^+$, (3) PD-L1$^+$ TIL$^-$, (4) PD-L1$^-$ TIL$^-$ (Ribas & Hu-Lieskovan 2016). Predictors of clinical response to PD-1 therapy have included CD8$^+$, PD-1$^+$ and PD-L1$^+$ cell density in the invasive tumour margin and inside tumours, rather than CD4$^+$ density (Tumeh et al. 2014). PD-L1 expression in cancer histologies is more frequently observed as a result of IFN-γ induction rather than constitutive PD-L1 expression (Ribas & Hu-Lieskovan 2016). The induction of PD-L1 expression on the invasive tumour margin by IFN-γ producing T cells would be opportune for blockade therapy due to the presence of an ongoing immune response. Patients who do not respond to anti-PD-1/PD-L1 are likely to be negative for PD-L1 and absent of an effector T cell infiltrate. In addition, blockade therapy in PD-L1$^+$ tumours without T cell infiltrate may not induce a response, although, clinical responses were observed in patients with PD-L1-negative tumours (Robert et al. 2014; Shen & Zhao 2018). This may have been affected by the heterogeneous expression of PD-L1 in tumours and that the sampling location can affect the staining of PD-L1 or perhaps due to molecular mechanisms that involve PD-L1 expression on non-cancerous cells.

PD-L1 expression can be a major factor in the response to anti-PD-1/PD-L1 agents, and the "inflamed" phenotype of the tumour (number of infiltrating CD8$^+$ T cells, immune recognition of tumours and TCR clonality) can be predictive of immune checkpoint inhibitor response (Voong et al. 2017; Khunger et al. 2017). Patients who have at least 50% of tumours cells expressing PD-L1 had better outcome (29-30% overall response rate) from anti-PD-1 therapy (pembrolizumab) in previously-treated NSCLC, than the overall number of patients (>1% PD-L1 expression, 18% response rate) (Herbst et al. 2016) (*overall response rate is defined as the number of patients with a tumour size reduction of a predefined amount for a minimum time period* (Pazdur 2008)). Furthermore, anti-PD-L1 (durvalumab) treatment in metastatic urothelial carcinoma had a higher overall response rate (27.6%) in patients with high PD-L1 (≥ 25% of tumour cells or immune cells staining for PD-L1) expression than PD-L1 negative (≤ 25%) patients (5.1%) (Powles et al. 2017). There are similar findings showing that there is an increased benefit associated with higher PD-L1 expression has been observed with a second anti-PD-L1 agent (atezolizumab) (Rosenberg et al. 2016). Analysis of overall response rate found a PD-L1-associated response in patients with metastatic urothelial cancer: PD-L1 ≥ 5% on infiltrating immune cells; 27% response, PD-L1 ≥ 1%; 18% and PD-L1 ≤1%; 8%. This also indicates that patients with low to none expression of PD-L1 on tumour-infiltrating immune cells or tumour cells can still respond to anti-PD-L1 therapy.

Conversely, clinical trials are affected by different parameters to classify PD-L1-negative tumours and the type of antibodies to detect expression of PD-L1 (cell surface or cytoplasmic). This can affect clinical data especially when expression of PD-L1 can be heterogeneous and not necessarily indicative of an ongoing immune response, such as in cases of IFN-γ-independent induction (Sun et al. 2018; Blank et al. 2016). Expression of PD-L1 alone is suggested to be insufficient as a prognostic biomarker since anti-PD-1/PD-L1 blockade can benefit both PD-L1 positive and PD-L1 negative tumours (Carbognin et al. 2015; Shen & Zhao 2018). Not all patients with PD-L1 positive tumours respond to therapy so the expression of PD-L1 should be thought more of a crude measure (Carbognin et al. 2015; Blank et al. 2016). Furthermore, there may be a role of PD-L1 outside the tumour microenvironment; could targeting PD-L1-expressing stromal/vascular cells with PD-L1 blockade improve the overall response rate?

The combination of anti-PD-1 with anti-CTLA-4 agents can enhance sensitivity to immunotherapy compared to a single agent alone (Gong et al. 2018). Combining both nivolumab (anti-PD-1) and ipilimumab (anti-CTLA-4) in the treatment of untreated melanoma has been shown to result in significantly longer progression-free survival and higher response rates than ipilimumab or nivolumab alone (Wolchok et al. 2013; Larkin et al. 2015; Postow et al. 2015). In addition, patients with PD-L1 negative tumours had the most benefit from combination therapy (11.2 months median progression-free survival) than either agent alone (nivolumab – 5.3 months; ipilimumab – 2.8 months), suggesting PD-L1 status could be a biomarker for choosing combination therapy over monotherapy (Larkin et al. 2015). In consideration, the number of treatment-related adverse events were higher in patients treated with nivolumab and ipilimumab (55.0%) than with nivolumab (16.3%) or ipilimumab (27.3%) (Larkin et al. 2015).

1.1.4.3 PD-L1 expression on host cells – target for immune checkpoint blockade?

There are implications that PD-L1 expression on host stromal cells can play an important role in the regulation of inflammatory responses since clinical responses can be observed in patients with PD-L1-negative tumours (Robert et al. 2014). The contribution of PD-L1 on tumour cell and host cells may determine the efficacy of anti-PD-1/PD-L1 blockade but the mechanistic target of these agents remains unclear (Sun et al. 2018; Tang & Zheng 2018). PD-L1 expression on host immune cells, as well as tumour cells, can contribute to immunosuppression and may be of importance as a predictive biomarker of response (Bellucci et al. 2015; Noguchi et al. 2017; Lau et al. 2017; Juneja et al. 2017). NK cells are an important source of IFN-γ and it was demonstrated that this release of IFN-γ can trigger tumour cell resistance to NK cell activity by upregulation of PD-L1 (Bellucci et al. 2015). In a mouse sarcoma model, tumour-associated macrophages (TAMs) were found to be a major

source of PD-L1 and retained the expression for a long period of time (Noguchi et al. 2017). The expression of PD-L1 on TAMs was IFN-γ-dependent and -independent requiring $CD4^+$ T cells. High PD-L1 expression on infiltrating myeloid DC and myeloid-derived suppressor cells in mice bearing PD-L1-deficient tumour cells, originating from murine colon carcinoma cell lines (MC38), can contribute to tumour escape by dampening cytotoxic activity of T cells (Lau et al. 2017). The relative contribution of tumour or host-derived PD-L1 is context dependent, based on the type of tumour (Juneja et al. 2017). PD-L1-deficient tumour cells (MC38 and BRAF.PTEN) were injected into wild-type mice. $PD\text{-}L1^{KO}$ MC38 tumours grew at a similar rate as control and some were eventually cleared. In contrast, the growth of $PD\text{-}L1^{KO}$ BRAF.PTEN tumours were slightly slowed and none of the tumours were cleared, suggesting a greater role of PD-L1 in non-tumour cells in this context (Juneja et al. 2017). In addition, MC38 tumours expressing PD-L1 were injected into mice lacking perforin, a cytolytic granule found in $CD8^+$ T cells that is required for delivering granzymes and killing target cells. Blockade with anti-PD-1 resulted in slowed tumour growth but did not lead to clearance, PD-L1 was found to reduce $CD8^+$ T cell cytotoxicity (Juneja et al. 2017).

Recent studies have provided further knowledge that the target of immune checkpoint blockade may be PD-L1 expressed by host cells, rather than tumour cells, in the tumour microenvironment (Tang et al. 2018; Lin et al. 2018). When PD-L1-deficient murine colon carcinoma cells (MC38) were transferred into PD-L1-knockout mice, anti-PD-L1 blockade did not induce an anti-tumour response (Lin et al. 2018). However, the transfer of PD-L1-deficient MC38 into wild-type mice and subsequent treatment with anti-PD-L1 reduced tumour growth in mice and activated T cells in the tumour-draining LNs and tumour tissues. In addition, host PD-L1 expression in MC38 tumour tissues was found on macrophages, MDSCs and DCs (which expressed the highest levels of PD-L1) in the tumour and in tumour-draining LNs. Expression of PD-L1-positive APCs were demonstrated to correlated with clinical responses using PD-1/PD-L1 blockade in a small subset of patients with melanoma (Lin et al. 2018). A second study in MC38 tumour-bearing mice also found that myeloid cells (macrophages, MDSCs and DCs) in tumour-draining LNs expressed higher PD-L1 than the same cells in tumour tissues (Tang et al. 2018). Inoculation of wild-type MC38 or PD-L1-deficient MC38 into a wild-type host showed similar tumour growth. Upon anti-PD-L1 blockade, the response of the PD-L1-deficient MC38 tumour was similar to that of the wild-type tumour, suggesting PD-L1 on tumour cells is dispensable in the response to immune checkpoint therapy. Moreover, a bone marrow chimeric model showed that the expression of PD-L1 on myeloid cells was essential in response to PD-L1 blockade. Inhibition of lymphocyte trafficking using an analogue of sphingosine 1-phosphate (S1P)

reduced the effects of anti-tumour immunity in the presence of PD-L1 blockade, suggesting the migration of activated T cells from draining LNs was important in maintaining overall responses (Tang et al. 2018). This may also include therapeutic inhibition of PD-L1 expression on LECs. Although, these studies suggest that tumour-derived PD-L1 is dispensable for the efficacy of PD-L1 blockade, this does not rule out that PD-L1 expression is important for cancer cell survival and tumour progression (Azuma et al. 2008; Gato-Cañas et al. 2017).

A factor that could be explored further is the relative expression of PD-L1 on stromal and vascular cells and whether this may affect the immune response in the tumour microenvironment. Stromal cells such as endothelial cells and fibroblasts are able to actively interact with infiltrating leukocytes and modulate anti-tumour immunity (Turley et al. 2015) (see Chapter 1.3). The above studies lacked investigation into the effect of PD-L1 expression on fibroblasts or endothelial cells in the response to PD-L1 blockade. Overall, the findings from these studies imply that PD-L1 expression on host cells (i.e. APCs, stromal) could serve as a biomarker and mechanistic target for the response to anti-PD-1/PD-L1 therapy.

1.1.5 Regulation of PD-L1

The regulation of PD-L1 in immune, non-transformed and tumour cells is highly complex, which is reflected in the number of signalling networks and emerging mechanisms that affect the stability and expression of mRNA and protein (Sun et al. 2018). Moreover, PD-L1 is regulated at the transcriptional, posttranscriptional and posttranslational levels.

1.1.5.1 Inflammatory signalling

The best characterised and most potent inflammatory signal for induction of PD-L1 on various cell types is IFN-γ, a type II interferon and pro-inflammatory cytokine predominantly produced by activated $CD4^+$ and $CD8^+$ T cells and NK cells (Freeman et al. 2000; Dong et al. 2002; Mazanet & Hughes 2002; Brown et al. 2003; Rodig et al. 2003; Loke & Allison 2003; Lee et al. 2005; Lee et al. 2006; Pardoll 2012; Bellucci et al. 2015; Garcia-Diaz et al. 2017). Typically, IFN-γ binds to the IFN-γ receptor (IFNGR) that is composed of two ligand-binding IFNGR1 chains and two signal-transducing IFNGR2 chains (Schroder et al. 2004). IFN-γ induces rapid dimerization of IFNGR1 chains that is then recognised by IFNGR2 to form the complete receptor. This initiates downstream signalling via phosphorylation of the Janus kinase (JAK) family and to further recruit and phosphorylate STAT proteins. Following phosphorylation, STAT proteins homodimerise and translocate to the nucleus to bind to IFN-γ-activated sequence (GAS) elements and promote expression of genes such as interferon regulatory factors (IRFs) (Schroder et al. 2004). IRF1 was found responsible for constitutive expression and IFN-γ-mediated PD-L1

upregulation in the A549 lung cancer cell line (Lee et al. 2006). Moreover, IFN-γ treatment resulted in a defined upregulation pattern of PD-L1 by the JAK2/STAT1/IRF1 axis in melanoma cells (Garcia-Diaz et al. 2017). There was also an increase in STAT2, STAT3 and IRF9 genes which could suggest an overlap between type II and type I interferon-signalling pathways. Two melanoma cell lines that have loss-of-function mutations for either JAK1 or JAK2 failed to respond to IFN-γ induction of PD-L1 (Garcia-Diaz et al. 2017). Mutations in JAK1/2 in melanoma may serve as a form of resistance since these particular tumours appeared to be unresponsive to PD-1/PD-L1 blockade therapy (Shin et al. 2017). A particular JAK2 mutation ($JAK2^{V617F}$) is characteristic of myeloproliferative neoplasms (MPNs) mutations which spontaneously activates downstream STAT signalling (Prestipino et al. 2018). PD-L1 expression was revealed to be induced via STAT3 and STAT5 phosphorylation in multiple cell types including megakaryocytes, which typically drive the disease in MPNs. Furthermore, MPNs were susceptible to anti-PD-1 (nivolumab) therapy with a higher ratio of effector to naïve $CD8^+$ T cells and improved survival observed (Prestipino et al. 2018).

IFN-γ upregulation of PD-L1 has been reported to be context dependent and that there are other signalling mechanisms involved as well as the JAK/STAT pathway. The promoter region of PD-L1 was found to contain a NF-κB responsive element that can be induced by IFN-γ or TNF (Kondo et al. 2010). $PD\text{-}L1^+$ myelodysplastic syndrome blasts were revealed to have greater intrinsic proliferative capacity and suppressed T cell proliferation and induced apoptosis (Kondo et al. 2010). PD-L1 was found to be induced by IFN-γ alone through NF-κB in melanoma cell lines (Gowrishankar et al. 2015). Little effect was shown with inhibition of STAT3 on the expression of PD-L1 suggesting another pathway that IFN-γ can signal to NF-κB. IFN-γ has been shown to induce NF-κB via the mitogen-activated protein kinase (MAPK) and PI3K pathway in human dermal fibroblasts (Lee et al. 2005). Inhibition of PD-L1 by a MAPK and PI3K reduced promoter activity of PD-L1 by 39% and 46%, respectively. The role of JAK/STAT signalling was not explored in this study.

TNF-α is a potent mediator of inflammation produced by macrophages, NK cells, T cells, endothelial cells and fibroblasts (Sedger & McDermott 2014). TNF-α binds to TNFR1 or TNFR2 to form a trimer on the cell surface. A prominent downstream effector of TNF-α is NF-κB which typically involves the recruitment of TNF receptor-associated factor 2 (TRAF2) that facilitates the signal transduction of TNF (Sedger & McDermott 2014). TRAF2 interacts with receptor interacting protein kinase (RIP) to activate the inhibitor of NF-κB kinase (IKK), leading to ubiquitination and degradation of IKK. This allows NF-κB to translocate into the nucleus and induce transcription by binding to DNA. Given that PD-

L1 has been reported to be induced by NF-κB through IFN-γ and TNF-α stimulation in both cancer cells and human dermal fibroblasts (Lee et al. 2005). TNF-α stimulation alone did not affect PD-L1 expression in human umbilical vein endothelial cells (HUVEC) but in combination with IFN-γ displayed a synergistic or add-on effect (Rodig et al. 2003; Mazanet & Hughes 2002). Furthermore, activation of NF-κB by TNF-α was shown to stabilise PD-L1 expression at the posttranslational level in breast cancer cells (Lim et al. 2016). Induction of COP9 signalosome 5 (CSN5) by the p65 subunit of NF-κB directly deubiquitinates and stabilises PD-L1 from degradation. The effect of TNF-α on PD-L1 appears to revolve around the role of stability or localisation of PD-L1 to the cell surface and similarly to IFN-γ stimulation is also context dependent.

PD-L1 is also induced by type I interferons IFN-α and -β (Eppihimer et al. 2002; Garcia-Diaz et al. 2017), IL-6 and IL-10-induced STAT3 (Wölfle et al. 2011) and lipopolysaccharide (LPS) through toll-like receptor 4 (TLR4)/ NF-κB signalling (Loke & Allison 2003). TLR4-mediated upregulation of PD-L1 was shown to be dependent on JAK2 and myeloid differentiation primary response 88 (MyD88) in human stromal cells derived from normal mucosa (Beswick et al. 2014). MyD88 is an adaptor protein that is linked to NF-κB, IRF and MAPK pathways and may play a critical role in PD-L1 expression (Kawasaki & Kawai 2014).

1.1.5.2 Oncogenic signalling

PD-L1 expression is often overexpressed in many cancers and has been implicated with several oncogenic signalling pathways that contribute to tumour growth, survival and proliferation. The majority of these mechanisms contribute to driving expression of PD-L1 which facilitate the inhibition of T cell responses. PD-L1 has been linked to oncogenic signalling from anaplastic lymphoma kinase (ALK) which promotes the expression of PD-L1 through induction of STAT3 in T cell lymphoma (Marzec et al. 2008).

The MAPK/ extracellular signal-regulated kinase (ERK) pathway (also called MEK/ERK) is involved in PD-L1 regulation through crosstalk between IFN-γ and TLR inflammatory signalling (Liu et al. 2007). Blockade of MyD88 and TRAF6 adaptor proteins and MEK/ERK signalling inhibit IFN-γ/STAT1 induced transcription of PD-L1 in multiple myeloma plasma cells. In addition, induction of PD-L1 by phorbol 12-myristate 13-acetate (PMA), a known inducer of the MEK/ERK pathway was blocked with a MEK/ERK inhibitor (Liu et al. 2007). The MAPK/ERK pathway includes the RAS family of small GTPases and predominantly signalling initiates at the cell surface receptor, an example being epidermal growth factor receptor (EGFR). Oncogenic RAS signalling was demonstrated to drive PD-L1 expression by modulating a posttranscriptional control

mechanism affecting PD-L1 mRNA stability (Coelho et al. 2017). Adenylate-uridylate (AU)-rich element (ARE) binding protein tristetraprolin (TTP) negatively regulates PD-L1 which could be inhibited by RAS/ERK activity. Epidermal growth factor receptor (EGFR) is a commonly mutated oncogene in patients with NSCLC and activation of the EGFR pathway induces an immunosuppressive environment, including PD-L1 expression (Akbay et al. 2013). In EGFR-driven murine lung cancer models, PD-1 blockade reduced tumour burden and improved the effector function of $CD8^+$ T cells, such as production of IFN-γ. Rare mutations of EGFR that cause over-activation of EGFR signalling upregulate PD-L1 in head and neck cancers, which was found to be dependent on JAK2/STAT1 (Concha-Benavente et al. 2016).

The PI3K/Akt/mTOR pathway is an important pathway that regulates normal cellular processes and its dysregulation which contributes to cell survival and proliferation is frequently observed in many cancers. Phosphatase and tensin homolog (PTEN) is a tumour suppressor gene that inhibits Akt. PD-L1 is increased after loss of PTEN and activation of S6K1, a downstream effector of the Akt pathway in glioma, breast and prostate cancer cells (Parsa et al. 2007; Crane et al. 2009). Polysomal recruitment by S6K1 upregulates PD-L1, by facilitating the movement of mRNA to polysomes to increase translation of PD-L1. IFN-γ induction of PD-L1 has been demonstrated to be mediated by mTOR activation in NSCLC cell lines (Lastwika et al. 2015). In addition, it was suggested that regardless of the oncogenic or cytokine stimuli, Akt/mTOR signalling is necessary for driving PD-L1 protein expression.

The MYC oncogene is a transcription factor that is involved in numerous growth signalling pathways that affect cell proliferation, differentiation and apoptosis (Dang 2012). MYC is estimated to be mutated in up to 70% of human cancers. MYC inactivation in both mice and human tumour cells induces tumour regression where PD-L1 mRNA and protein expression were also found to be suppressed (Casey et al. 2016). MYC can regulate PD-L1 by binding to the promoter suggesting a transcriptional mechanism of control.

Cyclin-dependent kinases (CDKs) regulate the stability cell cycle-related proteins during cell cycle progression. CDK5 is a serine-threonine kinase that facilitates the immune escape of medulloblastoma by maintaining expression of PD-L1 (Dorand et al. 2016). Disruption of CDK5 increases the abundance of IRF2, a competitive inhibitor of IRF-1-mediated activation and prevents further IFN-γ-mediated production of PD-L1. In contrast, inhibition of CDK4 but not CDK6 elevates PD-L1 protein levels by regulating the phosphorylation of a cullin 3-based E3 ubiqutin ligase (Cullin 3^{SPOP}), which mediates degradation of PD-L1 (Zhang et al. 2018). Deletion of the last eight amino acids of PD-L1 (283-290) ablated the

binding of PD-L1 to SPOP. Treatment with different inhibitors of CDK4/6 and anti-PD-1 immunotherapy increase the immunogenicity of cancer cells and enhance tumour regression (Zhang et al. 2018; Schaer et al. 2018).

Hypoxia represents non-physiological levels of oxygen in the tumour and hypoxia-inducible factor 1-alpha (HIF-1α) is typically induced in response to oxygen deficiency. HIF-1α was demonstrated by chromatin immunoprecipitation (ChIP) to directly interact with the hypoxia response element of the PD-L1 promoter in murine splenic myeloid-derived suppressor cells, human breast cancer and prostate cancer cells (Noman et al. 2014; Barsoum et al. 2014). In addition to HIF-1α, HIF-2α was shown to target PD-L1 at both mRNA and protein levels in human renal carcinoma cells (Messai et al. 2016).

Glycosylation of PD-L1 has been shown to affect the tumour-associated immune escape (Li et al. 2016). PD-L1 is extensively N-glycosylated at four glycan sites (N35, N192, N200 and N219), which mediate PD-L1 stability through protection against degradation. Glycogen synthase kinase 3β (GSK3β) was demonstrated to facilitate the degradation of non-glycosylated PD-L1 through formation of a complex with β-transducin repeats-containing protein (β-TrCP) (Li et al. 2016).

Two papers identified CKLF-like MARVEL transmembrane domain containing protein 6 (CMTM6) as a specific regulator of PD-L1 protein that maintains its cell surface expression in a broad range of cancer cells and primary DCs (Burr et al. 2017; Mezzadra et al. 2017). Mass spectrometry screening revealed PD-L1 as one of four interacting proteins of CMTM6 from 4,935 quantified proteins that were decreased by more than two-fold at the cell surface after Clustered Regularly Interspaced Short Palindromic Repeats (CRISPR)-Cas9-mediated disruption of CMTM6 (Burr et al. 2017). CMTM6 can bind directly to PD-L1 and facilitate protection against lysosome-mediated degradation (Burr et al. 2017; Mezzadra et al. 2017). Depletion of CMTM6 affects both constitutive and IFN-γ induced PD-L1 expression where the recycling of PD-L1 is markedly impaired. In addition, CMTM4 was identified as a second regulator of PD-L1 which shares the regulatory function with CMTM6 (Mezzadra et al. 2017).

1.1.5.3 Genetic alteration

PD-L1 is located on chromosome 9p24.1 and is 322 kb downstream of JAK2. Genetic amplification of the 9p24.1 chromosome and increased expression of PD-L1 was discovered in cases of Classical Hodgkin lymphoma (cHL) (6 of 16; 38%) and primary mediastinal large B cell lymphoma (PMBCL) (26 of 41; 63%) (Green et al. 2010). JAK2 amplification and increased expression was also detected and suggested to induce PD-L1 expression. A larger study of rearrangements in chromosome 9p of PMBCL showed an amplification

frequency of 29% and a break-point frequency of 20% in 125 cases (Twa et al. 2014). In addition, a large study in cHLs found that almost all cases had alterations in the 9p24.1 chromosome. Copy gain and amplification accounted for 56% (61 f 108) and 36% (39 of 108) of all analysed cases (Roemer et al. 2016). Moreover, a small number of patients with NSCLC were observed to have genetic amplification of the PD-L1 gene (5 of 89; 6%) which correlated with JAK2 gene amplification (Ikeda et al. 2016). Four of the five samples that showed PD-L1 gene amplification did not have PD-L1 protein overexpression. However, using the HCC4006 lung adenocarcinoma cell line which harbours PD-L1 and JAK2 gene amplification, the study showed that PD-L1 was significantly higher expressed after IFN-γ and TNF-α treatment compared to other cell lines without this amplification (Ikeda et al. 2016). In a small subset of SCLC patients (4 of 210; 2%), high-level and focal amplification of 9p24 was observed with high expression of PD-L1 (George et al. 2017). Whether patients with genetic alterations of the PD-L1 gene are sensitised to anti-PD-1/PD-L1 is less well-studied.

In addition, the 3'-untranslated region (UTR) is a crucial determinant of PD-L1 expression. Interestingly, an ovarian cancer patient harbouring a break-point in the 3'-UTR of PD-L1 had strong expression of the extracellular domain of PD-L1 (Bellone et al. 2018). The structural variant involved a translocation/insertion of a 32 nt fragment from chromosome 9, exon 5 of the plasminogen receptor, C-terminal lysine (PLGRKT) gene into the 3'-UTR of PD-L1 (Bellone et al. 2018). The patient had a chemotherapy and radiation-resistance, high grade ovarian cancer and was given pembrolizumab treatment. High PD-L1-expressing tumour cells co-localised with a heavy infiltration of $CD4^+$ and $CD8^+$ TILs and it was reported that the patient experienced a complete and sustained response (Bellone et al. 2018). Adult patients with T cell leukaemia/lymphoma, diffuse large B cell lymphoma and stomach adenocarcinoma were revealed to harbour structural variations that truncated the 3'-UTR of the PD-L1 gene (Kataoka et al. 2016). Disruption of the 3'-UTR of PD-L1 led to increased stability of PD-L1 transcripts and expression. Furthermore, CRISPR-Cas9 deletion of the PD-L1 3'-UTR determined that truncation of the 3'-UTR induced a greater upregulation of PD-L1 expression than that of IFN-γ. Moreover, the loss of the 3'-UTR was shown to promote tumour growth and immune escape in *in vitro* and *in vivo* models. This suggests that the 3'-UTR of PD-L1 might serve as a genetic marker to determine cancers that may respond to anti-PD-1/PD-L1 therapy. Moreover, the 3'-UTR of PD-L1 is relatively long (2710 bp) and potentially contains several regulatory regions including microRNA response elements that function as mechanisms for posttranscriptional control.

1.2 MicroRNAs

1.2.1 microRNA silencing

microRNAs (miRNAs) are a class of highly conserved, small non-coding RNA (~22-24 nt) that regulate gene expression at the posttranscriptional level of all biological pathways including cell development, differentiation and function (O'Connell, Rao, et al. 2010). The function of miRNAs is to guide the RNA-induced silencing complex (RISC) to target mRNAs. miRNA binding sites are typically in the 3'-UTR of mRNAs (Bartel 2009). Nucleotide position 2 to 7 at the 5'-end of miRNAs serve as the seed sequence which determines target recognition. In addition, nucleotide(s) 8 and 13-16 may also contribute to target-base pairing (Ha & Kim 2014). The miRNA mechanism of action is to induce translation repression or mRNA degradation which acts to fine-tune gene expression. Due to their short seed sequence (6-8 nt), many miRNAs can be involved in regulating a single mRNA target or that a single miRNA can be involved in regulating many mRNA targets (Mehta & Baltimore 2016). Over 4,000 miRNAs in humans have been catalogued by the miRNA database (miRBase v22, March 2018 release) (Griffiths-Jones et al. 2006). It is predicted that more than 60% of human protein-coding genes are under the control of at least one conserved miRNA and thought to be exceeded because of the potential number of non-conserved binding sites. Often in human diseases such as cancer, miRNAs can become dysregulated and function as potential oncogenes or oncosuppressor genes, and miRNA expression can be profiled to distinguish between normal and cancerous tissue (Iorio & Croce 2012). Now, although in its infancy, it has emerged that miRNAs can be used in the clinic as prognostic and predictive biomarkers through detection in biological fluids which provides an encouraging real-world use (Iorio & Croce 2012; Hayes et al. 2014).

1.2.2 microRNA biogenesis

In mammals, the canonical process of miRNA biogenesis encompasses the maturation of primary miRNA (pri-miRNA) transcripts (~1 kb) that are transcribed by RNA polymerase II in the nucleus (Figure 1.3). The majority of miRNAs undergoing the canonical process come from introns of non-coding or protein-coding genes that can share the promoter of the host gene, or from exonic regions (Ha & Kim 2014). Pri-miRNA transcripts consist of a stem-loop structure (apical loop and stem) and single-stranded RNA tails at both 5'- and 3'- ends (the location where the stem extends to the tails is termed basal junction), which are processed by the RNase III endonuclease Drosha and the dsRNA-binding protein DiGeorge syndrome critical region 8 (DGCR8) (Lee et al. 2003; Ha & Kim 2014). Drosha and two DGCR8 molecules form a Microprocessor complex where the tandem RNase III domains of Drosha cut the 5'- and 3'- ends, one helical turn away from the basal junction (Kwon et al. 2016). DGCR8 is recruited to facilitate RNA-binding activity for efficient pri-miRNA

processing. The C-terminus of DGCR8 can interact with Drosha through protein-protein interactions. Two dsRNA-binding domains (dsRBD) from DGCR8 can bind to haem of the pri-miRNA to provide a stable interface between Drosha and the pri-miRNA, leading to formation of a hairpin-shaped precursor miRNA (pre-miRNA, ~65 nt long) (Ha & Kim 2014).

As a side note, there have been reports of different non-canonical pathways, one of which involves the bypassing of the Drosha-mediated processing step through mRNA splicing such that a pre-miRNA is formed after a series of folds. These 'mirtrons' have extra sequences at the 5'- or 3'-end that requiring trimming by exonucleases (Ha and Kim, 2014). The vast majority of functional miRNAs follow the canonical pathway, where only 1% of conserved miRNAs are produced independently of Drosha or Dicer in vertebrates.

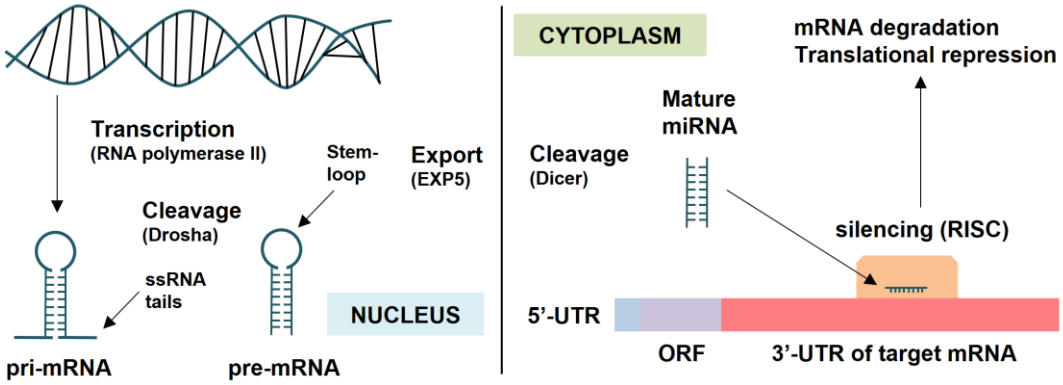

Figure 1.3. **The microRNA biogenesis canonical pathway**. Initially, RNA polymerase II transcribes pri-miRNA from DNA. The single-stranded RNA tails at 5'- and 3-'ends of the pri-miRNA are cleaved by the Microprocessor complex consisting of the RNase III endonuclease Drosha and its RNA-binding partner DGCR8, forming a pre-miRNA. Exportin-5 transports the pre-miRNA from the nucleus to the cytoplasm where a second cleavage takes place. The RNase III endonuclease Dicer assisted by its co factors TRBP and PACT cleaves the stem-loop giving arise to a mature miRNA. Next, the mature miRNA is unwound and a single 'guide' strand is loaded onto the RISC and directs the complex to a target mRNA to mediate mRNA degradation and/or translation repression. This figure is modified from previous publications (Ling et al. 2013; Ryan et al. 2015).

Following this processing, pre-miRNA are exported into the cytoplasm through a transport complex consisting of the protein exportin-5 (XPO5) and a GTP-binding nuclear protein (RanGTP). RanGTP is hydrolysed in order for the pre-miRNA to be released into the cytoplasm where it is further processed (Ha & Kim 2014). The RNase III endonuclease Dicer consists of a catalytic centre at the C-terminal and an N-terminal helicase that allows Dicer to cleave off the stem-loop of the pre-miRNA. In addition to having a similar structure

to Drosha, Dicer also has cofactors that facilitate processing efficiency, transactivating response RNA-binding protein (TRBP) and protein activator of the interferon-induced protein kinase (PACT) assist in this cleavage, giving arise to a miRNA duplex (Ha & Kim 2014).

Multiple publications have reported the importance of core miRNA biogenesis components in animal development including cases of embryonic lethality from Drosha and Dicer deficiency by embryonic day 7.5 (E7.5) (Chong et al. 2010; Bernstein et al. 2003). Furthermore, binding partners are also key and DGCR8 deficiency has been shown to affect the maturation of miRNAs and downstream silencing function (Wang et al. 2007).

1.2.3 microRNA function

Prior to unwinding of the duplex, RISC assembles with a member of the Argonaute (AGO) family of RNA-binding proteins that act as downstream effectors. There are 4 types in humans (AGO1-4), all of which are capable of inducing translational repression, mRNA deadenylation and mRNA decay. Only AGO2 can slice perfectly matched mRNAs, however, all four types of AGO can associate with miRNAs (Ha and Kim, 2014). Most miRNA duplexes have central mismatches (that prevent slicing) such that unwinding is a general process. Mismatches in the guide strand at nucleotide positions 2-8 and 12-15 promote unwinding. Of the miRNA duplex (~20 nt), one miRNA represents the 5'-strand and the other the 3'-strand. When the duplex is unwound, the 'guide' strand is packaged onto RISC whereas the other miRNA strand (the 'passenger' strand, denoted by miRNA*) is normally degraded (Kim et al., 2009). Determining which strand is degraded is related to the relative thermodynamic stability of the two ends of the duplex (Kim et al., 2009). The strand with relatively unstable base pairs, such as GU compared to GC, at the 5'-end typically becomes the guide strand (Kim et al., 2009). One other determinant, is the preference of AGO for guide strands with a U at nucleotide position 1 (Ha and Kim, 2014). Loading of the guide strand to the RISC is ATP-dependent with the aid of the heat shock cognate 70/heat shock protein 90 chaperone complex to facilitate binding of AGO to miRNA. In contrast, the release of the passenger strand is ATP-independent (Ha and Kim, 2014). The miRNA guides RISC to the 3'UTR region of target mRNAs leading to repression of protein-coding gene expression (Huntzinger and Izaurralde 2011). In mammals, the majority of miRNAs pair imperfectly with target mRNAs and direct translational repression, mRNA destabilisation or the combination of the two (Filipowicz et al. 2008; Bartel 2009).

1.2.4 microRNAs in the inflammatory response

miRNAs are a crucial regulatory body for development and normal function of the immune system (O'Connell et al. 2012). This section provides a brief overview about the importance

of miRNAs and miRNA biogenesis components for normal immune function. Deletion of Dicer during T cell development demonstrated the involvement of miRNAs in the maturation, proliferation and survival of T cells (Cobb et al. 2005; Muljo et al. 2005; Cobb et al. 2006). In addition, there is an overall reduction of $CD4^+$ and $CD8^+$ T cell numbers in the blood, LNs and spleen (Muljo et al. 2005). miRNAs are indispensable in inflammatory responses due to the regulation of T reg cells that repress spontaneous inflammation and autoimmunity (Chong et al. 2008; Liston et al. 2008; Zhou et al. 2008). Drosha and Dicer are required for the induction of forkhead box P3 (FOXP3), which regulates the development and function of T reg cells. Dicer is needed for the development of B cell lineage and antibody repertoire (Koralov et al. 2008). Gene-expression profiling identified a cluster of miRNAs, miR-17~92, which consists of six miRNAs (miR-17, -19a, -20a, -19b and -92) that share four distinct and conserved seed regions. High levels of the pro-apoptotic gene, Bim, and loss of miR-17~92 expression were found in Dicer knockout B cells. Bim was shown as a target of miR-17~92, which contains nine potential binding sites for miR-17~92 (Koralov et al. 2008).

miRNAs are implicated in a number of inflammatory conditions such as multiple sclerosis, rheumatoid arthritis and systemic lupus erythematosus (O'Connell et al. 2012). The first miRNAs associated with the inflammatory response were miR-155, miR-146a and miR-132 (O'Connell et al. 2007; O'Connell et al. 2009; Taganov et al. 2006; Tili et al. 2007; Shaked et al. 2009; Lagos et al. 2010). miR-155 and miR-146a are induced in monocytes, macrophages and DCs by NF-κB and activator protein-1 (AP-1) in response to a broad range of TLRs and cytokine signals such as LPS. Expression of miR-155 tightly upregulates inflammatory signalling by suppressing negative regulators of Akt and IFN pathways, SH2 domain-containing inositol 5'-phosphate 1 (SHIP1) and suppressor of cytokine signalling 1 (SOCS1), respectfully (O'Connell et al. 2009; Androulidaki et al. 2009; Lu et al. 2009). In contrast to miR-155, miR-146a is a negative regulator of the immune response and regulates proteins involved in the NF-κB pathway, IL-1 receptor-associated kinase 1 (IRAK1) and TRAF6 (Taganov et al. 2006; Boldin et al. 2011). Ablation of miR-146a expression in mice revealed the hyper-responsiveness of macrophages towards LPS and development of autoimmune disorder, characterised by multi-organ inflammation. This correlated with the activated phenotype of $CD8^+$ and $CD4^+$ T cells suggesting a loss of peripheral T cell tolerance (Boldin et al. 2011). Both miR-155 and miR-146a play opposing roles in the development of T follicular cells (Hu et al. 2014). Mice lacking miR-146a have elevated NF-κB activation which increases miR-155 in activated T cells. In addition, miR-155 is required for development of $CD4^+$ T follicular helper cells (Hu et al. 2014). Moreover in the context of anti-tumour immunity, miR-155 plays a protective role whereas miR-146a is

inhibitory and is demonstrated by their effects on the IFN-γ response of $CD4^+$ and $CD8^+$ T cells (Huffaker et al. 2012). Several other miRNAs have been implicated in regulation of the inflammatory response including miR-21 (Sheedy et al. 2010), let-7 (Iliopoulos et al. 2009) and miR-125b (Tili et al. 2007).

1.2.5 Regulation of PD-L1 by microRNAs

miRNAs have the potential to regulate the molecular pathways involved in the host immune response (Baltimore et al. 2008; O'Connell, Rao, et al. 2010; Mehta & Baltimore 2016). Recent evidence have placed miRNAs as one of the group of regulators of PD-L1 expression. The first miRNA implicated in regulation of PD-L1 is miR-513 (Gong et al. 2009). PD-L1 mRNA but not protein is detectable, unless with IFN-γ stimulation, in normal human cholangiocytes. A significant decrease of miR-513 was detected in IFN-γ-exposed cells and overexpression of miR-513 was found to bind to the 3'-UTR of PD-L1 and repress translation of PD-L1 mRNA, suggesting miR-513 inhibits IFN-γ-induced PD-L1 expression.

The remaining studies have linked miRNAs to PD-L1 expression in a broad range of cancers. Several miRNAs including miR-200, miR-34a and miR-138, have been found to be downregulated in cancer cells to allow PD-L1 expression (Chen et al. 2014; Cortez et al. 2016; Zhao et al. 2016). miR-200, a suppressor of metastasis by targeting zinc-finger E-box-binding homeobox 1 (ZEB1) was found to target PD-L1 expression in NSCLC, revealing a possible link between epithelial-mesenchymal transition and T cell dysfunction (Chen et al. 2014). miR-34 was shown to target PD-L1 in NSCLC via the tumour suppressor p53 that may facilitate tumour immune evasion because p53 is downregulated in most cancers (Wang et al. 2015; Cortez et al. 2016). Low miR-138-5p and high PD-L1 levels are correlated with tumour growth in colorectal cancer (Zhao et al. 2016). In pancreatic cancer, miR-142-5p expression was inversely correlated with PD-L1, and overexpression could block the PD-1/PD-L1 pathway (Jia et al. 2017). PD-L1 is repressed by miR-106b-5p and miR-93-5p which are part of the miR-25-93-106b cluster, in pancreatic cancer cells, myeloid-derived suppressor cells and bone marrow stromal cells (Cioffi et al. 2017). In gastric adenocarcinoma, miR-570 regulates PD-L1 via the 3-UTR of PD-L1 mRNA, a G-to-C mutation in the 3-UTR caused reduced binding affinity of miR-570, resulting in elevated PD-L1 (Wang et al. 2012; Wang et al. 2013). Helicobacter pylori infection results in higher PD-L1 expression in gastric cancer cells and both miR-152 and miR-200b are suppressed (Xie et al. 2017). It was identified that miR-152 and miR-200b can suppress PD-L1 expression by acting as tumour suppressors. In laryngeal cancer cells, miR-217 is found suppressed but overexpression of miR-217 was shown to target and repress PD-L1 protein levels (Miao et al. 2017). In melanoma, miR-17-5p is downregulated and shows an inverse correlation with PD-L1 (Audrito et al. 2017). In malignant pleural mesothelioma, miR-15a

and miR-16 were identified to target PD-L1 (Kao et al. 2017). Although, miR-193a is not predicted to have a target binding site on PD-L1, there was an alternative GU-containing target site that caused PD-L1 downregulation. Mutagenesis of miR-17-5p binding site in the 3'-UTR of PD-L1 mRNA was used to confirm binding specificity between miR-17-5p and PD-L1. Indirect regulation of PD-L1 by miRNAs were observed when miR-20b, miR-21 and miR-130b repress PTEN and resulted in PD-L1 overexpression in advanced colorectal cancer (Zhu et al. 2014). Furthermore, A miR-197/CKS1B/STAT3-mediated PD-L1 network was found to promote lung cancer (Fujita et al. 2015). Downregulation of miR-197 in lung cancer allows the cyclin-dependent CKS1B to promote PD-L1 expression via STAT3.

Although, there has been a great deal of progress in the identification of dysregulated miRNAs that regulate PD-L1 expression in various cancer cell types. There is also a lack of studies in miRNAs of non-transformed cells, particularly of stromal cells which would help to understand their contribution in the context of normal physiology, disease or response to anti-PD-1/PD-L1 therapeutics. Another question is whether miRNA-mediated regulation of PD-L1 expression in macrophages, DCs, fibroblasts or endothelial cells affect or predict the response to PD-1/PD-L1 immunotherapy?

1.3 Introduction to stromal/vascular cells

There has been a great deal of studies into PD-1/PD-L1 pathway which have focused on the role of these molecules in immune cells, cancer cells or infected cells. These studies have broadened our knowledge of the PD-1/PD-L1 mechanism and also the regulation of the pathway. The response to PD-1/PD-L1 treatment occurs in a subset of patients suggesting there is a complexity in the number of intrinsic resistance mechanisms. The influence of the stromal landscape and the dynamic relationship of the environments that surround immunological target sites should be considered. Stromal and vascular cells have emerged as active regulators of immunity which can shape the responsiveness to immunotherapy (Turley et al. 2015). Stromal cells incorporate a number of different cell types including fibroblasts, macrophages and endothelial cells (Mao et al. 2013).

Recent data has shown that transforming growth factor-β (TGF-β) signalling from fibroblasts is attributed to the lack of response from treatment with anti-PD-L1 in patients with metastatic urothelial cancer (Mariathasan et al. 2018). In particular, there was an exclusion of $CD8^+$ T cells from the tumour parenchyma, which were found sequestered in the peritumoural stroma. In addition, non-haematopoietic stromal cells contribute towards epithelial-mesenchymal transition (EMT)-related gene expression in urothelial cancer (Wang et al. 2018). Although there was a correlation between infiltrating numbers of T cells and

EMT-related gene expression, this was found to be associated with lower response rates to anti-PD-1 blockade, suggesting that stromal cells have a role in the resistance to anti-PD-1 blockade.

There is less known about the effect that PD-L1 expression on vascular/stromal cells has in the response to immune checkpoint blockade. In addition, the regulatory mechanisms behind PD-L1 expression and function in vascular/stromal cells, especially the role of miRNAs, under normal physiological responses need to be studied. This would help facilitate our understanding into the network of interactions between stromal or vascular cells and the immune response. The following subsections describe two different types of cells that interact with immune cells such as T cells to either activate or inhibit their function and response. These cell types are likely to play some role in the response to immune checkpoint blockade. Lymphatic endothelial cells (LEC) are reported to affect both T cell activity and lymphangiogenic pathways that can target the extravasation of T cells (Chapter 1.4) (Turley et al. 2015). Similarly, fibroblasts shape immune responses in local microenvironments through direct cell-cell contact or secreting chemokines and cytokines, affecting T cell responses (Turley et al. 2015) (Chapter 1.5).

1.4 Lymphatic endothelial cells (LECs)

The lymphatic system is a large transport network that is required for fluid clearance from tissues, including the trafficking of cytokines, immune cells and antigen to secondary lymphoid organs, such as LNs which orchestrate the adaptive immune response. The constant interaction between lymphatic vessels and the immune system enables the lymphatic system to serve as an important conduit in inflammation, infection, wound healing and cancer. The lymphatic system is also thought to link the brain and the immune system (Louveau et al. 2015).

1.4.1 Development and maintenance of the lymphatic system

Lymphatic vessels are made up of a single layer of partly overlapping LECs (Swartz 2001). The venous origin of the lymphatic system (Sabin 1902) has been supported by embryonic studies that have identified key transcription factors required for development and maintenance of the lymphatic system. Lymphatic differentiation and identity are characterised through expression of vascular endothelial growth factor receptor-3 (VEGFR3), lymphatic vessel hyaluronan receptor-1 (LYVE-1), podoplanin (Gp38) and prospero-related homeodomain protein 1 (PROX1) (Oliver 2004). VEGFR3 is a receptor tyrosine kinase for lymphatic-specific VEGF-C and VEGF-D (Tammela and Alitalo 2010). LYVE-1 is a widely-used lymphatic-specific marker, implicated in cellular trafficking and a homologue of the CD44 glycoprotein (Banerji et al. 1999; Jackson 2004). During early endothelial cell

development, both VEGFR3 and LYVE-1 are expressed and become restricted to LECs at later stages. VEGFR3 or VEGF-C knockout mice have defective lymphatic vascular development. In contrast, LYVE-1 knockout mice develop normal lymphatic vasculature (Gale et al. 2007).

The murine lymphatic system begins to form in a subpopulation of venous endothelial cells, LEC precursors, at embryonic day (E) 8.5 that express PROX1, LYVE-1 and VEGFR3 (Wigle & Oliver 1999). At E9.75, a lymphatic bias signal upregulates PROX1, LEC budding and formation of primary lymph sacs (Oliver 2004). PROX1-deficient embryos lack lymphatic vasculature, VEGFR3 or LYVE-1 expression, and are embryonic lethal at E14.5 (Oliver 2004). Two upstream transcriptional regulators of PROX1, SOX18 (Francois et al. 2008) and COUP-TFII promote the lymphatic bias signal until E13.5 (You et al. 2005; Srinivasan et al. 2010). Constant levels of PROX1 are required to maintain LEC lineage, which is supported by VEGF-C/VEGFR3 signalling (Srinivasan et al. 2014). Postnatal LECs have lower PROX1 expression compared with embryonic lymphatic endothelium suggesting low expression of PROX1 is sufficient to maintain LEC identity (Kazenwadel et al. 2010). Additional transcription factors and regulators of lymphatic development have been reported including neuropilin 2 (NRP2) (Yuan et al. 2002; Xu et al. 2010), NOTCH (Emuss et al. 2009; Kang et al. 2010), integrin-9α (Bazigou et al. 2009; Mishima et al. 2007), GATA2 (Kazenwadel et al. 2015), FOXC2 (Petrova et al. 2004; Norrmen et al. 2009) and c-MAF (Hansen et al. 2010).

Studies have highlighted the plasticity of LECs and that endothelial cell differentiation is reversible. Altering the levels of PROX1 expression during embryonic, postnatal or adult stages can reprogram LEC phenotype into blood endothelial cells (BECs) (Johnson et al. 2008; Petrova et al. 2002; Mishima et al. 2007). PROX1 deletion results in the upregulation of BEC-specific markers in human and murine LECs (Johnson et al. 2008). Conversely, BECs can be transcriptionally reprogrammed by overexpression of PROX1 in vitro, resulting in upregulation of VEGFR3 and podoplanin and suppression of BEC-specific transcripts such as the transcription factor STAT6 (Petrova et al. 2002; Hong et al. 2002). In adult vasculature, endothelial cells are quiescent but able to respond to angiogenic signals. Angiogenesis is the growth of new blood vessels from pre-existing vessels. Angiopoietin-1 (ANG-1) and ANG-2 are ligands for the receptor tyrosine kinase TIE2 and promote lymphatic vessel formation and patterning by VEGFR3 expression (Gale et al. 2002; Baluk et al. 2005; Morisada et al. 2005).

1.4.2 LECs in the inflammatory response

LECs are actively involved in immune regulation and inflammation. These interactions can occur within the lymphatic vessels as antigen and immune cells are transported from the periphery to nearby LNs where the dermal immune response is initiated, or when immune cells exit lymphatic sinuses in the LN. LECs are grouped in the category of lymph node stromal cells (LNSCs) which broadly are, non-haematopoietic cells that regulate immunity and self-tolerance (Malhotra et al. 2012), constituting ~1% of LN cellularity. These include: LECs ($gp38^+$ $CD31^+$), fibroblastic reticular cells (FRCs; $gp38^+$ $CD31^-$), BECs ($gp38^+$ $CD31^+$) and double-negative cells (DNCs; $gp38^-$ $CD31^-$). Transcriptomic analyses of mouse LNSC subsets identified that DNCs closely resemble FRCs in terms of global gene expression and cytokine production. Whereas, LECs and BECs have a closer developmental relationship and differ slightly in terms of expression of transcripts. LECs produce IL-7 transcripts whereas BECs do not (Malhotra et al. 2012). In addition, IL-7 was shown to be required for remodelling and homeostasis of the LN microenvironment after viral infection and transplantation (Onder et al. 2012). FRCs, BECs and LECs express TLR-4 and actively respond to the onset of inflammation by upregulation of IFN- and/or TLR-4-inducble genes including chemokine (C-X-C motif) ligand 9 (CXCL9) (Malhotra et al. 2012).

LECs express the chemokine (C-C motif) ligand (CCL21) that attracts and guides the interactions of CCR7-positive T, B and DCs to LNs via the afferent lymphatics (Förster et al. 2008). LN-LECs express different levels of CCL21 forming chemokine gradients that facilitate directional migration into the LNs through an atypical chemokine receptor, CCRL1 (Ulvmar et al. 2014). Pro-inflammatory cytokines such as TNF-α activate human dermal LECs (HDLECs) and induce vascular cell adhesion molecule 1 (VCAM-1), intercellular adhesion molecule 1 (ICAM-1) and E-selectin, facilitating adherence and transmigration of DCs (Johnson et al. 2006). Furthermore, chemokines secreted by activated HDLECs are significantly increased, including monocyte chemoattractant protein 1 (MCP-1 or CCL2), regulated on activation, normal T cell expressed and secreted (RANTES or CCL5) and macrophage inflammatory protein-3 (MIP-3α or CCL20), compared to resting HDLECs. Furthermore, ICAM-1 expression on inflamed HDLECs can directly regulate DCs via CD11b to suppress the co-stimulatory marker CD86, preventing effective T cell activation (Podgrabinska et al. 2009). Nitric oxide synthase 2 (NOS2 or iNOS) is a short-lived metabolic product that was demonstrated to regulate $CD4^+$ and $CD8^+$ T cell proliferation (Lukacs-Kornek et al. 2011). The combination of IFN-γ and TNF-α secreted by activated T cells elevated the levels of NOS2 and the immune checkpoint molecule indoleamine 2,3-dioxygenase (IDO) in primary LECs. Co-culture of wild-type LECs and IFN-γ-deficient splenocytes restored T cell proliferation suggesting IFN-γ is essential for NOS2 production.

In addition, co-culture of NOS2-deficient LECs with wild-type splenocytes ablated the immunosuppressive effect.

LECs have been demonstrated to induce peripheral tolerance of $CD8^+$ T cells along with other lymph node stromal cells (Nichols et al. 2007; Cohen et al. 2010; Lund et al. 2012; Tewalt et al. 2012; Hirosue et al. 2014). VEGF-C-activated LECs in B16 melanoma and LECs under steady-state conditions can scavenge and cross-present exogenous antigen through MHC class I, leading to dysfunctional activation of antigen-specific $CD8^+$ T cells (Lund et al. 2012; Hirosue et al. 2014). LN-LECs express endogenous peripheral tissue antigens (PTAs) that are independent of autoimmune regulator (AIRE) including tyrosinase (Nichols et al. 2007; Cohen et al. 2010). Direct presentation to tyrosinase-specific $CD8^+$ T cells led to their deletion (Nichols et al. 2007; Cohen et al. 2010). It is suggested that viral antigens are "archived" in LECs following viral infection for at least three weeks but are not presented by LECs (Tamburini et al. 2014). These antigens are transferred to DCs for cross-presentation to T cells in order to maintain memory $CD8^+$ T cell responses when the lymphatic endothelium contracts following lymphoangiogenesis.

Notably, LEC express PD-L1 and induce peripheral deletion of $CD8^+$ T cells mediated via PD-1/PD-L1 pathway (Fletcher et al. 2010; Cohen et al. 2014; Tewalt et al. 2012; Hirosue et al. 2014; Rouhani et al. 2015). Murine LECs from the LN can express PD-L1 after polyI:C stimulation (Fletcher et al. 2010). PD-L1 is expressed higher in LECs of the LN than peripheral tissues such as the diaphragm, colon or liver (Cohen et al. 2014; Michonneau et al. 2016). Radioresistant LECs could induce deletional tolerance to tyrosinase-specific $CD8^+$ T cells through a lack of 4-1BBL (CD137) co-stimulatory molecule expression, which resulted in the upregulation of PD-1 expression (Tewalt et al. 2012). As a consequence, PD-1/PD-L1 engagement blocked upregulation of IL-2R on CD8 T cells, necessary for survival. Blockade of PD-1 rescued $CD8^+$ T cells from deletion. Furthermore, LECs can present endogenous β-galactosidase (β-gal) antigen via MHC class I to β-gal-specific $CD8^+$ T cells and induce deletion through the PD-1/PD-L1 pathway (Rouhani et al. 2015).

LECs may act as non-professional antigen-presenting cells, LECs express MHC class II after activation and in some cases carry the capacity to acquire peptide-antigen for cross-presentation (Malhotra et al. 2012; Nörder et al. 2012; Baptista et al. 2014; Dubrot et al. 2014; Rouhani et al. 2015). LPS, ovalbumin and IFN-γ stimulation of human or murine LECs have been shown to induce MHC class II expression (Malhotra et al. 2012; Nörder et al. 2012). LECs were shown to present self-antigen to both OVA-specific $CD8^+$ OT-I and $CD4^+$ OT-II T cells *in vitro* which increased CD25 expression (Baptista et al. 2014). In contrast to the previous report, murine DCs can transfer functional peptide-loaded MHC

class II complexes to LECs under steady state conditions *in vitro* in mainly a cell-cell contact-dependent manner to promote $CD4^+$ T cell apoptosis (Dubrot et al. 2014). Additional evidence have suggested that LEC indirectly induce $CD4^+$ T cell anergy by transfer of PTAs to DCs (Rouhani et al. 2015). Moreover, LN-LECs were shown to express MHC class II molecules *in vivo* either through endogenous expression or from acquisition. LEC MHC class II was demonstrated to directly induce tolerance of β-gal-specific $CD8^+$ T cells via the lymphocyte activation gene 3 (LAG-3)/MHC class II immune checkpoint pathway. LECs were unable to directly present β-gal to MHC class II because they lack HLA-DM, which is required for loading of peptide to MHC class II (Rouhani et al. 2015). The mechanism of antigen transfer from LEC to DCs requires further clarification. The transfer of antigens from LECs to DCs could potentially pass through exosomes, gap junctions or DC phagocytosis of excess LEC generated by lymphangiogenesis or undergoing apoptosis (Randolph et al. 2017).

Inflammatory activation of the lymphatic system induces lymphatic remodelling in both peripheral tissues and in LNs (Kim et al. 2014). The main pathways that regulate inflammation-induced lymphangiogenesis include VEGF-C/VEGFR3 and VEGF-A/VEGFR2 signalling (Tammela & Alitalo 2010). Lymphangiogenesis is induced by the upregulation of VEGF-A, -C and -D from macrophages during acute inflammation of the skin or chronic infection of the airway, to facilitate antigen clearance and prevention of lymphedema (Baluk et al. 2005; Kataru et al. 2009). Overexpression of VEGF-C was demonstrated to restore lymphatic vessels during chronic skin inflammation (Huggenberger et al. 2010). In addition, treatment of inflamed skin with VEGF-C initiated LECs to generate anti-inflammatory prostaglandin synthase, leading to increased IL-10 on DCs and suppression of DC maturation (Christiansen et al. 2016). Production of VEGF can be enhanced by B cells in order to facilitate the growth of LN lymphatic vasculature and upregulate the trafficking of DCs to the LN (Angeli et al. 2006). In contrast, T cell production of IFN-γ can suppress the sprouting of LN lymphatic vasculature *in vivo* and suppress the expression of key LEC lineage factors PROX1, LYVE-1 and podoplanin *in vitro* in a mechanism that is JAK/STAT-dependent (Kataru et al. 2011). IFN-γ knockout mice express a higher baseline of lymphatic vasculature in the LN. During acute skin inflammation, the levels of PROX1, VEGFR3 and LYVE-1 are suppressed (Vigl et al. 2011; Huggenberger et al. 2011). In human dermal LECs, TNF-α stimulation or TGF-β can lead to reduced PROX1 and LYVE-1 expression (Johnson et al. 2007; Oka et al. 2008). In contrast, studies in a murine peritonitis model have indicated that NF-κB induction of PROX1 and VEGFR3, increased the sensitivity of pre-existing lymphatic vessels to leukocytes expressing VEGF-C and VEGF-D (Flister et al. 2010). Moreover, IL-3 can upregulate the

expression of PROX1 and podoplanin, which indicates that IL-3 is important for the maintenance of LEC phenotype *in vitro* (Gröger et al. 2004).

1.4.3 microRNA regulation in LECs

Several miRNAs have emerged as key determinants of LEC differentiation and inflammatory responses. miRNA biogenesis are crucial for vertebrate development and tissue-specificity of miRNAs has been found in angiogenesis in mice and human studies (Bernstein et al. 2003; Yang et al. 2005; Kuehbacher et al. 2007; Suárez et al. 2007). Deletion of Dicer in mice leads to improper vascular formation and maintenance, consequently results in embryonic lethality (Bernstein et al. 2003; Yang et al. 2005). Key vascular and growth factors such as TIE1, FLT1 (encoding for VEGFR1), KDR (encoding VEGFR2), ANG-1 and PTEN are significantly dysregulated in Dicer mutant embryos and HUVECs (Yang et al. 2005; Suárez et al. 2007). Of note, in human studies, knockdown of Dicer resulted in significant but not complete loss of mature miRNA expression suggesting the long half-life of endogenous miRNAs (Kuehbacher et al. 2008; Suárez et al. 2007).

A key miRNA in the normal function of endothelial cells is miR-126, which mediates maintenance and angiogenesis of vascular integrity (Harris et al. 2008; Wang et al. 2008; Fish et al. 2008; Pedrioli et al. 2010). Loss of miR-126 results in leaky vessels and embryonic lethality in a subset of mutant mice (Wang et al. 2008). The remaining mice survived to adulthood but were prone to defective cardiac rupture. Possible targets of miR-126 include sprout-related protein-1 (SPRED-1) and VCAM-1 in human and murine cells. VCAM regulates leukocyte adherence and contributes towards vascular inflammation (Harris et al. 2008). On the other hand, SPRED-1 is an inhibitor of angiogenic and MAP kinase signalling that regulates the expression of pro-angiogenic genes VEGF and fibroblast growth factor in mice (Wang et al. 2008). Moreover, VEGF induces miR-132 and promotes angiogenesis by suppressing p120RasGAP in human vascular endothelial cells (Anand et al. 2010). Anti-miR-132 was shown to inhibit angiogenesis and decrease tumour burden in a mouse model of human breast carcinoma. Activated LECs can be regulated by the microRNA biogenesis machinery (Leonov et al. 2015). An auto-regulatory feedback mechanism links AGO2 suppression by miR-132 to the regulation of the miR-221 and miR-146, which are involved in angiogenic and inflammatory responses, respectively.

Studies have identified the role of miRNA regulation in LEC lineage commitment. PROX1 has a long 3'-UTR (5.4kb) that is conserved among vertebrates (Yoo et al. 2010). The length of the 3'-UTR suggests that PROX1 expression may be posttranscriptionally regulated by miRNAs. Whereas, SOX18 has a short 3'-UTR (585bp) and less likely to have many miRNA binding sites. The characterisation of miRNAs in human LECs and BECs has led to

the finding that BEC miRNA signatures can regulate lymphatic development (Pedrioli et al. 2010). Overexpression of miR-31 was demonstrated to repress LEC-signature genes including FOXC2. PROX1 is regulated by both miR-31 and miR-181a and consequently repress LEC-specific genes, including VEGFR3, and development of vasculature in embryonic LECs (Pedrioli et al. 2010; Kazenwadel et al. 2010). In addition, signalling from bone morphogenetic protein (BMP) 2, a member of the TGF-β family, can inhibit PROX1 expression and lymphatic differentiation during development of zebrafish and mice (Dunworth et al. 2014). Moreover, signalling from BMP2 increased the expression of: miR-92a, miR-99a, miR-186, miR-194, and also of miR-31 and miR-181a (Dunworth et al. 2014). SMAD4 deletion by siRNA reduced the expression of miR-31 and miR-181a, suggesting BMP2 signalling acts as a negative regulator of LEC identity (Dunworth et al. 2014). In addition, PROX1 expression can be suppressed by miR-466 in human dermal LECs and both miR-181a and miR-466 were shown to inhibit corneal lymphangiogenesis in rats (Seo et al. 2015).

A substantial understanding of gene regulation in LECs comes from Kaposi's sarcoma (KS), a tumour of LEC origin and is the most common cancer in untreated HIV-positive patients (Cancian et al. 2013). Both LECs and BECs can be infected by Kaposi's sarcoma-associated herpesvirus (KSHV) and in doing so induces transcriptional reprogramming, giving rise to assorted phenotypes of LECs and BECs (Hong et al. 2004; Wang et al. 2004). KS resembles a LEC-like phenotype and occurs at sites rich in LECs such as LNs, skin and mucosa (Wang et al. 2004). Infection of human LECs by KSHV induces an initial anti-viral miRNA response from miR-132 and miR-146a and suppression of these miRNAs inhibits viral gene expression (Lagos et al. 2010). Overexpression of miR-132 negatively regulates inflammation by targeting the expression of IFN-β and interferon-stimulated gene 15 (ISG15). KSHV infection regulates the interferon response by interaction of miR-132 and the transcriptional co-activator p300. Moreover, KSHV can determine endothelial cell motility by downregulating the miR-221/miR-222 cluster and upregulating miR-31 (Wu et al. 2011). It is possible that upregulation of miR-31 may regulate PROX1 during KSHV infection but this remains unknown. Kaposin B, a KSHV latent gene, was found to stabilize PROX1 mRNA and drive lymphatic reprogramming of BECs (Yoo et al. 2010). Other KSHV targets include c-MAF, which represses BEC-specific identity in human LECs, and is downregulated throughout viral infection (Hansen et al. 2010; Hong et al. 2004). The KSHV orthologue of miR-155 was identified to be miR-K12-11 (Gottwein et al. 2007), which was demonstrated to regulate MAF in human LECs (Hansen et al. 2010).

In addition, rat mesenteric LECs have shown a distinct miRNA signature after TNF-α stimulation (Chakraborty et al. 2015). Numerous miRNAs involved in angiogenesis,

endothelial cell growth and migration were induced while miRNAs connected with cell survival and proliferation were suppressed after 24 or 96 h stimulation. NF-κB is a downstream effector of TNF-α signalling of which miR-9 was induced and also shown to directly target and regulate TNF-α-mediated inflammatory mechanisms. Furthermore, overexpression of miR-9 upregulates the expression of VEGFR3 and tube formation, suggesting a possible role in lymphangiogenesis. VEGFR3 was also demonstrated to be regulated by miR-1236, a mirtron generated from a spliced intron that is independent of Drosha processing in human LECs (Jones et al. 2012).

LECs have much heterogeneity throughout the body, including organ-specific functions (Ulvmar & Mäkinen 2016). There is evidence that the plasticity of LECs is under miRNA regulation and facilitates the swift response of lymphatic endothelium to inflammatory and angiogenic stimuli. Studying miRNAs in different types of lymphatic vessels and niches, such as the skin or LN will facilitate our knowledge in their contribution towards inflammation and peripheral tolerance.

1.5 Fibroblasts

Fibroblasts are a class of stromal cells that consist of a heterogeneous and quiescent population (Van Linthout et al. 2014). Typically, fibroblasts maintain the structural framework and remodel the extracellular matrix (ECM) of local tissues in order to manage the mechanical stress (Turley et al. 2015). The ECM structures allow similar cells to connect and interact with each other with a common biological function (Kendall & Feghali-Bostwick 2014). These structural scaffolds are important for tissue regeneration in wound healing, creating boundaries between epithelial and endothelial tissues as well as protecting against the migration and invasion of cancer cells. Fibrosis is a process where excess ECM proteins are deposited due to the activation and accumulation of fibroblasts, leading to scarring of tissue (Turley et al. 2015). Consequently, tissues or organs can become dysregulated in structure and function and in essence, fibrosis is an exaggeration of the wound healing response. Fibroblast characteristics can vary between tissues and from cellular origin, where cells can have a type of positional memory (Van Linthout et al. 2014). Primarily, fibroblasts are formed from primary mesenchymal cells but in some cases from transition of epithelial or endothelial to mesenchymal or from circulating mesenchymal stromal cells and fibrocytes (Van Linthout et al. 2014). These include tumour- or cancer-associated fibroblasts (TAFs/CAFs, referred to as CAFs from hereby) that promote tumour growth and resistance to therapy as well as influencing the immune response within the tumour microenvironment (Bussard et al. 2016). Fibroblasts are not a cell type that is terminally differentiated and have the plasticity to be differentiated into subtypes of fibroblast-like cells (Kendall & Feghali-Bostwick 2014). Myofibroblasts which are essential

for the wound healing response can differentiate into various other cells such as epithelial cells, endothelial cells, pericytes or even monocytes.

1.5.1. Fibroblasts in the inflammatory response

Like LECs, fibroblasts are also an active player of the immune system in addition to its structural role. Fibroblasts are highly responsive to components of innate and adaptive immunity, including cytokines, chemokines and growth factors (Van Linthout et al. 2014). Activated macrophages produce TGF-β, TNF-α and IL-1 which have been demonstrated to stimulate fibroblast secretion of ECM products (Sica & Mantovani 2012; Sullivan et al. 2009). TNF-α and TGF-β knockout mice fail to develop fibrosis in the lungs and it is thought that TNF-α induction of TGF-β via AP-1 is required for the appearance of pulmonary fibrosis (Sullivan et al. 2009). Moreover, fibroblasts are responsive to prostaglandins and leukotrienes that can enhance or inhibit the fibrotic response through modulation of fibroblast proliferation and collagen or matrix production (Kendall & Feghali-Bostwick 2014).

Fibroblasts modulate the behaviour of immune cells in the local environment by conditioning the cellular and cytokine microenvironment (Van Linthout et al. 2014; Turley et al. 2015). Similar to LECs, fibroblasts also express chemokines MCP-1, MIP-1, RANTES and IP-10 which can modulate the immune landscape of T cells, B cells and macrophages or have paracrine effects on other fibroblasts (Gharaee-Kermani et al. 1996; Turley et al. 2015). Activation of fibroblasts by MCP-1 was shown to lead to elevation of collagen expression and TGF-β secretion (Gharaee-Kermani et al. 1996). TGF-β has effects on the regulation of development and function of all immune cell types (Barnas et al. 2010). As well as the ability to induce oncogenic transformation of fibroblasts (Kendall & Feghali-Bostwick 2014). Moreover, stromal fibroblasts can modulate endothelial cell recruitment of lymphocytes and response to cytokines (McGettrick et al. 2009). This depended on whether the fibroblast was activated or not. Dermal fibroblasts from non-inflamed tissue were able to modulate the capacity of IFN-γ and TNF-α-activated HUVECs to recruit circulating lymphocytes, whereas fibroblasts from chronic inflamed tissue induced lymphocyte adhesion. IL-6 was found to have opposing effects, in the presence of IFN-γ and TNF-α, IL-6 inhibited the effects of fibroblast and TGF-β. Furthermore, fibroblasts can form physical interactions between leukocytes, with expression of CD40 on its cell surface (Yellin et al. 1995). IFN-γ upregulates CD40 on fibroblasts, whereas TNF-α has minimal effects. T cell and fibroblast CD40L-CD40 interactions induce VCAM-1 and ICAM-1 expression on fibroblasts as well as augmenting the production of IL-6 to enhance proliferation of fibroblasts.

Dermal fibroblasts were demonstrated to express PD-L1 upon IFN-γ activation, whereas IL-1β and TNF-α did not (Lee et al. 2005). Further investigation revealed that a putative NF-κB binding site in the PD-L1 promoter of the 5'-UTR played a large role in IFN-γ-mediated PD-L1 induction. IFN-γ stimulation of the ERK and PI3K pathway were then shown to activate NF-κB activity and inhibition of either pathway repressed some PD-L1 expression (Lee et al. 2005). Gut stromal myofibroblasts and fibroblasts were revealed to express PD-L1 and PD-L2 and contribute to regulation of $CD4^+$ T helper cell proliferation (Pinchuk et al. 2008). In addition, simultaneous blockade of PD-L1/2 partially rescued T cell proliferation. Furthermore, dermal fibroblasts were able to mediate suppression of allogeneic T cell activation through IFN-γ-mediated IDO secretion (Haniffa et al. 2007). IDO typically inhibits tryptophan accumulation and limits growth and survival of cells. Suppression of T cells was partly reversed by the addition of L-tryptophan. Murine mesenchymal stem cells (MSCs) which are fibroblast-like cells were shown to express PD-L1, IDO and prostaglandin E2 (PGE-2) after IFN-γ and TNF-α activation (English et al. 2007). Furthermore, MSCs were demonstrated to modulate the pro-inflammatory environment of allogeneic immune responses which was widely dependent on IFN-γ signalling.

CAFs are one of the most abundant stromal populations in the tumour microenvironment and can promote inflammation through the release of inflammatory cytokines (Bussard et al. 2016). IL-6 is a key regulator for the transition from normal fibroblasts to CAFs in prostate cancer (Giannoni et al. 2010). In addition, IL-6 stimulates the secretion of matrix metalloproteinases (MMPs) from activated fibroblasts to influence EMT of prostate cancer cells. Co-cultures of CAFs and tumour-associated T cells were demonstrated to both enhance and suppress the function of T cells responding to stimulation (Nazareth et al. 2007). In addition, CAFs were shown to express PD-L1 and PD-L2 in NSCLC and demonstrated that some CAFs elicited a suppressive effect on tumour-associated T cells via the PD-1/PD-L1 or PD-L2 pathway (Nazareth et al. 2007). CAFs from murine lung tumours can directly interact with $CD8^+$ T cells in an antigen-dependent manner via PD-L2 and Fas ligand (FasL) and induce T cell suppression (Lakins et al. 2018). PD-L2 ligation to PD-1 and FasL to Fas drove the death and dysfunction of tumour specific T cells. No significant change was observed with PD-L1 due to the lack of expression on the CAFs that were tested.

In rheumatoid arthritis (RA), where progressive joint damage is a result of aggressive proliferation of the synovial membrane (Miranda-Carus et al. 2004). Synovial and dermal fibroblasts express IL-15 on the cell surface which can enhance the secretion of cytokines, such as IFN-γ and TNF-α, and proliferation of T cells through direct cell contact independent of antigen recognition (Miranda-Carus et al. 2004; Rappl et al. 2001).

Overall, these studies show that these heterogeneous fibroblasts express a diverse repertoire of receptors, ligands including PD-L1, and secrete cytokines and chemokines that allow them to modulate both activation and inhibition of the local immune environment.

1.5.2. microRNA regulation in fibroblasts

Cancer cells have been shown to influence the transition from normal fibroblasts to CAFs. Microvesicles containing miR-155 that are derived from murine pancreatic cancer cells have been shown to induce the conversion of fibroblasts into CAF-like cells *in vitro* (Pang et al. 2015). Moreover, miR-31 and miR-214 were found downregulated while miR-155 was upregulated when comparing CAFs to normal fibroblasts in ovarian cancer patients (Mitra et al. 2012). Further investigation demonstrated that these miRNAs facilitate the conversion to CAFs through transfection of anti-miR-31, anti-miR-214 and pre-miR-155. This conversion could be reversed by performing the opposite experiment and led to reduced migration and invasion of co-cultured ovarian cancer cells (Mitra et al. 2012).

1.6 Summary of introduction

PD-1/PD-L1 immunotherapy has revolutionised current treatments for cancer and PD-L1 expression may serve as a biomarker. However, the complex regulation of PD-L1 has introduced resistance mechanisms to therapy. Thus, an increase depth of knowledge in the basic biological roles of these immune checkpoints can provide rational for development of new immunotherapies and combinations (Wei et al. 2018). PD-L1-positive cancer patients respond better to PD-1/PD-L1 therapy but there are also a subset of tumour PD-L1-negative responders (Sunshine & Taube 2015). One possibility is the role of host PD-L1 expression on stromal/vascular cells that cannot be ignored. Further understanding is required to appreciate the contribution of these cells towards regulation of the local immune response in both physiological and pathological contexts. In addition, the difference in the amount of studies in PD-L1 between non-transformed cells and cancer cells suggests that there is still a large amount of knowledge to be covered within normal physiological environments. These studies can also facilitate our awareness in the minimisation of immune-related adverse effects especially in the context of combination therapies. Such immune-related adverse effects refers to events of autoimmune origin that can affect almost any organ system and are relatively common in patients treated with immune checkpoint inhibitors (estimated 30% with anti-PD-1/PD-L1 therapies) (Calabrese et al. 2018). Checkpoint therapy is connected with revitalising T cell phenotype to become more active which is shown by the increased production of inflammatory cytokines. Anti-PD-1 therapy is commonly associated with hypothyroidism which is rarely seen in patients given anti-CTLA-4 drugs, meaning that adverse events can be associated with the pathways targeted (June et al. 2017).

miRNAs have been demonstrated to regulate a variety of inflammatory responses in a broad range of cell types, and miRNA expression can be highly tissue-specific. Changes in levels of inflammatory-related miRNAs could facilitate our understanding in the modulation of immune pathways (Paladini et al. 2016). IFN-γ is a major inducer of PD-L1 expression and downstream signalling has been shown to affect miRNA-mediated suppression of PD-L1 (Figure 1.4). In addition, miRNA-based signatures could serve as an approach to predict immune-related adverse events and as a biomarkers of therapeutic response. There is still a large gap for additional inflammatory miRNA networks that regulate PD-L1, particularly in non-transformed cells, awaiting to be revealed.

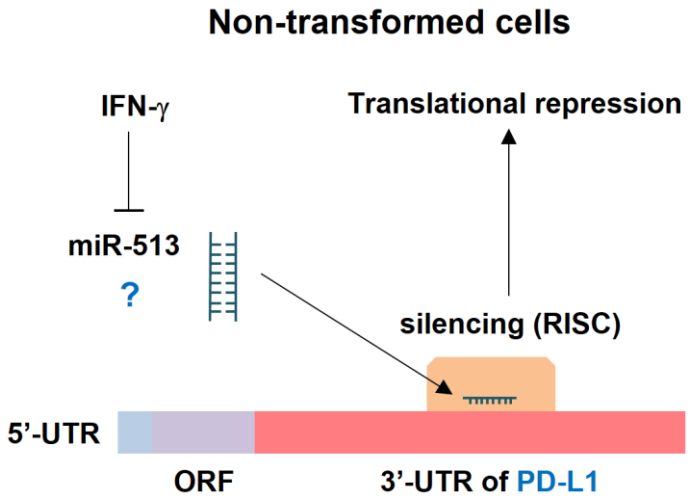

Figure 1.4. **IFN-γ signalling influences miRNA regulation of PD-L1.** IFN-γ is a major inducer of PD-L1 expression. In cholangiocytes, miR-513 was shown to suppress PD-L1 expression by directly binding to the 3'-UTR (Gong et al. 2009). IFN-γ was demonstrated to block the levels of miR-513, thereby enabling PD-L1 expression. Only one miRNA that interacts with PD-L1 has been shown to be regulated through IFN-γ signalling and it is likely that there are many more miRNAs to be identified due to the importance of the induction of PD-L1 by IFN-γ.

1.7 Thesis aims and hypotheses

This thesis aims to determine posttranscriptional regulation of PD-L1 by miRNAs in primary HDLECs, fibroblasts and cancer cells, and to elucidate this mechanism. In addition, to determine whether this mechanism is differentially controlled under inflammatory conditions when PD-L1 is induced and to develop a functional assay to test these findings.

Hypothesis: Expression and function of PD-L1 in stromal, vascular and cancer cells is posttranscriptionally regulated by inflammatory-driven microRNAs.

Aims:

- To characterise PD-L1 expression and under inflammatory conditions, using inflammatory mediators IFN-γ and TNF-α (Chapter 3).
- To determine the dynamics of the microRNA landscape in vascular and stromal cells exposed to inflammatory stimuli (Chapter 3).
- To investigate the effect of inflammatory-altered microRNAs on regulation of PD-L1 expression (Chapter 3).
- To compare microRNA-mediated mechanisms of PD-L1 expression between primary stromal cells and human cancer cell lines (Chapter 4).
- To develop a co-culture model that can be used to functionally test the relevance of the above findings, particularly the mechanism of a miRNA/PD-L1 regulatory loop (Chapter 5).
- To determine whether PD-L1 expression or signalling affects miRNA regulatory loops (Chapter 6).

2. Materials and Methods

2.1. Cell culture

All cultured cells were incubated at 37°C in a humidified atmosphere of 5% CO_2. Primary human dermal lymphatic endothelial cells (HDLECs) originating from an adult donor were purchased from Promocell (C-12219) and grown in endothelial cell growth media MV (Promocell, C-22020) supplemented with 10 ng/ml vascular endothelial growth factor C (VEGF-C) (R&D). Culture media was replaced every 48 h. HDLECs were cultured from passage 1 and split when 80-90% confluent using a 1:5 solution of trypsin-EDTA (Gibco) and PBS (Gibco). HDLECs were pelleted by centrifugation for 5 min at 259 x g. HDLECs were seeded at 500,000 cells per 100 mm (diameter) dish (Corning). At passage 4, HDLECs were cryopreserved in a 1 ml mixture of 10% dimethyl sulfoxide (DMSO) and fetal calf serum (FCS) (Hyclone). All experiments with HDLECs were performed at passage 5. Primary human foreskin fibroblasts (HFFs) of passages around 8-10 were obtained from frozen stocks in the Lagos lab. HFFs were grown in 100 mm dishes with Dulbecco's Modified Eagle Medium (DMEM) (Gibco) supplemented with 10% FCS, 1% L-glutamine and 1% pen/strep. Adherent cancer lines were grown in either 100 mm dishes or T75 flasks, all with Dulbecco's Modified Eagle Medium (DMEM) (Gibco) supplemented with 10% FCS, 1% L-glutamine and 1% pen/strep. The cells include lung cancer lines: A549, H838, HCC193, H1299, H358M and Hop62; breast cancer line: MDA-MB-231 and renal clear cell carcinoma lines: RCC4, RCC4 transfected with vector alone (RCC4-EV) and RCC4 transfected with VHL (RCC4 +VHL). All adherent cultured cells (exception being HDLECs) were split with trypsin-EDTA (0.25%) and pelleted by centrifugation for 5 min at 259 x g. Wild-type Jurkat T cells (E6-1) were a kind gift from Nathalie Signoret (University of York). Jurkat cells in suspension were grown in T75 flasks (Corning) containing Roswell Park Memorial Institute (RPMI) 1640 media (Gibco), supplemented with 10% FCS, 1% L-glutamine and 1% pen/strep. A modified Jurkat T cell line overexpressing PD-1 and harbouring a luciferase reporter construct under the control of a NFAT promote was generously donated by Grzegorz Dubin (Jagiellonian University, Poland). PD-1 NFAT-Luc Jurkat cells were cultured in RPMI 1640 media, supplemented with 10% FCS, 1% L-glutamine, 1% pen/strep and in constant presence of hygromycin B (50 μg/ml) and G418 (250 μg/ml) to maintain stable expression of transduced constructs. Hygromycin B and G418 were omitted from experiments. All Jurkat cell types were pelleted by centrifugation for 5 min at 162 x g.

2.2. Reagents

Human recombinant IFN-γ was obtained from Peprotech and used at 1000 U/ml. TNF-α was purchased from R&D was used at 25 ng/ml. Recombinant human PD-L1 Fc was acquired from R&D. Nivolumab or anti-hPD1-Ni-hlgG4 (S228P) was purchased from InvivoGen. AlamarBlue reagent was obtained from ThermoFisher Scientific.

2.3. RNA interference and miRNA inhibitors and mimics

Cells were seeded one day before transfection. A transfection mixture was prepared using Opti-MEM reduced serum medium with the GlutaMAX supplement (Gibco) and TransIT-siQUEST (Mirus Bio). The following nucleic acids (all from Dharmacon) were formulated with the transfection mixture: miRIDIAN hsa-miR-155-5p mimic (25-50 nM), hsa-miR-155-5p hairpin inhibitor (50-100 nM) based on the mature hsa-miR-155-5p sequence (5'-UUAAUGCUAAUCGUGAUAGGGGU-3') or siRNAs targeting PD-L1 (50 nM, On-TargetPlus Smartpool). All experiments utilized respective negative controls, for miRNAs this was based on mature sequences from *c. elegans* (i.e. cel-miR-67), or control siRNAs that have minimal targeting of human, mouse or rat genes, tested by the manufacturer (Dharmacon). 1 ml of media of which the cells are typically grown in was added 5 to 6 h posttransfection. The following day, cells were given fresh media and left to recover. 48 h posttransfection, cells were stimulated with IFN-γ and TNF-α for 24 h and further experimental analysis.

2.4. RNA isolation, cDNA synthesis and qRT-PCR

Total RNA was isolated based on the manufacturer's instructions for the miRNeasy Kit (Qiagen). In addition, extra RNA spin columns (NBS Biologicals, SD5008) and 1.5 ml RNase-free tubes (Appleton Woods) were purchased and used alongside pre-made concentrated buffers from the Qiagen kit. All samples for RNA isolation had 700 µl of QIAzol added to lyse the cells. Nucleic acids were separated from proteins and lipids by phenol-chloroform extraction. Subsequently, RNA was eluted in 30 µl RNase-free H_2O and purity was analysed on the NanoDrop ND 2000 (ThermoFisher Scientific) according to the A260/A280 ratio. An absorbance measurement of >2.0 is generally accepted for 'pure' RNA. Quantitative RT-PCR (qRT-PCR) was performed in a two-step manner.

Isolated RNA was first processed for either mRNA cDNA synthesis with either polyadenylated or random hexamer primers or microRNA (miRNA) cDNA synthesis using TaqMan primers. For mRNA cDNA synthesis with polyadenylated RNA of one sample, 1 µl of RNA (typically between 50-200 ng/µl) was combined with 0.75 µl anchored oligo(dT)23 primers (5 µM) (Sigma), 1 µl of dNTP (10 mM) (ThermoFisher Scientific) and made up to 12 µl with RNase-free H_2O (Qiagen). The reaction mixture was incubated at 70°C for 6 min

on Thermal Cycler 7500 system (Bio-Rad). After, the reaction mixture was combined with 4 µl 5x First-Strand buffer (Invitrogen), 2 µl DTT (0.1 M), 1 µl RNase OUT recombinant ribonuclease inhibitor (40 U, Invitrogen) and 1 µl SuperScript II Reverse Transcriptase (200 U, Invitrogen). The sample mix was placed on a thermal cycler at 42°C for 1 h and 70°C for 10 min (to inactivate reverse transcriptase) before being cooled on ice.

For mRNA cDNA synthesis with random hexamers of one sample, 1 µl of RNA was added to 1 µl of random hexamer primer (50 ng/µl, ThermoFisher Scientific), 1 µl of dNTP (10 mM) and made up to 12.5 µl with RNase-free H_2O. The reaction mix was incubated at 70°C for 6 min on a thermal cycler. Subsequently, the reaction mixture was combined with 4 µl 5x First-Strand buffer, 2 µl DTT (0.1 M), 1 µl RNase OUT (40 U) and 1 µl SuperScript III Reverse Transcriptase (200 U, Invitrogen). Samples were incubated at 25°C for 10 min, 50°C for 50 min and 85°C for 5 min (to inactivate the reverse transcriptase) before being cooled on ice.

miRNA cDNA synthesis was made using the TaqMan miRNA Reverse Transcription Kit (Applied Biosystems). 5 µl RNA (typically between 1-5 ng/µl) was mixed with 0.15 µl dNTP, 1.5 µl buffer, 0.19 µl RNase inhibitor, 0.5 µl reverse transcriptase, 0.5 µl TaqMan primer for specific miRNA and made up to 15 µl with RNase-free H_2O. The mixture was added to a thermal cycler and a program set for incubation at 16°C for 30 min, 42°C for 30 min and 85°C for 5 min (to inactivate the reverse transcriptase). All cDNA products were stored at -20°C until further use.

qRT-PCR was performed to determine expression of levels of mRNA, using SYBR Green Master Mix (Applied Biosystems) and mature miRNA using commercially available primers (Applied Biosystems). Primers were used at a final concentration of 300 nM in a 20 µl reaction. qRT-PCR runs were done on a StepOnePlus Real-Time PCR system (Applied Biosystems) with a default program of 40 cycles of amplification. Relative gene expression was calculated by the comparative CT method. This involved using GAPDH or β-actin as housekeeping genes for mRNA expression and U6 snRNA as a loading control for mature miRNAs.

Table 2.1. Primers for SYBR Green qRT-PCR

Target mRNA (human)	**Forward primer (5'-3')**	**Reverse primer (5'-3')**
CD274 (PD-L1)	CATCTTATTATGCCTTGGTGTAGCA	GGATTACGTCTCCTCCAAATGTG
PDCD1 (PD-1)	TGCGGACTACAAGCGAATCA	GATCCACGGAAATTCTCTGGTT
IL-1β	AGGATGACTTGTTCTTTGAAGCTGA	TGCCTGAAGCCCTTGCTG
IL-2	GAATCCCAAACTCACCAGGATGCTC	TAGCACTTCCTCCAGAGGTTTGAGT
ActB (β-actin)	CACCATTGGCAATGAGCGGTTC	AGGTCTTTGCGGATGTCCACGT
CD47	GGCAATGACGAAGGAGGTTA	ATCCGGTGGTATGGATGAGA
Vegfr2	CAGAATCCCTGCGAAGTACCTT	GTCAGTACATGCCCCGCTTTAA
Vegfr3	AGTACATCAAGGCACGCATCGA	ACCAAGAGCGTGTCAGGCTTGT
Prox1	CCCAGGACAGTTTATTGACCGA	GGTTGTAAGGAGTTTGGCCCAT
NR2F2 (COUP-TFII)	CACCGTCTCCTCCTCAGTCA	CATATCCCGGATGAGGGTTTC

2.5. PCR and agarose gel electrophoresis

A total of 300-500 ng/µl purified RNA was reverse transcribed to cDNA using random hexamer primers (described above). 1 µl cDNA (typically estimated to be 100 ng/µl) was combined with 10 µl 5X colourless GoTaq Flexi buffer (Promega), 2 µl $MgCl_2$ (25 mM, Promega), 1 µl dNTP (10 mM), 2.5 µl upstream primer, 2.5 µl downstream primer, 0.25 µl GoTaq (5 U/µl) Promega) and made up to 50 µl with RNase-free H_2O. The mixture was added to a thermal cycler which was programmed to run at 95°C for 2 min (initial denaturation), 95°C for a further 30 s (Step 2, denaturation), 57.5°C for 30 s (annealing, which was decreased by 1°C per every cycle, based on touchdown PCR (Korbie & Mattick 2008)), 72°C for 3 min (extension) and repeated from Step 2 (inclusive) for a further 9 cycles. Then samples were incubated at 95°C for 30 s (Step 5, denaturation), 47°C for 30 s (annealing), 72°C for 3 min (extension) and repeated from Step 5 (inclusive) for a further 24 cycles. A final extension at 72°C for 5 min was added and PCR products were incubated at 4°C prior to use. For agar gel electrophoresis, a 1% agar solution was made using Tris-acetate-EDTA (TAE) buffer and ethidium bromide was added to a final concentration of 0.8

μg/ml. 6X purple loading dye, no SDS (New England Biolabs) was added to each PCR product and loaded on to the agar gel which was ran at 140V for 30-40 min. Subsequently, DNA was detected using ultraviolet light and the brightness/contrast ratio was processed through GeneSnap software (Syngene).

Table 2.2. Primers for PCR of CD274 (PD-L1) 3'-UTR

PD-L1 3'-UTR sites	**Forward primer (5'-3')**	**Reverse primer (5'-3')**
Full length (2671 bp)	GATACACATTTGGAGGAG ACG	AATGGACATGCTGGTGTA CC
miR-155 binding sites (2nd half, 1446 bp)	GGAGGAAATAGGCCAAT GTG	AATGGACATGCTGGTGTA CC

2.6. Small RNA sequencing

RNA were isolated and enriched for small RNA using the PureLink miRNA isolation kit (Ambion). RNA integrity was assessed using the Agilent 2100 Bioanalyzer (Agilent Technologies). Sequencing libraries were generated using NEBNext Multiplex Small RNA Library Prep Set for Illumina (Set 1) (New England Biolabs) according to the manufacturer's instructions (performed by the Genomics lab at the Technology Facility, University of York). Samples were sequenced using Illumina MiSeq (pair ended, 75 bp, MiSeq v3). Sequencing reads were examined for quality and mapped against all annotated human mature and precursor miRNA sequences (miRBase version 21.0). Residual adapter sequences and indexes were removed with Cutadapt (version 1.8.3), in paired-end mode, first trimming any low-quality ends with a cutoff of Q10 (-q 10), then removing flanking Ns (--trim-n) and any reads with >20% Ns (--max-n 0.2). Reads were quality trimmed with Sickle (version 1.330), with a cutoff of >Q20 (-q 20), and truncating at the position of the first N (-n). Reads were mapped with Bowtie (version 1.0.1) with a seed length of 15 (-l 15), a maximum total quality score at mismatched positions of 99999 (-e 99999), reporting all valid alignments per read or read pair (-a) and the --best option to pick the best reported alignments. Reads were mapped separately for merged reads and a concatenated file of unmerged forward and reverse reads. Reads were counted using Subread featureCounts (version 1.5.0-p1), with a minimum fragment length of 5 (-d 5). Reads were counted against all features in the HsGRCh38 GFF file as well as against features from mirBASE release 21. Counts for the mapped merged reads were doubled and then added to the counts for the mapped unmerged reads. Duplicate features, i.e. those with identical numbers of mapped reads across all samples and identical lengths, were removed. RPKM (reads per kilobase transcript per million mapped reads) were calculated and then log2-transformed and 75th percentile-shifted. Reads mapping to protein-coding or pseudogenes were presumed to

correspond to degraded RNA and were excluded, from descriptive analyses of data. For each feature across all of the samples the baseline was set to the median value (i.e. the median subtracted from all of the values for that feature). A two-tailed t test and FDR p-value correction were used to assess statistical significance (analysis performed by the Genomics lab at the Technology Facility, University of York).

2.7. Western blot

All samples were initially washed once with ice-cold PBS. Subsequently, cells were lysed with either 30 or 50 μl of ice-cold radioimmunoprecipitation assay (RIPA) buffer (5 mM EDTA, 150 mM NaCl, 10 nM Tris HCl pH 7.2, 0.1% SDS, 0.1% Triton X-100 and 1% sodium deoxycholate) containing protease cocktail inhibitors P8340, P5726 and P0044 (Sigma). The lysate was kept on ice for approximately 15 min and then centrifuged at 10,000 x g for 15-20 min at 4°C to transfer the supernatant. Protein concentration was determined by the Pierce Bicinchoninic acid assay (BCA) protein assay kit (ThermoFisher Scientific) according to the manufacturer's protocol, using bovine serum albumin (BSA) to generate the standard curve. Samples were incubated at 37°C for 30 min and the absorbance was read on a VersaMax Microplate Reader (Molecular Devices) at 562 nm. Protein samples were denatured at 95°C with the use of 4X sample loading buffer (250 mM Tris HCl pH 6.8, 8% (w/v) SDS, 40% (v/v) glycerol, 5% (v/v) β-mecaptoethanol and 0.05% (w/v) bromophenol blue). Denatured proteins were resolved on 8, 10 or 12% SDS-PAGE gel containing acrylamide using a Bio-Rad PowerPac HC for 1.5 h at 120V and transferred onto PVDF membranes (Millipore) at 200 mA and voltage limited to under 25V for 1-1.5 h using a Trans-Blot SD semi-dry transfer cell (Bio-Rad). The PageRuler Plus Protein Ladder (ThermoFisher Scientific) was used to label size standards (10-250 kDa). Immediately after transfer, membranes were blocked with either 2% BSA (Fisher Scientific) or 5% non-fat dry milk (Sigma-Aldrich) in 0.1% (v/v) TBST for 1 h at room temperature. Membranes were probed overnight at 4°C or for 1 h at room temperature for GAPDH and β-actin (Table 2.3). Membranes were further incubated with horseradish peroxidase (HRP)-conjugated secondary antibodies (Dako, 1:5000). Membranes were washed with TBST, 3X for 5 min after each antibody incubation and finally visualized with ECL (GE Healthcare), according to the manufacturer's protocol. Band intensity was quantified using ImageJ v1.50e (NIH, Bethesda, Maryland).

Table 2.3. Primary antibodies for western blot

Supplier	Target (human)	Antibody (1:1000 unless stated)
Cell Signalling	PD-L1	E1L3N
	SOCS1	A156
	STAT1	9172
	P-STAT1 Tyr 701	D4A7
	STAT3	9132
	P-STAT3 Tyr 705	D3A7
	AKT	C67E7
	P-AKT Ser 473	D9E *(1:500)*
	P-AKT Thr 308	C31E5E
	ERK1/2	137F5
	P-ERK1/2 Thr202/204	D13.14.4E
	mTOR	7C10
	P-mTOR Ser 2481	2974
	rpS6	5G10
	P-rpS6 Ser 235/236	D57.2.2E
	Dicer	D38E7
	Drosha	D28B1
	AGO1	9388
	AGO2	C34C6
	TIE2	AB33
Abcam	Actin	AC-15
	GAPDH	6C5
	PACT	Ab31967
	TRBP	Ab42018
Proteintech	PROX1	11067-2-AP

2.8. PNGase F treatment

Peptide: N-glycosidase F (PNGase F) was acquired from New England Biolabs (P0704). PNGase F was added to denatured protein lysates according to the manufacturer's protocol and subsequently analysed by western blot.

2.9. PD-L1 3'-UTR luciferase assays

PD-L1 3'-UTR were amplified from HeLa cells and subcloned into the psiCheck2 vector using Xhol and Pmel enzymes. Mutations were introduced at the PD-L1 3'-UTR at the miR-155 binding site (Site1: 5'-AGCAUUA-3' to 5'-UCUACAG-3' and Site2: 5'-GCAUUAA-3' to 5'-UCUACAG-3') using Q5 site-directed mutagenesis kit (NEB) and confirmed by DNA sequencing. The PU.1 3'-UTR constructs were described previously (Vigorito et al. 2007). Luciferase assays were performed in HeLa cells transfected with hsa-miR-155-5p mimic (50

nM) and PD-L1 or PU.1 3'-UTR constructs for 48 h using JetPrime reagent. Samples were assayed with the Dual-Luciferase reporter assay system kit (Promega) for Firefly and Renilla luciferase activities and measured on a Perkin-Elmer Wallac Victor2 1420 multi-label counter (performed by Kunal Shah, Bart's Cancer Institute).

2.10. Flow cytometry / Fluorescence assisted cell sorting (FACS)

Cells were washed with ice-cold PBS before staining for the live/dead marker, Zombie Aqua (Biolegend) for 5 min on ice. Samples were subsequently washed with FACS buffer (1X PBS / 0.5% BSA / 0.05% sodium azide) and Ig Fc receptor-blocked with Human TruStain FcX (Biolegend) for a further 5 min on ice. Sodium azide can prevent capping and shedding or internalisation of the antibody-antigen complex. Next, samples were incubated with antibodies for 20-30 min on ice and then washed with FACS buffer x3. After the final wash, samples were transferred to FACS tubes and analysed on a BD LSR Fortessa (BD Biosciences) using FACS DIVA software. Post-analysis was done using FlowJo V10 (Tree Star).

For FACS, PD-1 NFAT-Luc Jurkat cells were prepared with no live/dead marker and antibody incubation was done in culture medium (described above). FACS analysis was performed on a MoFlo Astrios EQ Sorter (Beckman Coulter). Cells were sorted for purity (1 drop) with 80% efficiency. Sorted cells were immediately washed with media x2 to dilute sheath fluid and subsequently cultured (described above).

Table 2.4. Antibodies for flow cytometry

Supplier	Target (human)	Antibody	Isotype
Biolegend	PD-1	EH12.2H7 (APC)	Mouse IgG1, κ
	CD69	FN50 (FITC)	Mouse IgG1, κ
	PD-L1	29E.2A3 (PE)	Mouse IgG2b, κ
	HLA-DR	L243 (PE-Cy5)	Mouse IgG2a, κ
Lieping Chen lab	PD-L1	5H1 (Biotin)	Mouse IgG1, κ
eBioscience	CD80	2D10.4 (Biotin)	Mouse IgG1, κ
	HLA-ABC	W6/32 (PE-Cy5)	Mouse IgG2a, κ

2.11. Immunofluorescence confocal microscopy

Cells were cultured in 35 mm glass-bottom dishes with a 14 mm microwell (MatTek). After 48 h, cells were stimulated with IFN-γ or in combination with TNF-α for 24 h. Cells were fixed in 4% paraformaldehyde and permeabilized with 0.5% Triton X-100, and then blocked with 5% goat serum for 1 h. Samples were incubated overnight at 4°C with anti-PD-L1 (5H1, 1:50), washed with PBST x2, followed by goat anti-mouse secondary Alexa Fluor 488 (Invitrogen, 1:200) for 1 h and washed again with PBST x2. ProLong Gold antifade

mountant with DAPI (Invitrogen) was used to mount the slide and stain the nucleus. Slides were analysed and images were acquired with a Zeiss LSM 880 on a 40X oil immersion objective lens using Zeiss Zen software.

2.12. Enzyme-Linked Immunosorbent Assay (ELISA)

The Human IL-2 ELISA MAX Standard kit (Biolegend) was used for all ELISA experiments, following the instructions provided by the manufacturer. Rat monoclonal anti-human IL-2 (capture antibody) was coated overnight on Nunc MaxiSorp flat-bottom 96-well plates (ThermoFisher Scientific). The next day, wells were blocked with 5% FCS in 0.05% TBST and samples were added. A biotinylated goat polyclonal anti-human IL-2 (detection antibody) was incubated with supernatants and followed by avidin-HRP. Amount of IL-2 was detected using 3,3',5,5'-tetramethylbenzidine (TMB) substrate solution followed by a stop solution (2N H_2SO_4). Absorbance was read at 450 nm and 570 nm using the VersaMax Microplate Reader. An IL-2 standard curve (up to 500 pg/ml) was generated as shown: absorbance readings at *450 nm (TMB) – 570 nm (wavelength correction) – blank*.

2.13. Co-culture using wild-type Jurkat T cells / IL-2 ELISA

For most of the experiments, adherent cells (e.g. HFFs) were plated in 24 well plates in 500 μl DMEM at 15,000 cells/well and left to attach for 16-20 h. Next, media was replaced with fresh media consisting of IFN-γ and TNF-α for 24 h. If valid, transfection of cells with PD-L1 siRNA or miR-155 mimics would occur prior to stimulation, followed by an extra day to recover the cells. During seeding of HFFs, a separate parallel 24 well plate was set up containing wild-type Jurkat T cells in 500 μl RPMI. Subsequently, Jurkat cells were treated for 48 h with 1-5 μg/ml phytohaemagglutinin (PHA) and 50 ng/ml phorbol 12-myristate 13-acetate (PMA), both reagents were obtained from Sigma-Aldrich. On day 3, pre-activated Jurkat T cells were co-culture with pre-stimulated HFFs for 24 h and supernatants were collected for IL-2 ELISA.

2.14. Co-culture using PD-1 NFAT-Luc Jurkat T cells

Primarily, adherent cells (e.g. HFFs) were plated in flat bottom 96 well plates in 100 μl DMEM at 10,000 cells/well and left for 16-20 h. The following day, media was removed and cells were stimulated with IFN-γ and TNF-α in 100 μl for 24 h. If applicable, transfection of cells would occur prior to stimulation, followed by an extra day to recover the cells. Post-stimulation, the media was replaced with 75 μl RPMI 1% FCS containing PD-1 NFAT-Luc Jurkat T cells at 20,000 cells/well. Cells were preliminary co-cultured for 3 h at 37°C and then given anti-human CD3 (OKT3, Biolegend) and anti-human CD28 (CD28.2, Biolegend) stimulation at 2 μg/ml. CD3/CD28 antibodies were added in 25 μl solutions on top of the 75 μl present in the 96 well, and incubated for a further 3-4 h at 37°C. Following

this incubation, the 96 well plates were immediately analysed. First, the plates were equilibrated at room temperature for at least 10 min. The luciferase substrate Bio-Glo reagent (Promega) was brought to room temperature and 50 µl was added to each well for 8 min. Luminescence was measured by the CLARIOstar (BMG Labtech) plate reader, taking readings every 1 min for 5 cycles to determine stability of luciferase signal (equivalent to 8-12 min incubation of Bio-Glo, where the 10 min reading was used). Plate background signal was subtracted using measurements from blank wells with Bio-Glo only. Co-culture luciferase quantifications were normalised using PD-1 NFAT-Luc Jurkat only activated controls (set to 100%).

2.15. Statistical analysis

Statistical analysis and graphs were made using GraphPad Prism 8 (GraphPad Software Inc.) or RStudio. Statistical significance was determined by comparing the means of at least three independent experiments ($n \geq 3$), performed on different days, using two-sided unpaired Student's *t* tests between two experimental groups or by one-way analysis of variance (ANOVA) with Tukey for more than two experimental groups. A *p-value* < 0.05 is generally considered to be statistically significant. Unspecified indicates no significance. An unpaired t-test was used because there are two different experimental conditions (e.g. NTC or miR-155) that were tested such as in Chapter 3 (i.e. Figures 3.14, 3.15, 3.16, 3.18, 3.22 and 3.23). Experimental results are presented as mean ± standard deviation (S.D).

3. Posttranscriptional regulation of PD-L1

3.1 Introduction

Th1 $CD4^+$ and $CD8^+$ T cells commonly secrete pro-inflammatory cytokines IFN-γ and TNF-α upon activation, which are required for their effector function (Zhu et al. 2010; Zhang & Bevan 2011). As described (Chapter 1), IFN-γ activation is a principal inducer of PD-L1 expression. In addition, PD-L1 has been demonstrated to be induced in HUVECs by IFN-γ and TNF-α between 24 and 48 h of activation using a concentration of 100-1000 U/ml IFN-γ and 10-25 ng/ml TNF-α (Mazanet & Hughes 2002; Rodig et al. 2003). However, the expression of PD-L1 has not been studied in primary HDLECs that line the lymphatic system. Using this cellular model, I characterised HDLEC response to IFN-γ and TNF-α treatment using similar concentrations to Mazanet, Rodig and colleagues. PD-L1 expression was analysed using various cellular biology techniques: western blot, qRT-PCR, flow cytometry and microscopy to determine levels of total protein, mRNA, surface expression and cellular localisation, respectfully. Furthermore, I determined the effects of IFN-γ and TNF-α on the miRNA landscape in HDLECs using small RNA sequencing. In addition, I characterised the expression of PD-L1 in primary human foreskin fibroblasts (HFFs) to determine whether my findings were cell-type specific or not. This chapter highlights that primary stromal fibroblasts/vascular cells are strongly responsive to IFN-γ and TNF-α inflammatory stimuli, which synergise to induce downstream genes such as PD-L1, and in parallel activate small RNA networks within miRNAs that act to fine-tune PD-L1. I propose that this is a response to inflammation during a physiological immune response to avoid prolonged immune suppression and provides new understanding into the regulation of immune checkpoints in human primary cells.

3.2 HDLEC response to IFN-γ and TNF-α activation

The majority of nucleated cells express MHC class I and not MHC class II surface receptors, which are typically found on professional APCs. HDLECs display HLA-ABC molecules, which represent MHC class I cell surface receptors that can present peptides to $CD8^+$ T cells (Figure 3.1). Treatment with IFN-γ and TNF-α induced an increase in the surface expression of HLA-DR, suggesting HDLECs possess the expression of MHC class II receptors that present peptides to $CD4^+$ T cells (Figure 3.1). Stimulation of HDLECs with TNF-α alone did not change expression of HLA-DR compared to untreated cells. These data indicate similar findings to previous reports, suggesting HDLECs express MHC class II receptors when responding to IFN-γ activation. However, further evidence is required to understand whether HDLECs can present peptides through MHC class I or II molecules.

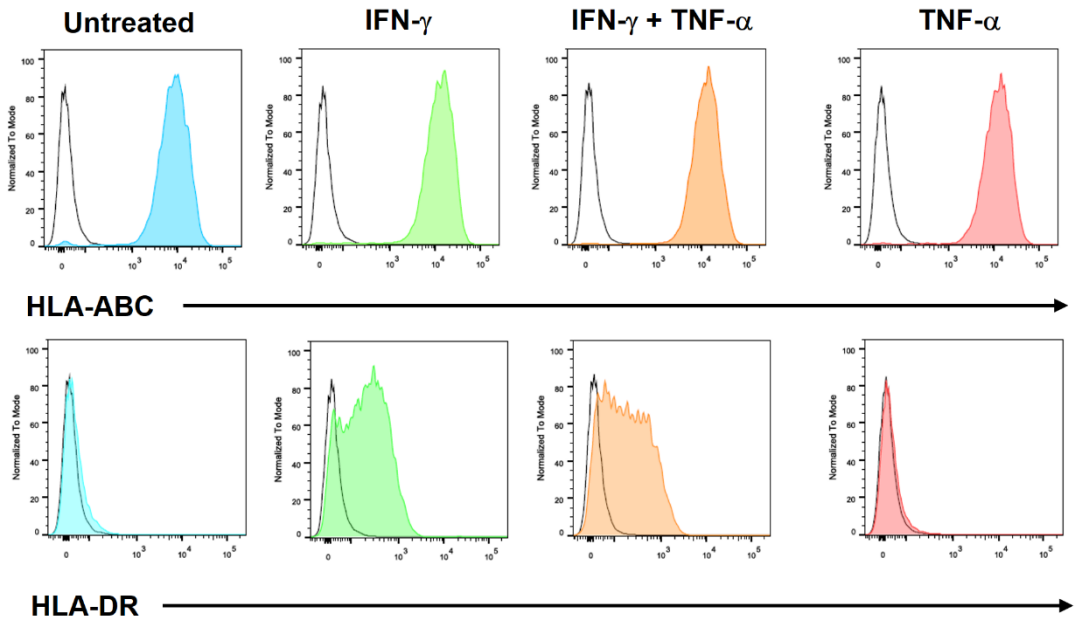

Figure 3.1. **HDLECs express MHC class II molecules after IFN-γ stimulation.** Pilot study to show the response of HDLECs to inflammatory activation. HDLECs were harvested after stimulation with IFN-γ, TNF-α or both cytokines (24 h) for flow cytometry analysis and stained for HLA expression. Data showing HLA-ABC (MHC class I) or HLA-DR (MHC class II) surface expression, measured by median fluorescence intensity, MFI, of cells gated on singlets. MFI of HLA-ABC staining: IFN-γ + TNF-α = 12814, IFN-γ = 12688, TNF-α = 12226 UT = 8396. MFI of HLA-DR staining: IFN-γ + TNF-α = 178, IFN-γ = 213, TNF-α = 25.9 UT = 27.8, Black = unstained cells (MFI = 17.9 to 19.7). n = 1 experiment.

Furthermore, the effect of IFN-γ and TNF-α was looked in various signalling pathways (Figure 3.2A). Phosphorylation of Akt at serine 473 is mediated by mTOR complex 2 (mTORC2) and constitutes to activation of Akt. Phosphorylation of S473 was initially induced by IFN-γ and TNF-α after 30 min but the effect was lost at 4 h compared to untreated cells. At 16 and 24 h, the cells had lower phosphorylation of Akt S473, suggesting IFN-γ and TNF-α affected mTORC2-mediated effects. On further investigation, at lower concentrations of IFN-γ stimulation this appeared to drive downregulation of Akt S473 which could be restored with addition of TNF-α (Figure 3.2B). However, increasing the concentration of IFN-γ drove further downregulation which was then enhanced with the addition of TNF-α. Stimulation with TNF-α alone slightly decreased Akt S473 phosphorylation. Downstream effector of the Akt pathway, ribosomal protein S6 phosphorylation at S235/236 was increased upon IFN-γ and TNF-α stimulation compared to untreated cells. Whereas, the phosphorylation of ERK at threonine 202/204 was transient but

noticeably increased at 16 and 24 h post-stimulation. These data indicate that IFN-γ and TNF-α activation can modulate the transient expression of key signalling molecules in HDLECs.

HDLEC lineage commitment markers were assessed after stimulation with IFN-γ and TNF-α. PROX1 protein expression was decreased by IFN-γ alone, TNF-α alone and further downregulated in the combination of both cytokines (Figure 3.3A). This was further supported by an observe decrease at mRNA level in all tested lineage commitment markers of LECs (PROX1, VEGFR3, COUP-TFII and LYVE1) (Figure 3.3B). This highlights the lineage plasticity of HDLECs and suggests IFN-γ and TNF-α-activation causes the loss of HDLEC identity, which may lead to suppression of HDLEC growth *in vitro*.

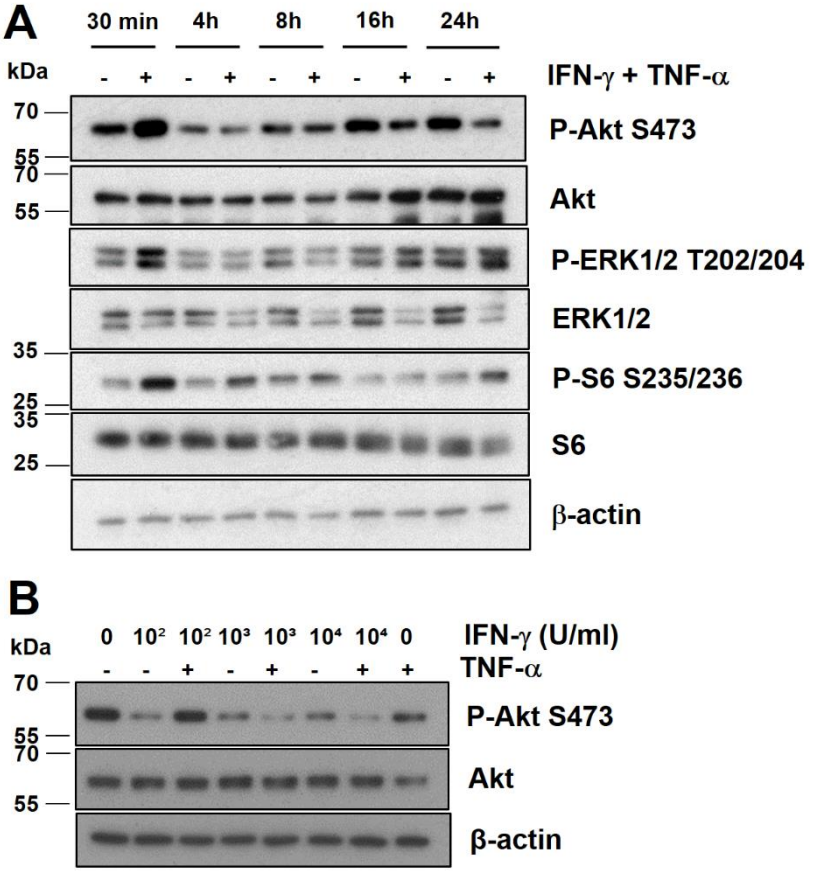

Figure 3.2. **Effect of IFN-γ and TNF-α on AKT or ERK pathways.** Another preliminary study to show responsiveness of HDLECs to cytokine activation. HDLECs were treated with or without IFN-γ and TNF-α in 6-well plates for up to 24 h and lysed for western blot analysis at time-points indicated above. A) Protein expression following a time-course of IFN-γ and TNF-α stimulation in HDLECs showing various effects on the phosphorylation (P) of AKT, ERK and S6 proteins. B) Protein expression following a titration of IFN-γ with and without TNF-α stimulation (24 h). n = 2 independent experiments.

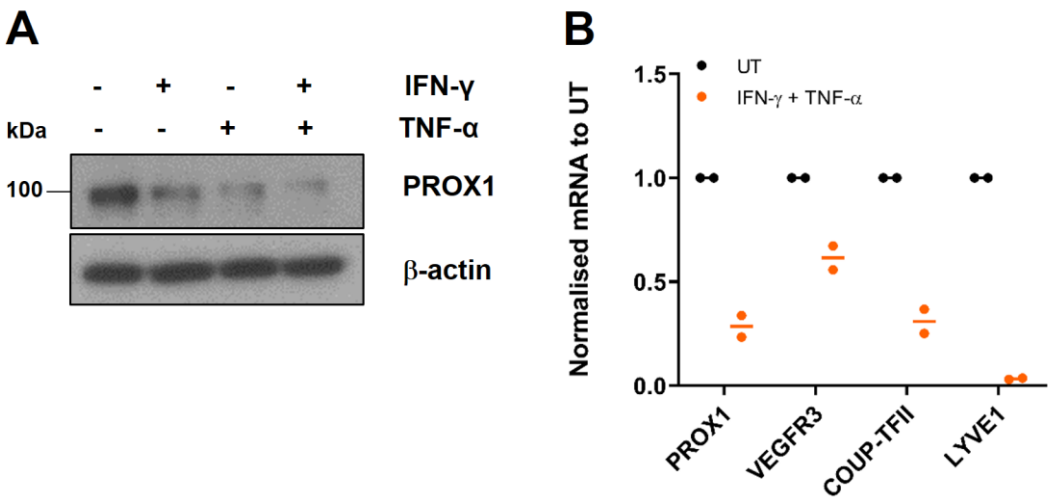

Figure 3.3. **IFN-γ and TNF-α activation of HDLECs results in loss of lineage commitment markers.** Experiment to show the effects of inflammatory cytokines on lineage markers associated with LECs. A) Western blot analysis showing the PROX1 expression in HDLECs after IFN-γ and TNF-α stimulation (24 h). B) qRT-PCR showing mRNA expression of PROX1, VEGFR3, COUP-TFII and LYVE1 after IFN-γ and TNF-α stimulation (24 h), gene expression is normalized to their respective untreated control, using β-actin as a reference gene when calculating fold change expression. n = 2 independent experiments.

3.3 HDLEC characterisation of PD-L1 expression and kinetics

PD-L1 expression in HUVECs show a strong induction after IFN-γ and TNF-α activation, where peak levels of mRNA transcripts were between 12 and 24 h (Mazanet & Hughes 2002). In addition, surface expression of PD-L1 was highest around 24 h post-stimulation (Mazanet & Hughes 2002). In this study, PD-L1 expression was measured at basal levels and after IFN-γ and TNF-α stimulation at time-points between 30 min and 24 h in HDLECs (Figure 3.4A and B). PD-L1 protein expression was notably induced after 4 h of stimulation and this upregulation was increased further by 24 h. Two distinct protein bands were observed for PD-L1 (around 40-50 kDa) in western blot analysis. IFN-γ signalling is capable of activating both STAT1/3. In HDLECs, phosphorylation of STAT1 at the activating tyrosine residue (P-STAT1 Y701) positively correlated with the increase of PD-L1 whereas the kinetics of STAT3 activation were transient but remained induced. Consistent with these results, PD-L1 mRNA levels were upregulated in activated HDLECs (Figure 3.5A). IFN-γ treatment resulted in a ten-fold induction of PD-L1 mRNA levels at 24 h post-treatment, compared to basal expression. The effect was significantly elevated by concurrent addition of TNF-α, although addition of TNF-α alone did not significantly affect PD-L1 mRNA

levels, demonstrating that the effect of stimulating with both cytokines was synergistic. Importantly, IFN-γ and TNF-α enhanced surface PD-L1 expression (Figure 3.5B), where the functional relevance of PD-L1 has been described.

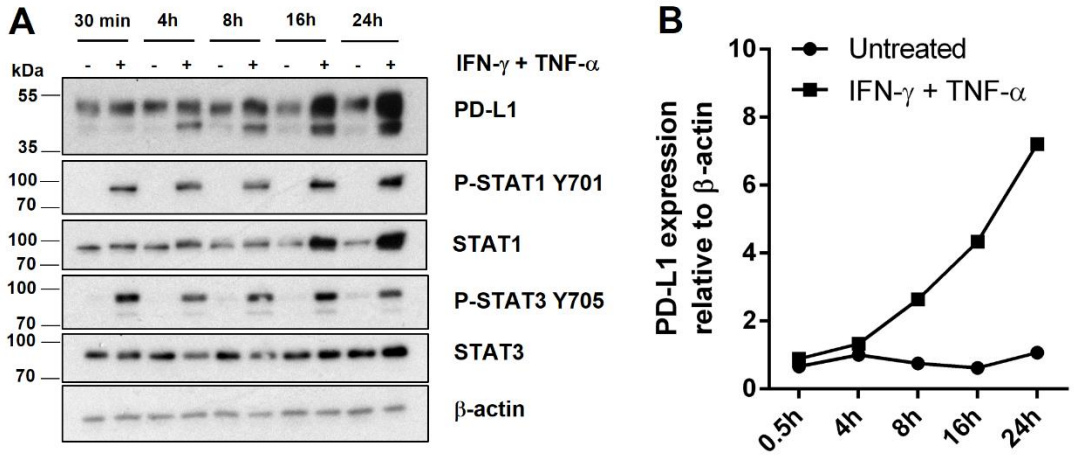

Figure 3.4. **PD-L1 is expressed in HDLECs and can be induced by IFN-γ and TNF-α**. A) Western blot analysis following a time-course of IFN-γ and TNF-α stimulation in HDLECs, compared to untreated. The phosphorylation of STAT1/3 proteins shows that HDLECs respond to canonical IFN-γ and TNF-α signalling. B) Western blot quantification from A (left) in untreated and IFN-γ and TNF-α-treated samples, relative to β-actin, showing PD-L1 protein expression. n = 2 independent experiments, showing one representative blot.

Furthermore, titrating IFN-γ stimulation showed an upwards trend of PD-L1 mRNA expression, which was further augmented in combination with TNF-α (Figure 3.6A). At the protein level, TNF-α stimulation alone had no effect on PD-L1 or P-STAT1 (Figure 3.6B). TNF-α in combination with IFN-γ induced further expression of P-STAT1 whilst having minimal effects on total PD-L1 protein levels in comparison to treatment with IFN-γ alone. Immunofluorescence determined the effect of IFN-γ and TNF-α on PD-L1 expression in permeabilised cells (Figure 3.7). PD-L1 was localized at the cell membrane and throughout the cytoplasm following stimulation. There was increased perinuclear PD-L1 staining from the synergistic effect between IFN-γ and TNF-α, which suggested that in IFN-γ-treated HDLECs, TNF-α can affect PD-L1 localization. Expression of IL-1β mRNA, a downstream target of NF-κB pathway, was upregulated in a similar synergistic manner between IFN-γ and TNF-α (Figure 3.8A). PD-L1 mRNA was measured at 8 h where it was strongly induced and remained at the same level at 24 h, consistent with the cumulative increase in PD-L1 protein levels (Figure 3.8B). To confirm specificity of PD-L1 signal, transfection of small interfering RNA (siRNA) targeting PD-L1 abolished detection of both bands in western blot (Figure 3.9A). PNGase F is an enzyme which cleaves oligosaccharides from N-linked

glycoproteins. De-glycosylation treatment using PNGase F led to total disappearance of both PD-L1 bands and a new band appearing at 33 kDa, which is the expected molecular weight of unmodified PD-L1 (Figure 3.9B). Taken together, these data indicated that, as in the case of macrovascular endothelial cells, PD-L1 is inducible at the transcriptional level in HDLECs responding to inflammatory stimuli.

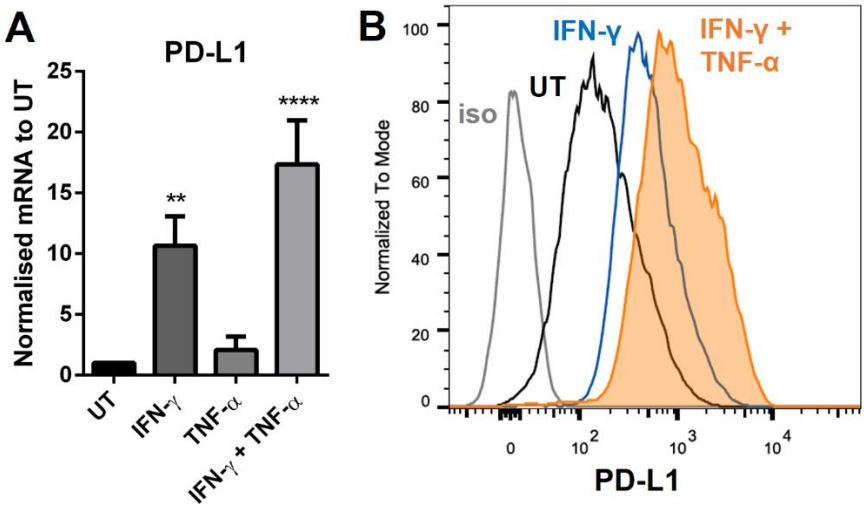

Figure 3.5. **PD-L1 transcription is induced by IFN-γ and TNF-α**. A) PD-L1 mRNA fold change measured by qRT-PCR after stimulation (as shown, 24 h), normalised to untreated (UT) HDLECs. B) Flow cytometric analysis showing PD-L1 surface expression (median fluorescence intensity, MFI) after stimulation (24 h) on live HDLECs. An isotype control (iso) was used as a negative control and lacks the specificity to bind PD-L1. MFI of PD-L1 staining: IFN-γ + TNF-α = 994, IFN-γ = 485, UT = 168, iso = 8.62. One-way analysis of variance (ANOVA) was calculated with Tukey's multiple comparisons test. **, $p < 0.01$ and ****, $p < 0.0001$. n = at least 3 independent experiments.

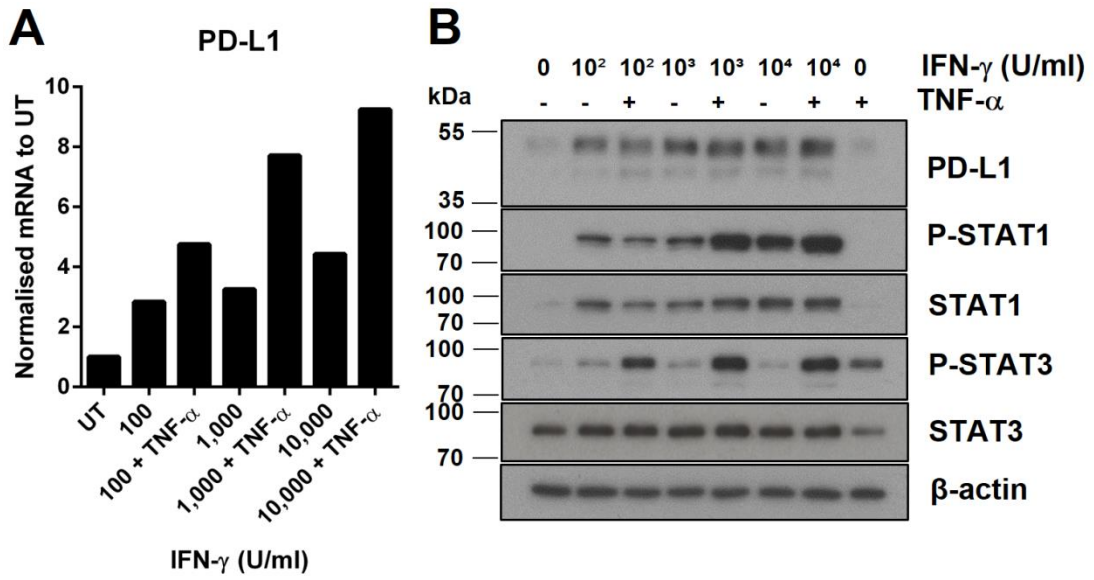

Figure 3.6. **The effect of titrating IFN-γ concentration with and without TNF-α on PD-L1 expression.** HDLECs were treated (24 h) with increasing amounts of IFN-γ with or without TNF-α to observe the effect on PD-L1 mRNA and protein expression. A) qRT-PCR showing PD-L1 mRNA expression in HDLECs, normalised to UT, in order of increasing IFN-γ concentration. n = 1 experiment. B) Expression of PD-L1 and STAT protein analysed from HDLEC lysates. n = 2 independent experiments, showing one representative experiment.

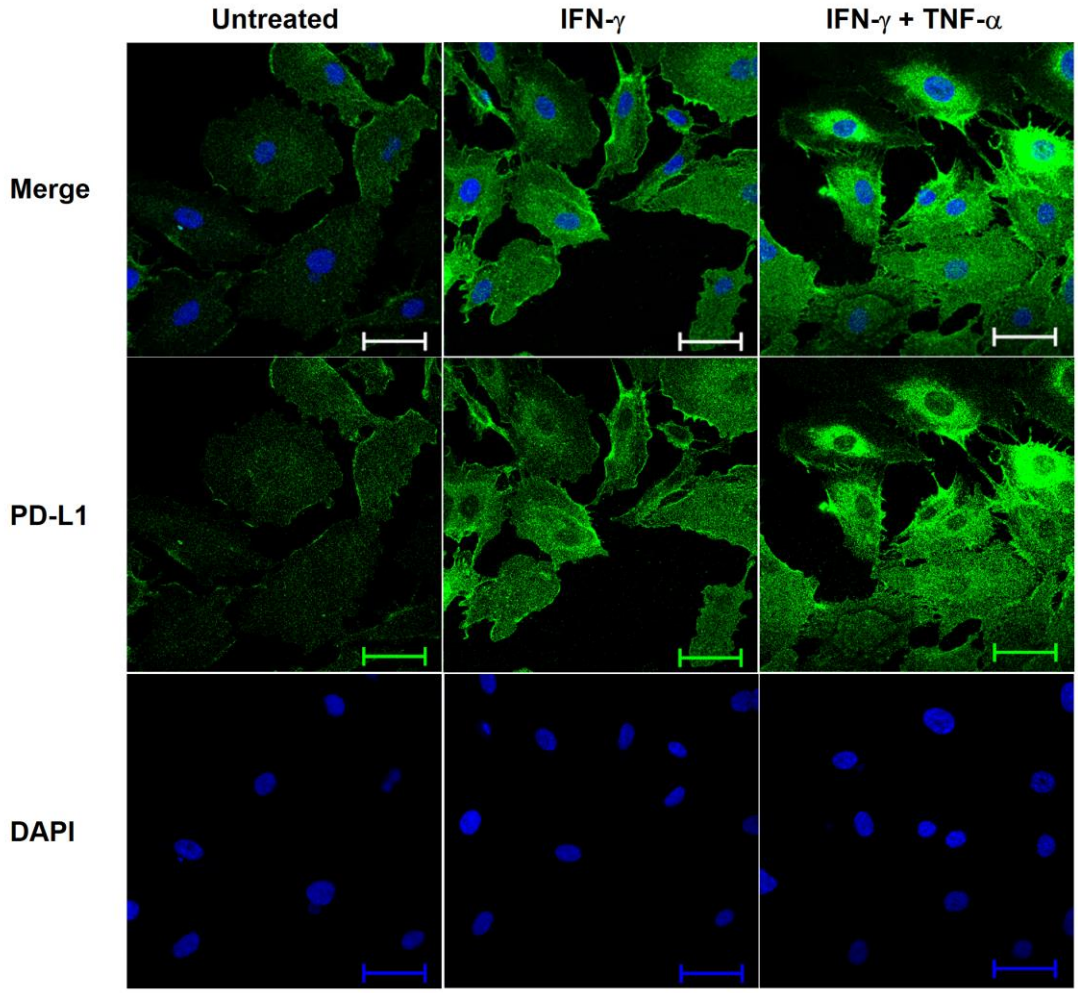

Figure 3.7. **PD-L1 expression is increased by the combination of IFN-γ and TNF-α.** Immunofluorescence microscopy showing PD-L1 (Alexa Fluor 488) in HDLECs after stimulation (24 h) with IFN-γ, or in combination with TNF-α. Cells were fixed and permeabilized prior to staining to show total PD-L1 expression on the surface and in the cytoplasm. DAPI (blue) is shown to mark the nucleus. Scale bar = 50 μm. n = 1 experiment.

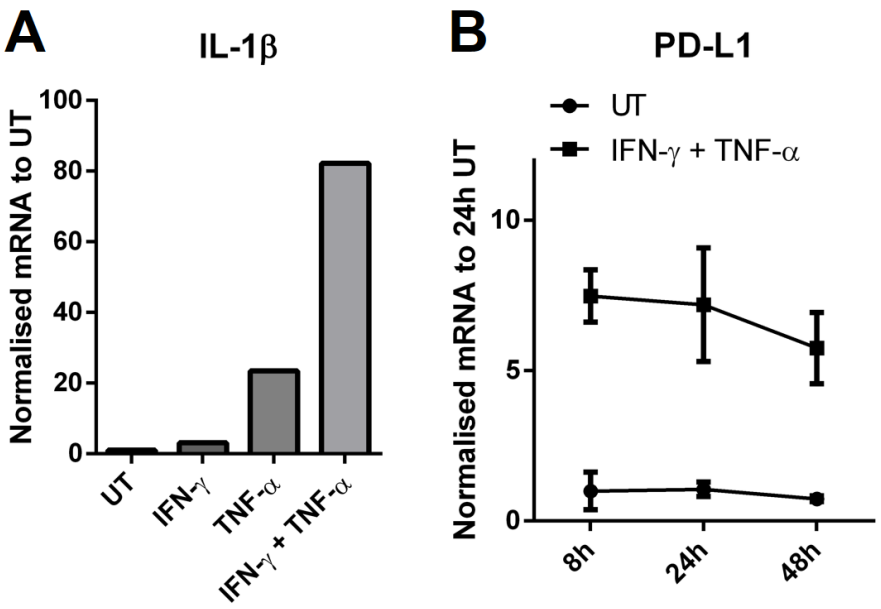

Figure 3.8. **The expression of PD-L1 and IL-1β following IFN-γ and TNF-α stimulation.** A) IL-1β is a known downstream target of TNF-α signalling. IL-1β levels were measured by qRT-PCR following 24 h stimulation in HDLECs. n = 1 experiment. B) qRT-PCR showing time-course of PD-L1 mRNA expression in cells treated with IFN-γ and TNF-α for 8, 24 and 48 h and normalized to untreated (24 h). n = average of 3 independent experiments.

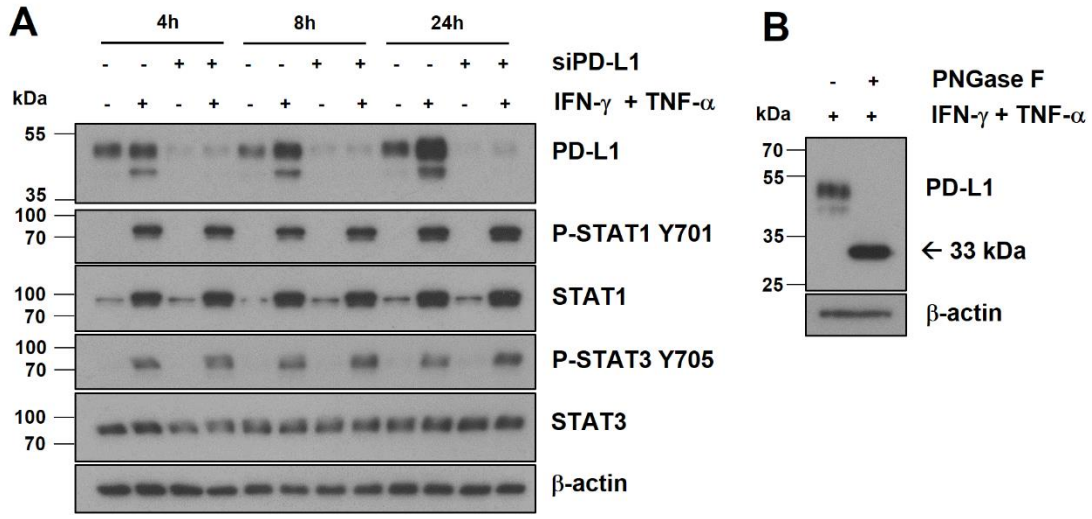

Figure 3.9. **Validation of antibody used to detect PD-L1 protein expression.** These experiments show that the antibody (E1L3N) used to detect PD-L1 is specific from testing the knockdown of PD-L1 by siRNA and de-glycosylation of PD-L1. A) Western blot analysis following 48 h transfection of siRNA targeting PD-L1. HDLECs were stimulated with IFN-γ and TNF-α for 4, 8 and 24 h after siRNA transfection and harvested for protein lysates. (B) IFN-γ and TNF-α stimulated lysates were treated with PNGase F and the resultant protein was analyzed for de-glycosylation by western blot. 33 kDa marks the size of unmodified PD-L1 protein. n = 2 independent experiments, showing one representative experiment.

3.4 Small RNA sequencing of IFN-γ and TNF-α-stimulated LECs reveal inflammation-responsive miRNAs

In the previous section, I characterised PD-L1 expression in HDLECs and showed that IFN-γ and TNF-α induce significant PD-L1 transcription and affect different pathways of characteristics of HDLECs. As described before (Chapter 1), IFN-γ and TNF-α are known to regulate miRNA expression in a number of inflammatory conditions. From these results, I continued to investigate the effect of inflammatory stimuli on small RNAs using HDLECs, where the role of IFN-γ and TNF-α on the small RNA transcriptome had not been determined at this point. This would lead to identification of possible candidates that were involved in posttranscriptional regulation of PD-L1 during inflammatory responses of primary human cells. To achieve this aim, small non-coding RNAs were analysed in HDLECs stimulated with or without IFN-γ and TNF-α for 24 h. Harvested RNA were then enriched for small RNAs, and processed using next-generation sequencing via the Illumina MiSeq workflow (performed by Genomics Technology Facility, University of York). Sequencing analysis confirmed detection of small nuclear RNAs (snRNAs), small nucleolar

RNAs (snoRNAs) and miRNAs, which made up ~22% of the analysed sample size (Figure 3.10A). As a result, 48 miRNAs were identified to be differentially regulated by IFN-γ and TNF-α (adjusted $p < 0.1$) (Figure 3.10B). A small sample of 11 miRNAs that were upregulated or downregulated were selected for further assessment by qRT-PCR (Figure 3.10C). We found that IFN-γ and TNF-α resulted in significant upregulation of miR-155-5p, miR-4485-3p, miR-218-5p and miR-146a-5p and downregulation of miR-582-5p, miR-582-3p, miR-93-5p, miR-217 and miR-125b-5p (Figure 3.10 and Tables 3.1A). Analysis of gene ontology utilising the miRNA enrichment analysis and annotation tool (Backes et al. 2016) indicated that predicted targets of these differentially regulated miRNAs were associated with cytokine-mediated signalling and regulation of inflammatory response (Figure 3.10D). These data suggest that the miRNA landscape in HDLECs is highly responsive to inflammatory stimuli and feedback into pathways associated with stress, proliferation and the inflammatory response.

I tested the following miRNAs which are reported to regulate essential cellular responses from angiogenesis to immune responses, for their response to IFN-γ and TNF-α stimulation after 24 h to understand the wide-spread effect of inflammatory activation in HDLECs (Figure 3.11A, Tables 3.1B). Both miR-126 and miR-221 have been reported to be involved in the regulation of angiogenesis (Wang et al. 2008; Fish et al. 2008; Nicoli et al. 2012); miR-16 is a regulator of apoptosis and the cell cycle (Cimmino et al. 2005; Linsley et al. 2007); miR-29a, miR-132 and miR-21 have been demonstrated to regulate different arms of immunity (Park et al. 2009; Ma et al. 2011; Lagos et al. 2010; Kumarswamy et al. 2011). Expression of miRNA was measured using qRT-PCR, miR-221, miR-126 and miR-16 were downregulated after activation. Whereas, inflammatory-associated miR-29a and miR-21 were upregulated by IFN-γ and TNF-α. Time-course experiments showed that only after 8 h of stimulation, the expression of miR-146, miR-21, miR-126 and miR-221 were up- or downregulated compared to untreated cells (Figure 3.11B). In comparison to small RNA-seq data, there were some discrepancies between the two different forms of expression, particularly with miR-21, which is a highly expressed miRNA in HDLECs (Table 3.1B). In general, some of the selected miRNAs that are linked key cellular processes responded to IFN-γ and TNF-α activation, indicating various cellular processes could be affected by changes to the miRNA landscape in HDLECs after inflammatory activation. However, the altered expression in most of these miRNAs were modest, compared to the significant upregulation of miR-155-5p.

3.5 miR-155 is synergistically induced by IFN-γ and TNF-α in HDLECs.

Having analysed differentially regulated miRNAs from small RNA sequencing, I cross-compared these with 82 miRNAs predicted to target the 3'-UTR of PD-L1 using TargetScan software (Agarwal et al. 2015) Figure 3.12A). 49 detected miRNAs in basal or inflamed HDLECs also had predicted binding sites for PD-L1, this amounted to ~8% of total miRNAs detected in HDLECs and ~60% of total miRNAs predicted to target PD-L1. Amongst these candidate miRNAs was miR-155-5p (referred to as miR-155), which was abundant in normal expression and also significantly induced by IFN-γ and TNF-α (Figure 3.12B). Other highly induced miRNAs were lowly expressed and can be subjected to high variance.

I focused on miR-155 as a potential posttranscriptional regulator of PD-L1 expression in inflamed HDLECs. First, miR-155 response to IFN-γ and TNF-α was profoundly due to TNF-α as the primary inducer (Figure 3.12C). IFN-γ stimulation alone did not change miR-155 levels but significantly elevated the effect of TNF-α on miR-155 expression, suggesting a synergistic effect similar to activation of PD-L1. Upregulation of miR-155 by IFN-γ and TNF-α was observed as early as 4 h and had a gradual rise, remaining at high levels after 48 h (Figure 3.12D and E). Increasing the concentration of IFN-γ induced further miR-155 expression (Figure 3.12F).

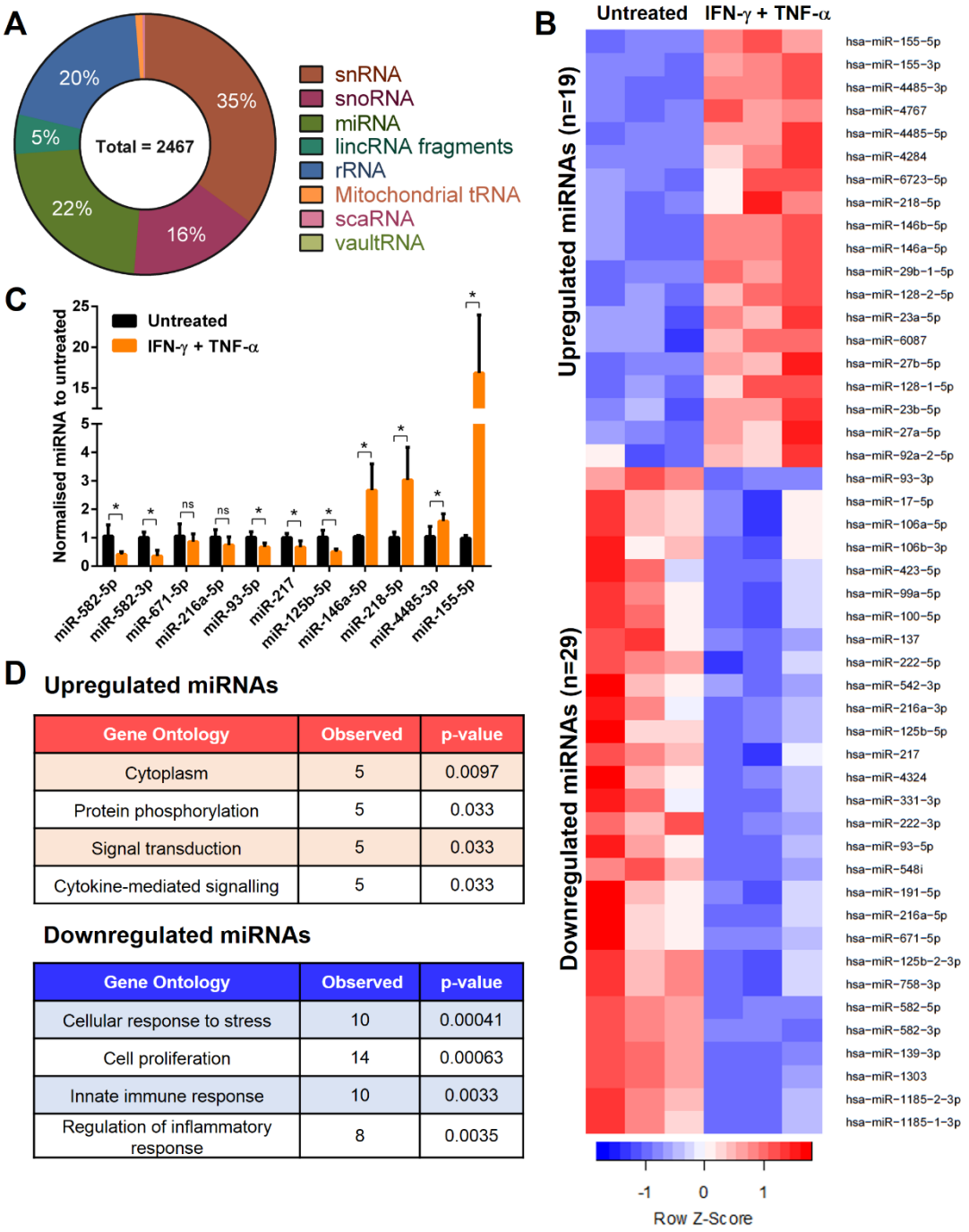

D

Upregulated miRNAs

Gene Ontology	Observed	p-value
Cytoplasm	5	0.0097
Protein phosphorylation	5	0.033
Signal transduction	5	0.033
Cytokine-mediated signalling	5	0.033

Downregulated miRNAs

Gene Ontology	Observed	p-value
Cellular response to stress	10	0.00041
Cell proliferation	14	0.00063
Innate immune response	10	0.0033
Regulation of inflammatory response	8	0.0035

Figure 3.10. **Identification of several inflammation-responsive miRNAs by small RNA sequencing of inflamed HDLECs.** A) Percentage distribution of sequencing results from HDLECs, showing the total number of hits after a threshold to filter lowly expressed genes was applied (>50 RPKM). B) Heat map showing fold-change in expression of 48 miRNAs after IFN-γ and TNF-α stimulation (24 h) in HDLECs (adjusted $p < 0.1$). Row Z-score represents mean ± S.D., n = 3 independent samples performed in triplicate. C) Validation of selected IFN-γ- and TNF-α-regulated miRNAs targets by qRT-PCR. Unpaired Student's t test comparing IFN-γ and TNF-α treated samples to UT per miRNA, *, $p < 0.05$, n = 3 independent samples. D) Gene ontology analysis of 48 IFN-γ and TNF-α-regulated miRNAs.

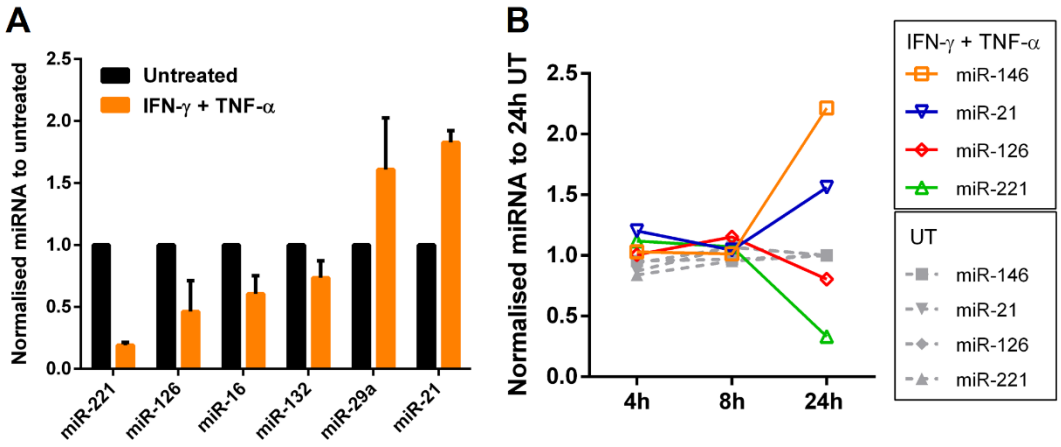

Figure 3.11. **The effects of IFN-γ and TNF-α on selected miRNAs.** A) miRNA expression in HDLECs measured by qRT-PCR after IFN-γ and TNF-α stimulation (24 h) normalized to untreated samples. n = average of 2 independent experiments. B) Time course showing kinetics of miRNA expression in HDLECs after 4, 8 or 24 h stimulation, normalised to untreated samples (24 h). n = average of 2 independent experiments.

A

miRNA	Sequencing fold change	qRT-PCR fold change
miR-582-5p	0.36	0.38
miR-582-3p	0.35	0.36
miR-671-5p	0.45	0.82
miR-216a-5p	0.49	0.72
miR-93-5p	0.52	0.67
miR-217	0.60	0.66
miR-125b-5p	0.60	0.49
miR-146a-5p	3.33	2.56
miR-218-5p	3.43	2.99
miR-4485-3p	6.57	1.51
miR-155-5p	17.03	17.16

B

miRNA	Sequencing fold change	qRT-PCR fold change
miR-221-3p	0.67	0.19
miR-126-3p	0.87	0.46
miR-16-5p	0.87	0.61
miR-132-3p	0.87	0.74
miR-29a-3p	1.29	1.60
miR-21-5p	1.03	1.83

Tables 3.1A and B. **Validation of IFN-γ and TNF-α regulated targets.** A) Table showing data from small RNA sequencing and qRT-PCR (Figure 3.10). Values represent average fold change of miRNA expression following IFN-γ and TNF-α stimulation (24 h) in HDLECs. B) Table showing the effect of IFN-γ and TNF-α stimulation (24 h) on tested select miRNAs that have been reported in the literature to regulate angiogenesis, apoptosis or inflammation. Increase (red shading) or decrease (blue shading) in miRNA expression after IFN-γ and TNF-α treatment (24 h) compared to untreated samples.

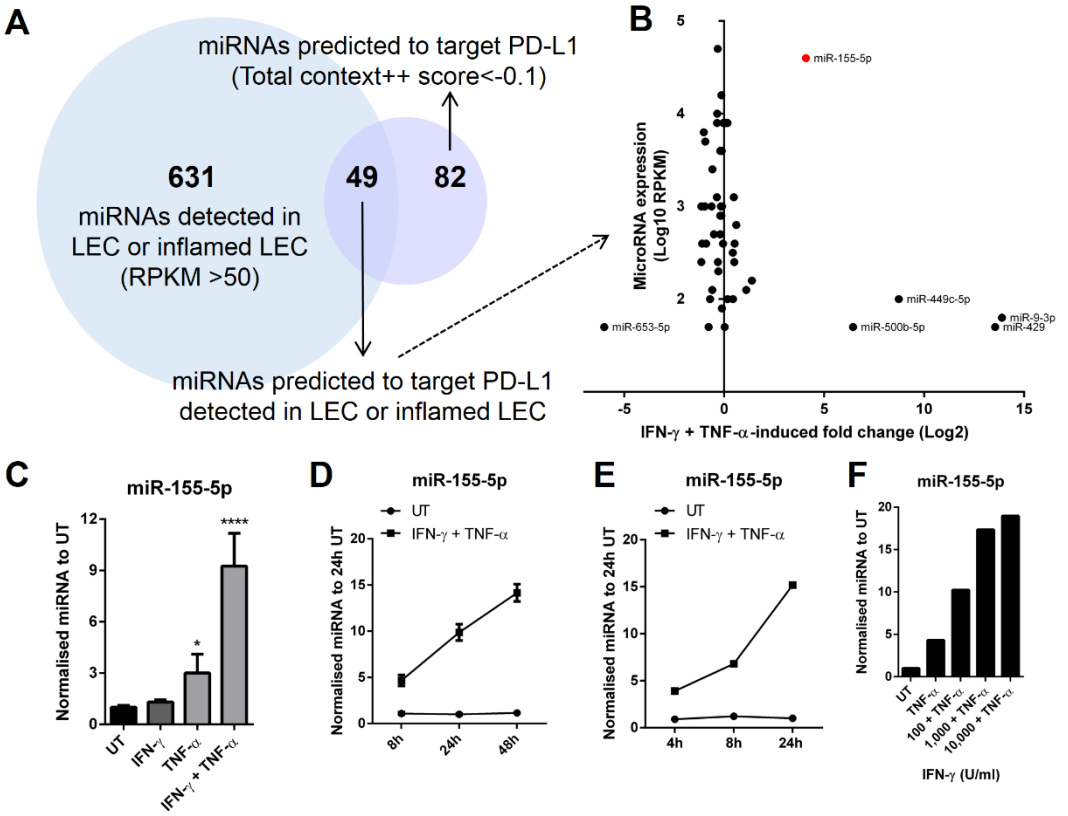

Figure 3.12. **miR-155 is synergistically induced by IFN-γ and TNF-α**. A) Representing the overlap between the total number of detected miRNAs in HDLECs from small RNA sequencing and number of miRNAs predicted to target PD-L1 (TargetScan). B) Comparison of the 49 miRNAs detected in LECs and predicted to target PD-L1 between average expression (log10 RPKM) and change in fold-expression after 24 h IFN-γ and TNF-α stimulation (log2). C) Levels of miR-155 were measured by qRT-PCR after stimulation (24 h) with IFN-γ, TNF-α, or both, normalized to untreated. Statistical test used was ANOVA using Tukey's multiple comparisons test, n = at least 3 independent samples. D) Time course of miR-155 expression following IFN-γ and TNF-α stimulation (8, 24, and 48 h), normalized to untreated (24 h). E) Time course of miR-155 expression following IFN-γ and TNF-α stimulation (4, 8, and 24 h), normalized to untreated (24 h). F) Expression of miR-155 were measured by qRT-PCR after stimulation (24 h) with TNF-α, or in combination with increasing dosage of IFN-γ, normalized to untreated. *, $p < 0.05$ and ****, $p < 0.0001$.

3.6 miR-155 directly binds to PD-L1 3'-UTR

There are two potential binding sites for miR-155 on the 3'-UTR of PD-L1 (Figure 3.13A) that are conserved in human and mice. Site 1 is located at the far end of the 3'-UTR (2587-2593) and Site 2 is situated in the middle of the 3'-UTR (1335-1341). Luciferase reporter assays were performed to determine direct regulation of PD-L1 by miR-155 (done by Kunal Shah, Barts Cancer Institute, UK) (Figure 3.13B). These are reporters that are transfected

into cells that can provide an indication of translation efficiency of the mRNA 3'-UTR. In addition, this provides an evaluation of the functional relevance of miRNAs on target mRNAs. A dual luciferase reporter system (Firefly/Renilla luciferase) is used to provide normalisation for the assay and to prevent off-target effects from transfection. The Renilla luciferase coding sequence is situated upstream of the 3'-UTR so that any regulation of the luciferase, or change in luminescence, is linked to the 3'-UTR itself. While a transfection control is provided by the Firefly luciferase. Furthermore, the assay required co-transfection of miR-155 mimic which are double-stranded RNA olignonucleotides that are designed to function as endogenous, mature miRNAs. A non-targeting mimic was used as a control for this particular transfection.

To investigate whether miR-155 can directly bind to the 3'-UTR of PD-L1, mutagenesis of the miR-155 binding sites was performed to prevent binding. Wild-type, single or double mutated miR-155 binding sites were co-transfected with miR-155 mimics in HeLa cells (Figure 3.13C). Mutation of Site 1 in the PD-L1 3'-UTR led to a significant increase (~35%) in luciferase reporter activity compared to wild-type 3'-UTR. Whereas, mutation of Site 2 had a lower effect (~22%). Mutation of both miR-155 binding sites further enhanced luciferase activity (~49%). Constructs containing the wild-type and mutated version of PU.1 3'-UTR, a previously validated miR-155 target (Vigorito et al. 2007), were used as controls for these assays. Compared to wild-type, mutation of PU.1 increased luciferase activity by 52%. These data suggest that the activity of miR-155 on the 3'-UTR of PD-L1 is relatively similar to a known target mRNA.

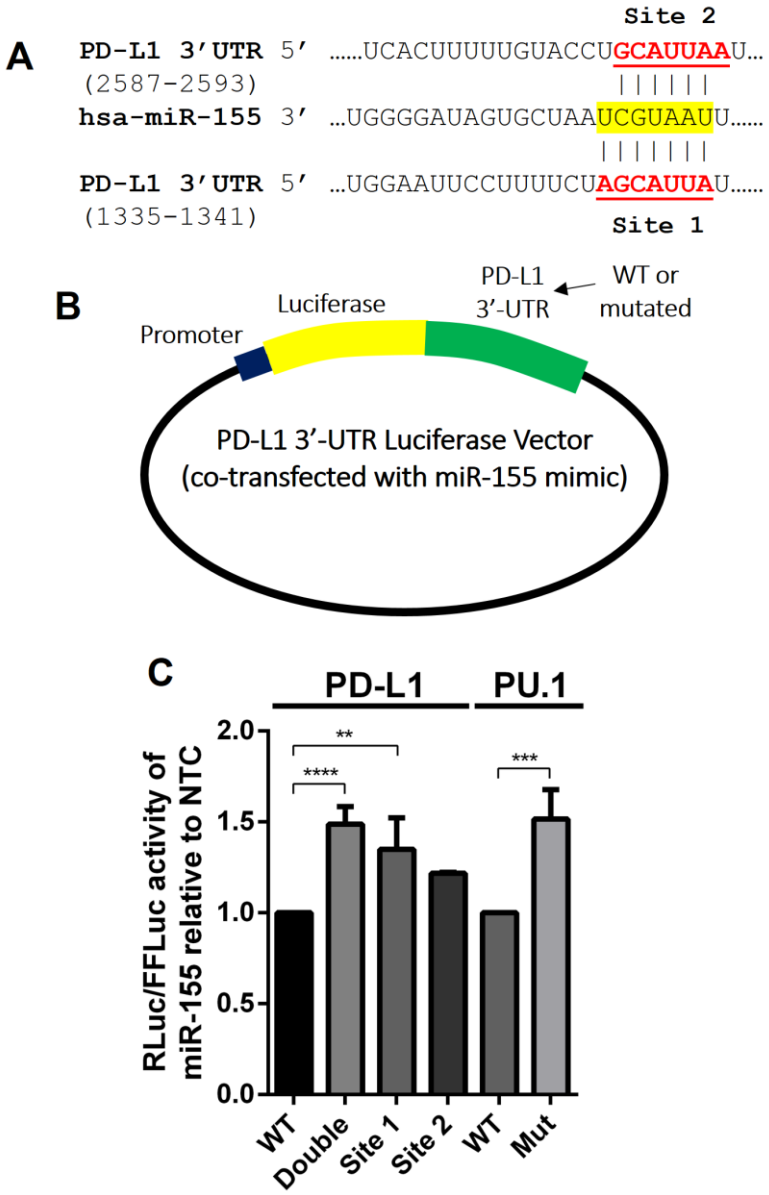

Figure 3.13. **miR-155 directly binds to PD-L1 3'-UTR.** A) Computer prediction software (Targetscan) identified two possible miR-155 binding sites on PD-L1 3'-UTR. B) The PD-L1 3'-UTR from HeLa cells was subcloned either as wild-type or with mutations introduced at miR-155 binding sites (as described in Materials and Methods). A luciferase coding sequence is located upstream and linked to the 3'-UTR to measure translation efficiency. C) Relative Renilla luciferase (RLuc) to Firefly luciferase (FFLuc) activity for PD-L1 wild-type (WT) 3'-UTR, PD-L1 double mutant 3'-UTR, PD-L1 mutant 3'-UTR at 1335-1341 (Site 1) and 2587-2593 (Site 2), performed in HeLa cells transfected with miR-155 mimics (48 h). The WT and mutated 3'-UTR of PU.1, a known miR-155 target, was used as control. Statistical test used was one-way ANOVA using Tukey's multiple comparisons test, n = 3–4 independent experiments, normalized to non-targeting control (NTC). **, $p < 0.01$; ***, $p < 0.001$; ****, $p < 0.0001$.

3.7 miR-155 regulates PD-L1 expression in response to IFN-γ and TNF-α

To determine the effect of miR-155 expression on PD-L1, I transfected miR-155 mimics into HDLECs to overexpress miR-155 activity (Figure 3.14A and B). This introduced a 10^4-fold increase in mature miR-155 expression compared to the NTC mimic. Overexpression of miR-155 increased the levels of PD-L1 mRNA in both untreated and IFN-γ and TNF-α-activated HDLECs (Figure 3.14C and D). At protein level, miR-155 overexpression resulted in significant downregulation of induced PD-L1 expression after IFN-γ and TNF-α stimulation (Figure 3.14E-G). No change in expression was observed in untreated cells. Moreover, the expression and phosphorylation of STAT1 were significantly increased in untreated and stimulated HDLECs (Figure 3.15A-C).

Next, I established the function of endogenous miR-155 on PD-L1 expression using miRNA inhibitors. These are single-stranded, RNA oligonucleotides that can bind specifically to the target miRNA and sequester the function of the miRNA strand. Inhibition of miR-155 resulted in significant upregulation of IFN-γ and TNF-α-induced PD-L1 expression (Figure 3.16A-C). No significant change was observed in untreated cells or at the mRNA level in activated HDLECs. Suppressor of cytokine signalling 1 (SOCS1), a reported target of miR-155 in macrophages and T reg cells (Androulidaki et al. 2009; Lu et al. 2009) was noticeably increased after inhibition of miR-155, although no change upon overexpression of miR-155 was observed in HDLECs (Figure 3.14). No change in the fold induction of PD-L1 mRNA after IFN-γ and TNF-α stimulation was observed, compared to NTC (Figure 3.16D).

The kinetics of miR-155 activity on the induction of PD-L1 expression were assessed using an earlier (8 h) and later (48 h) time-point for IFN-γ and TNF-α stimulation (Figure 3.17A and B). Inhibition of miR-155 showed an increase in PD-L1 protein expression at all time-points compared to NTC. Where between 8-24 h the effect of miR-155 was most noticeable and is consistent with my findings on the kinetics of PD-L1 induction by IFN-γ and TNF-α in HDLECs. The level of STAT1 was significantly increased in IFN-γ and TNF-α-stimulated cells but resulted in no overall change in relative phosphorylation (Figure 3.18A-E). Inhibition of miR-155 also increased expression of SOCS1 and STAT3. Taken together, these data demonstrate that miR-155 carries the functional capacity to affect the onset and maximal levels of PD-L1 expression following IFN-γ and TNF-α activation. This may represent an incoherent feed-forward loop where activated HDLECs produce both PD-L1 and miR-155, which in turn fine-tunes the induction of PD-L1 protein expression.

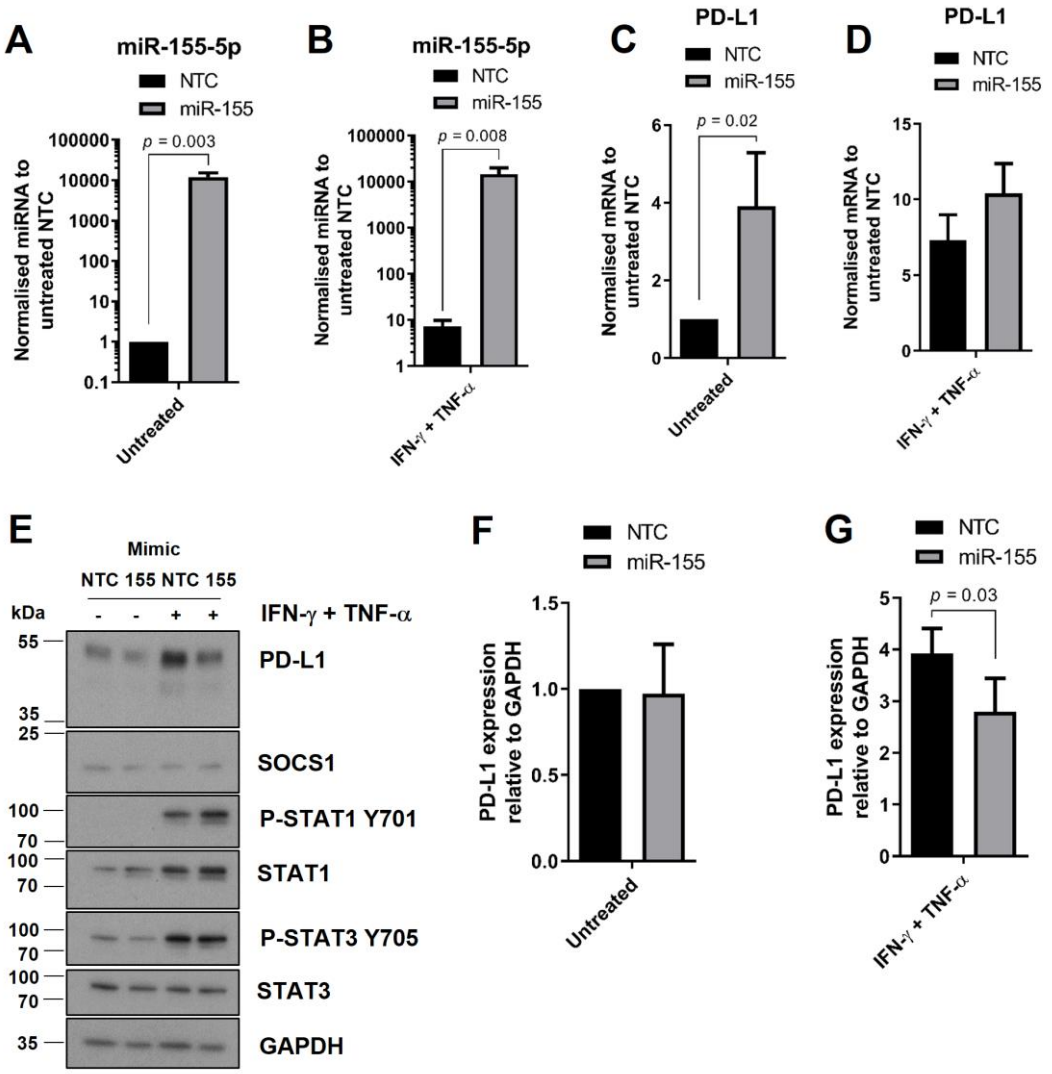

Figure 3.14. **miR-155 regulates PD-L1 expression in response to IFN-γ and TNF-α.** HDLECs were transfected with miR-155 or NTC mimics (48 h) and treated with IFN-γ and TNF-α (24 h). A and B) The expression of miR-155 in (A) untreated cells (no cytokine stimulation) and (B) IFN-γ and TNF-α treated cells was measured by qRT-PCR and normalised to untreated NTC. C and D) PD-L1 mRNA expression was determined in (C) untreated cells and (D) treated cells after transfection of NTC / miR-155 mimic and with either nil or IFN-γ and TNF-α stimulation by qRT-PCR and normalised to untreated NTC. E) Protein expression analysed by western blot following IFN-γ and TNF-α stimulation (24 h) in HDLECs transfected with miR-155 mimics (48 h). F and G) Quantification of western blot analysis on PD-L1 expression in (F) untreated cells and (G) IFN-γ and TNF-α-treated cells following miR-155 mimic transfection, normalized to untreated (NTC) and GAPDH expression. Unpaired Student's t test was used to compare NTC/miR-155-transfected within untreated or IFN-γ and TNF-α-treated subgroups. Significance is marked with a *p* value. n = 3 independent experiments.

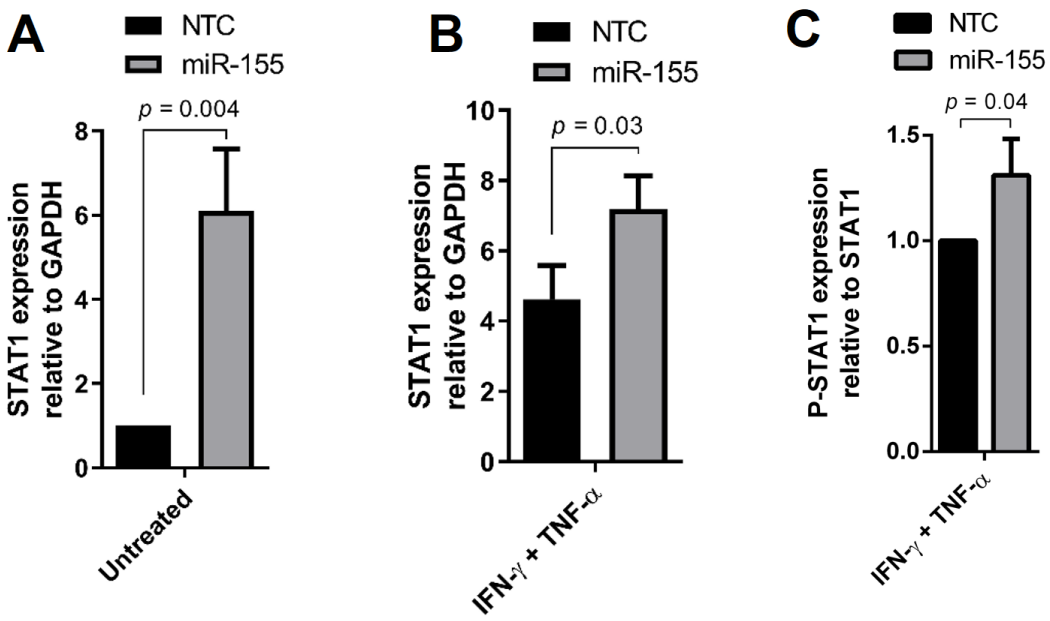

Figure 3.15. **miR-155 overexpression affects STAT1 protein expression.** HDLECs were transfected with miR-155 mimics or NTC (48 h) and treated with IFN-γ and TNF-α (24 h). Cells were subsequently harvested for protein lysates. A-C) Western blot quantification of STAT1 normalised to GAPDH expression in (A) untreated and (B) IFN-γ and TNF-α-stimulated samples, (C) phosphorylated STAT1 expression normalised to total STAT1 levels in stimulated samples. Unpaired Student's t test was used to compare NTC/miR-155-treated samples within either untreated (no cytokine stimulation) or IFN-γ and TNF-α-treated subgroups. Significance is marked with a *p* value. n = 3 independent experiments.

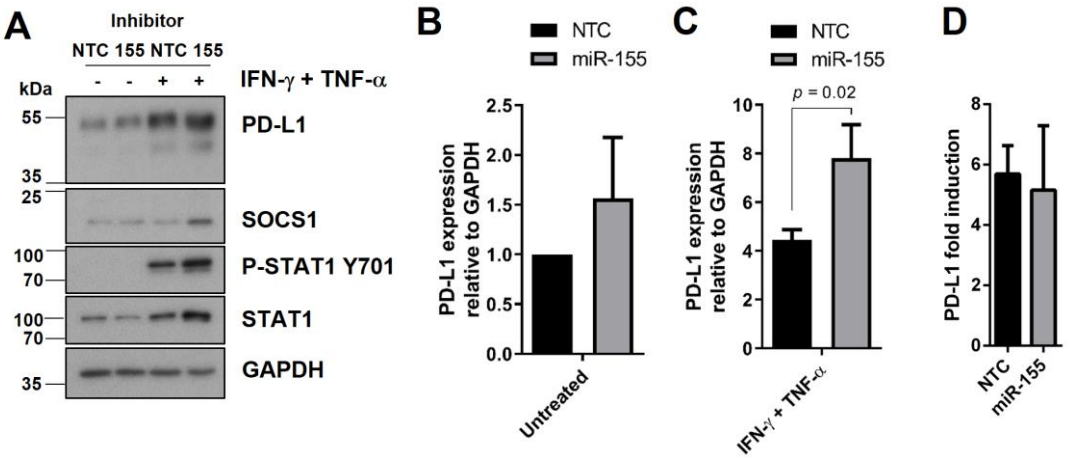

Figure 3.16. **Inhibition of miR-155 results in increased PD-L1 expression following IFN-γ and TNF-α activation.** HDLECs were transfected with miR-155 or NTC inhibitors (48 h) and treated with IFN-γ and TNF-α (24 h). A) Cells were harvested and analysed for protein expression by western blot. B and C) Western blot quantification of PD-L1 expression in the presence of miR-155 inhibitors in (B) untreated and (C) IFN-γ and TNF-α samples, normalized to untreated (NTC) and GAPDH expression. D) PD-L1 mRNA fold-induction following IFN-γ and TNF-α stimulation (24 h) in HDLECs transfected with miR-155 inhibitors (48 h), measured by qRT-PCR and normalised to respective untreated samples. Unpaired Student's t test was used to compare miR-155-treated and NTC samples within either untreated (no cytokine stimulation) or IFN-γ and TNF-α-treated subgroups. Significance is marked with a *p* value. n = 3 independent experiments.

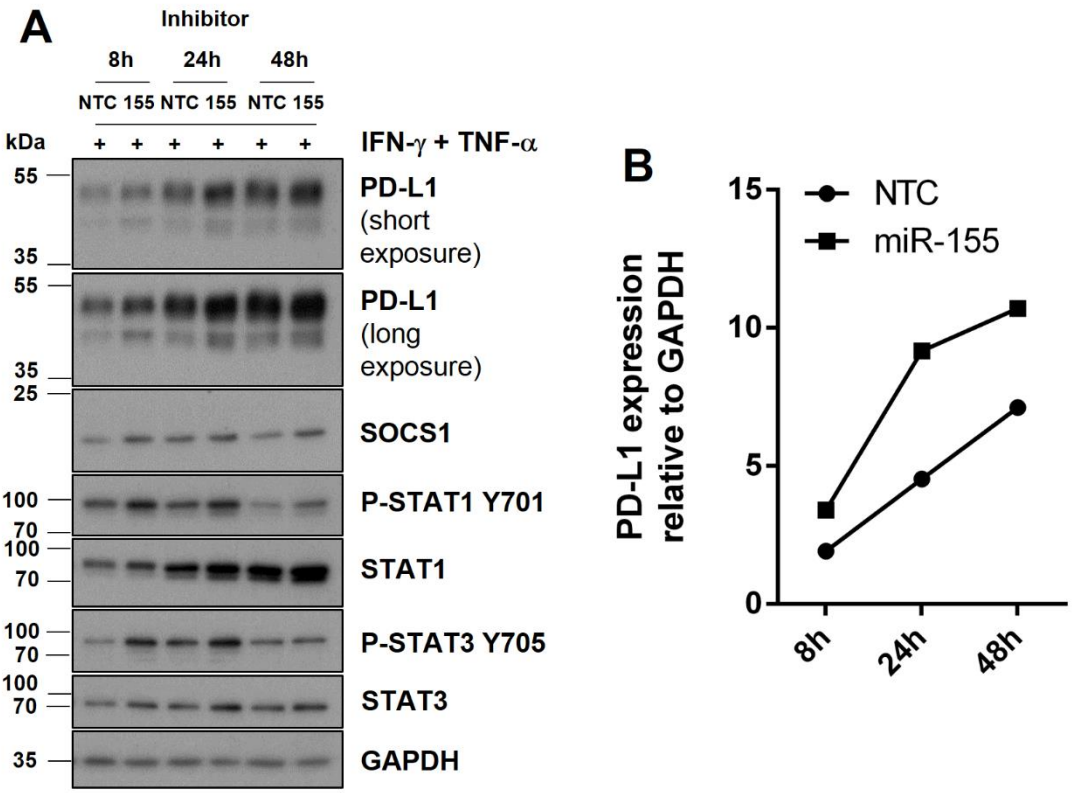

Figure 3.17. **miR-155 regulates the kinetics of PD-L1 induction.** HDLECs were transfected with miR-155 or NTC inhibitors (48 h) and treated with IFN-γ and TNF-α. A) Lysates were analysed for protein expression by western blot. B) Western blot quantification of time course (A) showing expression of PD-L1 after transfection of miR-155 inhibitors, compared to NTC and relative to GAPDH expression. n = 1 experiment.

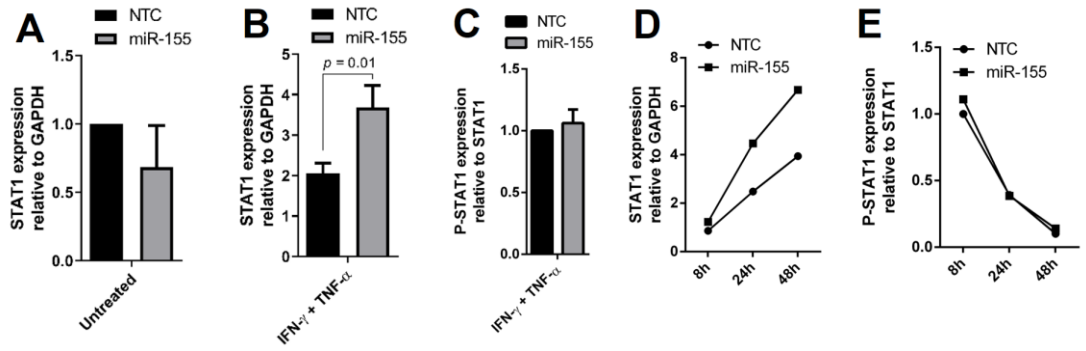

Figure 3.18. **miR-155 inhibition affects induced STAT1 expression but not phosphorylation.** HDLECs were transfected with miR-155 inhibitors (48 h), treated with IFN-γ and TNF-α (8, 24 or 48 h) and analysed by western blot. A and B) Quantification of STAT1 protein expression after 24 h in (A) untreated and (B) IFN-γ and TNF-α-activated samples, normalised to GAPDH, as assessed by western blot. C) Quantification of phosphorylated STAT1 expression after 24 h, normalised to total STAT1 levels. D) Western blot quantification of STAT1 protein expression from time course (Figure 3.17), normalised to GAPDH. E) Quantification of phosphorylated STAT1 compared to total levels of STAT1 from time course (Figure 3.17). Unpaired Student's t test was used to compare miR-155-treated and NTC samples within either untreated (no cytokine stimulation) or IFN-γ and TNF-α-treated subgroups. Significance is marked with a *p* value. n = 3 independent experiments.

3.8 HFF characterisation of PD-L1 expression and kinetics

Next, I wanted to determine whether regulation of PD-L1 by miR-155 in vascular cells could occur in a stromal cell type. To this aim, primary human foreskin fibroblasts (HFFs) were characterised for PD-L1 and miR-155 expression. At basal levels, PD-L1 is lowly expressed but inducible by IFN-γ and TNF-α in HFFs (Figure 3.19A). IFN-γ was the main inducer of PD-L1 and expression correlated with an increase in phosphorylation of STAT1. This was further amplified in combination with TNF-α, which was translated to expression at the cell surface level (Figure 3.19B). PD-L1 is transcriptionally induced by IFN-γ and transcripts are clearly elevated in a synergistic pattern in combination with TNF-α stimulation (Figure 3.20A). Expression of IL-1β is also enhanced by TNF-α and further increased with IFN-γ (Figure 3.20B). Although, IFN-γ stimulation alone does not affect IL-1β. I found that miR-155 is similarly induced in response to inflammatory stimuli at a similar fold change to HDLECs (Figure 3.21A and B). In activated HFFs, miR-155 reached peak levels of expression at 24 h and stayed at high levels until 48 h.

Next, I overexpressed miR-155 expression using mimics in HFFs, which resulted in downregulation of induced PD-L1 protein expression (Figure 3.22A-C). An increase in phosphorylated STAT1 was observed as well as increased PD-L1 mRNA. Inhibition of miR-155 in activated HFFs led to an increase in PD-L1 expression (Figure 3.23A-C). No significant change in PD-L1 mRNA. Furthermore, a time-course showed that overexpression of miR-155 controlled the kinetics of miR-155 induction between 8 and 48 h (Figure 3.24). Whereas, the effects of inhibiting miR-155 activity were also seen as early as 8 h on PD-L1 expression. Altogether, these results suggest that miR-155-mediated suppression of PD-L1 is not limited to HDLECs and is observed in other primary dermal cells reacting to inflammatory stimuli.

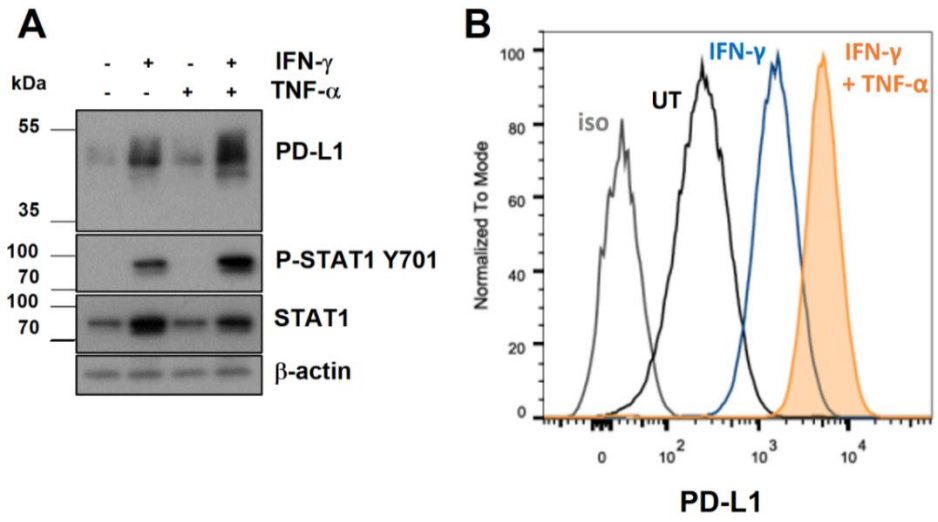

Figure 3.19. **PD-L1 is expressed in HFFs and can be synergistically induced by IFN-γ and TNF-α**. Human foreskin fibroblasts (HFFs) were assessed for expression of PD-L1 at both total and surface protein level using two different analytical techniques. A) Western blot analysis following 24 h stimulation of HFFs with IFN-γ and TNF-α. B) Flow cytometric analysis showing PD-L1 surface expression (MFI) after stimulation (24 h) on live HFFs. MFI of PD-L1 staining: IFN-γ + TNF-α = 5301, IFN-γ = 1583, UT = 255, iso = 25.7.

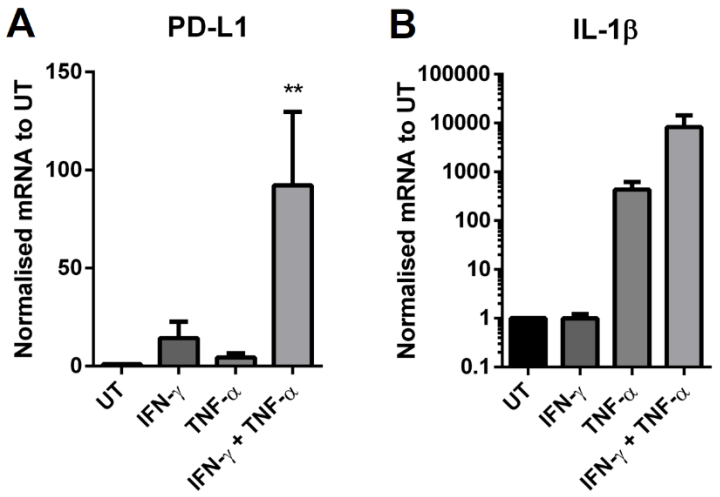

Figure 3.20. **Effect of IFN-γ and TNF-α activation on PD-L1 and IL-1β transcription.** A) PD-L1 and B) IL-1β mRNA levels in HFFs were measured by qRT-PCR after stimulation (24 h), data is normalized to untreated. One-way ANOVA was calculated with Tukey's multiple comparisons test for (A), n = average of 3 independent experiments. (B), n = average of 2 independent experiments. **, $p < 0.01$.

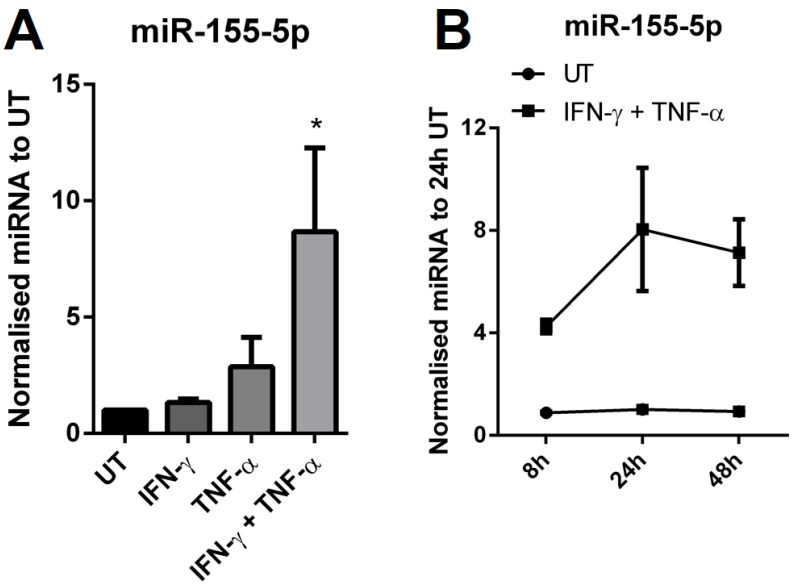

Figure 3.21. **Effect of IFN-γ and TNF-α activation on miR-155 expression levels.** A) miR-155 expression was measured by qRT-PCR following stimulation (24 h) in HFFs and normalized to untreated. Statistical test used was one-way ANOVA using Tukey's multiple comparisons test. B) Time course of miR-155 expression after IFN-γ and TNF-α stimulation (8, 24, and 48 h) and normalized to untreated (24 h), n = 3 independent samples.

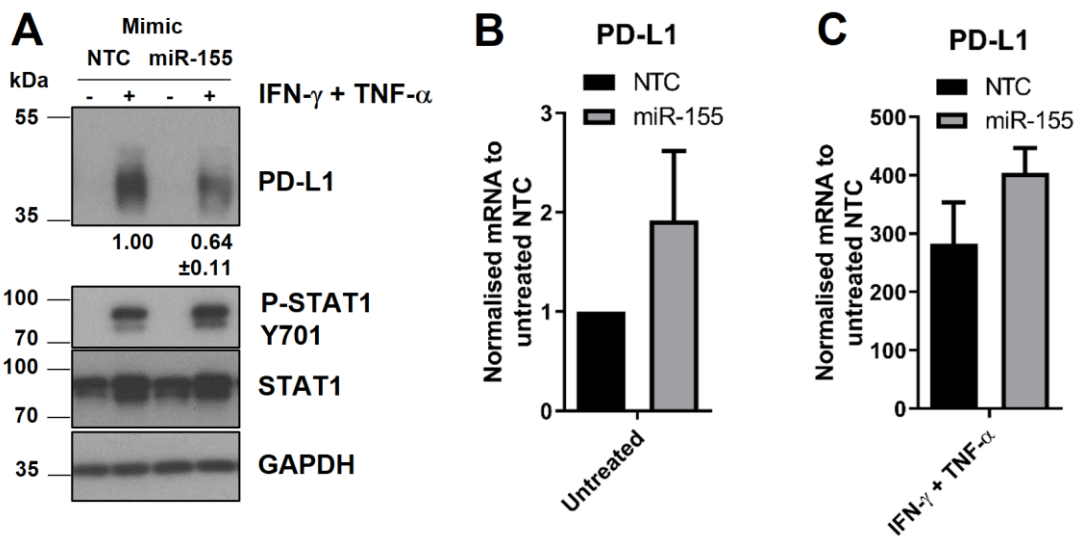

Figure 3.22. **miR-155 regulates PD-L1 expression in response to IFN-γ and TNF-α in HFFs.** A) Protein expression following IFN-γ and TNF-α stimulation (24 h) in HFFs transfected with miR-155 mimics (48 h). Western blot quantification of PD-L1 normalized to IFN-γ and TNF-α treated NTC with average expression and standard deviation stated below (n = 2 independent experiments). B and C) PD-L1 mRNA expression in (B) untreated or (C) IFN-γ and TNF-α-stimulated (24 h) HFFs transfected with miR-155 mimics (48 h).

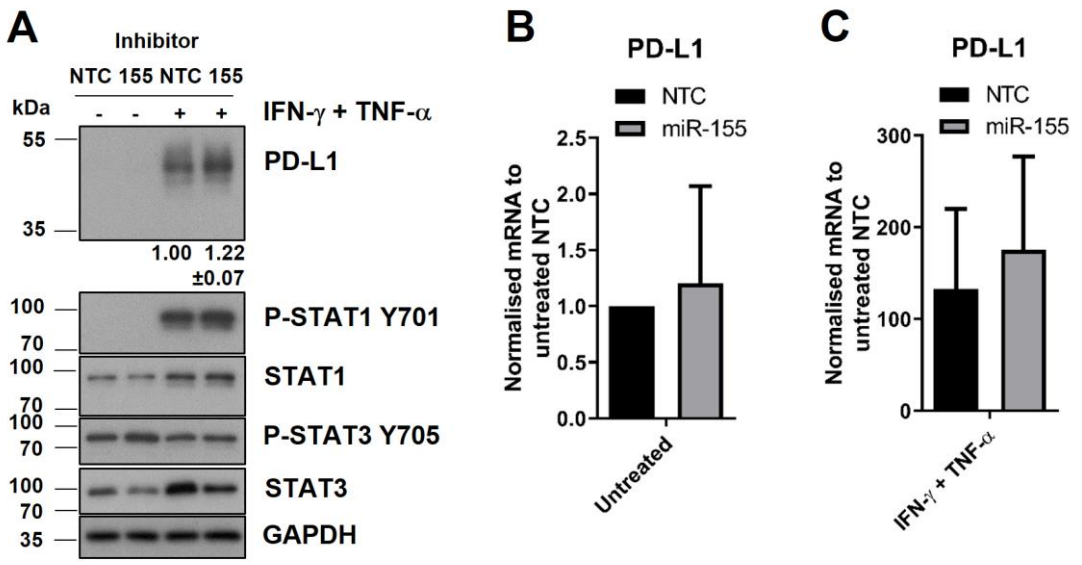

Figure 3.23. **Inhibition of miR-155 increases PD-L1 expression following IFN-γ and TNF-α activation in HFFs.** A) Protein expression following IFN-γ and TNF-α stimulation (24 h) in HFFs transfected with miR-155 inhibitors (48 h). Western blot quantification of PD-L1 normalized to IFN-γ and TNF-α treated NTC with average expression and standard deviation stated underneath (n = 2 independent experiments). B and C) PD-L1 mRNA expression in (B) untreated or (C) IFN-γ and TNF-α-stimulated (24 h) HFFs transfected with miR-155 inhibitors (48 h).

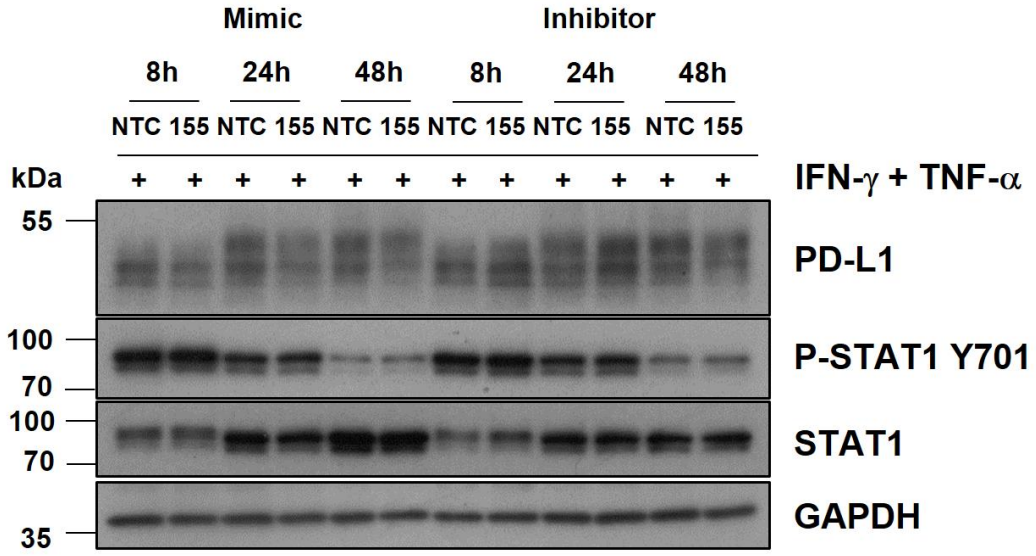

Figure 3.24. **Time-course to show effect of overexpression/inhibition of miR-155 on PD-L1 expression following IFN-γ and TNF-α activation in HFFs.** Protein expression following IFN-γ and TNF-α stimulation (8, 24, 48 h) in HFFs transfected with miR-155 mimics (left side) or miR-155 inhibitors (right side) (48 h). n =1 experiment.

3.9 Overexpression of miR-218 alters constitutive and induced PD-L1 expression

From the small RNA sequencing, I identified other miRNAs that are regulated by IFN-γ and TNF-α stimulation including the expression of miR-218-5p (referred to as miR-218) (Figure 3.10B). Validation of miR-218 showed that this was on average the second highest miRNA induced by IFN-γ and TNF-α (~3 fold) (Figure 3.10C). Furthermore, miR-218 is strongly induced by TNF-α and to a lesser extent by IFN-γ, however, there seemed to be no synergistic activation of miR-218 with both cytokines (Figure 3.25A). Similar to experiments with miR-155, I transfected miR-218 mimics into HDLECs to determine its functional relevance (Figure 3.25B). Although, Targetscan did not predict any binding sites for PD-L1, overexpression of miR-218 resulted in an increase to constitutive and induced PD-L1 protein expression HDLECs (Figure 3.26A). Levels of PD-L1 mRNA expression were also increased with miR-218 overexpression compared to NTC but in a similar manner to miR-155 (Figure 3.26B). In addition, there was an increase to phosphorylated levels of STAT1. The 3'-UTR of PROX1 was predicted to have miRNA binding sites for miR-155 and miR-218, however, protein expression of PROX1 remained unchanged after overexpression of either miRNA (Figure 3.26A).

To test miR-218 regulation of PD-L1 expression in other cell types, I found that miR-218 is also induced in HFFs by IFN-γ and TNF-α (Figure 3.27A). Overexpression of miR-218

using mimics elevated PD-L1 expression in both untreated and treated cells and similarly PD-L1 mRNA expression was increased compared to NTC (Figure 3.27B and C). These data suggest that there may be a form of regulation of PD-L1 by miR-218, however, the mechanism of action remains unclear since there are no predicted miR-218 binding sites on the 3'-UTR of PD-L1. Other possibilities could include miR-218-mediated activation of PD-L1 translation via the 5'-UTR or relief of repression by suppressing a negative regulator of PD-L1 (Vasudevan 2012).

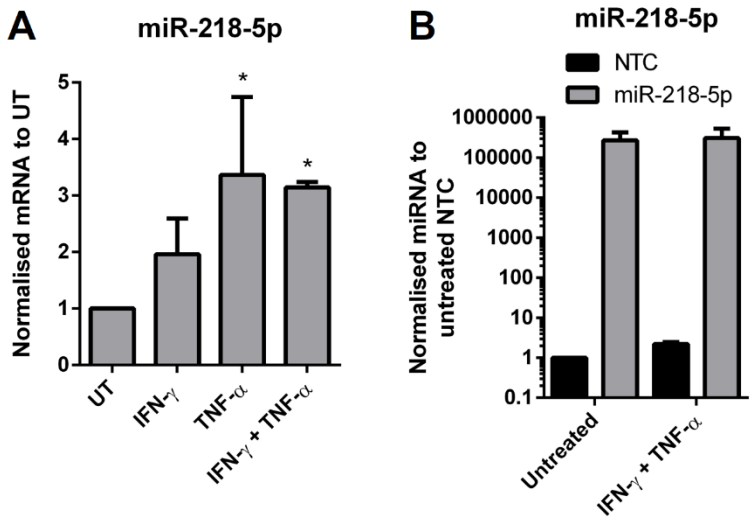

Figure 3.25. **miR-218 expression is regulated by IFN-γ and TNF-α.** A) miR-218 expression was measured by qRT-PCR following stimulation (24 h) in HDLECs and normalized to untreated. Statistical test used was one-way ANOVA using Tukey's multiple comparisons test. n = 3 independent experiments. B) HDLECs were transfected with miR-218 mimics (48 h) and treated with IFN-γ and TNF-α (24 h). The expression of miR-218 was measured by qRT-PCR and normalised to untreated NTC. *, $p < 0.05$.

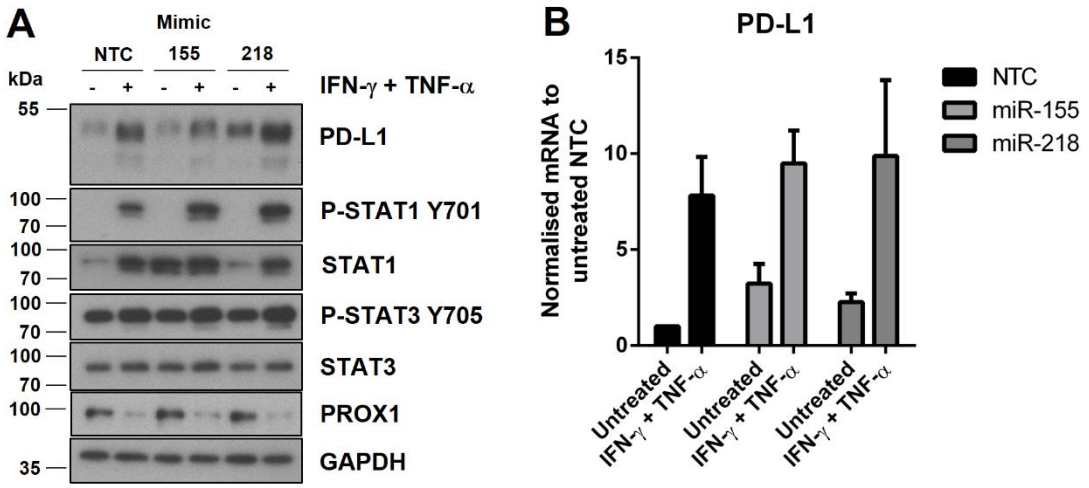

Figure 3.26. **Overexpression of miR-218 induces expression of PD-L1 in HDLECs.** HDLECs were analysed following IFN-γ and TNF-α stimulation (24 h) in cells transfected with miR-155 or miR-218 mimics (48 h). A) Protein expression assessed by western blot and B) PD-L1 mRNA expression measured by qRT-PCR. n = 2 independent experiments.

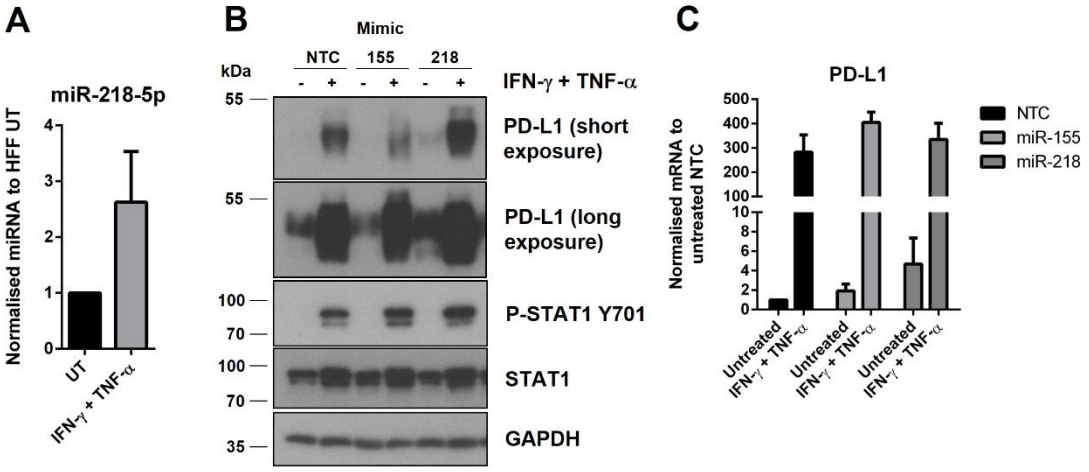

Figure 3.27. **Overexpression of miR-218 induces expression of PD-L1 in HFFs.** A) miR-218 expression was measured by qRT-PCR in HFFs treated with IFN-γ and TNF-α (24 h). B and C) HFFs were analysed following IFN-γ and TNF-α stimulation (24 h) in cells transfected with miR-155 or miR-218 mimics (48 h). B) Protein expression assessed by western blot and C) PD-L1 mRNA expression measured by qRT-PCR. n = 2 independent experiments.

3.10 Dicer knockdown does not affect PD-L1 protein expression in LECs

Having demonstrated that PD-L1 protein expression is regulated at the posttranscriptional level by miRNAs, I further investigated whether Dicer activity had the capacity to modulate PD-L1. Dicer is essential for the majority of miRNA biogenesis and silencing (Kim et al.

2016), and has been shown in HUVECs to regulate a subset of miRNA profiles including miR-126 and angiogenesis (Kuehbacher et al. 2007; Suárez et al. 2007). By silencing Dicer, this would potentially provide information on the larger effect of miRNA regulation of PD-L1. These experiments analysed the knockdown of Dicer in untreated and IFN-γ and TNF-α-stimulated LECs. I confirmed loss of Dicer expression after cells were transfected with siRNAs targeting Dicer (Figure 3.28A). PD-L1 protein expression remained largely unaffected in cells with Dicer knockdown, compared to control, and there was some decrease in PD-L1 mRNA expression (Figure 3.28B). In addition, Dicer knockdown had a modest decrease in the expression of miR-126, miR-155 and miR-218 in untreated cells but did not have any effect in the induced expression of miR-155 or miR-218 (Figure 3.28C). Altogether, these data show that Dicer knockdown in LECs result in an incomplete inhibition of miRNAs, and that Dicer does not directly affect PD-L1 protein expression. Kuehbacher *et al.* also reported that a subset of miRNAs were reduced after Drosha and Dicer silencing, which may be due to insufficient knockdown of protein or a higher stability of some miRNAs (Kuehbacher et al. 2007). This could suggest that some miRNAs have a longer half-life and a time-course experiment to observe the effects of Dicer knockdown could be performed (Rüegger & Großhans 2012). An alternative method would be to knockdown AGO2, which is reported to be the most critical of all AGO in the miRNA pathway and can significantly affect both protein activity and mRNA levels (Schmitter et al. 2006).

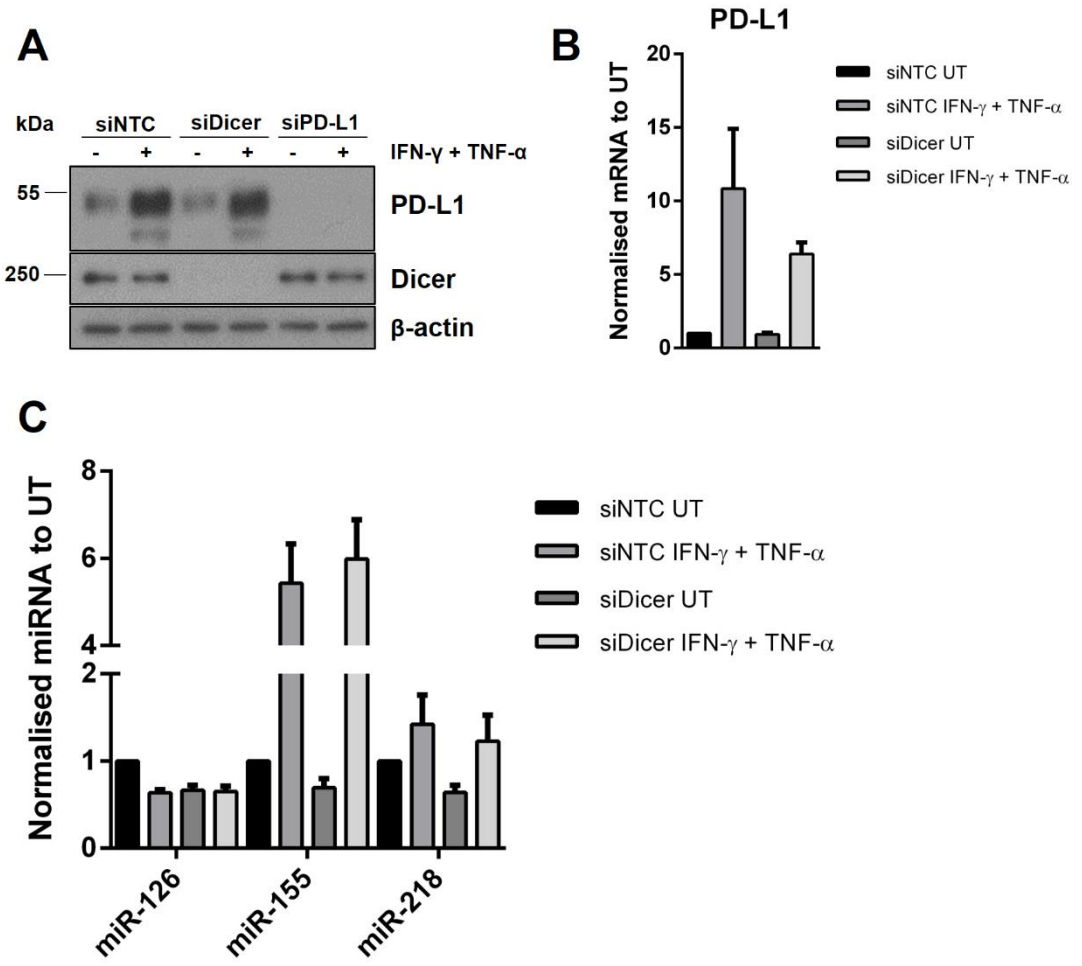

Figure 3.28. **Dicer knockdown does not affect PD-L1 protein expression in LECs.** Transfection of LECs with siRNAs targeting non-targeting control (NTC), Dicer and PD-L1 (48 h) was followed by IFN-γ and TNF-α stimulation (24 h). A) Protein expression in untreated and IFN-γ and TNF-α-stimulated LECs. B) PD-L1 mRNA expression was measured by qRT-PCR. C) miR-126, miR-155 and miR-218 expression were analysed by qRT-PCR. n = 3 independent experiments.

3.11 Chapter discussion

In this chapter, I assessed PD-L1 expression, the miRNA landscape and lineage commitment markers of primary cells in response to pro-inflammatory cytokines IFN-γ and TNF-α. The main finding in this chapter reveals an incoherent feed-forward loop that is initiated by IFN-γ and TNF-α which induces PD-L1 expression (Figure 3.29). Concurrently, IFN-γ and TNF-α promotes the induction of PD-L1 targeting miRNAs. I identified miR-155 as a posttranscriptional regulator of PD-L1 that fine-tunes the kinetics and maximal levels of PD-L1 induction in primary dermal cells responding to inflammation. This is in contrast to miR-513 which blocks the induction of PD-L1 but is suppressed by IFN-γ signalling (Gong et al.

2009). In addition, miR-218 is also induced by IFN-γ and TNF-α in primary cells and acts to increase PD-L1 expression. Overall, the data reveal that miRNAs induced in response to inflammation are critical components of regulatory loops that can control the expression of immune checkpoint molecules and thereby mediate a functional role in immunosuppression.

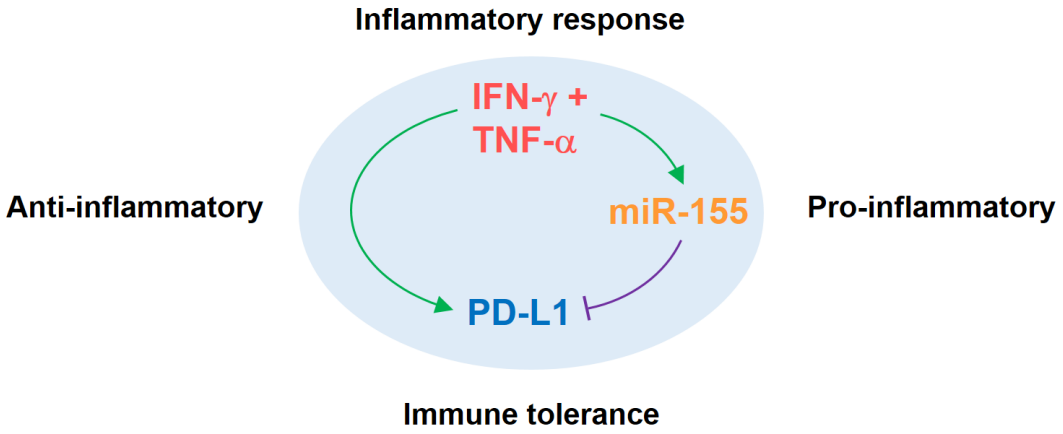

Figure 3.29. **The IFN-γ/TNF-α/miR-155/PD-L1 incoherent feed-forward loop**. Cartoon depicting the inflammatory activation of cells by IFN-γ and TNF-α, which leads to the production of both PD-L1 and miR-155. PD-L1 expression mediates immune tolerance, whereas the effect of miR-155 is to directly inhibit the induced expression of PD-L1 protein to promote inflammation. IFN-γ and TNF-α regulates the initial induction of PD-L1 and fine-tunes the expression of PD-L1 via miR-155 in a balance between inflammation and tolerance.

miR-155 regulates PD-L1 protein expression

The finding that miR-155 regulates PD-L1 expression is significant. As briefly mentioned, miR-155 is a known multifunctional modulator of immune system and primary component of the inflammatory response (Chapter 1.2.4). The mechanism of this regulatory loop is presumed to be the blocking of PD-L1 translation or protein synthesis rather than affecting the degradation of PD-L1 mRNA. In addition, the effects of miR-155 on the JAK/STAT pathway cannot be ruled out and may contribute towards overall PD-L1 protein expression.

miR-155 is described in many aspects of the immune system, where it has a crucial role towards to the development and maintenance of the immune response. miR-155 was first described as B-cell integration cluster (bic) in chickens (Tam et al. 1997). The precursor of miR-155 in chickens is encoded within bic exon 2 and that miR-155 is also expressed in mice and humans (Lagos-Quintana et al. 2002). The stem-loop sequence of pre-miR-155 has high evolutionary conservation in the region that corresponds to mature miR-155. In several types of B cell lymphomas and solid tumours, miR-155 expression is abnormally expressed,

where it is regarded as an oncomir and associated with unfavourable prognosis (Eis et al. 2005; Volinia et al. 2006; Yanaihara et al. 2006). In the mammalian immune system, miR-155 is responsible for regulating a broad range of immune cell types including subsets of T cells, B cells and DCs. Mice with mutant miR-155 have normal numbers of most lymphoid and myeloid subsets (Vigorito et al. 2013). However, the importance of miR-155 is shown upon activation of cells, where mutant bic/miR-155 mice are found to be immune-deficient and have impaired lymphocyte responses, including failure of DCs to efficiently activate T cells (Rodriguez et al. 2007). In response to B cell receptor (BCR) activation, miR-155 is induced where it directly inhibits the transcription factor PU.1 (Lu et al. 2014). This enables plasma cell commitment in the germinal centre due to downregulation of PAX5. If the miR-155 binding site on PU.1 mRNA is mutated, this leads to increased PU.1 expression during B cell activation with defective class-switch recombination and plasma cell differentiation. Moreover, activation-induced deaminase (AID), required for class-switch recombination and somatic hypermutation, is upregulated in response to BCR signalling and the expression of AID can be repressed by miR-155 affecting B cell immune function (Teng et al. 2008). In addition, miR-155 is required for production of immunoglobulin class-switch differentiation of B cells by targeting transcription factor PU.1 (Vigorito et al. 2007). Upon T cell activation, miR-155 is induced and promotes Th1 differentiation by targeting IFN-γRα in Th1 cells (Thai et al. 2007; Banerjee et al. 2010). Given that miR-155 regulates several processes in immune cells, my results show an additional mechanism that miR-155 can potentially regulate the activation of the immune response through immune checkpoint expression.

A broad range of inflammatory cytokines induce the activation of miR-155 including LPS, poly I:C and TNF-α (O'Connell et al. 2007; Tili et al. 2007; Stanczyk et al. 2008; Ceppi et al. 2009). Induction of miR-155 was found to be dependent on TNFR1 and JNK signalling in macrophages (O'Connell et al. 2007). Both IFN-γ and TNF-α were shown to induce miR-155 expression in mesangial cells and cells of the retinal pigment epithelium (Imaizumi et al. 2010; Villarino et al. 2017). Here, I identified a consistent finding in primary dermal cells that miR-155 is synergistically enhanced by IFN-γ and TNF-α. Up to now, TNF-α was associated with stabilisation of PD-L1 through NF-κB signalling (Lim et al. 2016). I show here that TNF-α is required for maximal induction of PD-L1 where it may also regulate the localisation of PD-L1 to the cell surface.

The association between inflammatory activation, miR-155 and PD-L1 reveals the existence of an incoherent feed-forward loop in primary stromal fibroblasts/vascular cells. Moreover, a regulatory loop involving miR-155 was found in macrophages where TLR4 signalling is

activated by LPS (Androulidaki et al. 2009). This led to differential expression of miRNAs such as miR-155 which enhanced TLR4 signalling. Stimulation of LPS also induced expression of Akt, which was found to regulate miR-155 expression and response of macrophages to LPS. My findings show that at least the phosphorylation of Akt S473 is downregulated at 16 and 24 h which may affect the expression of miR-155.

SOCS1 is a regulatory negative feedback mechanism of several cytokine signalling pathways including IFN-γ/STAT1 signalling which inhibits the activity of JAK phosphorylation and has been demonstrated to be a direct target of miR-155 in human and mice (Androulidaki et al. 2009; Lu et al. 2009). In some cases, miR-155 expression is inversely correlated with SOCS1, as shown in breast cancer (Jiang et al. 2010). Overexpression of miR-155 has been shown to decrease SOCS1 and increase phosphorylation levels of JAK2 and phospho-STAT3 (Jiang et al. 2010; Zhao et al. 2013; Rasmussen et al. 2015). Furthermore, disrupting miR-155 regulation of SOCS1 in T regs, $CD8^+$ T cells and NK cells was shown to affect the immune response during autoimmunity and infection (Lu et al. 2015).

Interestingly, miR-155 suppresses expression of SOCS1 leading to enhanced STAT1 phosphorylation in macrophages (Wang et al. 2010), miR-155-deficient $CD8^+$ T cells display enhanced levels of STAT1 phosphorylation (Gracias et al. 2013). I observed that inhibition of miR-155 increased SOCS1 expression although overexpression of miR-155 did not affect SOCS1 levels in HDLECs. Moreover, we found no increase in STAT3 after miR-155 overexpression but rather an increase in phospho-STAT3 at 8 h after inhibiting miR-155. Additionally, I found that overexpression and inhibition of miR-155 both increased the levels of STAT1 indicating the existence of dose-dependent effects, in agreement with previous reports (Gracias et al. 2013; Lin et al. 2015). Inflammatory conditions promote the expression of miR-155, which through the regulation of SOCS1 and PD-L1 in different cell types, can have potential pro-inflammatory effects.

Overexpression of miR-218 regulates PD-L1 protein expression

Of the validated miRNAs that were selected from small RNA sequencing, miR-93-5p as part of the miR-25-93-106b cluster (Cioffi et al. 2017) and miR-217 (Miao et al. 2017) were later shown to regulate PD-L1 in cancer cells. I also identified that miR-218 is induced by IFN-γ and TNF-α. miR-218 has been shown to affect endothelial cell angiogenesis and migration (Small et al. 2010) and LPS-induced inflammation (H. Zhao et al. 2014) through targeting of the Slit-Robo pathway. Slit2 upregulates miR-218 expression which in turn inhibits Robo1 protein expression and produces an anti-inflammatory effect by suppressing LPS-induced signalling of the NF-κB pathway. In some cancers, miR-218 is downregulated suggesting

miR-218 acts as a tumour suppressor (Venkataraman et al. 2013; Mathew et al. 2014). An indirect target of miR-218 was found to be HIF-2α through its activity on multiple components of receptor tyrosine kinase signalling pathways such as EGF (Mathew et al. 2014). My findings show that overexpression of miR-218 increases the expression of PD-L1, while not a direct 3'-UTR target of miR-218. Although HIF-2α has been shown to regulate PD-L1 in hypoxic conditions (Messai et al. 2016), it is unlikely that primary dermal cells would produce much HIF-2α to affect PD-L1 expression. In untreated cells, overexpression of miR-218 increased some PD-L1 expression suggesting this may not be due to the anti-inflammatory effects of miR-218. This mechanism of miR-218 regulation of PD-L1 expression remains unexplained. RNA-binding proteins such as Pumilio (PUM1, PUM2) bind to the 3'-UTR of certain mRNAs and can act on mRNA stability or repression of translation (Vasudevan 2012). Using TargetScan, miR-218 has conserved binding sites for both PUM1 and PUM2 that could relief repression of PD-L1 mRNA translation. Overall, I showed that IFN-γ and TNF-α activation of miRNAs can lead to up- and downregulation of PD-L1 expression.

Loss of LEC lineage commitment markers in response to IFN-γ and TNF-α treatment

There was a significant decrease in all tested LEC lineage commitment markers (PROX1, VEGFR3, COUP-TFII and LYVE1) after IFN-γ and TNF-α activation. PROX1 and VEGFR3 regulate LEC differentiation and maintenance of lineage and downregulation of these molecules suggests that the integrity or growth of LECs was affected. Several reports have indicated that inflammation or TNF-α stimulation can lead to reduced PROX1 and LYVE-1 expression (Vigl et al. 2011; Huggenberger et al. 2011; Johnson et al. 2007; Oka et al. 2008). Activation of lymphatic vasculature can limit skin inflammation through promotion of fluid drainage and reduction of edema formation (Huggenberger et al. 2011). In addition, T cells can suppress growth of lymphatic vasculature through the production of IFN-γ, whereas B cells do not *in vivo* (Kataru et al. 2011). In T cell deficient models, there is an increase of LN lymphatic vasculature accompanied with higher levels of antigen-carrying DCs. T cells moderate immune responses through the lymphatic vasculature which respond to IFN-γ in order to maintain homeostasis (Kataru et al. 2011). A further study using a mouse melanoma model (K14-VEGFR3-Ig) that lacked LYVE-1^+ dermal lymphatic vessels found that lymphatic vessel remodelling and drainage was key for tumour-associated inflammation and immunity (Lund et al. 2016). There was a decrease in the number of infiltrating immune cells ($CD8^+$ T cells) and reduced trafficking of DCs from the tumour to the LN.

IL-3 has been reported to upregulate PROX1 through NF-κB activation and both IL-3 and LPS can upregulate VEGFR3 expression, indicating inflammatory factors can also induce LEC commitment markers (Gröger et al. 2004; Flister et al. 2010). PROX1 synergises with the p50 subunit but not p65 of NF-κB to induce VEGFR3 expression (Flister et al. 2010). Since NF-κB is also an effector of downstream TNF-α signalling, my results support that NF-κB regulates PROX1 expression. However, the stimulus may affect how the expression of PROX1 is regulated. Another explanation for the loss of lineage commitment markers could be due to the de-differentiation of LECs to BEC-like cells in response to physiological challenge (Srinivasan et al. 2007; Johnson et al. 2008). The plasticity of endothelial cells has been demonstrated from the switch between BEC to LEC in Kaposi's sarcoma (Hong et al. 2004; Wang et al. 2004).

Conclusion

Based on the above, I propose that miR-155 affects the JAK/STAT pathway through multiple mechanisms, likely in a cell type-specific manner. The observed effects of miR-155 mimics and inhibitors on PD-L1 protein expression in combination with the direct binding of the miRNA to the PD-L1 3'-UTR, demonstrate that direct targeting of PD-L1 by miR-155 is a crucial component of the cytokine receptor (IFNGR or TNFR)/miR-155/PD-L1 network. Overall, this study provides a novel perspective on the posttranscriptional regulation of PD-L1 during inflammation. I reveal a number of potentially PD-L1-targeting miRNAs as responsive to inflammatory challenge. These include miR-155, a multifunctional miRNA which plays a primary role in inflammation and can be induced by a broad range of inflammatory mediators. Concomitantly, I show that PD-L1 is induced in HDLECs upon inflammation and contributes towards immune suppression which is in line with previous findings in macrovascular endothelial cells (Mazanet & Hughes 2002; Rodig et al. 2003). Having shown that both IFN-γ and TNF-α are required for miR-155 regulation of PD-L1 *in vitro*, it would be unlikely in this context that either IFN-γ or TNF-α stimulation alone could induce this regulation. A limitation of this study would be that inflammatory environments are more complex than two cytokines and further experiments would be required to test this mechanism in pathological contexts such as in chronic inflammation. I show that in dermal vascular and stromal cells, miR-155 acts to suppress PD-L1 induction to potentially fine-tune the immune response. Moreover, miR-155 is expressed by a variety of immune cells and frequently overexpressed in cancer and chronic inflammatory diseases. miR-155 was shown to regulate the expression of CTLA-4, a negative regulator of T cell activation, in atopic dermatitis suggesting miR-155 contributes to chronic inflammation (Sonkoly et al. 2010). My findings contribute to the overall understanding of PD-L1 regulation in physiological and pathological contexts.

4. miRNA regulation of PD-L1 in in cancer cells

4.1. Introduction

From Chapter 1, I outlined the regulation of PD-L1 in cancer and in Chapter 3, identified miRNAs that regulate PD-L1 protein expression with a focus on miR-155. Both PD-L1 and miR-155 can have aberrant expression in several types of cancer (X. Wang et al. 2016; Bayraktar & Van Roosbroeck 2018). PD-L1 is expression is associated with poor clinical outcome in multiple cancers including renal cell carcinoma, bladder cancer (X. Wang et al. 2016). However, the expression of PD-L1 in lung cancer and melanoma can have both positive and negative prediction values suggesting using PD-L1 as a predictive biomarker can be limited. The expression of PD-L1 is heterogeneous which can be affected by a number of factors as described in Chapter 1, including miRNAs. Additional biomarkers could be used to facilitate those patients that can benefit from immunotherapy such as using miRNA biomarkers. Levels of miR-155 are often overexpressed in a variety of cancers such as B cell lymphoma, acute myeloid leukaemia, and solid tumours (breast, colon, lung cancers), frequently associated with poor prognosis (Eis et al. 2005; Faraoni et al. 2012). There are multiple cellular processes that miR-155 can affect which include tumour growth, migration and invasion of cells and EMT (Bayraktar & Van Roosbroeck 2018). Additionally, miR-155 has been associated with resistance to systemic chemotherapy and radiotherapy in different types of cancer. There is a requirement for more understanding in the function and immunoregulatory role of miR-155 in cancer cells. The findings of this chapter characterise the levels of PD-L1 and miR-155 found in a selection of cancer cell lines and indicate that miR-155 could regulate PD-L1 expression in cancer cells.

To extend my findings from primary cells, I investigated whether the mechanism of PD-L1 regulation by miR-155 is similar in cancer cells. The Cancer Genome Atlas (TCGA) Research Network has produced a large amount of data that is publicly available (The Cancer Genome Atlas Research Network et al. 2013). The data was accrued from characterisation of 33 different cancer types including 10 rare cancers (see Table 4.1 for specific details) which were selected for their poor prognosis and overall public health impact. The TCGA aimed to generate and interpret, quality-controlled molecular profiles at the DNA, RNA, protein and epigenetic levels for several hundreds of clinical tumours. The Pan-Cancer analysis project was a collaboration between many researchers of the TCGA research network that coordinated a collection of data at the Broad Institute's Firehose and the Memorial Sloan-Kettering Cancer Centre's cBioPortal for automated analysis. Sequencing data included miRNA and mRNA sequencing data. The TCGA data for miRNA sequencing were then analysed by Chu and colleagues using a computational pipeline as to

allow for consistent comparison with other TCGA sequencing datasets (Chu et al. 2016). I used the normalised data (available at https://gdc.cancer.gov/about-data/publications/pancanatlas) to understand the different levels of tumour expression of PD-L1 and miR-155 in cancer cells that I would be experimenting with. I matched the corresponding RNA or miRNA value (these are obtained from two separate files named 'RNA (Final)' and 'miRNA (Batch Effects Normalised miRNA data') with the patient and type of cancer (which can be found in the 'Merged_sample-quality_annotations' and 'sample list' files) found in the supplemental data section.

Overall, there is a large variation of PD-L1 and miR-155 expression in the different tumour types analysed. There is no clear positive or negative correlation between miR-155 and PD-L1 suggesting the possibility of tumour-specific posttranscriptional regulation.

4.2. RNA expression of miR-155 and PD-L1 in 33 tumour types

Using publicly available sequencing data from TCGA, the median expression of miR-155 could be presented to show comparisons between 33 different tumour types. Of note, the data does not draw comparisons between non-transformed or cancer cells and in addition there were a low quantity of glioblastoma multiforme (GBM) samples analysed for miRNA sequencing. miR-155 is associated with the pathogenesis of various types of haematological malignancies. The data showed that the levels of miR-155 were highest in diffuse large B cell lymphoma (DLBC), acute myeloid leukaemia (LAML) and in skin cutaneous melanomas (SKCM) (Figure 4.1 and Figure 4.2). Moreover, miR-155 expression was lowest in cancers of the CNS and endocrine as determined by the median expression of these cancer types. In terms of PD-L1, mRNA expression was also highest in a rare haematological cancer, thymoma, followed closely by two types of lung cancer, lung squamous cell carcinoma and lung adenocarcinoma, and head and neck squamous cell carcinoma (HNSC) (Figure 4.3). Lowest expression of PD-L1 was found in rare cancers uterine carcinosarcoma (UCS) and adrenocortical carcinoma (ACC). By comparing both miR-155 and PD-L1 together, DLBC express high levels of both miR-155 and PD-L1, whereas LAML only expresses high levels of miR-155 (Figure 4.3). Relatively, both lung cancer types and head and neck cancers express high levels of PD-L1 and above global median levels of miR-155. Although there is high expression of PD-L1, low expression of miR-155 is found in pheochromocytoma and paraganglioma (PCPG), kidney chromophobe (KICH) and prostate adenocarcinoma (PRAD). These data show that miR-155 and PD-L1 expression differ in many types of cancer, including within the same broad category of cancer and there is no clear correlation between the two factors, across the 33 tumour types analysed (Pearson r correlation coefficient = +0.1523).

Abbrev.	Cancer type	Category	Sample size miR-155	Sample size PD-L1
ACC	Adrenocortical carcinoma*	Endocrine	79	78
BLCA	Bladder Urothelial Carcinoma	Urologic	429	423
BRCA	Breast invasive carcinoma	Breast	1165	1188
CESC	Cervical squamous cell carcinoma and endocervical adenocarcinoma	Gynaecologic	311	306
CHOL	Cholangiocarcinoma*	GI	45	45
COAD	Colon adenocarcinoma	GI	431	480
DLBC	Lymphoid Neoplasm Diffuse Large B-cell Lymphoma	Haematologic	47	48
ESCA	Esophageal carcinoma	GI	195	193
GBM	Glioblastoma multiforme	CNS	5	174
HNSC	Head and Neck squamous cell carcinoma	Head and Neck	565	560
KICH	Kidney chromophobe*	Urologic	89	89
KIRC	Kidney renal clear cell carcinoma	Urologic	570	587
KIRP	Kidney renal papillary cell carcinoma	Urologic	321	587
LAML	Acute Myeloid Leukaemia	Haematologic	188	173
LGG	Brain Lower Grade Glioma	CNS	528	532
LIHC	Liver hepatocellular carcinoma	GI	421	421
LUAD	Lung adenocarcinoma	Thoracic	555	569
LUSC	Lung squamous cell carcinoma	Thoracic	511	537
MESO	Mesothelioma*	Thoracic	87	87
OV	Ovarian serous cystadenocarcinoma	Gynaecologic	486	273
PAAD	Pancreatic adenocarcinoma	GI	182	161
PCPG	Pheochromocytoma and Paraganglioma*	Endocrine	186	186
PRAD	Prostate adenocarcinoma	Urologic	544	545
READ	Rectum adenocarcinoma	Urologic	156	166
SARC	Sarcoma*	Soft tissue	260	260
SKCM	Skin Cutaneous Melanoma	Skin	452	473
STAD	Stomach adenocarcinoma	GI	474	436
TGCT	Testicular Germ Cell Tumours*	Urologic	155	155
THCA	Thyroid carcinoma	Endocrine	569	567
THYM	Thymoma*	Haematologic	126	122
UCEC	Uterine Corpus Endometrial Carcinoma	Gynaecologic	556	563
UCS	Uterine Carcinosarcoma*	Gynaecologic	56	57
UVM	Uveal Melanoma*	Head and Neck	80	80
	Total		**10824**	**11121**

Table 4.1. **33 tumour types were sampled by the TCGA network.** Table shows details of acquired sequencing data from TCGA (see Figure 4.1 for full details), showing number of samples for all 33 tumour types, with abbreviations described. CNS = central nervous system; GI = gastrointestinal. *denotes rare cancers, 10 of which were characterised in the study. Sample size was determined by the number of data available from supplementary files found on the NCI Genomic Data Commons data portal (https://gdc.cancer.gov/about-data/publications/pancanatlas). Note: not all samples had both values for miR-155 and PD-L1 (i.e. see GBM).

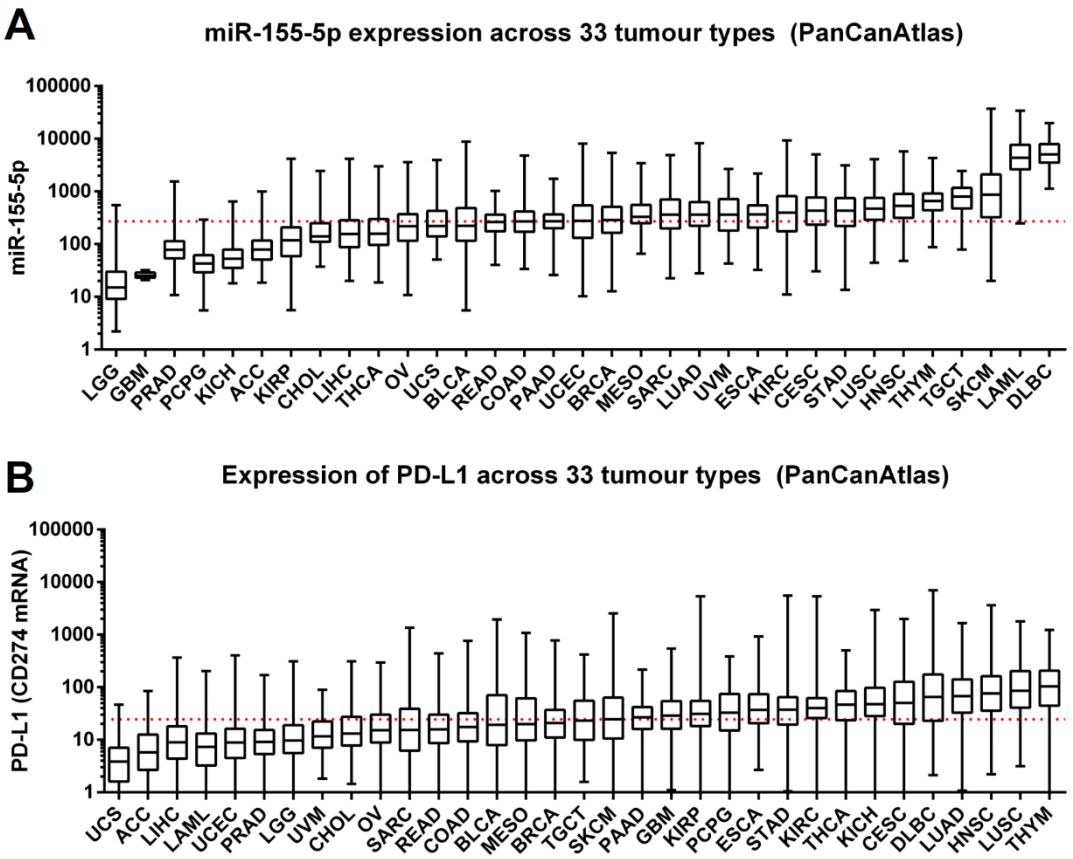

Figure 4.1. **The expression of miR-155 and PD-L1 across 33 tumour types.** Pre-normalised sequencing data from The Cancer Genome Atlas (TCGA) comparing 33 tumour types gathered by the Pan-Cancer Atlas initiative was acquired from the NCI Genomic Data Commons data portal (https://gdc.cancer.gov/about-data/publications/pancanatlas). A) miRNA-seq analysis showing expression of miR-155 (normalised to reads per million mapped reads, RPM), data was originally generated by the Michael Smith Genome Sciences Centre and normalised using a computational pipeline (Chu et al. 2016). Tumour type and expression miR-155 of samples were then paired and sorted from low to high expression. A global median (271.7422 RPM) across all tumour types was calculated (red dotted line). B) RNA-seq analysis showing expression of PD-L1 mRNA expression (data was normalised using two related methods: fragments per kilobase of transcript per million mapped reads, FPKM, and FPKM upper quartile methods). Tumour type and expression PD-L1 mRNA of samples were also paired and sorted from low to high expression. A global median (24.5025 FPKM) across all tumour types was calculated (red line). Abbreviations for tumour types detailed in Table 4.1. For sample size, see Table 4.1.

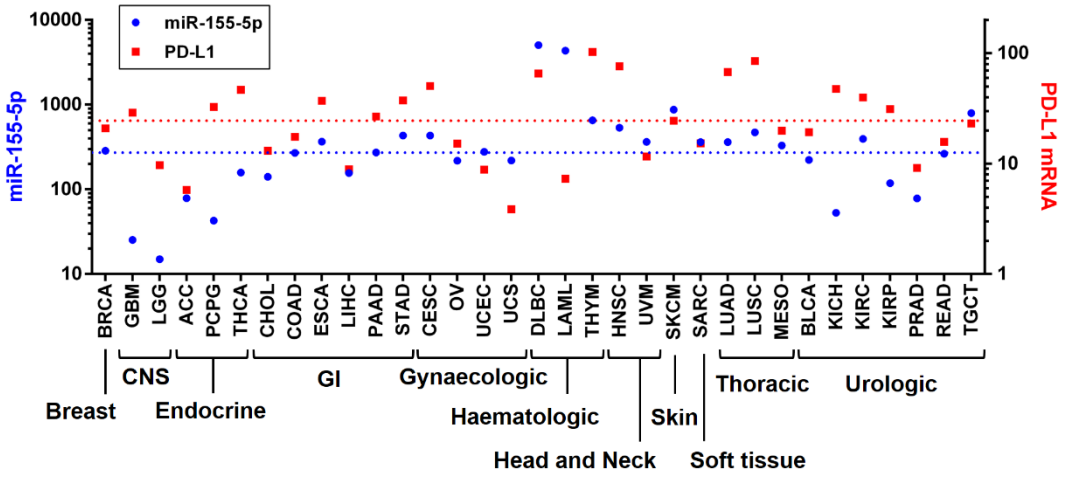

Figure 4.2. **Expression of miR-155 (blue) and PD-L1 mRNA (red) in different types of tumours**. Different cancers were grouped based on location and the median value of PD-L1 mRNA (red) and miR-155 (blue) expression for each tumour type was calculated and plotted on the above graph. The global median value taking into consideration all 33 tumour types was then calculated to allow comparison for each tumour type: miR-155 (blue line; 271.7422 RPM) and PD-L1 (red line; 24.5025 FPKM). CNS = central nervous system; GI = gastrointestinal. For sample size, see Table 4.1.

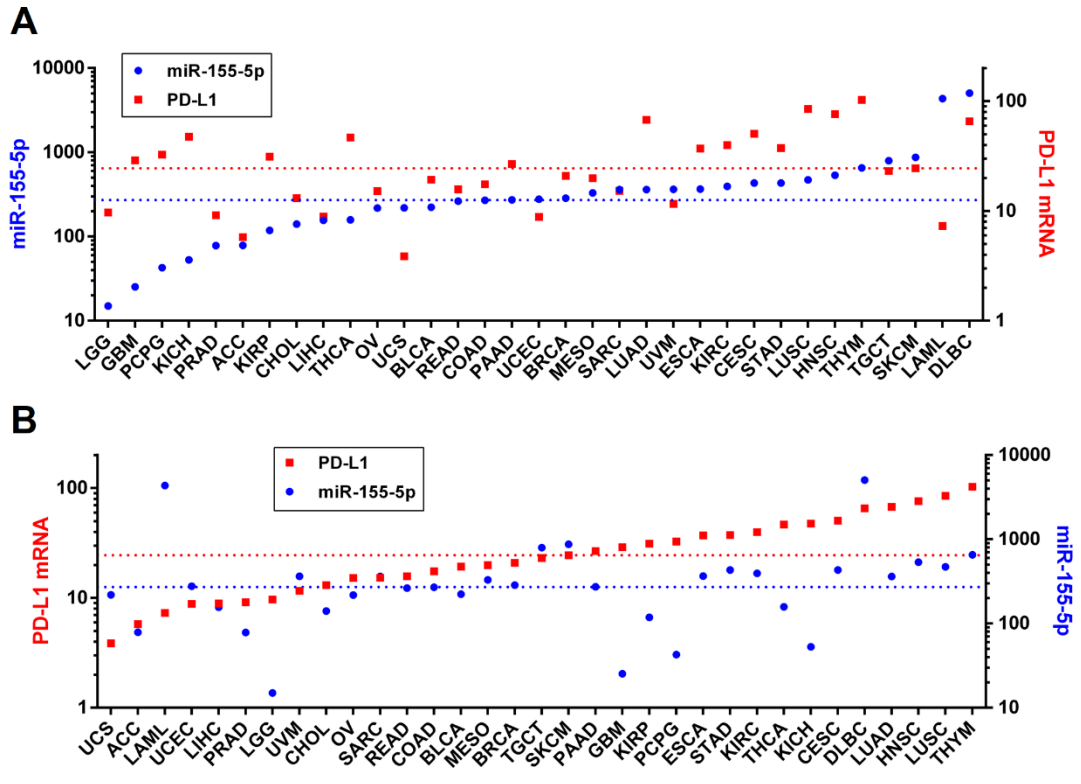

Figure 4.3. **Tumour types sorted for increasing expression of either miR-155 (blue) or PD-L1 mRNA (red).** The median value of PD-L1 mRNA (red) and miR-155 (blue) expression for each tumour type was sorted in terms of increasing expression. Expression of miR-155 (blue) with PD-L1 mRNA (red), A) where miR-155 expression is sorted from low to high-expressing tumour types and PD-L1 expression is unsorted. B) Where PD-L1 mRNA expression is sorted from low to high-expressing tumour types and miR-155 levels are unsorted. Data shown represents the median expression for each tumour type based on the sample size from Table 4.1. Global medians, calculated across all tumour types, are displayed for miR-155 (blue line; 271.7422 RPM) and PD-L1 (red line; 24.5025 FPKM).

4.3. Expression and kinetics of miR-155 and PD-L1 in human cancer cell lines

Next, I investigated PD-L1 expression in a series of human cancer cell lines, including a renal cell carcinoma line (RCC4), a metastatic breast adenocarcinoma cell line (MDA-MB-231) and a lung adenocarcinoma cell line (A549). All three cancer cell lines expressed differing levels of PD-L1 and miR-155 upon induction by inflammatory stimuli which could be used to test whether miR-155 regulation of PD-L1 was a general mechanism in different cancer cell types. I aimed to characterise PD-L1 and miR-155 expression in the available cancer cell lines and investigate the interaction between miR-155 and PD-L1 in this context.

4.3.1. miR-155 regulates PD-L1 in a renal cell cancer line

Renal cell carcinoma (RCC) accounts for up to ~85% of kidney cancer diagnoses, of which the clear cell renal cancer subtypes form around ~75% of renal cell cancers. RCC subtypes are generally characterised by loss-of-function mutations of the tumour suppressor von Hippel-Lindau (VHL) gene in up to 90% of clear cell RCC (Brodaczewska et al. 2016). VHL is associated with regulation of HIF, acting as an E3 ubiquitin ligase which targets HIF for proteasomal degradation. HIF is involved in a number of cellular processes such as growth, apoptosis, angiogenesis and metabolism (Brodaczewska et al. 2016). HIF-1α has been shown to upregulate PD-L1 expression in various types of cancer cells (Noman et al. 2014; Barsoum et al. 2014). Furthermore, VHL mutation status was demonstrated to correlate with PD-L1 expression in clear cell renal tumours (Messai et al. 2016; Kammerer-Jacquet et al. 2017).

The RCC4 line is a clear cell renal cancer that has mutated VHL and the cell line is often used to model VHL-dependent mechanisms in comparison to RCC4 cells that have been transfected with VHL to restore this function. Suppression of HIF-1α or HIF-2α caused a significant decrease in PD-L1 mRNA and protein expression in RCC4 cells (Messai et al. 2016). Moreover, VHL was reported to be involved in regulation of miRNAs in renal cancer including miR-155 (Neal et al. 2010). It was demonstrated that in RCC4 cells without VHL, miR-155 was upregulated compared to RCC4 cells with transfected VHL. Induction of miR-155 was determined to be a HIF-dependent mechanism. Furthermore, miR-155 is expressed significantly higher in renal tumours than in normal tissue. Herein this chapter, I used the RCC4 cell line to investigate the levels of PD-L1 and miR-155 expression.

According to TCGA data (Figures 4.1, 4.2 and 4.3), kidney renal clear cell carcinoma (KIRC) displays above median expression of miR-155 and PD-L1, which places it in the top third of all tumour types characterised. Compared to other renal cancers (KICH and kidney renal papillary cell carcinoma (KIRP), KIRC has similar expression of PD-L1 but displays higher miR-155 levels based on median expression. RCC4 cells were used as an *in vitro* model of clear cell renal carcinoma to characterise PD-L1 expression, RCC4 cells that have stably transfected empty vector (RCC4-EV), restored VHL (RCC4 +VHL) and wild-type were also tested. Treatment of RCC4-EV with IFN-γ and TNF-α induced higher PD-L1 expression compared to treated RCC4 +VHL cells (Figure 4.4A). Two bands of HIF-1α were detected (~120 kDa), where presumably the upper band is phosphorylated HIF-1α, which has been attributed previously (Minet et al. 2000). The upper band was present in RCC4-EV cells but not in RCC4 +VHL. Furthermore, total STAT1 levels were higher in RCC4-EV than RCC4 +VHL cells. Analysis of PD-L1 surface expression by flow cytometry corroborated the

results of western blot (Figure 4.4B). RCC4-EV cells displayed higher levels of PD-L1 in both IFN-γ and TNF-α-treated and untreated conditions. Similar results were shown by measuring PD-L1 mRNA expression (Figure 4.5A). Altogether, the results validate previous reports (Noman et al. 2014; Barsoum et al. 2014; Messai et al. 2016) that restoration of VHL in RCC4 cells suppresses PD-L1 expression.

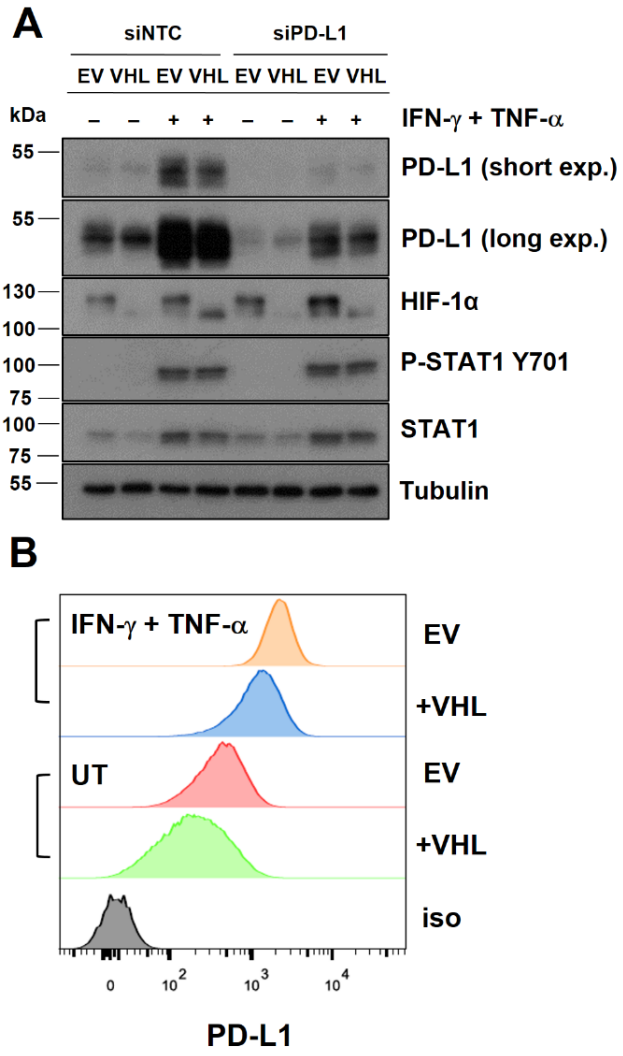

Figure 4.4. **Expression of VHL regulates the levels of PD-L1.** A) Protein expression analysis of renal cell carcinoma line (RCC4) cells with stable transfection of empty vector (EV) or von Hippel-Lindau (VHL), transfected with siRNA targeting PD-L1 or control (NTC) (48 h) and treated with IFN-γ and TNF-α (24 h). B) Surface expression of PD-L1 was measured in RCC4-EV or +VHL cells treated with IFN-γ and TNF-α (24 h) or left untreated (UT) in comparison to isotype (iso). MFI of PD-L1 staining: RCC4-EV (IFN-γ + TNF-α) = 2274, RCC4 +VHL (IFN-γ + TNF-α) = 1304, RCC4-EV (UT) = 452, RCC4 +VHL (UT) = 210, iso = 8.60. n = 1 experiment.

Next, I determined that VHL also regulates miR-155 expression with and without inflammatory stimulation (Figure 4.5B). RCC4-EV cells displayed higher levels of miR-155 than RCC4 +VHL cells. Overexpression of miR-155 in RCC4 wild-type cells showed suppression of PD-L1 protein levels notably after 24 h of treatment with IFN-γ and TNF-α (Figure 4.6). In contrast, inhibition of endogenous miR-155 resulted in an increase in PD-L1 at 24 h post-stimulation. This suggests that miR-155 regulates PD-L1 expression in renal cancer cells.

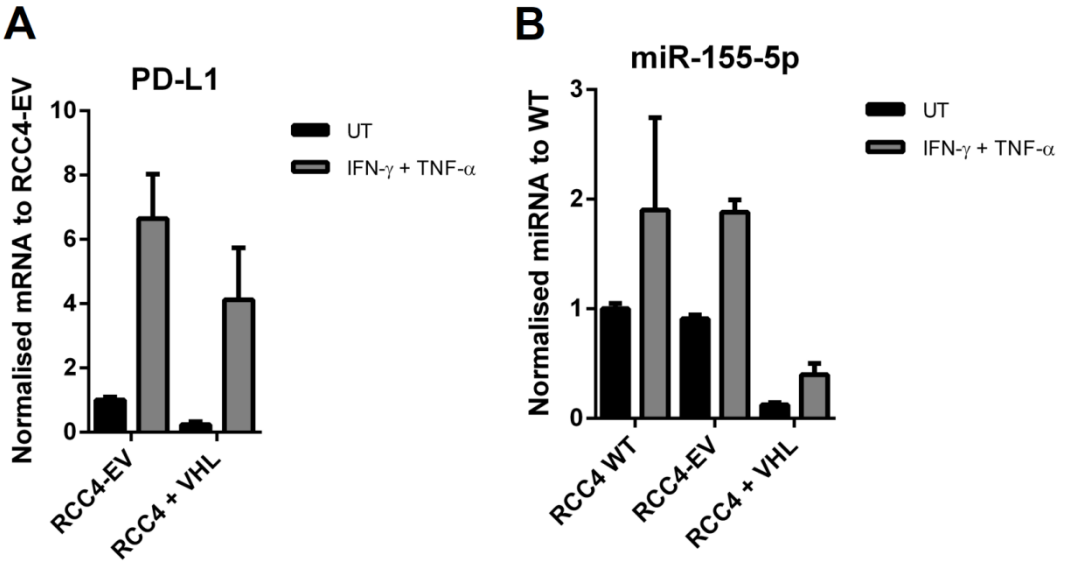

Figure 4.5. **Expression of PD-L1 and miR-155 in RCC4 cells.** A) PD-L1 mRNA expression was analysed by qRT-PCR in RCC4-EV or +VHL cells treated with IFN-γ and TNF-α (24 h) or untreated (UT). B) miR-155 expression was analysed by qRT-PCR in RCC4 wild-type, RCC4-EV or +VHL cells treated with IFN-γ and TNF-α (24 h) or left untreated (UT). n = mean of 2 independent experiments.

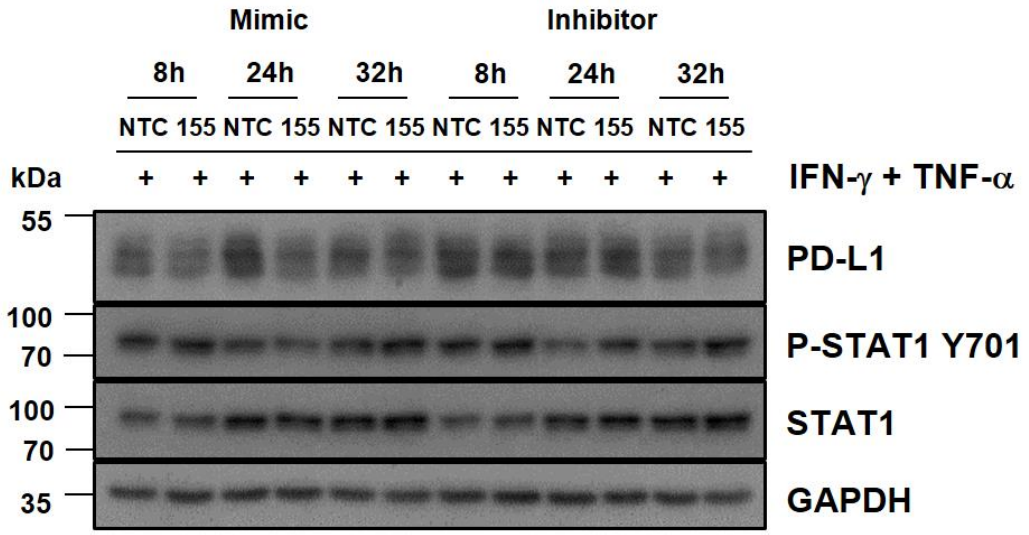

Figure 4.6. **miR-155 expression regulates PD-L1 in RCC4 cells.** RCC4 cells were tested to understand whether miR-155 could regulate the expression of PD-L1 in a renal cancer cell line. Protein expression following IFN-γ and TNF-α stimulation (8, 24, 32 h) in RCC4 wild-type cells transfected with miR-155 mimics (left side) or miR-155 inhibitors (right side) (48 h). n = 1 experiment.

4.3.2. miR-155 regulates PD-L1 in a metastatic breast cancer cell line

The MDA-MB-231 cell line represents a mesenchymal-like breast cancer type. These are triple negative for receptors of the hormones oestrogen, progesterone and human epidermal growth factor receptor 2 (HER2), a member of the EGFR family, representing 10-20% of breast cancers. MDA-MB-231 cells are highly invasive and metastatic-derived from a pleural effusion, the excess fluid that is accumulated in the fluid-filled space surrounding the lungs. MDA-MB-231 cells have been shown to express PD-L1 which can be induced further by knockdown of PTEN (Mittendorf et al. 2014). Levels of miR-155 can be increased by inflammatory cytokines TNF-α or LPS in MDA-MB-231 at 24 h post-stimulation (Tili et al. 2011).

TCGA data suggested that participants with breast invasive carcinoma (BRCA) had levels of miR-155 and PD-L1 that were close to the global median of all tumour types (Figures 4.1, 4.2 and 4.3). Similar to RCC4 cells, both PD-L1 mRNA and miR-155 levels are induced by IFN-γ and TNF-α (Figure 4.7). Overexpression of miR-155 in MDA-MB-231 cells led to decreased PD-L1 protein expression at 24 h (Figure 4.8). Conversely, when endogenous expression of miR-155 was inhibited this led to an increase in PD-L1 expression. These results suggest the capacity of miR-155 to regulate induction of PD-L1 expression in a metastatic breast cancer cell line.

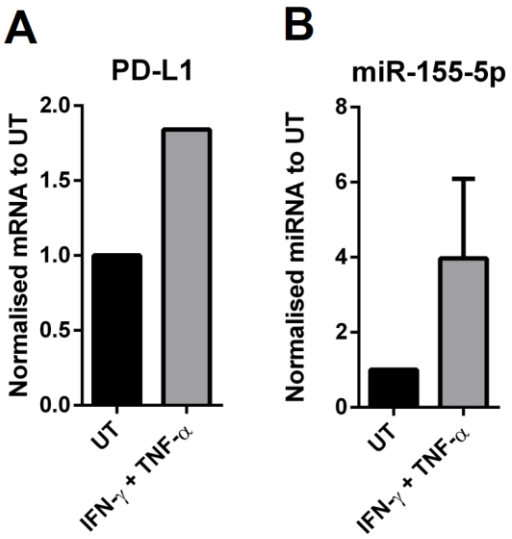

Figure 4.7. **Expression of PD-L1 and miR-155 in MDA-MB-231 cells.** A) PD-L1 mRNA expression was analysed by qRT-PCR in MDA-MB-231 cells treated with IFN-γ and TNF-α (24 h) or untreated (UT). n = 1 experiment. B) miR-155 expression was analysed by qRT-PCR in MDA-MB-231 cells treated with IFN-γ and TNF-α (24 h) or left untreated (UT). n = 3 independent experiments.

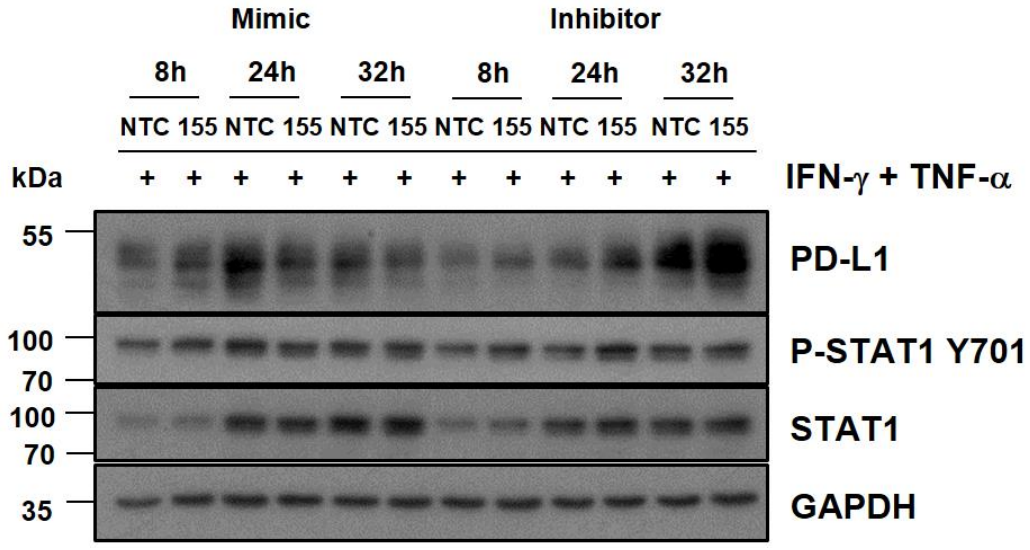

Figure 4.8. **miR-155 expression regulates PD-L1 in MDA-MB-231 cells.** MDA-MB-231 cells were tested to understand whether miR-155 could regulate the expression of PD-L1 in a breast cancer cell line. Protein expression following IFN-γ and TNF-α stimulation (8, 24, 32 h) in MDA-MB-231 cells transfected with miR-155 mimics (left side) or miR-155 inhibitors (right side) (48 h). n = 1 experiment.

4.3.3. Different regulation of PD-L1 by miR-155 in a lung adenocarcinoma cell line

Alveolar type II cells have a compact shape that cover 5% of the alveolar surface, as compared to alveolar type I cells that cover 95% (Mason 2006). These type II cells restructure the alveolar epithelium after damage has occurred to type I cells. A characteristic of type II cells is the lamellar bodies that produce and secrete pulmonary surfactant to prevent the collapse of lungs during breathing out. Human A549 lung adenocarcinoma cells fall within the range of NSCLC tissues, originating from the basal epithelium of alveoli and are considered alveolar type II cells. A549s have weak PD-L1 signal at basal levels (Chen et al. 2015; Hong et al. 2016) but were shown to upregulate PD-L1 following IFN-γ treatment (24 h) (Anantharaman et al. 2016). Expression of miR-155 is higher expressed in lung cancer tissues (adenocarcinoma and squamous carcinoma) than para-cancerous and normal tissues (Zang et al. 2012). However, A549 cells express almost undetectable miR-155 levels (Rather et al. 2013).

TCGA data analysis (Figure 4.3) indicated that lung adenocarcinoma (LUAD) and lung squamous cell carcinoma (LUSC) express levels of PD-L1 and miR-155 above the global median, compared to other tumour types. Further characterisation in A549 cells saw that IFN-γ and TNF-α synergise to induce PD-L1 mRNA expression (Figure 4.9A). Similarly, miR-155 is induced in A549 cells by the same inflammatory cytokines (Figure 4.9B). Moreover, the synergistic induction of PD-L1 translated to cell surface expression (Figure 4.9C). Untreated A549s displayed very low levels of PD-L1 which were elevated upon stimulation. Upon overexpression of miR-155 using mimics, PD-L1 expression was increased and not suppressed as seen in the RCC4 and MDA-MB-231 cell lines at all time-points (Figure 4.10). The increase in protein expression was observed in western blot in an upper band of PD-L1 that was noticeable after 24 h post-stimulation. The lower band of PD-L1 did not change. In contrast, inhibition of miR-155 did not affect PD-L1 expression. Phosphorylation of STAT1 was increased after overexpression of miR-155 compared to NTC. No increase was seen after inhibition of miR-155. This suggests that miR-155 may affect PD-L1 protein expression in A549 cells by a different mechanism that could be cell-type specific.

4.4. Regulation of PD-L1 by miR-155 in lung cancer cell lines

Next, I validated that all tested cancer cell lines have an intact PD-L1 3'-UTR to indicate that the regulatory mechanism of miRNAs can occur in these cells, since in some cancers the 3'-UTR of PD-L1 is truncated (Kataoka et al. 2016). The average length of a human 3'-UTR is ~950 bp long (Sood et al. 2006). The PD-L1 gene is 3691 bp long, containing a 5'-UTR sequence (108 bp), an open reading frame (ORF) (873 bp) which encodes the functional protein and a long 3'-UTR (2710 bp). The two miR-155 binding sites are situated in the

latter half of the 3'-UTR. First, I designed primer pairs that enclosed the whole 3'-UTR ('F1:R1') and the latter half ('F2:R1') containing the miR-155 binding sites, based on the dominant PD-L1 mRNA isoform that represents the longest transcript (*NM_014143.3*) (Figure 4.11A). I tested RCC4, MDA-MB-231, A549 and HFF cells and confirmed the presence of the full length (F1:R1) PD-L1 3'-UTR in all cell types (Figure 4.11B and C), including the regions where miR-155 binding sites are situated. This suggests that all of the tested cell types express the dominant mRNA isoform of PD-L1. However, this does not test whether other isoforms are expressed such as truncated forms. In addition, the PCR products require further sequencing to investigate whether the miR-155 binding sites are not mutated and therefore expected to have functional capability. By examining miR-155 expression in the tested cell types, I determined that HFFs and RCC4s expressed higher levels of miR-155 than A549 or MDA-MB-231 (Figure 4.11D). As described before, all cell types induce miR-155 upon inflammatory activation.

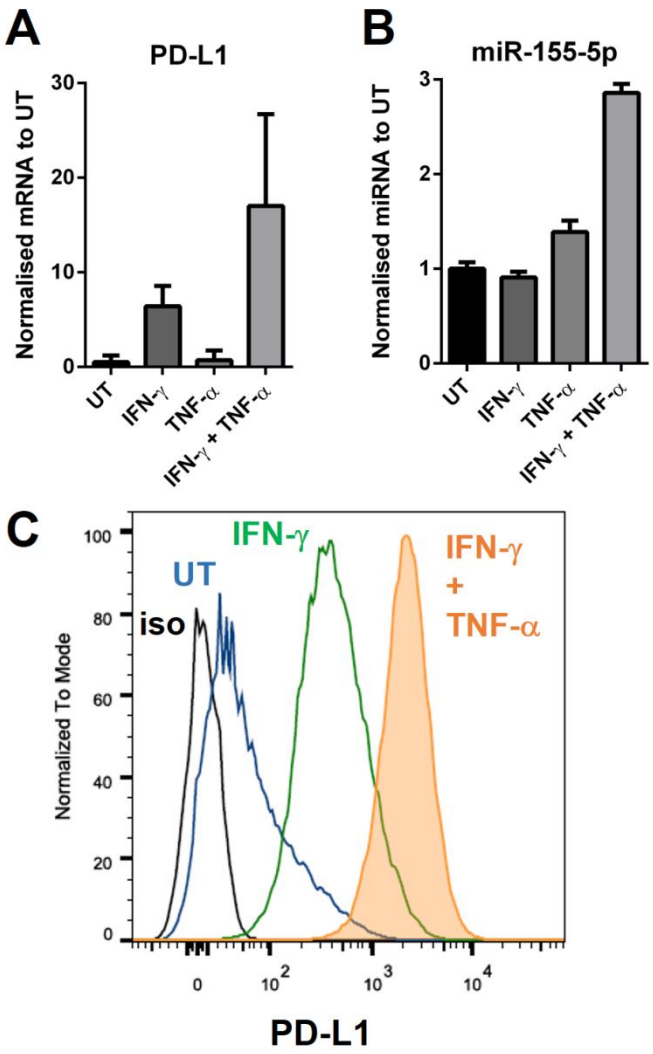

Figure 4.9. **Expression of PD-L1 and miR-155 in A549 cells.** A) PD-L1 mRNA expression was analysed by qRT-PCR in A549 cells treated with IFN-γ and TNF-α (24 h) or untreated (UT). B) miR-155 expression was analysed by qRT-PCR in A549 cells treated with IFN-γ and TNF-α (24 h) or left untreated (UT). C) Surface expression of PD-L1 in A549 cells untreated or treated with IFN-γ, or both IFN-γ and TNF-α (24 h). MFI of PD-L1 staining: IFN-γ + TNF-α = 2236, IFN-γ = 421, UT = 48.9, iso = 7.92. n = 2 independent experiments.

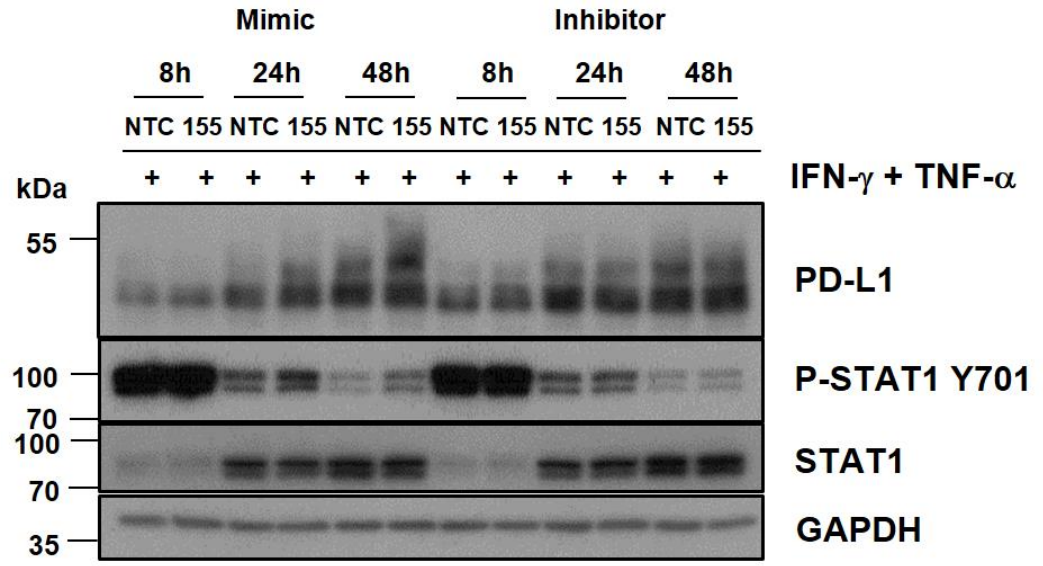

Figure 4.10. **Different regulation of PD-L1 by miR-155 in A549 cells.** A549 cells were tested to understand whether miR-155 could regulate the expression of PD-L1 in a lung cancer cell line. Protein expression following IFN-γ and TNF-α stimulation (8, 24, 48 h) in A549 cells transfected with miR-155 mimics (left side) or miR-155 inhibitors (right side) (48 h). n = 1 experiment.

The low levels of miR-155 expressed in A549 cells suggest that in general this cell type deviates from the median expression of lung cancers that were analysed by the TCGA (Figure 4.12A). As described before, lung cancer cells express above median levels of both miR-155 and PD-L1 based on the data from the TCGA (Figure 4.12B). I found no correlation of miR-155 levels with PD-L1 in either LUAD or LUSC cell types (Figure 4.12C and D). Since it was found that PD-L1 was suppressed by overexpressing miR-155 in RCC4 and MDA-MB-231, two cell types that express different levels of miR-155, this indicated that cell-specific effects may contribute to the regulation of PD-L1 by miR-155. Furthermore, to investigate potentially different regulatory mechanisms of PD-L1 by miR-155 in lung cancer cells I characterized five additional lung cancer cell lines. These included NSCLC lines: H838, HCC193, H1299, H358M and Hop62 of various stages of cancer. H838, H1299 and H358M are all metastatic-derived. H838 and H1299 cells are derived from the lymph node while H358M was isolated from a primary bronchioalveolar carcinoma of the lung. Moreover, all three cancer types are sourced from a male whereas HCC193 and Hop62 come from females. Both H1299 and H358M do not express the tumour suppressor p53 protein. All lung cancer cell types including A549 were transfected with miR-155 mimics and treated with IFN-γ and TNF-α (Figure 4.13A). These lung cancer cell lines displayed different expression levels and glycosylation patterns of PD-L1. miR-155 mimic suppressed PD-L1

expression in H838, H1299 and H358M but not HCC193, Hop62 and A549 cell lines. It was observed that overexpression of miR-155 in HCC193 and A549 appeared to increase upper glycosylated bands of PD-L1.

I found that all lung cancer cell lines contain the 3'-UTR of PD-L1 at a similar level to that of expressed PD-L1 protein (Figure 4.13B). As described before, sequencing would be required for further analysis of the miR-155 binding sites and PD-L1 3'-UTR. The expression of miR-155 was characterised in all lung cancer cells with variability in the levels that were detected (Figure 4.13C). Hop62 cells expressed the most miR-155 of all tested lung lines, which were similar levels to that of HFFs. A549 cells expressed the lowest amount of endogenous miR-155 and do not follow the previously described mechanism of PD-L1 expression by miR-155 (Chapter 3). These data propose that miR-155 regulation of PD-L1 is not correlative to the levels of miR-155 or the pattern of PD-L1 expression. Instead, this refers back to cell-type specific events within cancer subtypes of similar origin that may affect miRNA-mediated regulation of mRNAs.

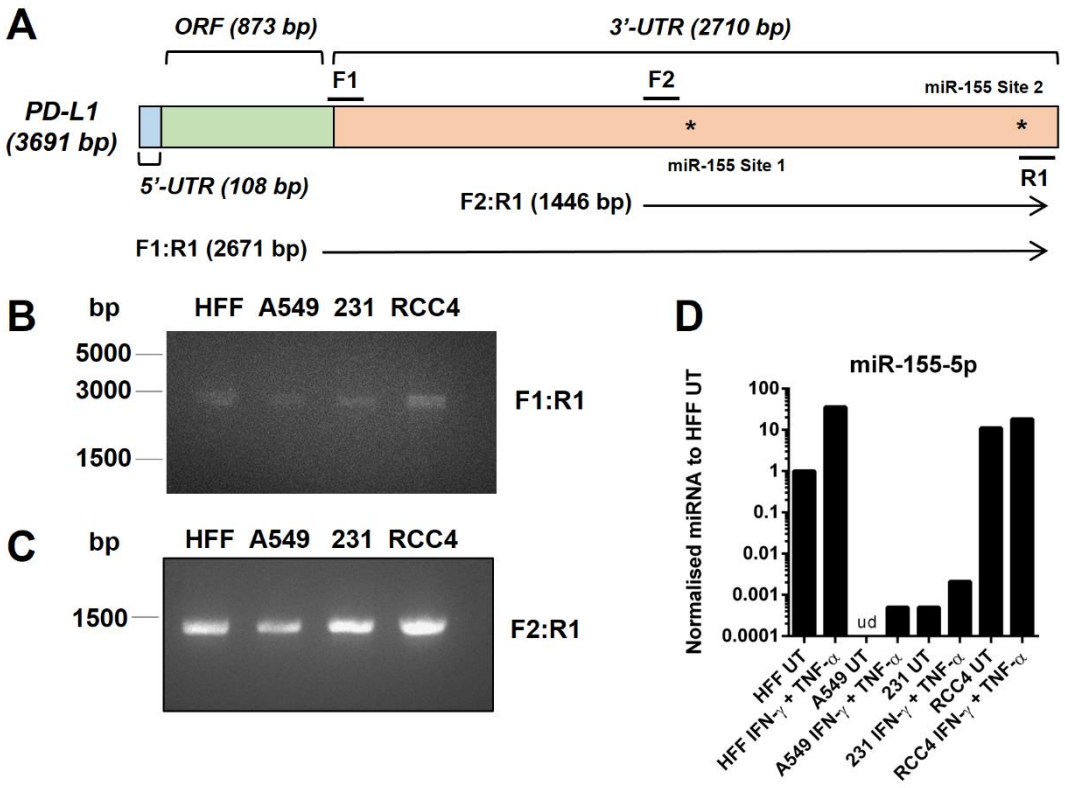

Figure 4.11. **Expression of PD-L1 3'-UTR and miR-155 in cancer cells.** A) The 3'-UTR of PD-L1 covers 2710 bp of the whole length of the PD-L1 gene (3691 bp). Within the 3'-UTR of PD-L1, there are two binding sites for miR-155 of PD-L1, Site 1 (1335-1341) and Site 2 (2587-2593). PCR primers were designed to amplify a product that covers the majority of the 3'-UTR (F1:R1, 2671 bp) or the latter half of the 3'-UTR (F2:R1, 1446 bp), inclusive of the two miR-155 binding sites. B) cDNA synthesised from HFFs and various cancer cells (A549, MDA-MB-231 and RCC4) were amplified using PCR and the product (F1:R1) was analysed by agar gel electrophoresis. C) Similar to (B) using primers to amplify PCR product (F2:R1) from cDNA and analysed by agar gel electrophoresis. F = Forward, R = Reverse primer. D) miR-155 expression was analysed by qRT-PCR in HFFs and various cancer cells treated with IFN-γ and TNF-α (24 h) or left untreated (UT). ORF = open reading frame. n = 1 experiment.

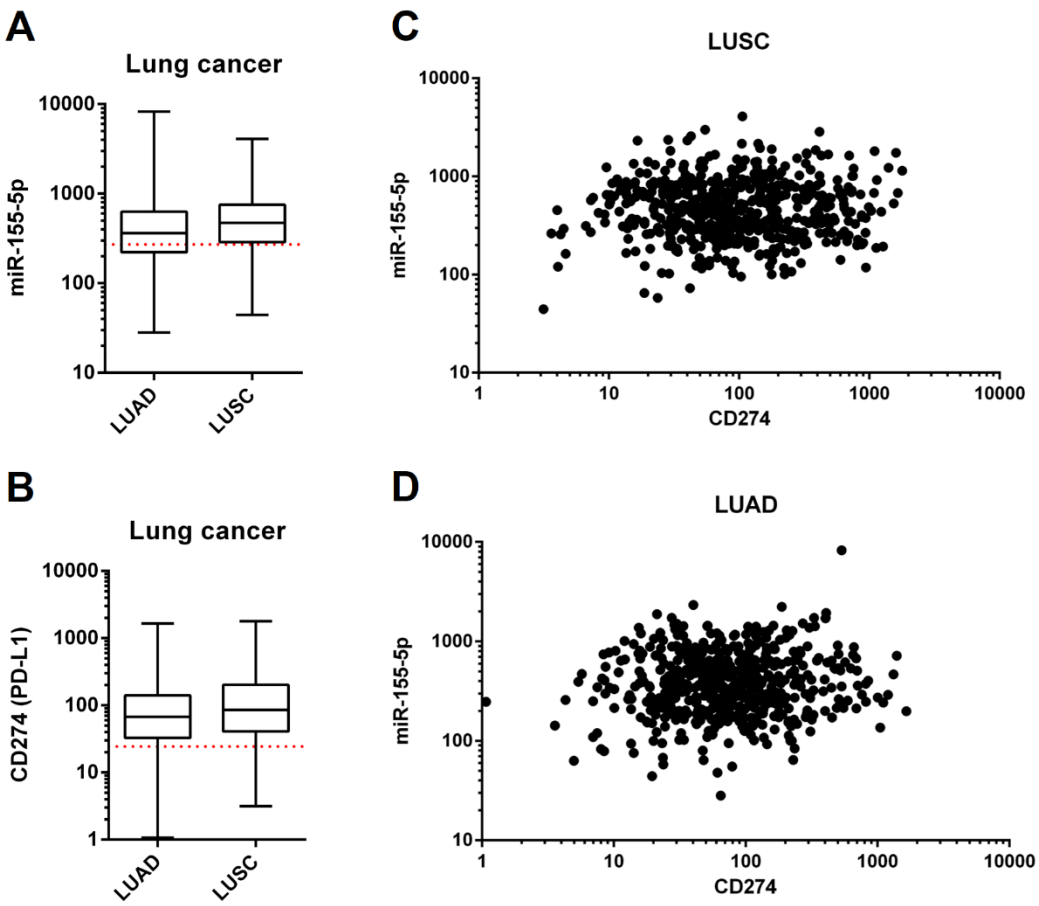

Figure 4.12. **Normalised lung cancer sequencing data obtained from TCGA for LUAD and LUSC** (see Figure 4.1 for details). A) Expression of miR-155 with whiskers showing minimum and maximum for both LUAD and LUSC tumour types. The red line represents the global median (271.7422 RPM) of all 33 tumour types. B) Expression of PD-L1 mRNA in both LUAD and LUSC tumour types, the red line represents the global median (24.5025 FPKM). C) Scatter plot showing both expression of PD-L1 mRNA and miR-155 for each individual sample in LUSC (Pearson r correlation coefficient = +0.05542) and D) LUAD (Pearson r correlation coefficient = +0.07275) to observe any correlation. LUSC = lung squamous cell carcinoma; LUAD = lung adenocarcinoma.

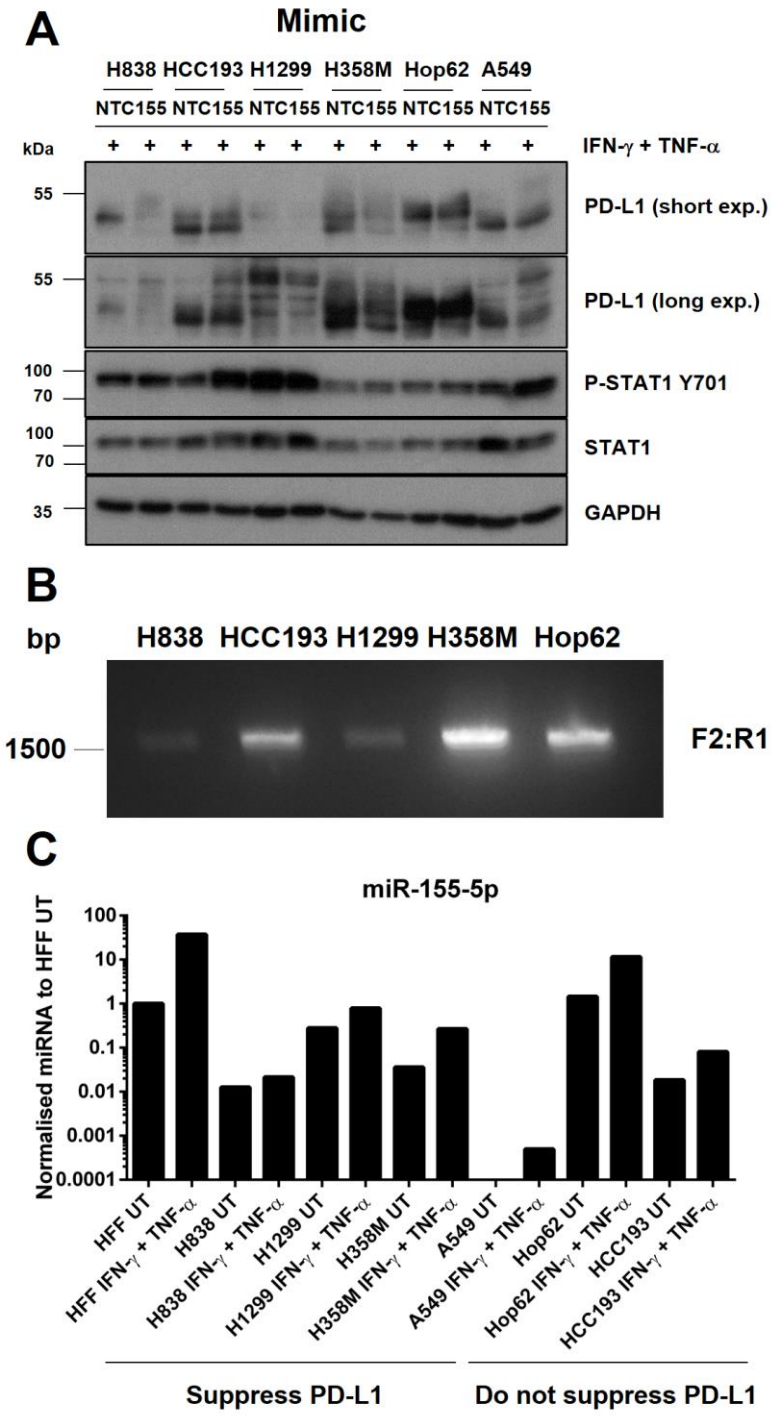

Figure 4.13. **miR-155 expression and regulation of PD-L1 in lung cancer cell lines.** A) Protein expression following IFN-γ and TNF-α stimulation (24 h) in lung cancer cell lines (H838, HCC193, H1299, H358M, Hop62 and A549) transfected with miR-155 mimics (48 h) and analysed by western blot. B) PCR product (F2:R1) from cDNA synthesised from lung cancer cell lines (see above) and analysed by agar gel electrophoresis. C) miR-155 expression was analysed by qRT-PCR in HFFs and in lung cancer cell lines treated with IFN-γ and TNF-α (24 h) or left untreated (UT). n = 1 experiment.

4.5. miR-218 regulation of PD-L1 in cancer cell lines

In Chapter 3, I first looked at miR-218 regulation of PD-L1 in primary cells. Here, I continued investigating the effect of miR-218 on PD-L1 in cancer cell lines. I compared overexpression of miR-218 in A549, MDA-MB-231 and RCC4 cell lines with HFFs (Figure 4.14). All cells were stimulated with IFN-γ and TNF-α and analysed for protein expression of PD-L1 after 24 h. In line with previous results, overexpression of miR-218 in HFFs induces the expression of PD-L1 more so than IFN-γ and TNF-α alone. There was no noticeable increase in PD-L1 expression in the tested cancer cell lines, apart from a small increase in A549 cells. Upon measuring miR-218, both HFF and MDA-MB-231 expressed the higher levels of miR-218 and A549 expressed the lowest (Figure 4.15A). IFN-γ and TNF-α induced miR-218 in all cells except in RCC4. Moreover, testing the additional lung cancer cell lines showed that miR-218 was suppressed following IFN-γ and TNF-α activation in H838, HCC193, H358M (Figure 4.15B). These data suggested a differential regulation of miR-218 induction in cancer cells as opposed to HDLECs/HFFs cells which may account for the mechanism by which PD-L1 is affected by miR-218 overexpression in non-transformed cells.

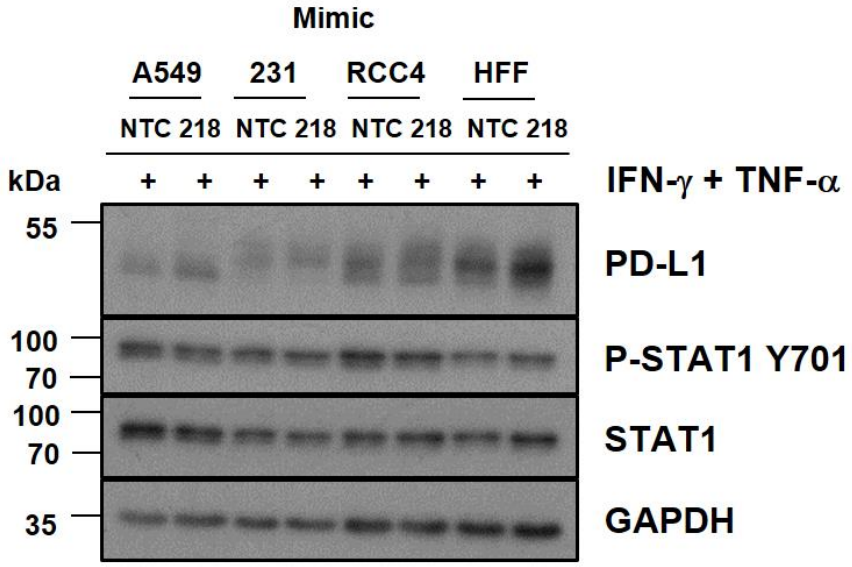

Figure 4.14. **The effect of miR-218 overexpression in cancer cell lines.** Protein expression following IFN-γ and TNF-α stimulation (24 h) in A549, MDA-MB-231, RCC4 and HFF cells transfected with miR-218 mimics (48 h). n = 1 experiment.

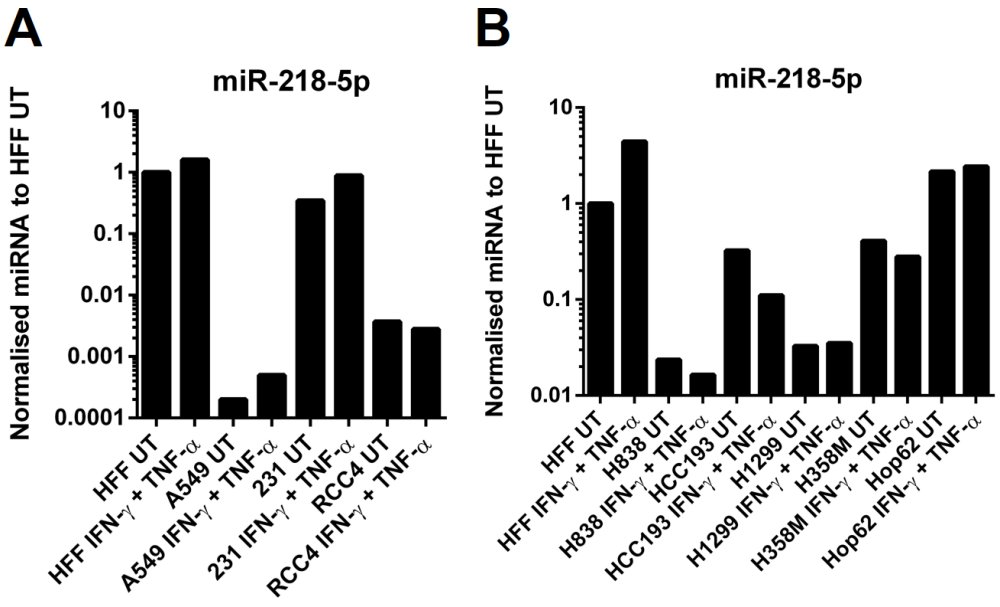

Figure 4.15. **miR-218 expression in HFFs and cancer cell lines.** A) miR-218 expression was analysed by qRT-PCR in HFFs and various cancer cells (A549, MDA-MB-231 and RCC4) treated with IFN-γ and TNF-α (24 h) or left untreated (UT). B) Similar to (A), miR-218 expression analysed in lung cancer cell lines. Both sets of data were normalised to expression of miR-218 in untreated HFFs. n = 1 experiment.

4.6. Chapter discussion

This chapter primarily addresses miRNA-mediated regulation of PD-L1 and in some cases, specifically whether the mechanism by which PD-L1 is regulated by miR-155 in HDLECs/HFFs could be extended to cancer cell lines. The tested cancer cell lines align within the categories of renal (RCC4), breast (MDA-MB-231) and lung cancer (A549). Regulation of PD-L1 by miR-155 extended in a similar pattern in inflammatory-activated RCC4 and MDA-MB-231 cells. However, in A549 cells, miR-155 had the opposite effect on PD-L1 expression. Upon testing of additional lung cancer cell lines, I identified a subset following the initial finding that miR-155 suppresses PD-L1 expression. These preliminary findings identify a larger scope of miR-155 regulation of PD-L1 beyond healthy cells, which could be studied in further detail in a disease context.

In the beginning, I analysed expression of PD-L1 and miR-155 in multiple tumour types using clinical data from the TCGA Research Network. This provided an overview to understanding any potential relationships between PD-L1 and miR-155 in different cancer subtypes. Between various cancer subtypes, the expression of PD-L1 and miR-155 is varied especially in haematological cancers such as DLBC and LAML. B cell lymphomas were found to have up to 10- to 30-fold higher copy numbers of miR-155 than normal circulating

B cells (Eis et al. 2005). Patients with the activated B cell (ABC) phenotype of DLBC have increased levels (2- to 3-fold) of miR-155 compared to a non-germinal centre B cell (GCB) phenotype. In a study where 1253 DLBC samples were analysed, PD-L1 expression was significantly associated with the GCB phenotype and had poor prognosis (Kiyasu et al. 2015). It would be interesting to establish whether miR-155 regulates PD-L1 expression in DLBC samples due to the high expression of both molecules. Moreover, I analysed that miR-155 expression was high in LAML compared to other tumour types but expressed PD-L1 at a lower level. Similar findings on PD-L1 expression were reported where a study found 18% of patients expressing PD-L1 (Berthon et al. 2010). However, these studies showed that LAML cells were inducible by IFN-γ and upregulated PD-L1 upon stimulation (Berthon et al. 2010; Krönig et al. 2014). miR-155 is overexpressed and repeatedly linked with poor prognosis in LAML (Narayan et al. 2018). The levels of miR-155 (intermediate or high) in LAML can affect the targeting of genes, such that intermediate miR-155 expression will target lowly expressed genes and as the levels of miR-155 rise this allows more highly expressed mRNAs to be regulated. This is another possible context to explore the miR-155/PD-L1 interaction in more detail.

In the present work, I demonstrated that miR-155 and PD-L1 were differentially expressed at basal levels and induced by IFN-γ and TNF-α in diverse orders of magnitude. In RCC4, I confirmed previous reports (Messai et al. 2016; Kammerer-Jacquet et al. 2017) that VHL is a crucial regulator of PD-L1 and miR-155 expression. It has also been demonstrated previously that upregulation of miR-155 can target VHL in breast cancer and therefore there may be an add-on effect on PD-L1 expression in RCC4 cells from regulation of VHL (Kong et al. 2014).

Both RCC4 and MDA-MB-231 cells displayed similar regulation of PD-L1 using miR-155 mimics in line with results from primary cells as described (Chapter 3). Only three of six tested lung cancer cell lines demonstrated a similar regulatory pattern despite overexpression of miR-155. There was also no distinct correlation between endogenous miR-155 and PD-L1 expression in individual lung cancer tissues. Despite the differences in miR-155 expression between the cancer cell lines, the miR-155/PD-L1 mechanism can occur in selected cell types. This suggests that for the interaction to occur, there are more factors to understand than the expression of miR-155 or PD-L1. This may explain the lack of correlation between PD-L1 and miR-155 from the lung cancer data. My experiments so far cannot rule out indirect regulation by miR-155 on signalling pathways that can affect PD-L1 expression, such as the JAK/STAT cascade. Moreover, conducting luciferase assays (similar to that in Chapter 3) to demonstrate that miR-155 can bind directly to the 3'-UTR of PD-L1 in all

tested lung cancer cell lines would provide further knowledge on the accessibility of the binding site.

All lung cancer cell lines had an intact 3'-UTR of PD-L1 inclusive of miR-155 binding sites which suggests against the incidence of a shortened 3'-UTR in cancer cells caused by alternative cleavage or polyadenylation (Mayr & Bartel 2009). Sequencing of the 3'-UTR would be required to determine whether there are alterations of the miR-155 binding sites and/or surrounding sequences. The site accessibility is reported to be as important as the matching of the seed sequence in miRNA-mediated translational repression (Kertesz et al. 2007). It would be important to know whether the binding sites are functionally accessible for binding of miR-155 to sites on PD-L1 3'-UTR in lung cancer cells (discussed below).

The 3'-UTR of PD-L1 is twice as long as the average human 3'-UTR. This opens up the possibility that PD-L1 is heavily regulated by factors that affect the stability, translation, localisation, transport and polyadenylation/deadenylation of the mRNA (Hu & Coller 2012). Although miRNAs can functionally cleave target mRNAs, the majority of mechanisms are not and require the role of mRNA decay factors that contribute towards mRNA deadenylation (Huntzinger & Izaurralde 2011). How does miR-155 exert its regulation on PD-L1 and why does this mechanism not occur in some cell types? It has been reported that translational repression can precede mRNA deadenylation and decay, such as repression of translation initiation (Djuranovic et al. 2012; Bazzini et al. 2012). A genome-wide scale study found that there was poor correlation between the changes in protein production and mRNA fold change at a time-scale of 8 h and 32 h after miR-1 transfection (Selbach et al. 2008). Many of the miRNA targets were regulated at the protein level at 8 h and at a later time-point protein and mRNA levels were similarly suppressed. In contrast, other studies have suggested that the majority of miRNA targets are repressed at the mRNA level (Baek et al. 2008; Guo et al. 2010; Eichhorn et al. 2014). A small number of targets (10-25% of overall repression) are repressed at the translational level without change to mRNA expression. Additionally, depletion of decapping factors can relieve miRNA-mediated silencing of mRNAs (Eulalio et al. 2007).

In Chapter 3, overexpression of miR-155 did not reduce PD-L1 mRNA levels and in some cases increased the amount of mRNA in primary cells. In spite of this, the protein expression of PD-L1 was suppressed. Generally, this indicates that miR-155-mediated gene silencing of PD-L1 in primary cells occurs through translational repression. PD-L1 mRNA levels were not measured after overexpression of miR-155 in cancer cell lines to confirm whether this was the case in these particular cells. In addition, regulation of PD-L1 by miR-155 occurs in cells responding to inflammatory stimuli rather than in untreated cells.

Some mechanisms have been proposed that explain how miRNAs in animals might repress translation. These include involvement of GW182 family of proteins that interact directly with Argonaute (AGO) proteins and are involved in mRNA decay (Iwakawa & Tomari 2015). GW182-mediated dissociation of eukaryotic initiation factor 4F (eIF4F) from poly (A)-binding protein (PABP) compromises translation initiation and contributes to overall miRNA-mediated translational repression. Furthermore, GW182 recruits downstream translational repressors such as DEAD-box RNA helicase 6 (DDX6) to target mRNAs (Iwakawa & Tomari 2015). Dissociation of the RNA helicase eIF4A from target mRNAs can abolish ribosome binding (Iwakawa & Tomari 2015). In zebrafish embryos, injection of miR-155 duplexes caused mostly translational repression at an early stage of miR-155 targets but shifted towards mRNA destabilisation at a later phase due to the length of the poly (A)-tail (Subtelny et al. 2014). Tail lengths in early zebrafish were associated with translational efficiency which was diminished in non-embryonic samples.

The mechanism by which miR-155 affects PD-L1 in the 3'-UTR could be cell-type specific depending on the accessibility of the 3'-UTR and other factors that may regulate PD-L1 in the 3'-UTR such as RNA-binding proteins. RISC proteins can hinder base-pairing interactions between miRNA and the target site (Kertesz et al. 2007). Control of protein levels via the 3'-UTR and is not only regulated by miRNAs but also by adenylate-uridylate (AU)-rich elements (AREs) which also lead to rapid mRNA decay (Mayr 2017). ARE-mediated degradation of mRNA has been shown to require cooperation between miRNAs and ARE-binding proteins (Jing et al. 2005). Moreover, the ARE-binding protein, HuR was shown to de-repress the 3'-UTR of cationic amino acid transporter 1 (CAT-1) mRNA from miR-122-induced inhibition (Bhattacharyya et al. 2006). Additionally, RNA-binding proteins (RBPs) can bind to the mRNA and modify its translatability. Binding of Pumilio to the 3'-UTR of p27 can alter the secondary structure and accessibility of miR-221 and miR-222 to their binding sites (Kedde et al. 2010). In contrast, expression of dead end 1 (Dnd1) can bind mRNAs and inhibit the association of miRNAs to their target sites (Kedde et al. 2007). Recently, RAS-MEK signalling was demonstrated to stabilise the expression of PD-L1 by enhancing the phosphorylation of the ARE-binding protein TTP (ZFP36) (Coelho et al. 2017). TTP negatively regulates PD-L1 expression and inhibition of MEK increased TTP expression. In addition, restoration of TTP expression increased the effectiveness of anti-tumour immunity which was dependent on the regulation of PD-L1 mRNA (Coelho et al. 2017). From these studies, there is a possibility that the activity of RNA-binding proteins or ARE-binding proteins could affect miR-155 regulation of PD-L1 expression. Using TCGA data, low levels of TTP found in lung adenocarcinoma patients were observed to correspond to high levels of PD-L1 (Figure 4.16). No similar relationship with PD-L1 is observed with

Pumilio or DND1 regardless of expression suggesting the relationship between TTP and miR-155 regulation of PD-L1 expression could be further investigated.

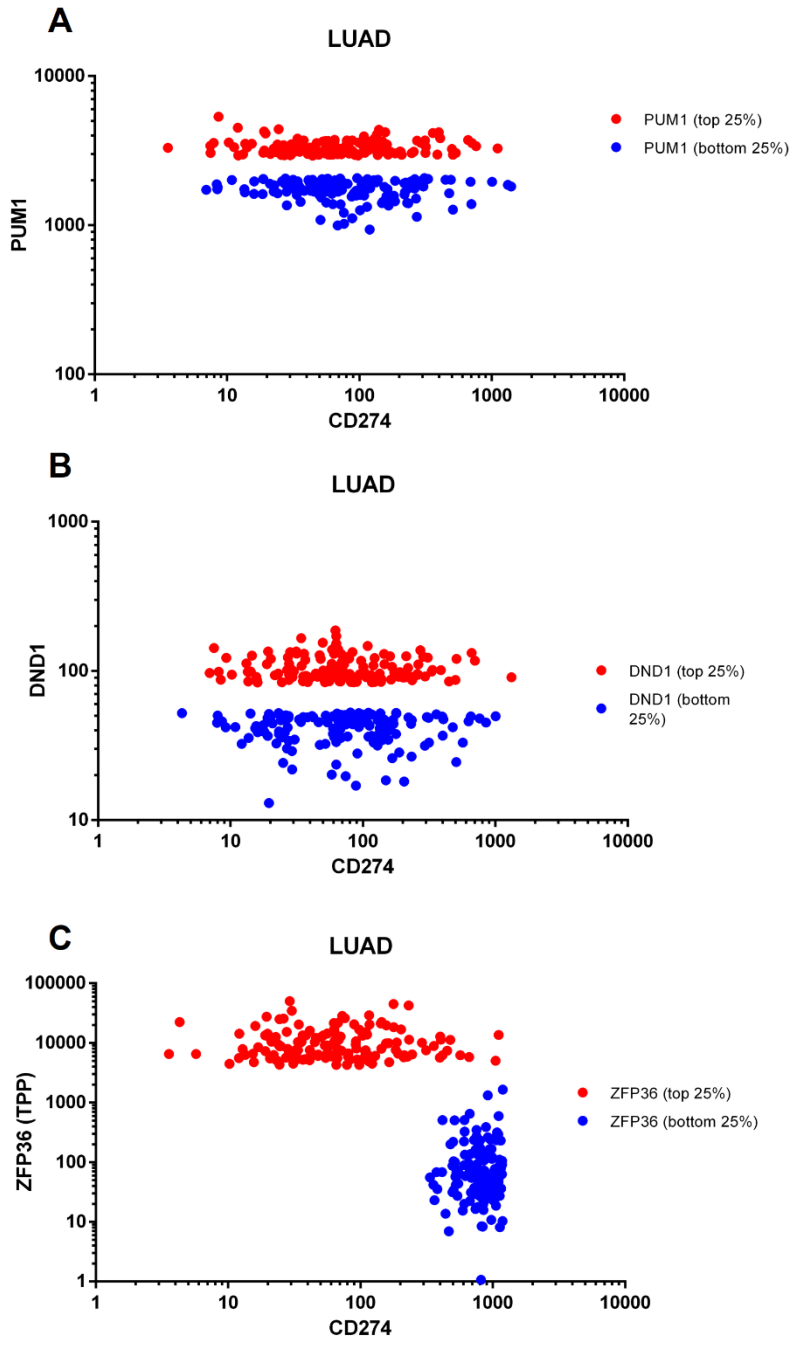

Figure 4.16. **Low expression of ZPF36 correlates with high expression of PD-L1 mRNA.** Scatter plots showing TCGA data from LUAD of the expression of A) PUM1 B) DND1 C) ZFP36 (TTP) against the expression of CD274 (PD-L1). Comparing the top 25% and the bottom 25% values of each gene on the y-axis (PUM1, DND1, ZFP36) with its corresponding/matching CD274 value in each tumour sample. LUAD = lung adenocarcinoma.

Additionally, results in this chapter have suggested miR-155 affects posttranslational modification of PD-L1. I saw that miR-155 decreased the intensity of all glycosylated PD-L1 bands (Figure 4.13A). However, in some cases where miR-155 increased PD-L1 expression (HCC193 and A549), these were associated with glycosylated bands at a higher size than the main PD-L1 band. In contrast, H1299 cells expressed PD-L1 with a primary intensity on the upper bands which were suppressed following overexpression of miR-155. The stability of PD-L1 is associated with N-glycosylation, which prevents ubiquitination of the protein, and is important for the immunosuppressive function of PD-L1 upon engagement to PD-1 (Li et al. 2016; C. W. Li et al. 2018). In addition, EGF signalling was shown to induce PD-L1 glycosylation which is mediated at the posttranslational level. EGF upregulates the β-1,3-N-acetylglucosaminyl transferase (B3GNT3) glycosyltransferase to facilitate glycosylation of PD-L1 in triple-negative breast cancer cells (C. W. Li et al. 2018). Monoclonal antibodies targeting the glycosylated version of PD-L1 blocked interaction with PD-1 and promoted internalisation and degradation of PD-L1. Lung cancer cell lines, including HCC193, display different levels of signalling complexes associated with the EGFR pathway (Toki et al. 2016). Moreover, glycosylation has been shown to be affected by miRNAs (Vaiana et al. 2016). GSK3β was shown to mediate destabilisation of unglycosylated PD-L1 (Li et al. 2016). Interestingly, there is one predicted conserved miR-155 binding site in the 3'-UTR of GSK3β (4794-4800) among mammals. Furthermore, miR-155 was reported to inhibit the activity of GSK3β directly or indirectly by affecting β-arrestin-2 in mice (J. Zhao et al. 2014). This suggests that within my subset of lung cancer cell lines there exists different forms of glycosylated PD-L1. There is some possibility that miR-155 activity, either directly via GSK3β or indirectly, could affect the glycosylation of PD-L1.

In the subset of lung cancer cells where miR-155 suppressed PD-L1 expression, these belonged to cells that were derived from metastatic sites such as the lymph node. Thus, this could affect responses to PD-L1 treatment. A comparative study between primary and metastatic pulmonary adenocarcinomas observed a number of cases where the majority had regional nodal metastasis (Kim et al. 2017). There was a high concordance of PD-L1 expression between primary and metastatic pulmonary adenocarcinomas. This was based on the proportion of tumour cells expressing PD-L1. This high concordance was observed in both low expressing (<1%) and high expressing (>50%) PD-L1^{+} tumour cells. However, there was a low concordance in cases with >1% and <50% PD-L1 expression between primary and metastatic tumours. This was suggested by the authors to be due to the vulnerability of tumour cells to extrinsic regulation (Kim et al. 2017). Furthermore, lymph node metastases of triple-negative breast cancer were found to have higher PD-L1

expression (59.41%) than paired primary tumours (38.61%) (M. Li et al. 2018). Similar reports of weak correlation in PD-L1 expression between primary and metastatic tumours have been reported in RCC (Jilaveanu et al. 2014) and bladder cancer (Mukherji et al. 2016). Although, it appears that higher expression of PD-L1 is found in metastatic tumours compared to primary tumours, the effect of miR-155 activity has not been detailed in PD-1/PD-L1 immunotherapy.

Overall, the implication of these findings demonstrate that the mechanism by which miR-155 regulates PD-L1 expression in HDLECs/HFFs can be found in cancer cell lines after treatment with IFN-γ and TNF-α. Overexpression of miR-155 in several cancer cell lines suppressed the levels of PD-L1. In some lung cancer cell lines, the type of miR-155 regulation of PD-L1 was different. I speculate that this is either due to how miR-155 specifically binds and regulates PD-L1 expression, whether the 3'-UTR of PD-L1 is altered in terms of accessibility to miRNAs in different cancer cell types or the effect of posttranslational regulation of PD-L1. The regulation of PD-L1 by miR-155, now found, in cancer cells adds to the possibility that miR-155 can potentially influence tumour response to anti-PD-1/PD-L1 therapeutic agents, in addition to its regulatory effect in stromal/vascular cells.

5. Development of a co-culture assay to determine the PD-L1 interaction from primary stromal fibroblast/vascular cells

5.1. Introduction

The effects of miRNA regulation can affect several mRNA targets but the downregulation of mRNA or protein expression is typically modest (Lim et al. 2005; Selbach et al. 2008). For example, knockdown of miR-223 which is highly expressed in mouse neutrophils, resulted in hundreds of repressed genes although to a modest degree (<33%) at the protein level (Baek et al. 2008). Targets that underwent further repression also showed de-stabilisation at the mRNA level (Baek et al. 2008). My results in Chapter 3 did not demonstrate that PD-L1 mRNA levels were repressed after miR-155 regulation of PD-L1. However, the protein expression of PD-L1 was regulated by miR-155 to a mild extent. To further understand the significance of this regulatory loop, the functional relevance of these effects should be tested in stromal fibroblasts/vascular cells. Here, I investigated whether surface expression of PD-L1 on stromal fibroblasts/vascular cells suppresses T cell activation via PD-1 engagement using an *in vitro* co-culture system.

The Jurkat cell line is a widely known model of cultured human $CD4^+$ T cell suspension from leukemic origin (Abraham & Weiss 2004). Jurkat cells release large amounts of IL-2 upon stimulation which can be used as a marker of T cell activation for *in vitro* model systems. IL-2 is crucial for maintenance of antigen-activated T cells where it controls proliferation, development and survival (Boyman & Sprent 2012). In addition, transcription of IL-2 is mediated by transcription factors including nuclear factor of activated T cells (NFAT) and activator protein-1 (AP-1) (Boyman & Sprent 2012). Jurkat cells could be activated with phytohaemagglutinin (PHA) to produce IL-2 (Abraham & Weiss 2004). PHA is a lectin that binds and crosslinks sugars on glycosylated surface proteins, including the αβ-heterodimer of the TCR and the CD3 co-receptors, and in doing so indirectly activates the TCR. An additional signal is required which can be fulfilled by phorbol 12-myristate 13-acetate (PMA). PMA diffuses through to the cytoplasm where it directly activates protein kinase C, leading to activation of NF-κB, NFAT and AP-1. Other known combinations that have been used to activate T cells include ionomycin and PMA as well as anti-CD3/CD28 stimulation (Abraham & Weiss 2004). Upon ligation, the CD3 chains of the TCR cluster/aggregate and a conformational change is induced (Minguet et al. 2007). A second co-stimulatory signal can be provided by ligation of CD28. This type of stimulation

represents a more physiologically relevant activation of T cells than with pharmacological agents.

Co-culture techniques allow us to observe cell-cell interactions in a closed environment (Goers et al. 2014). Previously, a co-culture assay was used to determine the effect of PD-L1 on uveal melanoma cells (Yang et al. 2008). PHA and PMA were added to induce PD-1 expression on Jurkat T cells which do not express PD-1 unless activated. IFN-γ-treated melanoma cells were co-cultured with Jurkat cells and supernatants were harvested and assessed for IL-2 by ELISA. Co-culture resulted in significant reduction of IL-2 production which was demonstrated to be in a cell contact-dependent manner. Blockade of PD-1 or PD-L1 resulted in a restoration of IL-2 production by Jurkat cells (Yang et al. 2008). Measuring IL-2 expression on activated Jurkat cells has also been used to demonstrate GSK3β regulation of PD-L1 on tumour cells (Li et al. 2016). Moreover, Jurkat cells were found to enhance PD-1/PD-L1-mediated drug resistance in tumour cells (Black et al. 2016). Jurkat cells cannot fully replace primary T cell biology and harbour mutations that make it an unique transformed T cell line (Abraham & Weiss 2004). Jurkat cells lack expression of PTEN, which can lead to constitutive activation of the PI3K pathway that could alter T cell signal transduction (Gioia et al. 2018). In addition, Jurkat cells do not express SHIP1, Syk or CTLA-4, which are associated with T cell receptor signalling.

However, these co-culture models provide *in vitro* testing of T-like cells that are ease of use and low expense that can supplement the data generated from *in vivo* approaches. By using co-culture assays, this would enable me to test the PD-L1-expressing cells in conjunction with the Jurkat T cell line to study the effect of PD-L1 regulation on T cell activation. First, this would involve testing the interaction of PD-L1 on HFFs or HDLECs with Jurkat cells to see whether there is suppression of T cell activation via the PD-1/PD-L1 pathway. Further, to investigate whether miRNA regulation of PD-L1 affects the PD-1/PD-L1 interaction and consequently activation of T cells. This chapter describes the development of two co-culture assays using wild-type or engineered Jurkat T cells and techniques including ELISA to measure IL-2 production and luciferase assays to measure NFAT activation.

5.2. IL-2 secretion upon activation of wild-type Jurkat cells with PHA/PMA

5.2.1. Activation of Jurkat cells with PHA and PMA induces PD-1 expression

For this first co-culture assay, I characterised wild-type Jurkat T cells (E6-1) using the pharmacological agents PHA and PMA to induce the expression of PD-1. I also measured CD69 expression, an independent marker of T cell activation by flow cytometry. Of the two agents, PHA had a prominent role in PD-1 induction whereas PMA alone had no effect on

PD-1 expression (Figure 5.1A and B). PD-1 expression did not increase with the addition of PMA to PHA (Figure 5.1B). Although, Jurkat cells activated with both PHA and PMA generated the highest CD69 levels indicating higher activation of T cells than with PHA alone (Figure 5.1C). PHA and PMA activation led to a decrease in the number of live cells (~43%), compared to PHA (64% live) and PMA (80% live). Furthermore, activation of Jurkat cells found that the production of IL-2 was higher at 48 h compared to 24 h or 6 h post-activation (Figure 5.2A). The initial co-culture setup was based on the previously described report (Yang et al. 2008), replacing the uveal melanoma cells with HFFs. The reason for using HFFs was due to having a sustainable supply of cells to test and optimise the co-culture assay, whereas HDLECs are slower growing and can only be used up to a limited number of passages. HFFs were pre-treated with IFN-γ and TNF-α stimulation to increase PD-L1 expression or left untreated (Figure 5.2B). Jurkat T cells were added on top of the HFFs and the cells were treated with PHA/PMA to increase PD-1 expression for 48 h. Jurkat cells were titrated between ratios of 1:2, 1:4, 1:8 and 1:20 (i.e. 20 Jurkat cells to 1 HFF) in order to optimise the co-culture setup. IL-2 was measured by ELISA to study changes to T cell activation. I found that at ratios 1:2 and 1:8, that IFN-γ and TNF-α stimulated HFFs significantly decreased the amount of IL-2 detected compared to untreated HFFs (~20% reduction). This suggested that activated HFFs could affect the production of IL-2 from Jurkat T cells.

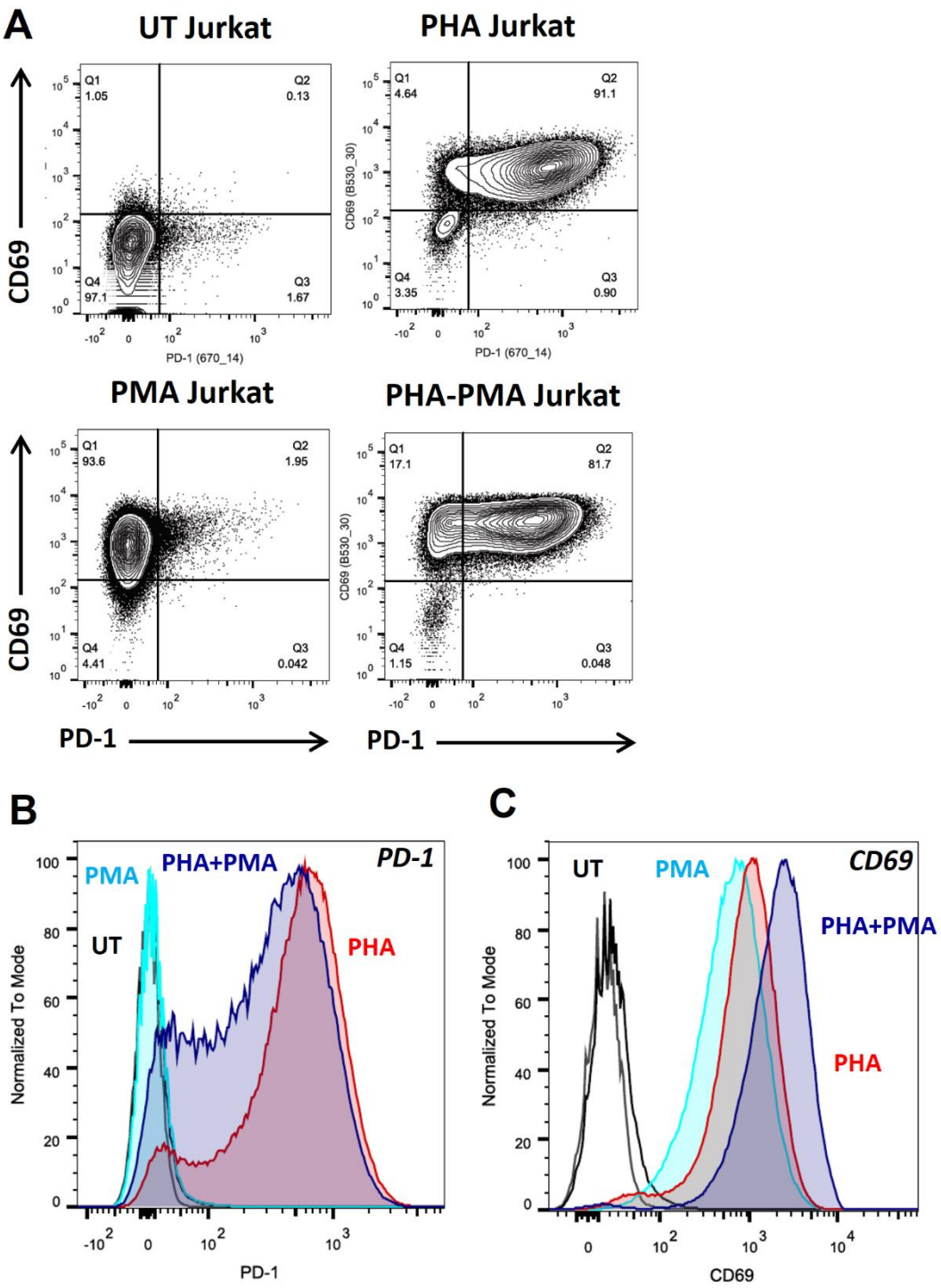

Figure 5.1. **PHA and PMA induce PD-1 on Jurkat T cells**. A) Jurkat cells were treated with PHA, PMA or both (48 h) and analysed for surface expression of PD-1 (x-axis) and the T cell activation marker CD69 (y-axis) by flow cytometry. B and C) Histograms showing overlaid data from (A), MFI (median fluorescence intensity) of PD-1 (PHA+PMA = 319, PHA = 560, PMA = 8.18, UT = 6.46, isotype = 2.37) and CD69 = (PHA+PMA = 2450, PHA = 1096, PMA = 734, UT = 27.9, isotype = 20.0). n = 3 independent experiments.

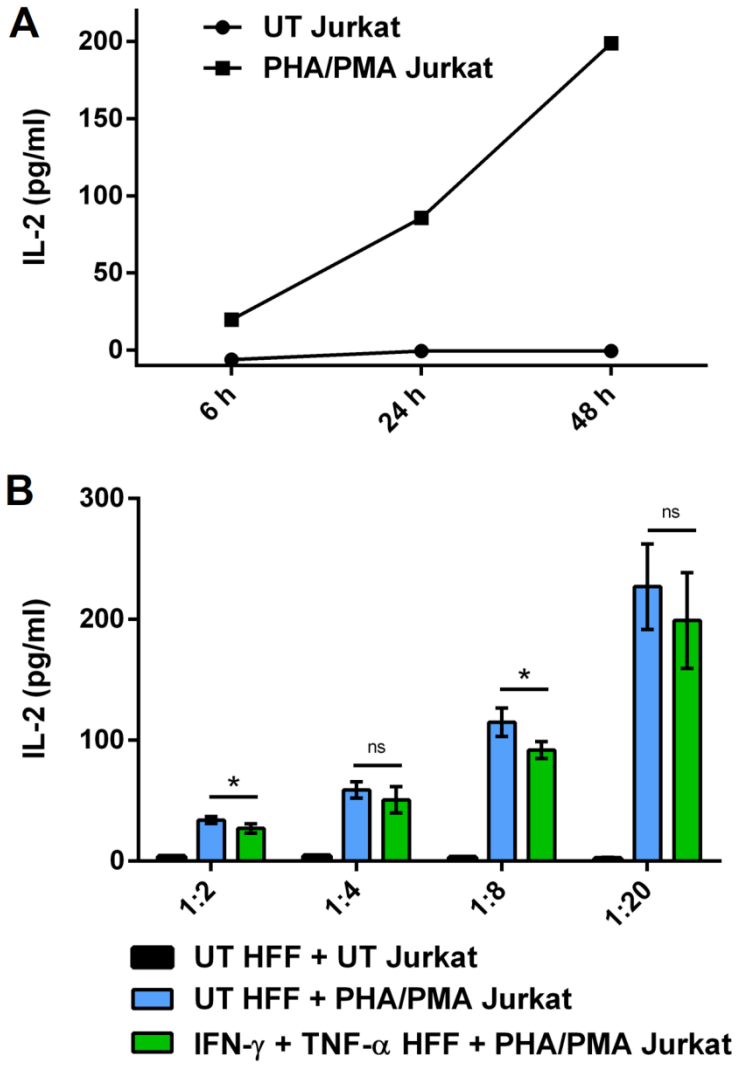

Figure 5.2 **IL-2 levels as a marker of Jurkat T cell activation.** A) Jurkat T cells were treated with PHA and PMA or left untreated (UT) for 6, 24 and 48 h and IL-2 production was measured by ELISA. n = 1 experiment. B) Co-culture of HFFs with Jurkat cells. In this particular case, IFN-γ and TNF-α pre-treated (24 h) HFFs were co-cultured with Jurkat cells in the presence of PHA and PMA (48 h) and supernatants were measured for IL-2 levels by ELISA. Unpaired Student's t test was used to compare 'UT HFF + PHA/PMA Jurkat' and 'IFN-γ and TNF-α HFF + PHA/PMA Jurkat' in each ratio. Ratio means HFF: Jurkat cells. *, $p < 0.05$. n = 4 samples in quadruplicate.

Since PHA/PMA could possibly introduce external factors that may affect the co-culture assay such as activation of signalling pathways in HFFs, I separated the activation of Jurkat cells with PHA/PMA from the co-culture with HFFs. Therefore, pre-activated Jurkat T cells (48 h) were placed on top of pre-treated HFFs and co-cultured for 24 h (Figure 5.3). Both untreated and treated HFFs increased IL-2 expression of Jurkat T cells in co-culture compared to the levels observed with Jurkat cells alone. Similarly, pre-treated HFFs

prevented secretion of IL-2 at 1:4 and 1:8 ratios. Following this, I sought to investigate the effect of cell-cell contact compared to the secretion of chemokines and cytokines by HFFs on Jurkat cells. I utilised Transwell inserts that prevent cell-cell contact meanwhile maintaining the transfer of media across a 0.4 µm pore (Figure 5.4). The increase of IL-2 production of Jurkat T cells during co-culture was reduced but remained above Jurkat only controls, and this was more noticeable with untreated HFFs, suggesting HFFs secrete pro-inflammatory mediators that induce T cell activation. Moreover, there was a significant increase in IL-2 secretion observed with the co-culture of treated HFFs compared to untreated HFFs in Transwell. This suggests anti-inflammatory cell-cell interactions that occur between treated HFFs and Jurkat cells were suppressed. These data indicate that HFFs differentially affect the amount of IL-2 produced by Jurkat cells via cell-cell contact or by the secretion of chemokines/cytokines where this response can depend on inflammatory activation of HFFs.

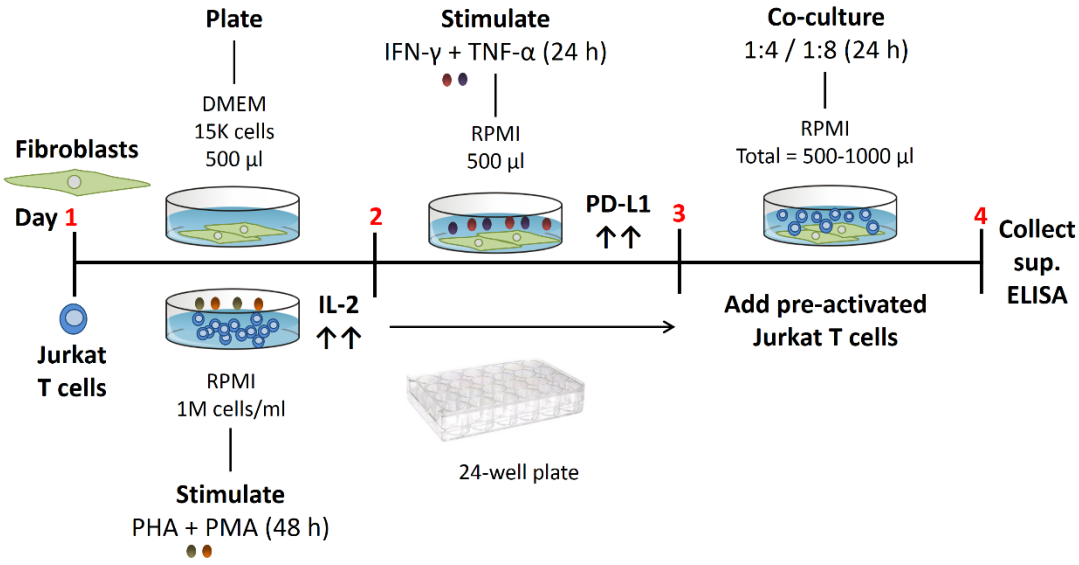

Figure 5.3. **Experimental procedure for IL-2 ELISA co-culture assays.** Jurkat T cells were pre-activated with PHA/PMA (48 h) which produce IL-2 upon activation. Meanwhile, human foreskin fibroblasts (HFFs) were plated on 24-well plates and stimulated with IFN-γ and TNF-α (24 h) the following day to increase PD-L1 expression. After pre-activation, Jurkat T cells were co-cultured with HFFs in a ratio such as 1:4 or 1:8 (HFF: Jurkat) in a volume of 500 to 1000 µl fresh media per well. Supernatants of each co-culture were harvested 24 h later for analysis by IL-2 ELISA to determine the change in levels of secreted IL-2.

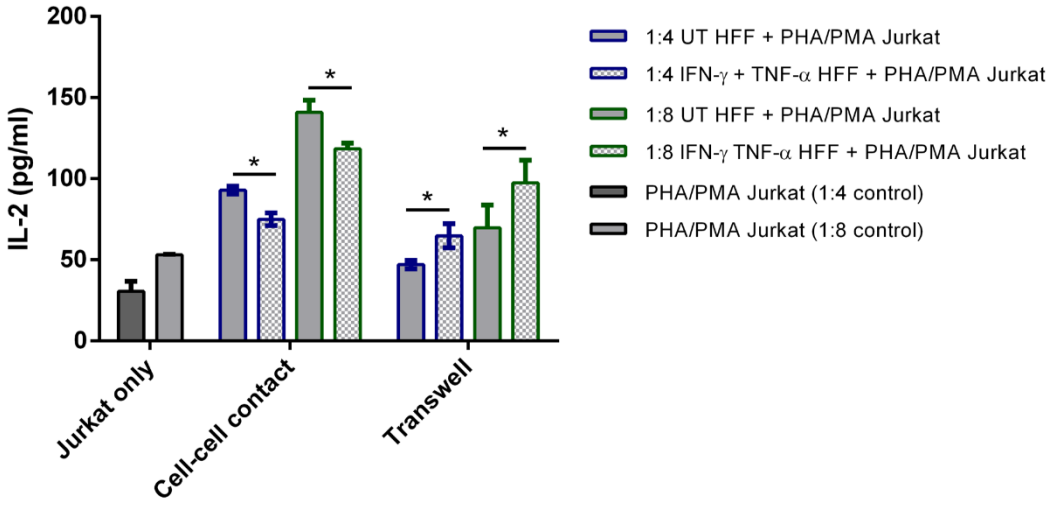

Figure 5.4. **HFFs affect the production of IL-2 by Jurkat T cells.** Jurkat T cells pre-treated with PHA/PMA (48 h) were added to UT or IFN-γ and TNF-α-treated (24 h) HFFs and co-cultured for 24 h. Data marked with 'Transwell' used 0.4 μm pore Transwell inserts to separate from cell-cell contact. Whereas the label 'cell-cell contact' did not restrict any interaction between the two cell types. Wells designated with Jurkat only were used as controls for IL-2 levels. IL-2 production was assessed by ELISA. Unpaired Student's t test was used to compare 'UT HFF + PHA/PMA Jurkat' and 'IFN-γ and TNF-α HFF + PHA/PMA Jurkat' for the same ratio in each condition. Ratio means HFF: Jurkat cells. *, $p < 0.05$. n = 3 independent experiments run in triplicate.

5.2.2. Blockade of PD-L1 interaction does not affect IL-2 expression

To investigate the effect of PD-L1 on IL-2 expression, I investigated whether the levels of IL-2 were affected by blockade of PD-L1 expression. In several reports, anti-PD-L1 clone 29E.2A3 has been used to block the expression of PD-L1 which has led to restoration of T cell function (Butte et al. 2008; Haile et al. 2014; Black et al. 2016; Watanabe et al. 2017). IFN-γ and TNF-α induces PD-L1 surface expression which was partially blocked by anti-PD-L1 antibody (29E.2A3) (Figure 5.5). Of note, the same antibody was used to block the PD-L1 site and to measure the surface expression by flow cytometry. PD-L1 expression was reduced compared to blockade with an isotype control with increasing concentration of blocking antibody (~85% reduction with the highest concentration). No difference was observed with the effect of anti-PD-L1 blockade on IL-2 levels compared to the isotype control (Figure 5.6). To test the effect of PD-L1 in the co-culture system in an alternative approach, I used siRNA to target PD-L1 (Figure 5.7 and 5.8). No difference in IL-2 levels was observed between knockdown of PD-L1 and non-targeting control in HFFs (Figure 5.7), although, there was an 80% knockdown in PD-L1 expression that was maintained

throughout co-culture (Figure 5.8). In addition, there was no difference observed with PD-1 or CD69 expression in Jurkat T cells following co-culture (Figures 5.9A and B). These data showed that the loss of PD-L1 on HFFs did not affect T cell activation as observed by levels of IL-2. These findings indicated that the lack of effect from PD-L1 disruption suggested the possibility of some limiting factors such as the expression of PD-1. In addition, the effect of PHA/PMA activation on Jurkat cells which resulted in a high proportion of cell death; using PHA alone to increase PD-1 expression would have not generated sufficient IL-2 to measure. The approach could be optimised by engineering PD-1 expression on Jurkat cells and using a different form of T cell activation.

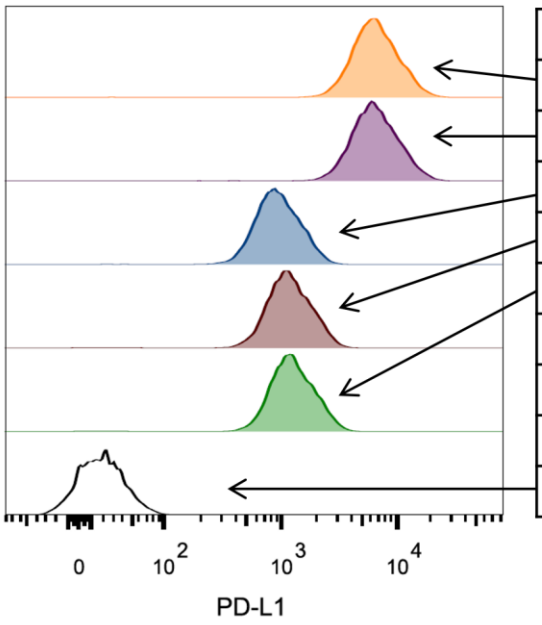

All samples IFN-γ + TNF-α treated	MFI
No block / PD-L1	6606
Iso block / PD-L1	6543
PD-L1 block (20 μg/ml) / PD-L1	955
PD-L1 block (10 μg/ml) / PD-L1	1197
PD-L1 block (5 μg/ml) / PD-L1	1267
PD-L1 block (20 μg/ml) / iso	20.4
PD-L1 block (10 μg/ml) / iso	20.4
PD-L1 block (5 μg/ml) / iso	21.3
No block / iso	20.4

Figure 5.5. **Induced PD-L1 expression is partially blocked by antibody blockade.** HFFs were treated with IFN-γ and TNF-α for 24 h. Next, HFFs were harvested and incubated with unconjugated anti-PD-L1 antibody (29E.2A3, 5, 10 and 20 μg/ml) for 30 min on ice to block the PD-L1 site. Then, cells were incubated with PE-conjugated anti-PD-L1 (29E.2A3, 2 μg/ml) for 30 min on ice to determine the surface expression of PD-L1 by flow cytometry. n = 1 experiment.

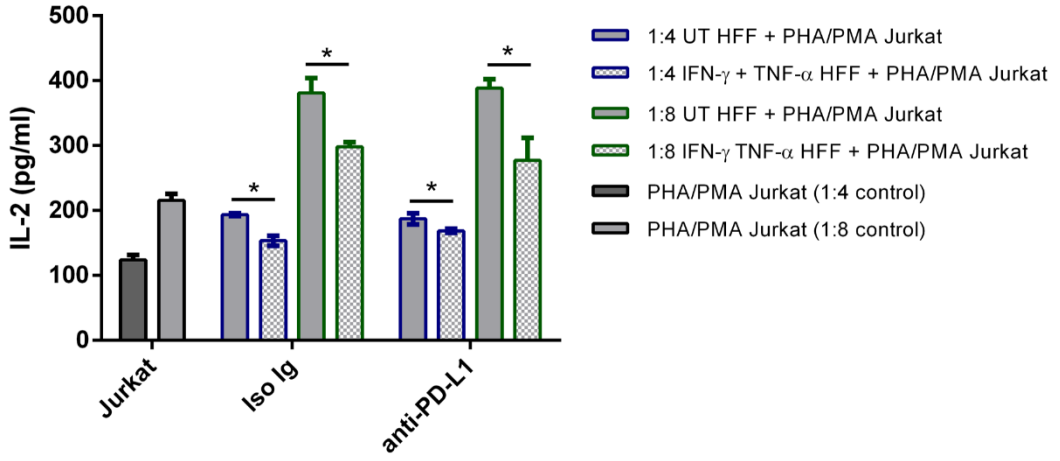

Figure 5.6. **Co-culture with antibody blockade of PD-L1.** HFFs were pre-stimulated with IFN-γ and TNF-α (24 h) and co-cultured with pre-treated Jurkat T cells (PHA and PMA, 48 h) with either anti-PD-L1 antibody (29E.2A3, 5 μg/ml per well) or isotype control (24 h). Supernatants were harvested for IL-2 ELISA 24 h later. Unpaired Student's t test was used to compare 'UT HFF + PHA/PMA Jurkat' and 'IFN-γ and TNF-α HFF + PHA/PMA Jurkat' for the same ratio in each condition. Ratio means HFF: Jurkat cells. *, $p < 0.05$. n = 3 samples run in triplicate.

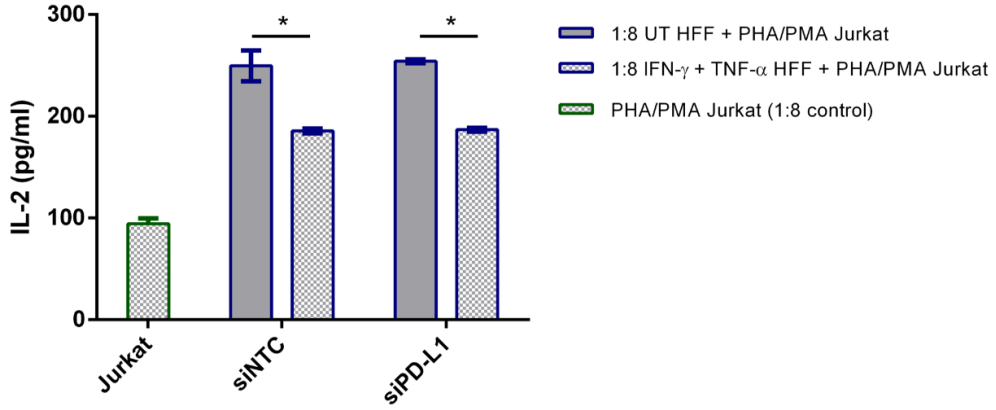

Figure 5.7. **IL-2 levels secreted by Jurkat T cells following co-culture are not affected by PD-L1 knockdown of HFFs.** HFFs were transfected with PD-L1 siRNA (48 h) and treated with IFN-γ and TNF-α (24 h). In parallel, Jurkat T cells were pre-treated with PHA and PMA (48 h), prior to co-culture with HFFs (24 h). Supernatants were collected following co-culture incubation period and IL-2 levels were determined by ELISA. Unpaired Student's t test was used to compare 'UT HFF + PHA/PMA Jurkat' and 'IFN-γ and TNF-α HFF + PHA/PMA Jurkat' for the same ratio in each condition. Ratio means HFF: Jurkat cells. *, $p < 0.05$. n = 3 samples run in triplicate.

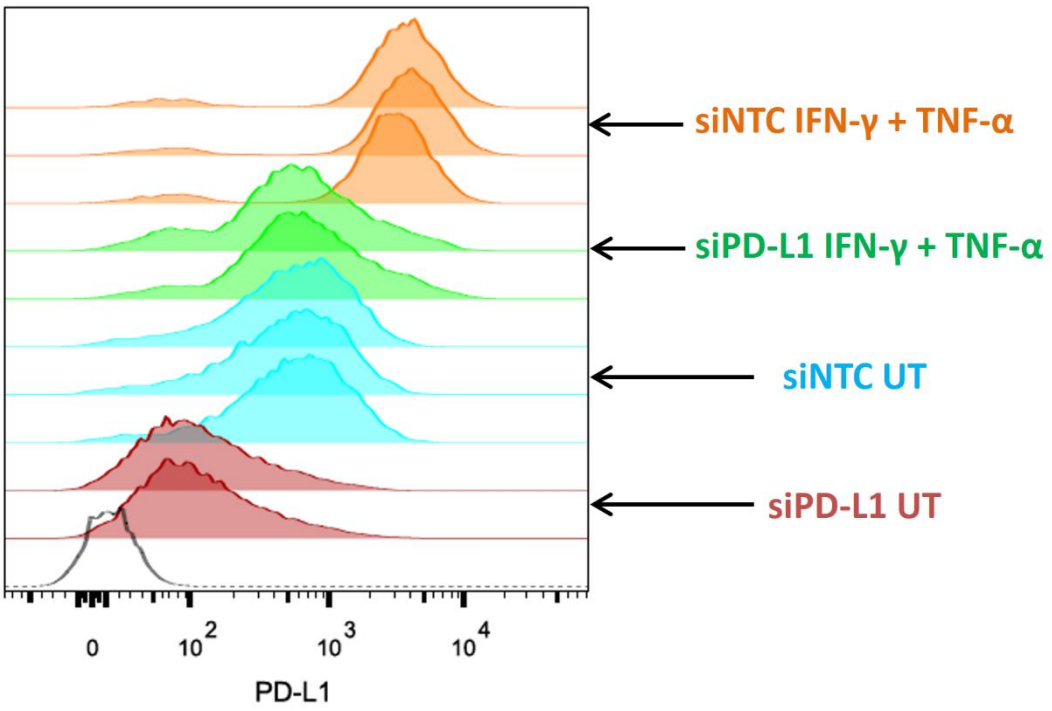

Figure 5.8. **HFF PD-L1 surface expression following co-culture with Jurkat T cells.** HFFs were transfected with siRNAs targeting PD-L1 (48 h) or non-targeting control (NTC) and subsequently treated with IFN-γ and TNF-α for 24 h or left untreated (UT). HFFs were co-cultured with pre-treated Jurkats (PHA and PMA, 48 h) for 24 h and collected for analysis by flow cytometry. Average MFI of PD-L1 staining: siNTC IFN-γ + TNF-α = 3486, siPD-L1 IFN-γ + TNF-α = 631, siNTC UT = 582, siPD-L1 UT = 115. Black = isotype control (MFI = 16.0). n = 2-3 samples run in triplicate.

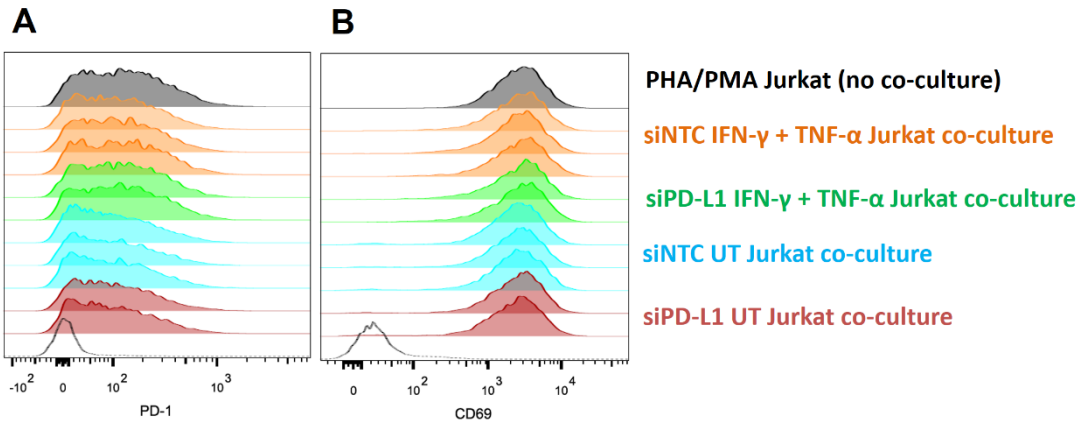

Figure 5.9. **PD-1 and CD69 expression of Jurkat T cells following co-culture with HFFs.** Jurkat cells were pre-treated with PHA and PMA (48 h) prior to co-culture with PD-L1 siRNA transfected HFFs (24 h), see Figure 5.8 for further details. Levels of PD-1 and CD69 in Jurkat T cells were measured by flow cytometry. Average MFI of PD-1 staining when co-cultured with HFFs: siNTC IFN-γ + TNF-α = 112, siPD-L1 IFN-γ + TNF-α = 119, siNTC UT = 91, siPD-L1 UT = 91, PHA and PMA Jurkat control = 128. Black = isotype control (MFI = 6.5). Average MFI of CD69 staining when co-cultured with HFFs: siNTC IFN-γ + TNF-α = 3012, siPD-L1 IFN-γ + TNF-α = 3090, siNTC UT = 2742, siPD-L1 UT = 2742, PHA and PMA Jurkat control = 3048. Black = isotype control (MFI = 20.7). n = 2-3 samples run in triplicate.

5.3. NFAT activation upon stimulation of engineered Jurkat cells with anti-CD3/CD28 antibodies

A second co-culture assay was set up in order to overcome the potential limiting factors such as PD-1 expression on T cells and the high proportion of activation-induced cell death. This approach used an engineered Jurkat T cell line (PD-1/NFAT-Luc Jurkat, defined as PD-1 Jurkat from here onwards) that overexpress CD3, PD-1 and carry a luciferase reporter tagged to the promoter of NFAT, similar to a previously published report (Skalniak et al. 2017). This would enable the quantification of T cell activation such that NFAT-responsive cells would express a higher level of luciferase upon activation. Downstream signalling from the TCR can lead to NFAT activation through the mobilisation of calcium from the plasma membrane to the cytoplasm (Smith-Garvin et al. 2009). This involves the activity of phospholipase C (PLCγ) to catalyse the hydrolysis of phosphatidylinositol-4,5-bisphosphate (PIP_2) to inositol-1,4,5-triphosphate (IP_3) and diacylglycerol (DAG) (Smith-Garvin et al. 2009). The build-up in cytosolic calcium concentration leads to activation of calcineurin which dephosphorylates NFAT via a calcineurin-binding domain. This enables nuclear translocation of NFAT to associate with its nuclear component, AP-1, to promote

transcription of genes such as IL-2 via a Rel-homology DNA binding domain that is required for regulation of T cell differentiation, proliferation and survival. In addition, NFAT is also activated through downstream co-stimulatory CD28 signalling. PI3K (phosphoinositide 3-kinase) is an effector of CD28 signalling, which converts PIP_2 to PIP_3, where PIP_3 can serve as a docking site for PDK1 (phosphoinositide-dependent kinase 1). PDK1 precedes activation of Akt which can indirectly increase NFAT activation through NF-κB signalling and also regulate the inhibitory effects of GSK3 on NFAT (Smith-Garvin et al. 2009). Overall, the increase in intracellular free Ca^{2+} represents a triggering signal for T cell activation.

The co-culture model has been previously used for antibody screening to test anti-PD-1 and anti-PD-L1 antibodies (Skalniak et al. 2017). This consisted of the PD-1 Jurkat cell line and a Chinese hamster ovary (CHO) cell line (PD-L1+ aAPC/CHO-K1), which overexpresses PD-L1 and an engineered ligand to activate the TCR, simulating an APC. These were two of the factors to overcome in order to implement HFFs/HDLECs into the set up. IFN-γ and TNF-α were used to stimulate PD-L1 expression and anti-CD3 and/or anti-CD28 antibodies to activate the PD-1 Jurkat cells (Figure 5.10) (Trickett & Kwan 2003). The co-culture would allow the two types of cells to interact and to determine the effect of PD-1/PD-L1 interaction on T cell activation, which is linked to NFAT response. Of note, this approach differs because the PD-L1 expressing cells do not provide an antigenic stimulus.

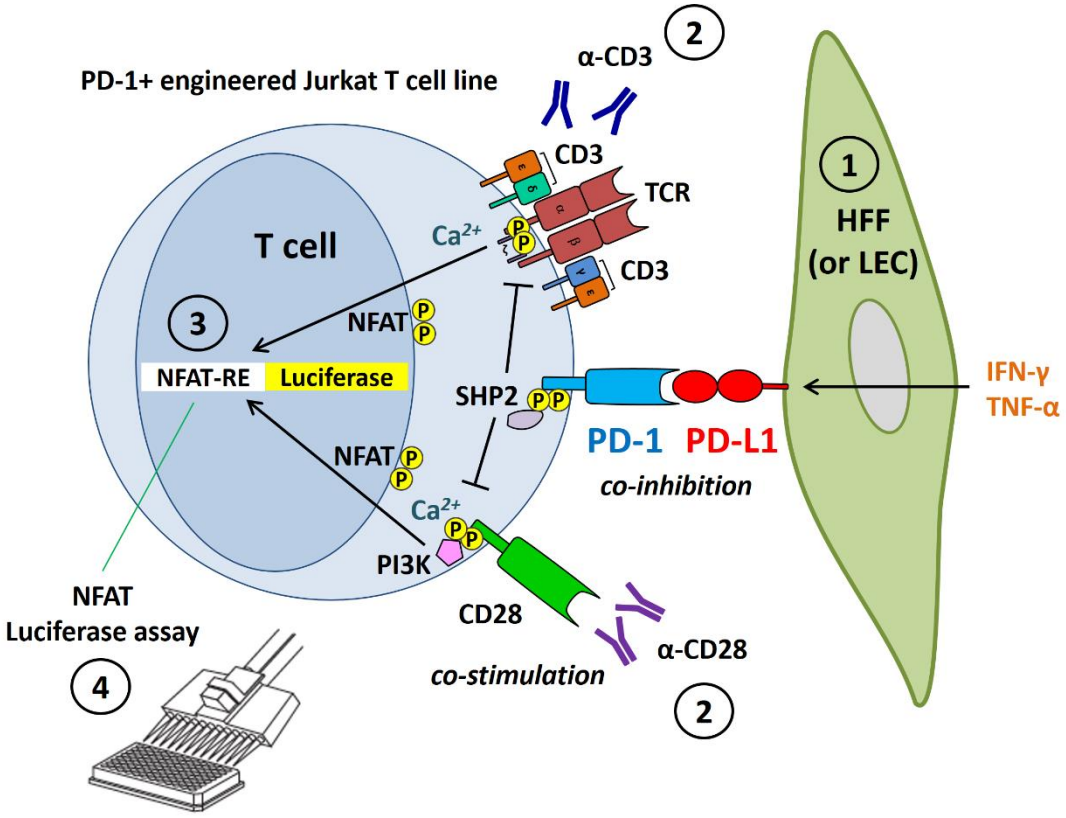

Figure 5.10. **Experimental pathway for PD-1 engineered Jurkat T cell luciferase assay.** PD-1 Jurkat T cells are engineered to constutively to express PD-1. These cells also have a luciferase reporter that is coupled to the transcriptional activity of nuclear factor of activated T cells (NFAT, response element (RE)) which is upregulated upon T cell activation and thereby represents a measurable form of T cell activation response. 1) The assay consists of PD-L1-expressing cells that are treated with IFN-γ and TNF-α to induce maximal PD-L1 expression that would interact with PD-1 expressed by modified Jurkat cells. 2) PD-1 expression is increased upon T cell activation which can be induced by using antibodies against CD3 and CD28 to stimulate the T cell receptor (TCR) and co-stimulatory pathways, respectively. This is used due to the lack of antigen presentation or TCR-activating ligand by the primary cells in this assay. 3) Activation of both of these pathways increase the amount of intracellular calcium levels that further facilitate the translocation and expression of NFAT in the nucleus which acts to promote transcription of cytokines such as IL-2. Overall, binding of PD-L1 to PD-1 prevents activation of T cells which would decrease the levels of NFAT and can be measured by luciferase assay to determine the effect of co-culture between PD-L1 expressing and Jurkat cells.

5.3.1. Activation of PD-1 Jurkat cells with anti-CD3 and anti-CD28

To activate the PD-1 Jurkat cells with anti-CD3 and/or anti-CD28, I used either plate-bound, soluble (Figure 5.11) or coated beads. Plate-bound activation of T cells provides a better crosslinking effect than soluble activation, the idea that receptor or ligands are brought closer in a specific area which would enable prolonged engagement of the TCR and sustained signalling. In addition, PD-1 expression is induced following TCR crosslinking of $CD4^+$ $CD8^+$ double positive T cells using plate-bound anti-CD3 antibodies (Keir et al. 2005). In contrast, the soluble activating format would be in alignment with the previous co-culture format, allowing the PD-L1-expressing cells to adhere to the bottom of the well prior to the addition of Jurkat cells and stimulating factors.

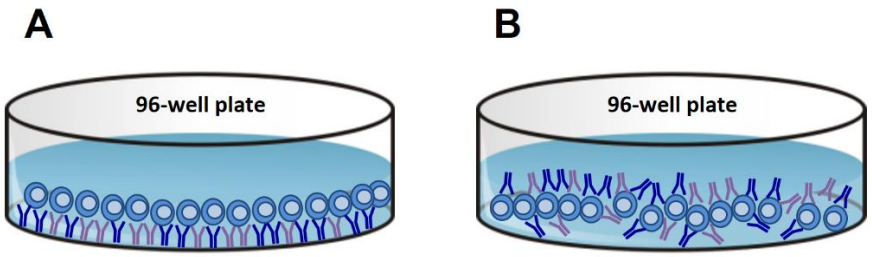

Figure 5.11. **Plate-bound versus soluble T cell activation: crosslinking difference.** Crosslinking means to bring receptors or ligands together in a specific area of the cell membrane leading to a strong point signal. In vitro method of activation of T cells can determine the response of T cells. A) Plate-bound or immobilised antibodies are coated on 96-well plates and can send a strong proliferative signal to T cells, allowing gradual accumulation of signalling events over time. B) Soluble antibodies in the media can also activate T cells where there is uniform distribution of antibody on the cell surface and engagement of most receptors. However, there is no continuous receptor triggering or sustained signalling. Therefore plate-bound activation provides better activation of T cells.

I tested both the plate-bound and soluble format. Although, these cells were engineered to overexpress PD-1, I determined that at basal level these PD-1 Jurkat cells expressed a modest level of surface PD-1 expression (~50-60%) (Figure 5.12A). Plate-bound or immobilised anti-CD3 coated at the bottom of the well generated a strong increase to both PD-1 and CD69 signal after 24 h compared to the modest increases generated from soluble, free-floating antibodies (Figure 5.12A-C). Live-stained cell count was ~70-85% in both untreated and anti-CD3-treated cells (Figure 5.12B-C). Similar findings were observed using the luciferase assay, NFAT activity was higher with plate-bound activation (Figure 5.12D). In addition, there was a further increase in the activation of PD-1 Jurkat T cells by using media with lower serum content (1%) (Figure 5.12D). To determine the effect of PD-L1 Fc

on PD-1 Jurkat cells, recombinant PD-L1 Fc was added at the same time as anti-CD3 (Figure 5.12A-D). There was a decrease in detectable PD-1 expression and a modest reduction in CD69 signal from flow cytometry analysis. However, there was no difference in NFAT signal when quantified through the luciferase assay. Soluble anti-CD3 activation of NFAT activity in PD-1 Jurkat cells could be enhanced in combination with anti-CD28 (Figure 5.13A-B). In addition, levels of NFAT activation were higher at 6 h compared to 24 h activation. There was a decrease in PD-1 signal and a small rise in NFAT activation after applying PD-L1 Fc, suggesting that PD-L1 Fc partially blocks the PD-1 site rather than mitigating the activation of T cells. Moreover, the number of live-stained cells was ~80-90% in both untreated and anti-CD3/CD28-treated cells (Figure 5.13B). Overall, these data indicate that both plate-bound and soluble anti-CD3 and/or anti-CD28 application can activate PD-1 Jurkat cells to increase PD-1, CD69 and NFAT expression. Although, the effect of soluble activation is noticeably weaker. This allows some flexibility with the setup of the co-culture with the aim to optimise a system that can determine the effect of PD-1/PD-L1 interaction on the initialisation and maintenance of T cell activation.

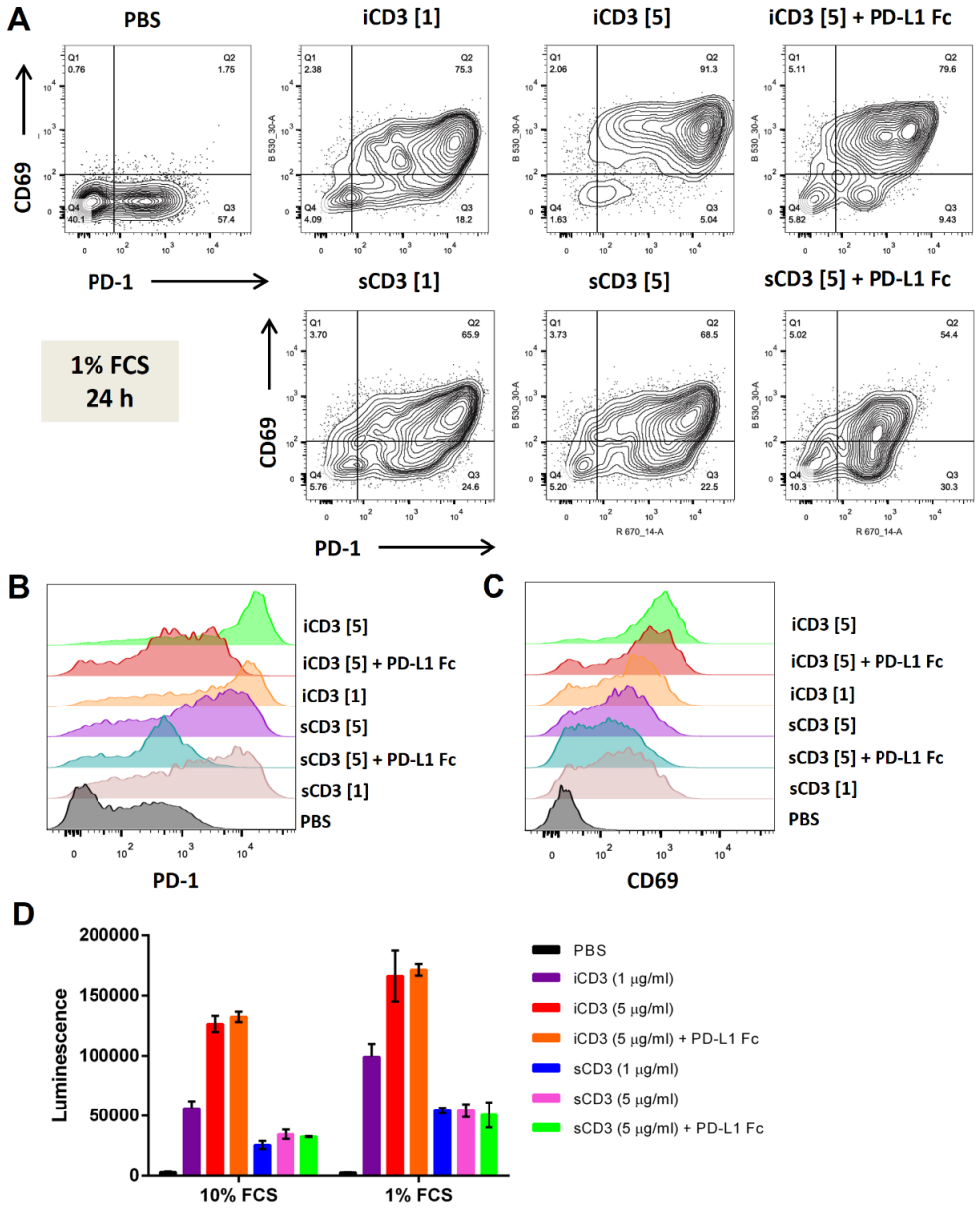

Figure 5.12. **Effect of plate-bound or soluble antibody activation of NFAT expression in T cells.** PD-1 Jurkat T cells were treated with 1 or 5 µg/ml anti-CD3 for 24 h in RPMI 1% FCS either in wells that have been coated with anti-CD3 (plate-bound) or anti-CD3 that was soluble in the media. If applicable, recombinant PD-L1 Fc was added at the same time as anti-CD3 to attempt to block the PD-L1 binding site. A) Cells were analysed for surface expression of PD-1 and CD69 by flow cytometry. B and C) Histograms showing intensity of PD-1 and CD69 expression, D) NFAT activation was subsequently analysed for luminescence following addition of luciferase substrate (Bio-Glo). n = 3 samples run in triplicate. iCD3 = immobilised anti-CD3, sCD3 = soluble anti-CD3 and PBS = no activating factors. Average MFI of PD-1: iCD3 [5] = 11220, iCD3 [5] + PD-L1 Fc = 908, iCD3 [1] = 4763, sCD3 [5] = 2513, sCD3 [5] + PD-L1 Fc = 492, sCD3 [1] = 2063 and PBS = 130. Average MFI of CD69: iCD3 [5] = 1001, iCD3 [5] + PD-L1 Fc = 655, iCD3 [1] = 357, sCD3 [5] = 232, sCD3 [5] + PD-L1 Fc = 142, sCD3 [1] = 217 and PBS = 23.7.

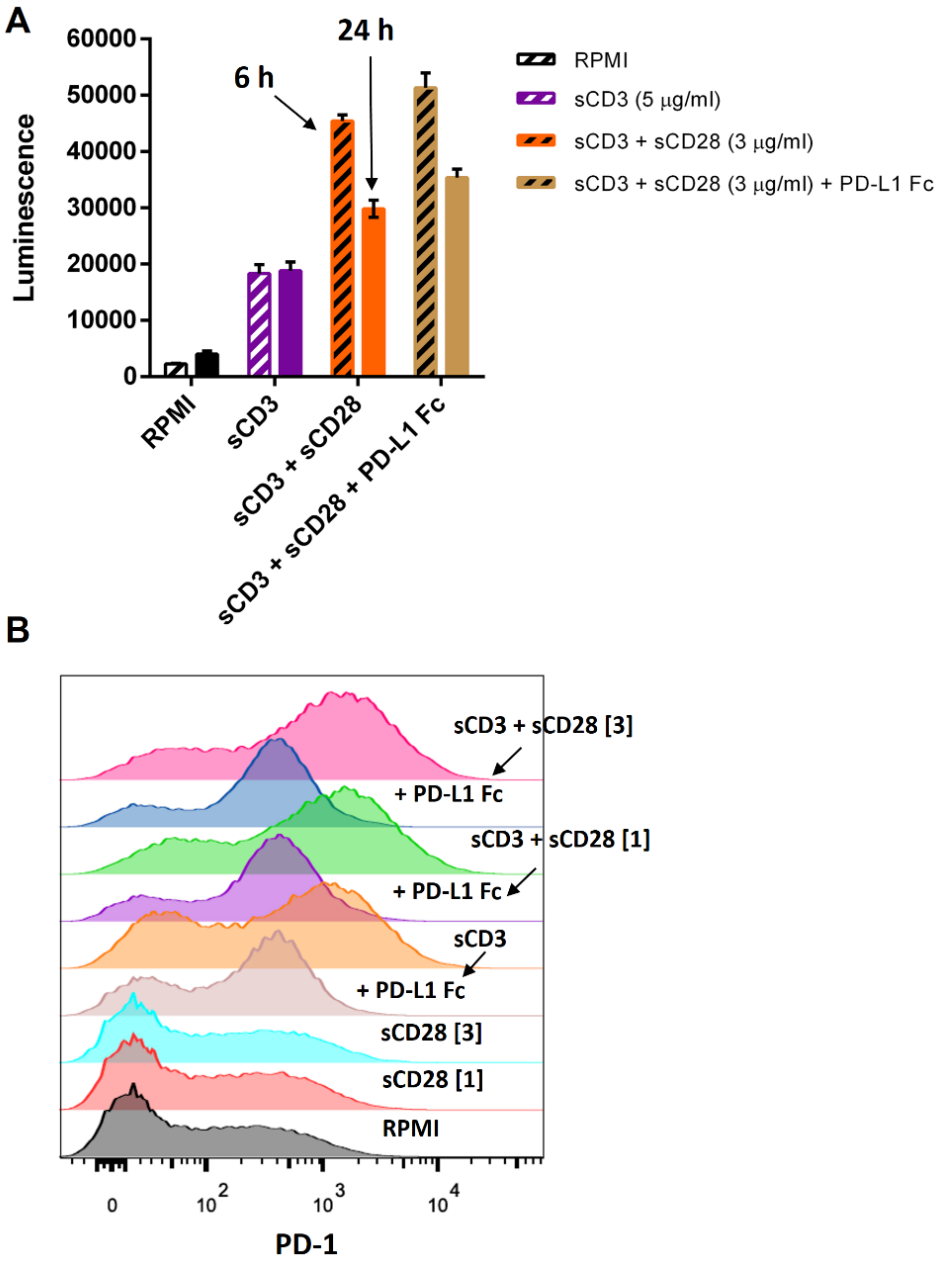

Figure 5.13. **NFAT Activation of Jurkat T cells with soluble CD3/CD28.** PD-1 Jurkat T cells were treated with 5 µg/ml anti-CD3 and either 0, 1 or 3 µg/ml anti-CD28 for 6 or 24 h in RPMI 1% FCS. A) NFAT activation was subsequently analysed for luminescence following addition of luciferase substrate (Bio-Glo). Striped bars = 6 h time-point and bars with no pattern = 24 h time-point. n = 3 samples in triplicate. B) Cells were analysed by flow cytometry for surface PD-1 expression after 24 h. Average MFI of PD-1: sCD3 + sCD28 [3] = 1038, : sCD3 + sCD28 [3] + PD-L1 Fc = 385, sCD3 + sCD28 [1] = 983, sCD3 + sCD28 [1] + PD-L1 Fc = 392, sCD3 [3] = 565, sCD3 + PD-L1 Fc = 297, sCD28 [3] = 104, sCD28 [1] = 96.2, RPMI = 78.7.

5.3.2. Co-culture of primary cells with plate-bound activated PD-1 Jurkat cells

Having determined two forms of activation of PD-1 Jurkat cells, the next step was to establish a protocol for the co-culture. Plate-bound antibody activation of PD-1 Jurkat cells gave the higher level of activation and PD-1 expression compared to using soluble antibodies. PD-1 Jurkat cells were pre-activated on anti-CD3/CD28 coated wells for ~4 h prior to the addition of pre-stimulated HFFs on top of the PD-1 Jurkat cells (IFN-γ and TNF-α, 24 h) (Figure 5.14A). This meant that additional time was required for the HFFs to adhere. Following co-culture for ~16 h, activation of NFAT in PD-1 Jurkat cells were analysed by luciferase assay. For this co-culture method, I tested HFFs transfected with siRNAs for non-targeting control (siNTC) or PD-L1 (siPD-L1) as well as two anti-PD-1 antibodies (EH12.2H7, Figure 5.14B and nivolumab, Figure 5.14C) to determine PD-1/PD-L1 interaction. It was expected that knockdown of PD-L1 would increase activation of NFAT in PD-1 Jurkat cells. Co-culture had a modest decrease to NFAT signal in PD-1 Jurkat cells, which was also not affected by the depletion of PD-L1. As activation of NFAT in samples treated with non-targeting control were higher than samples where PD-L1 was knockdown. Addition of HFFs to Jurkat T cells decreased T cell activation. In addition, samples with Jurkat only controls had increased NFAT signal compared to counterpart isotype controls and was more noticeable in samples treated with nivolumab. These results suggest that the protocol with plate-bound activation above does not demonstrate that PD-1/PD-L1 interaction affects the activation of NFAT in PD-1 Jurkat cells. Although, plate-bound activation of PD-1 Jurkat cells generates the higher form of activation, it is complicated by other factors such as the addition of HFFs to the well, such as the suspension of PD-1 Jurkat cells that may be displaced from the bottom of the well due to this movement and thereby detach from plate-bound anti-CD3/CD28.

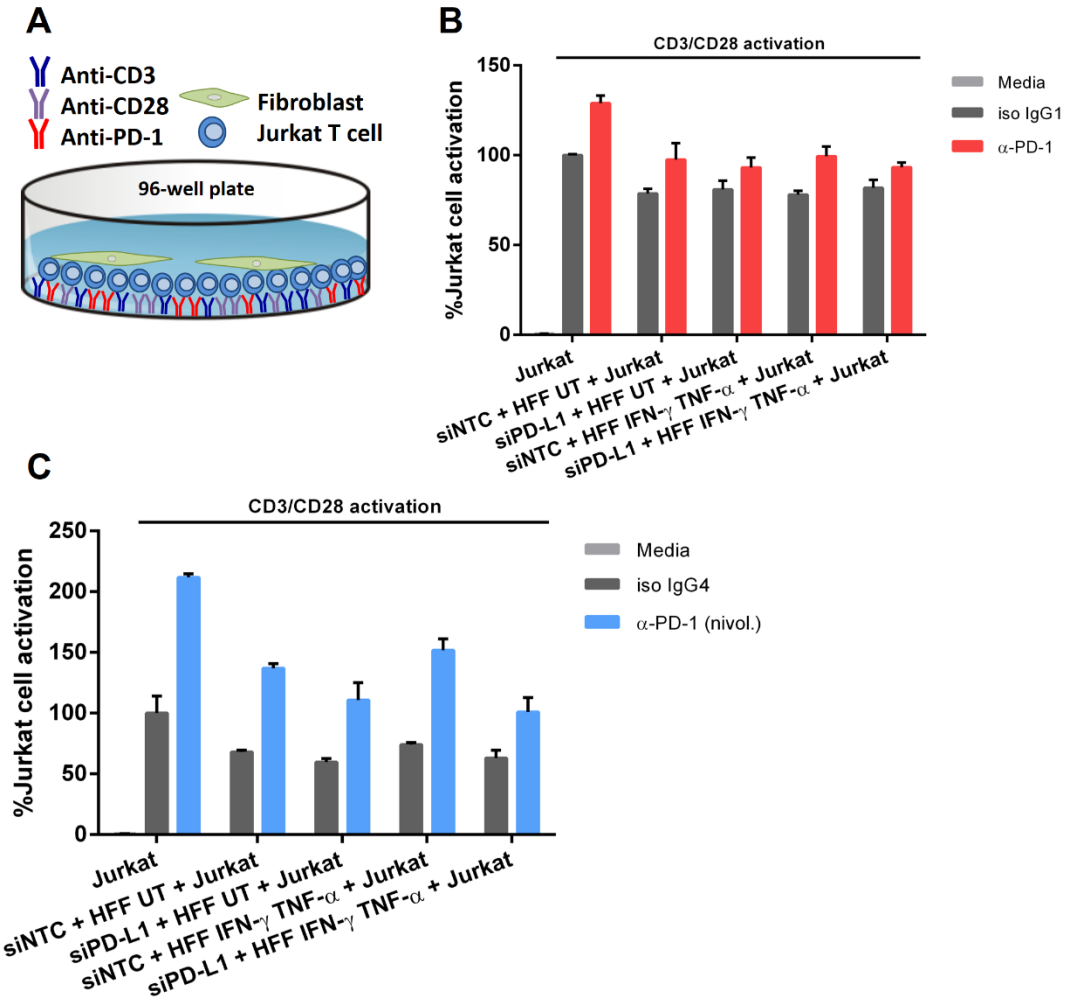

Figure 5.14. **Effect of co-culture on plate-bound activated PD-1 Jurkat cells.** A) Jurkat T cells were incubated with plate-bound anti-CD3/CD28 with anti-PD-1 (panel B, EH12.2H7, red), anti-PD-1/nivolumab (panel C, blue) or isotype IgG control in a 96-well plate. After 4 h, pre-stimulated HFFs which were either siRNA transfected with non-targeting control (NTC) or PD-L1, were added and cells were co-cultured for 16 h. For Jurkat control, the same volume in media was added. This means the Jurkat cells were pre-activated prior to addition of HFFs and anti-CD3/CD28 remained in the media during co-culture. Cells were subsequently analysed for luminescence following addition of luciferase substrate (Bio-Glo). % Jurkat cell activation is calculated from normalisation of all luciferase readings to the average of the relevant Jurkat isotype control. n = 3 samples run in triplicate.

5.3.3. Co-culture of primary cells with soluble activated PD-1 Jurkat cells

As an alternative, soluble anti-CD3/CD28 antibodies were used for activation of PD-1 Jurkat cells (Figure 5.15). HFFs were adhered and stimulated with IFN-γ and TNF-α (24 h) to increase PD-L1 expression. I tested the addition of PD-1 Jurkat cells, overlaying these cells on top of HFFs for different periods (Figure 5.16A). I also adjusted the times before anti-

CD3/CD28 antibodies were applied to start the activation of T cells, as there may be a pre-incubation time required for the HFFs and PD-1 Jurkat cells to form an interface or immunological synapse (Figure 5.16A). Suppression of NFAT activation was more evident with 3-4 h of pre-incubation. Upon further testing, I activated the PD-1 Jurkat cells for a lesser time and found that as early as 3 h activation there was a decrease in NFAT signal with 3 h pre-incubation (Figure 5.16B). Activation times of 1-2 h for PD-1 Jurkat cells may be too short to see a difference. Further 3 h pre-incubation periods with longer activation (up to 9 h) yielded a similar decrease in NFAT activity (Figure 5.17A). This suggested that for HFFs, a pre-incubation period is required to suppress T cell activity. By titrating the starting number of HFFs versus PD-1 Jurkat cells, there was a significant amount of suppression of NFAT activity with increasing density of IFN-γ and TNF-α stimulated HFFs (Figure 5.17B). Untreated HFFs can also suppress T cell activation which is then further decreased when HFFs were treated with IFN-γ and TNF-α (Figure 5.18A). There was no disparities between using fresh media or conditioned media that was collected from HFFs treated with IFN-γ and TNF-α to test for possible factors in the media that affected the activation of T cells, indicating that the suppression was primarily mediated by cell-cell contact.

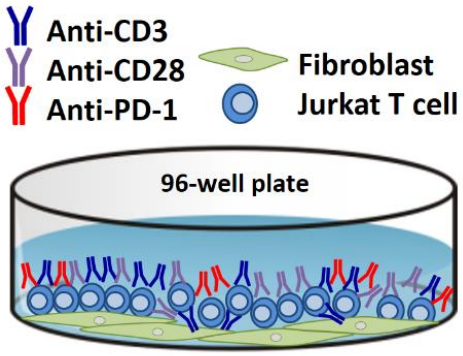

Figure 5.15. **Effect of co-culture on soluble activated PD-1 Jurkat cells.** In the final version of this assay. HFFs were seeded in 96-well plate format for up to 24 h. Untreated PD-1 Jurkat T cells were added to IFN-γ and TNF-α stimulated (24 h) HFFs and co-cultured without activating antibodies for up to 3 or 4 h to establish cell-cell interactions. Subsequently, anti-CD3, anti-CD28 and anti-PD-1 (if applicable) were added to the well to initialise activation of PD-1 Jurkat cells whilst in contact with HFFs for up to a total of 8 to 24 h co-culture.

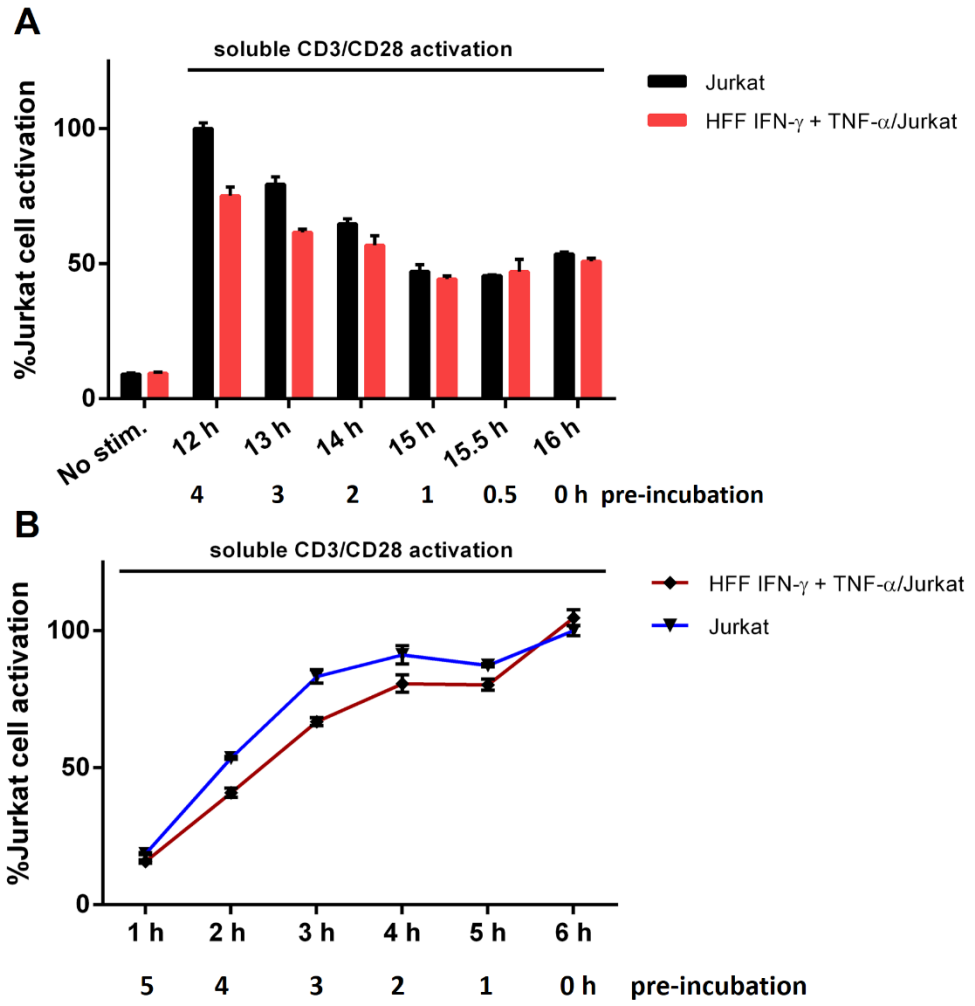

Figure 5.16. **Pre-incubation prior to anti-CD3/CD28 activation is required for suppression of Jurkat cell activation.** Untreated PD-1 Jurkat T cells were added to IFN-γ and TNF-α stimulated (24 h) HFFs and co-cultured without activating antibodies (defined as pre-incubation) for the time-period indicated. Subsequently, anti-CD3 and anti-CD28 were added to activate the Jurkat cells that are in co-culture with HFFs. Total co-culture time is notified by the number on the top row; bottom row indicates the pre-incubation time. A) Total co-culture up to 16 h with pre-incubation between 0-4 h, Jurkat cells were analysed by luciferase assay to assess NFAT activation. B) Total co-culture up to 6 h with pre-incubation between 0-5 h. Jurkat cells were analysed by luciferase assay to assess NFAT activation. % Jurkat cell activation is calculated from normalisation of all luciferase readings to the average of the anti-CD3/CD28-treated Jurkat only control. n = 3 samples run in triplicate.

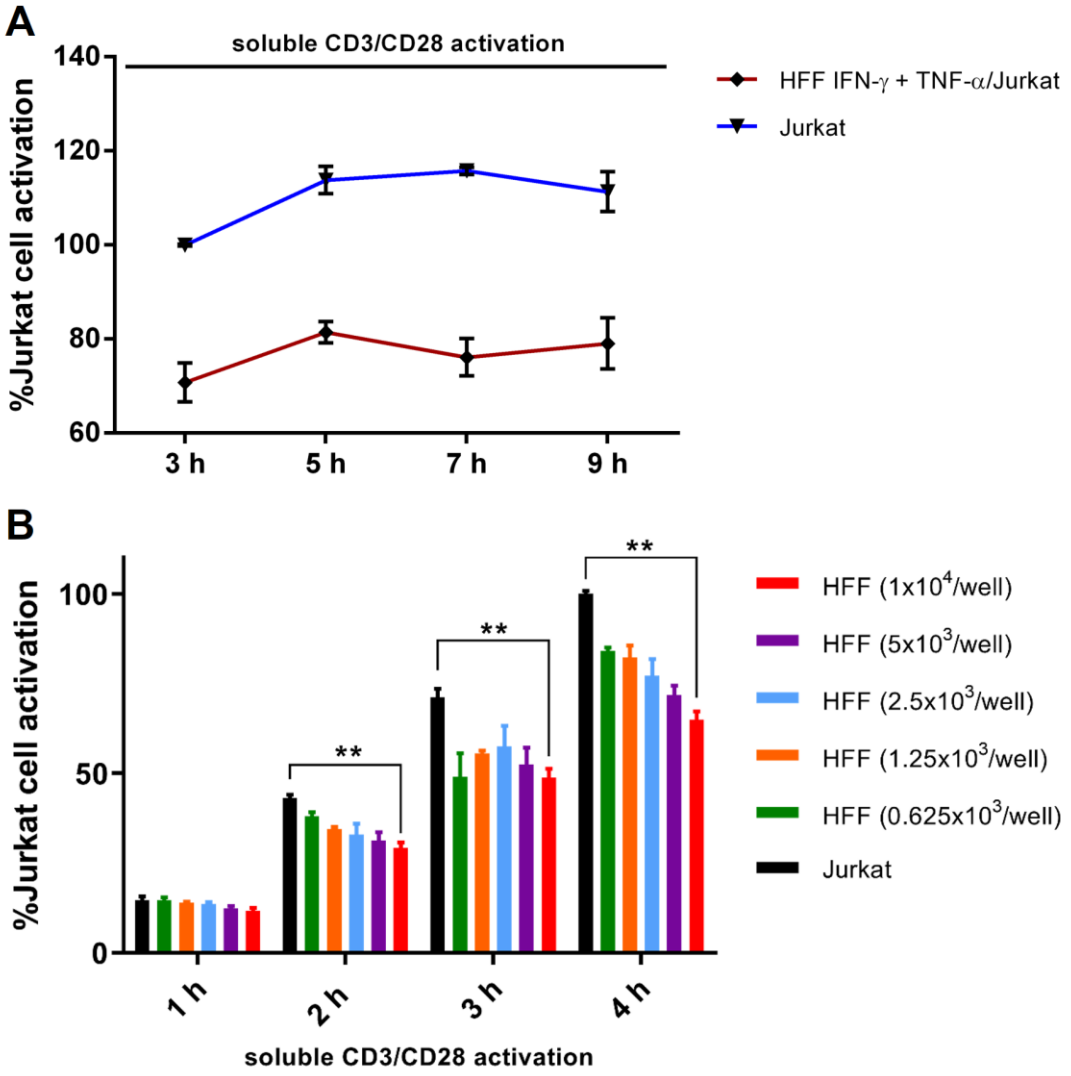

Figure 5.17. **HFFs inhibit activation of PD-1 Jurkat T cells.** A) Untreated PD-1 Jurkat T cells were added to IFN-γ and TNF-α stimulated (24 h) HFFs and pre-incubated initially without activating antibodies (3 h). Subsequently, anti-CD3 and anti-CD28 were added to activate the Jurkat cells that were in co-culture with HFFs, length of activation is indicated on the x-axis. Following co-culture, Jurkat cells were analysed by luciferase assay to assess NFAT activation. B) Similar preliminary setup to A) but with titration of number of HFFs per well (i.e. this is the starting number of HFFs in the well). Pre-incubation of Jurkat and HFFs occurred for 3 h before activation of Jurkat with anti-CD3 and CD28 for the time indicated on the x-axis. % Jurkat cell activation is calculated from normalisation of all luciferase readings to the average of the anti-CD3/CD28-treated Jurkat only control. Two-way analysis of variance (ANOVA) was calculated with Tukey's multiple comparisons test, here showing the difference between Jurkat control and HFF ($1x10^4$/well). **, $p < 0.01$. n = 3 samples run in triplicate.

Next, I transfected HFFs with siRNAs for NTC and PD-L1 (Figure 5.18B). There was no noticeable difference apart from a small increase from the knockdown of PD-L1 on NFAT activity. I also transfected miR-155 mimics, which previously described to decrease PD-L1 expression, generated a small decrease on T cell activation (Figure 5.18B). Previously, nivolumab (anti-PD-1 antibody) was shown to affect the activation of PD-1 engineered Jurkat T cells (Skalniak et al. 2017). Blockade of PD-1 using nivolumab partially restored NFAT signal but there were some technical difficulties since nivolumab affected the luciferase signal given by PD-1 Jurkat cells (Figure 5.19A). Specifically, the PD-1 Jurkat control cells were generating decreased luciferase signal after nivolumab was added to the co-culture compared to the isotype control, suggesting nivolumab was affecting the PD-1 Jurkat cells themselves. The reason for this is unknown and testing for cell viability using the Alamar Blue assay did not indicate that the PD-1 Jurkat cells were dying (Figure 5.19B).

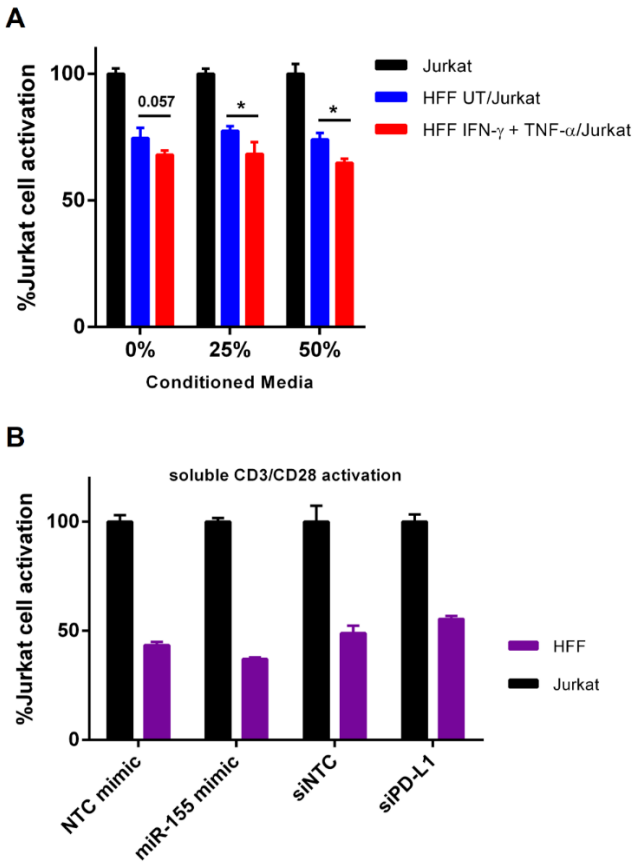

Figure 5.18. **IFN-γ + TNF-α treated HFFs suppress Jurkat T cell activation but is not restored by blocking PD-1/PD-L1 interaction.** A) Conditioned media was collected from IFN-γ and TNF-α stimulated HFFs (2 h) and added at the same time as untreated PD-1 Jurkat T cells were added to HFFs and co-cultured initially without activating antibodies (3 h). Percentage indicates the ratio of conditioned to fresh media. Subsequently, anti-CD3 and anti-CD28 were added to activate the PD-1 Jurkat cells that are in co-culture with HFFs (3 h). B) HFFs were transfected with miR-155 mimic or PD-L1 siRNA (48 h) and treated with IFN-γ and TNF-α (24 h). PD-1 Jurkat cells were co-cultured with HFFs for 3 h without activating factors and then anti-CD3 and anti-CD28 were added to activate the Jurkats (3 h). Following co-culture, Jurkat cells were analysed by luciferase assay to assess NFAT activation. % Jurkat cell activation is calculated from normalisation of all luciferase readings to the average of the anti-CD3/CD28-treated Jurkat only control. n = 3 samples run in triplicate. Unpaired Student's t test was used to compare 'HFF UT/Jurkat' and 'HFF IFN-γ + TNF-α/Jurkat'. *, $p < 0.05$. n = 3 samples run in triplicate.

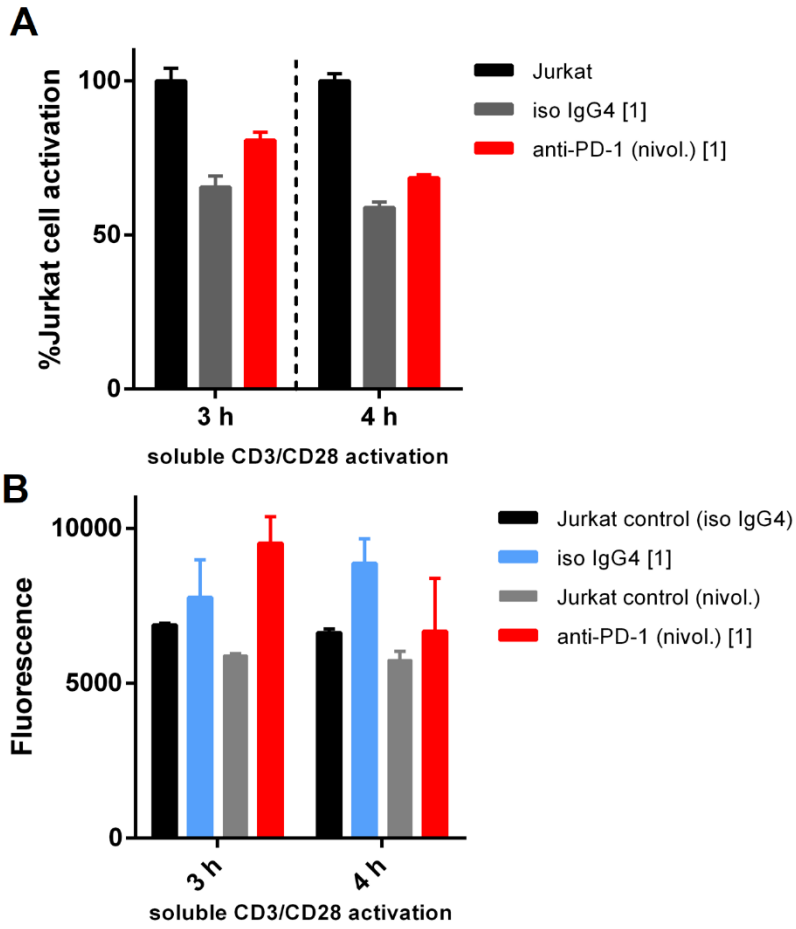

Figure 5.19. **Effect of nivolumab on the blockade of PD-1/PD-L1 interaction in this assay.** A) Jurkat T cells were incubated with pre-treated HFFs (IFN-γ and TNF-α, 24 h) and anti-PD-1/nivolumab or isotype IgG control for 3 h and then activated with anti-CD3/CD28 were for 3 or 4 h. Cells were subsequently analysed for luminescence following addition of luciferase substrate (Bio-Glo). % Jurkat cell activation is calculated from normalisation of all luciferase readings to the average of the relevant anti-CD3/CD28-treated Jurkat isotype control. B) In a parallel setup to A), Alamar Blue was added to wells at the final step (instead of the luciferase substrate) to determine cell viability and the fluorescence was measured. HFF only controls were used to determine the contribution of Jurkat cells within the co-culture to the fluorescence reading. [1] denotes 1 μg/ml. n = 3 samples run in triplicate.

To investigate the effect of HDLECs on PD-1 Jurkat cell activation, a similar approach was undertaken whereby HDLECs were titrated versus Jurkat cells (Figure 5.20). Untreated HDLECs did not display any difference, in contrast, IFN-γ and TNF-α treated HDLECs significantly suppressed PD-1 Jurkat cell activation. The highest density of HDLECs used had the most suppressive effect. These data indicate that both IFN-γ and TNF-α activated HFFs and HDLECs can suppress NFAT activity in PD-1 Jurkat cells.

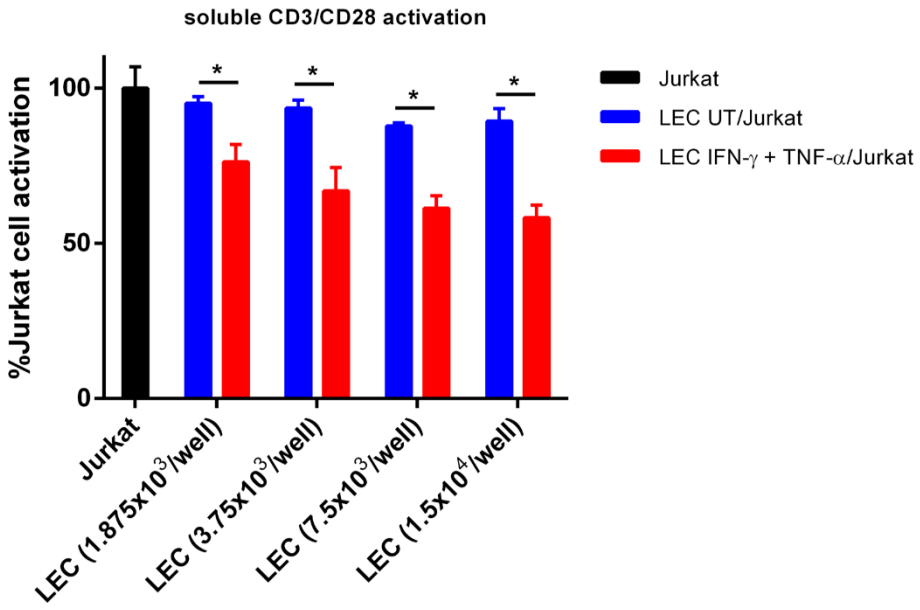

Figure 5.20. **HDLECs inhibit activation of PD-1 Jurkat T cells.** Untreated PD-1 Jurkat T cells were added to IFN-γ and TNF-α stimulated (24 h) HDLECs (number per well is shown on x-axis) and co-cultured initially without activating factors (3 h). Subsequently, anti-CD3 and anti-CD28 were added (3 h) to activate the Jurkat cells that were in co-culture with HDLECs. Following co-culture, Jurkat cells were analysed by luciferase assay to assess NFAT activation. % Jurkat cell activation is calculated from normalisation of all luciferase readings to the average of the anti-CD3/CD28-treated Jurkat only control. n = 3 samples run in triplicate. Unpaired Student's t test was used to compare 'LEC UT/Jurkat' and 'LEC IFN-γ + TNF-α/Jurkat'. *, $p < 0.05$. n = 3 samples run in triplicate.

5.3.4. PD-L1 knockdown does not affect T cell activation in PD-1^{hi}-sorted Jurkat cells

To assess whether the weak effect of PD-1 blockade (or PD-L1 siRNA knockdown) on NFAT activity was dependent on PD-1 expression, PD-1 Jurkat cells were FACS sorted based on high expression of PD-1 (Figure 5.21). Untreated pre-sorted PD-1 Jurkat cells were gated on the higher expressing PD-L1 population of cells (based on MFI) and were sorted into a new population defined as PD-1^{hi} Jurkat cells (Figure 5.21A and C). Activation of PD-1^{hi} Jurkat cells with soluble anti-CD3/CD28 (3 h) increased the expression of PD-1 from untreated levels (84.5% to 93.8% of cells) and gained 2-fold MFI over activated pre-sorted Jurkat cells (Figure 5.21B and D). Co-culture experiments were repeated with the sorted PD-1^{hi} Jurkat cells using soluble anti-CD3/CD28 activation similarly to the previous setup (Figure 5.22A). Compared to previous results (Figure 5.17B), the addition of HFFs to PD-1^{hi} Jurkat cells resulted in reduced suppression of NFAT activation with both untreated or IFN-γ and TNF-α treated HFFs. There was no noticeable difference in the activation of PD-1^{hi}

Jurkat cells when co-cultured with HFFs that were depleted of PD-L1 (Figure 5.22B). However, there was further decrease in activation of PD-1^{hi} Jurkat cells when IFN-γ and TNF-α stimulated HFFs were transfected with miR-155 mimics but not with untreated HFFs (Figure 5.22B). Similar to HFFs, co-culture of PD-1^{hi} Jurkat cells with IFN-γ and TNF-α treated HDLECs resulted in a reduced effect of suppression (Figure 5.23A). Neither knockdown of PD-L1 or transfection of miR-155 mimics in HDLECs affected NFAT activation in PD-1^{hi} Jurkat cells (Figure 5.23B). Overall, stimulation of HFFs or HDLECs with IFN-γ and TNF-α induced a suppressive effect on NFAT activation. However, blocking PD-1/PD-L1 interaction did not affect NFAT activation.

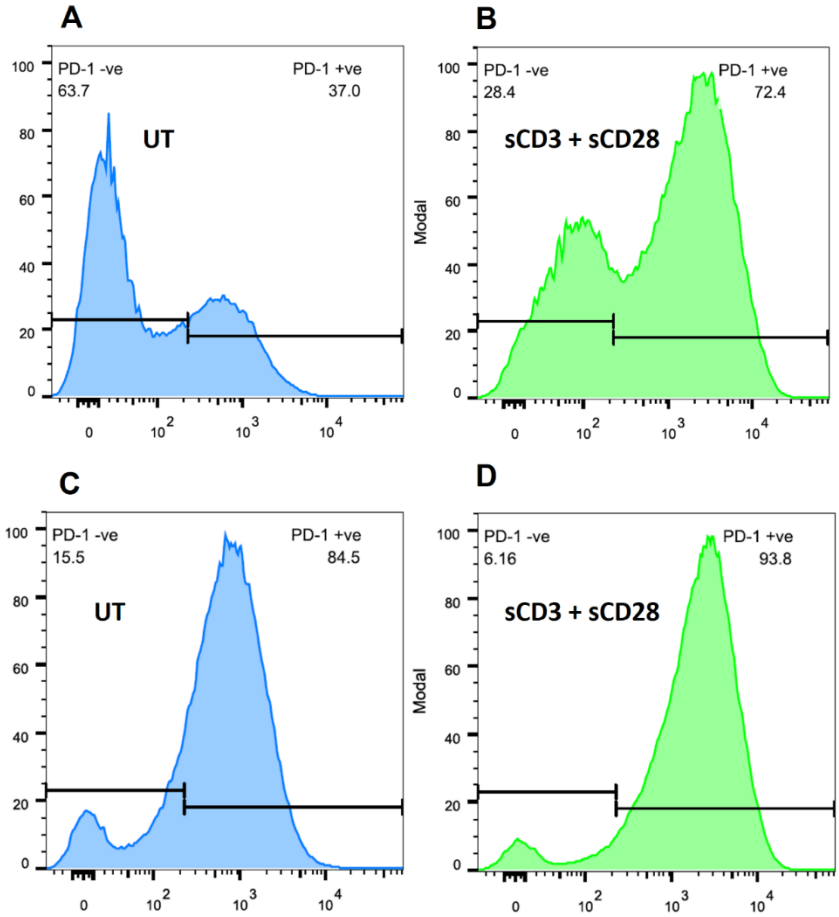

Figure 5.21. **PD-1 expression on pre- and post-sort of PD-1 Jurkat T cells.** PD-1 Jurkat T cells were sorted for high expression of PD-1 by FACS and compared to pre-sorted Jurkat T cells. A) and B) Pre-sorted Jurkat cells were activated with anti-CD3 and anti-CD28 (3 h) or left untreated and analysed by flow cytometry for surface PD-1 expression. C and D) Post-sorted Jurkat cells were activated with anti-CD3 and anti-CD28 (3 h) or left untreated. PD-1 MFI: untreated pre-sorted PD-1 Jurkat cells = 67, soluble anti-CD3/CD28 activated pre-sorted PD-1 Jurkat cells = 1188, untreated post-sorted PD-1^{hi} Jurkat cells = 767, soluble anti-CD3/CD28 activated post-sorted PD-1^{hi} Jurkat cells = 2356. n = 1 experiment.

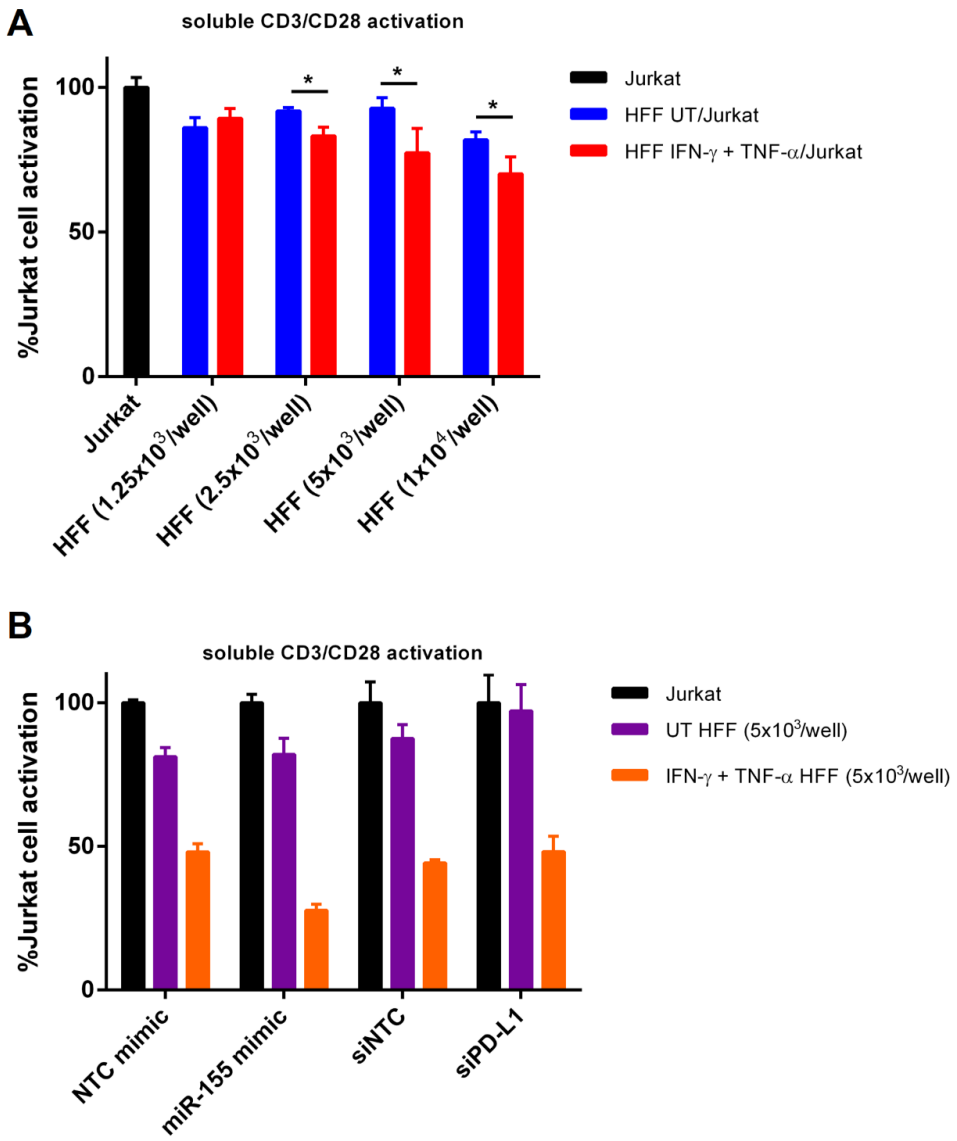

Figure 5.22. **PD-L1 knockdown in HFFs has no effect in the co-culture model.** A) Sorted PD-1^{hi} Jurkat T cells were co-cultured with titrated number of IFN-γ and TNF-α stimulated HFFs (3 h) prior to addition of anti-CD3 and anti-CD28 (3 h). B) HFFs were transfected with miR-155 mimic or PD-L1 siRNA (48 h) and treated with IFN-γ and TNF-α (24 h). Sorted PD-1^{hi} Jurkat cells were co-cultured with HFFs for 3 h without activating factors and then anti-CD3 and anti-CD28 were added to activate the Jurkats (3 h). Following co-culture, Jurkat cells were analysed by luciferase assay to assess NFAT activation. % Jurkat cell activation is calculated from normalisation of all luciferase readings to the average of the anti-CD3/CD28-treated Jurkat only control. Unpaired Student's t test was used to compare 'HFF UT/Jurkat' and 'HFF IFN-γ + TNF-α/Jurkat'. *, $p < 0.05$. n = 3 samples run in triplicate.

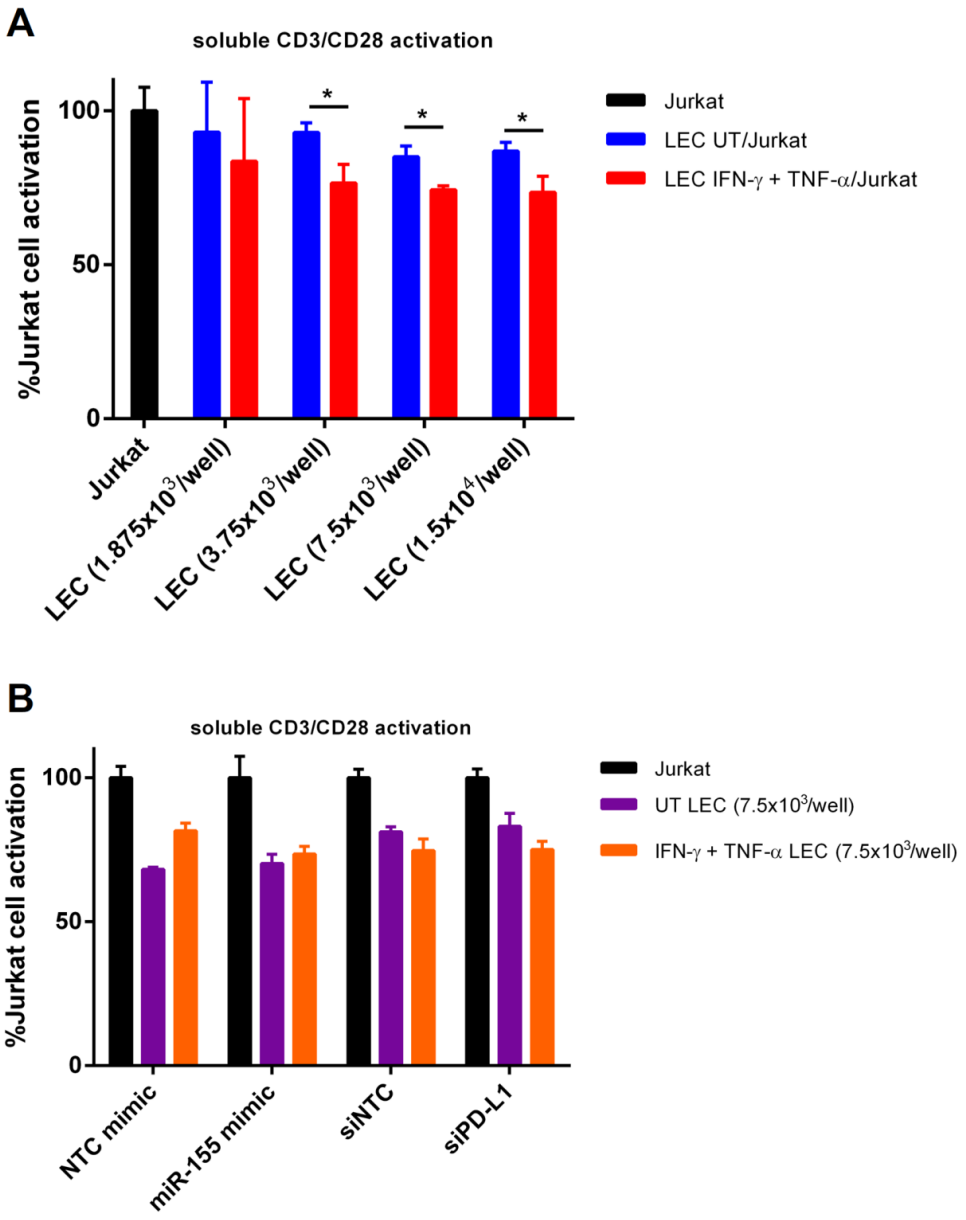

Figure 5.23. **PD-L1 knockdown in HDLECs has no effect in the co-culture model.** A) Sorted PD-1^{hi} Jurkat T cells were co-cultured with titrated number of IFN-γ and TNF-α stimulated HDLECs (3 h) prior to addition of anti-CD3 and anti-CD28 (3 h). B) HDLECs were transfected with miR-155 mimic or PD-L1 siRNA (48 h) and treated with IFN-γ and TNF-α (24 h). Sorted PD-1^{hi} Jurkat cells were co-cultured with HDLECs for 3 h without activating factors and then anti-CD3 and anti-CD28 were added to activate the Jurkats (3 h). Following co-culture, Jurkat cells were analysed by luciferase assay to assess NFAT activation. % Jurkat cell activation is calculated from normalisation of all luciferase readings to the average of the anti-CD3/CD28-treated Jurkat only control. Unpaired Student's t test was used to compare 'LEC UT/Jurkat' and 'LEC IFN-γ + TNF-α/Jurkat'. *, $p < 0.05$. n = 3 samples run in triplicate.

5.4. Chapter discussion

This chapter focused on the development of co-culture assays to study the effect of PD-L1 expression and regulation on T cell activation, using both wild-type and engineered Jurkat cells as a model for T cells. Both co-culture models were developed off previously reported systems (Yang et al. 2008; Skalniak et al. 2017) to test PD-1/PD-L1 interaction with primary stromal fibroblasts/vascular cells that have been used in previous chapters. The experimental setup required extensive optimisation and was far more complex than first thought. Both NFAT and IL-2 were used as measures of Jurkat T cell activation of which NFAT is an essential component that contributes towards IL-2 expression (Chow et al. 1999) and both factors have been used to characterise PD-1/PD-L1 interaction (Yang et al. 2008; Skalniak et al. 2017). In addition, surface levels of CD69 were used, which serves as an independent early activation marker (Sancho et al. 2005). There was a noticeable and reproducible difference in IL-2 or NFAT after co-culture with HFFs or HDLECs (Figures 5.4, 5.17B, Figure 5.20), suggesting that HFFs/HDLECs did interact with the activation of Jurkat cells in both co-culture models. In contrast, neither of the two co-culture models which utilised different measures of T cell activation showed an effect that was dependent on PD-1/PD-L1 interaction since depletion of PD-L1 by siRNA or blockade of PD-1 with antibodies made no difference to the described markers of T cell activation.

Presentation of specific antigen activates T cells and upregulates PD-1 expression, which is dependent on the concentration of antigen and duration of antigen stimulation (Xu-Monette et al. 2017). The importance of antigen expression on the PD-L1-expressing cell may influence whether PD-1/PD-L1 interaction occurs as co-localisation of PD-1 with CD3 and/or CD28 is required for suppression of T cell activation (Chemnitz et al. 2004). Purified primary $CD4^+$ T cells were coated with artificial APCs that were constructed using magnetic beads comprised of anti-CD3, anti-CD28, anti-MHC class I and anti-PD-1. T cells were activated with anti-CD3/CD28-coated beads in the production of IL-2 mRNA, compared to using anti-MHC class I which served as the negative control. CD28 stimulation was required for rapid increase of PD-1 mRNA. Moreover, SHP2 was recruited to the cytoplasmic tail of PD-1 upon TCR-induced cell activation but only upon PD-1 engagement can SHP2 mediate inhibition of T cell activation. In addition, low levels of PD-1 surface expression on $CD4^+$ T cells were sufficient for inhibitory effects and SHIP1 did not bind to PD-1 cytoplasmic tail (Chemnitz et al. 2004). These findings suggest that for further optimisation of the PD-1 Jurkat co-culture assay, anti-MHC class I antibodies could be used to test whether antigen-dependent stimulation is required for PD-1/PD-L1 interaction to occur.

In co-culture assays using Jurkat cells to investigate PD-1/PD-L1 interaction, Raji B cells were pre-incubated with the superantigen staphylococcal enterotoxin E (SEE) that binds to MHC class II molecules and the TCR (Tian et al. 2015; Zhao et al. 2018; Fraser et al. 1992). This would enable Jurkat cells to recognise antigen-loaded Raji B cells and become activated upon interaction. The advantage of using superantigens is that it only requires binding to the TCR to induce acute inflammatory responses (Pinchuk et al. 2008) and SEE has been shown to activate NFAT and IL-2 in wild-type Jurkat cells (Antón et al. 2008). In addition, superantigens can be used to bind to a diverse number of cell types via MHC class II molecules. I have shown that IFN-γ and TNF-α-activated HDLECs can express MHC class II molecules, and fibroblasts have been demonstrated in a previous paper to express MHC class II upon activation (Ilangumaran et al. 2002). To further optimise the co-culture assay, primary stromal fibroblasts/vascular cells could be pre-loaded with superantigen SEE (or similar) prior to co-culture (Brogan et al. 2004), instead of using anti-CD3/CD28 antibodies to activate Jurkat cells. In some studies, PD-1/PD-L1 interaction has been demonstrated between wild-type Jurkat cells and human melanoma or breast cancer cells without the use of superantigen or antigen presentation on PD-L1-expressing cells (Yang et al. 2008; Black et al. 2016; Li et al. 2016). This may be due to the level of immunogenicity of these tumour cells as a result of mutations that give rise to tumour-associated antigens, enabling further interactions between cancer cells and Jurkat cells (Escors 2014). Overall, the use of pre-loaded antigens on PD-L1-expressing cells can enable these cells to function as non-professional APCs in order to analyse PD-1/PD-L1 interaction in a physiological manner.

For the first co-culture model involving IL-2, which was based on a previously described system, uveal melanoma cells overall decreased the amount of IL-2 produced by Jurkat cells (Yang et al. 2008). In addition to IL-2, the production of IFN-γ, TNF-α and IL-10 have been characterised after PD-1 blockade in T cell co-cultures with lymphoma cell lines, to determine the activation of T cells (Quan et al. 2015). In contrast to the report that this co-culture procedure was based on (Yang et al. 2008), Jurkat cells were pre-treated with PHA and PMA instead of this addition at the co-culture step. This meant that HFFs were unaffected by PHA and PMA treatment, where PMA has been shown to affect the growth of fibroblasts and induce cyclooxygenase-2 (COX-2) expression, an inflammatory mediator (Ning & Mamrack 1994; Cheng et al. 2014). An additional reason was that PD-1 expression induced by PHA and PMA treatment on Jurkat cells requires up to 48 h to reach maximal levels. This meant that the measurement of IL-2 production from Jurkat cells took place at a different stage of T cell activation compared to the previous report (Yang et al. 2008). Overall, HFFs induced IL-2 secretion of pre-treated Jurkat cells and this induction was

suppressed with IFN-γ and TNF-α stimulated HFFs. By eliminating cell-cell contact using a Transwell system, the induction of IL-2 by untreated HFFs was suppressed but not with treated HFFs suggesting the presence of anti-inflammatory cell-contact-dependent interactions that are induced by IFN-γ and TNF-α. A titration of increasing density of HFFs to Jurkat cells could have shown a range of effect on T cell activation with and without Transwell inserts. Furthermore, PHA stimulation can induce apoptosis of Jurkat cells in a concentration-dependent manner, a process termed activation-induced cell death (Zhang et al. 2017). I found some similarity in the number of live-stained cells (~43% PHA/PMA treated) in my results comparing to PHA stimulation in the previously described report (Zhang et al. 2017), indicating that there were fewer Jurkat cells to interact with HFFs which may decrease any effect of PD-1/PD-L1 interaction that could be observed.

Therefore, I investigated whether a second co-culture model could demonstrate PD-1/PD-L1 interaction using PD-1 engineered Jurkat cells. In this second approach, the limiting factors that were thought to be associated with the first approach (i.e. PD-1 expression, live number of cells) could be taken into consideration in order to observe PD-1/PD-L1 interaction. This method utilised PD-1 engineered Jurkat cells with a luciferase reporter linked to NFAT, which can be used to measure luminescence and improve the sensitivity of the assay. Activation of PD-1 Jurkat cells with anti-CD3/CD28 antibodies expressed more levels of PD-1 than PHA/PMA activated wild-type Jurkat cells without requiring a longer period of stimulation that could cause activation-induced cell death. This was demonstrated by a difference of ~43% live-stained cells with PHA/PMA-treated Jurkat cells compared with ~70-80% live cells using anti-CD3/CD28 with PD-1 engineered Jurkat cells. There were two different developments of this assay that deviated from the previously described method that presented a challenge (Skalniak et al. 2017), involving the use of plate-bound or soluble activation to stimulate PD-1 Jurkat cells. As this was to replace engineered CHO cells that overexpressed PD-L1 and a ligand to activate the TCR (Skalniak et al. 2017). In another report that showed a similar PD-1 NFAT system, a membrane-anchored anti-CD3 antibody (OKT3) fragment was engineered onto CHO cells (L. Wang et al. 2017). The difference between my experimental procedure and the previously described reports (Skalniak et al. 2017; L. Wang et al. 2017) is there are two specific interactions, such that an APC can activate and inhibit the same Jurkat cell. In my setup, anti-CD3/CD28 antibodies were used to activate PD-1 Jurkat cells and IFN-γ and TNF-α to induce PD-L1 expression on HFFs/HDLECs. Thus, this represents only one interaction from the PD-L1-expressing cell and increases the variability of the type of interactions that can occur. For example, an IFN-γ and TNF-α stimulated HFF could make contact with an unstimulated PD-1 Jurkat cell. The pre-incubation of both Jurkat and PD-L1-expressing cells was essential in demonstrating an

effect on PD-1 Jurkat cell activation. The idea was to facilitate the assembly of an interface between the two cell types or the immunological synapse where PD-1 can be recruited upon TCR engagement (Pentcheva-Hoang et al. 2007; Yokosuka et al. 2012). The interaction between PD-1/PD-L1 is characterised as entropy-driven and relies on relatively weaker interactions, compared to CD28/CTLA-4 (Cheng et al. 2013; Parry et al. 2005). The suppressive effect mediating by HFFs/HDLECs was not found to be dependent on PD-1/PD-L1 interaction and suggests a lack of MHC-peptide antigen may be the issue. Antigenic peptide-MHC binding can induce restructuring of the actin cytoskeleton that leads to PD-1 accumulation at the immunological synapse, which can be stabilised by PD-L1 (Pentcheva-Hoang et al. 2007). The formation of PD-1/PD-L1 checkpoint interaction may have been prevented between HFFs/HDLECs and PD-1 Jurkat cells, or there was a lack of downstream effector signalling if the two molecules did engage (Pentcheva-Hoang et al. 2007). A positive control for this co-culture procedure would be to use the CHO-K1 cells that express a TCR ligand and PD-L1 to determine whether the same PD-1 Jurkat T cells require the interaction at the TCR to initiate the PD-1/PD-L1 interaction that is described in published reports (Skalniak et al. 2017; L. Wang et al. 2017).

The role of miR-155 in $CD4^+$ T cells has been shown to be important for influencing IFN-γ signalling and generating a bias for Th1 differentiation (Rodriguez et al. 2007; Lu et al. 2009; Banerjee et al. 2010). Moreover, miR-155 is required for optimal responses of CD8+ T cells by enhancing cytokine signalling through the targeting of SOCS1 (Dudda et al. 2013; Gracias et al. 2013). The expression of miR-155 was shown to regulate LCMV-mediated $CD8^+$ T cell exhaustion (Stelekati et al. 2018). miR-155 was shown to influence T cell differentiation through the balance of AP-1 family members where overexpression of miR-155 resulted in decreased expression of NFAT1 and Fosl2. Of note, the overexpression of miR-155 did not complement the efficacy of anti-PD-L1 blocking antibody treatments in exhausted $CD8^+$ T cells (Stelekati et al. 2018). What effect may miR-155 expression in stromal fibroblasts/vascular cells have on the inflammatory response, in particular on T cell activation in a paracrine manner? Previously, miR-155 expression was demonstrated to decrease PD-L1 expression (Chapter 3) which suggested that using miR-155 mimics in HFFs/HDLECs may lead to an increase in Jurkat cell activation. In contrast, the addition of miR-155 mimics to IFN-γ and TNF-α-stimulated but not untreated HFFs was found to have a modest decrease on NFAT activation in $PD\text{-}1^{hi}$ Jurkat cells, suggesting the overall effect of miR-155 in HFFs may have a suppressive effect on T cell activation. However, the findings are limited because it was not possible to observe whether miR-155-dependent regulation of PD-L1 expression affects T cell activation.

In sum, I aimed to investigate the functional relevance of the effects of miRNA regulation of PD-L1 protein expression on the activation of T cells using stromal fibroblasts/vascular cells. I can determine that HFFs/HDLECs affect markers of T cell activation (NFAT, IL-2) and that IFN-γ and TNF-α stimulation of HFFs/HDLECs suppresses activation of Jurkat cells. The experimental setups of these co-cultures are influenced and interlinked by a number of limitations and variables that include: the type of cells used (with/without genetic engineering of antigen or PD-L1 expression), the activation of Jurkat cells, the type of PD-1/PD-L1 blockade used, the period of co-culture, the concentration of cells per co-culture and the controls that are used for normalisation of IL-2 or NFAT signal (Goers et al. 2014). A "small" adjustment in the system could widely affect the results of the co-culture. These setups have generated reproducible results using IL-2 or NFAT expression upon repeated experiments but have yet to show an effect on T cell activation that is dependent on PD-1/PD-L1 interaction in their current state. Further optimisation is required for the co-culture assays as these will determine whether regulatory effects of PD-L1 expression on HFFs/HDLECs can affect T cell activation.

6. PD-L1 silencing in primary cells

6.1. Introduction

Previously, I showed that inflammatory cytokines and inflammatory-regulated miRNAs can affect the expression of PD-L1. At the time of those experiments it was relatively weakly understood whether PD-L1 had any forward signalling or feedback mechanisms to the effects on its expression in a cell-intrinsic manner. This chapter explored the capabilities of PD-L1 by silencing its expression and investigating the resulting effects specifically on key STAT proteins and miRNA levels in an exploratory fashion.

The cytoplasmic region of human PD-L1 is short (30 aa) and relatively conserved in pigs, cattle, mice and rats (Figure 6.1A) (Keir et al. 2008). Human PD-L2 also has a short intracellular tail (30 aa) but in mice and rats there are a loss of amino acid residues towards the end of the PD-L2 tail sequence (Figure 6.1B) (Latchman et al. 2001). Initially, PD-L1 was thought to have no signalling motifs or any known signalling function. Emerging evidence have shown that PD-L1 may indeed have a role in intracellular signalling (Azuma et al. 2008; Jin et al. 2011; Chang et al. 2015; Clark et al. 2016; Gato-Cañas et al. 2017; Lucas et al. 2018). In studies using mouse tumour models, tumour expression of PD-L1 was demonstrated to regulate mTOR activity and glycolytic metabolism in tumour cells as blockade of PD-L1 decreased phosphorylation of Akt (S473) and mTOR target proteins and glycolysis enzymes (Chang et al. 2015). These findings were supported by another study that found tumour expression of PD-L1 regulated cell proliferation, mTOR signalling and autophagy without the need for engagement of PD-1 (Clark et al. 2016).

PD-L1 was indicated to have a functional role in corneal angiogenesis (Jin et al. 2011). Knockdown of PD-L1 by siRNA transfection was demonstrated to increase VEGFR2 and proliferative levels of MS1 pancreatic islet endothelial cells (obtained from a C57BL/6 mouse). A higher level of angiogenesis was observed in PD-L1 knockout mice compared to wild-type mice but there was no change in expression of inflammatory cytokines after induction of inflammation. This suggests that PD-L1 expression limits endothelial cell division. Additionally, inhibition of a potential binding partner of PD-L1, CD80 affected similar targets including VEGFR2 which may be addressed by possible interaction between PD-L1 and CD80 (Jin et al. 2011). Typically, CD80 provides a co-stimulatory signal for activation of T cells by binding to CD28 on the surface of T cells but can also interact with the immune checkpoint CTLA-4 to attenuate T cell immune responses. Moreover, PD-L1 was reported to receive a signal from PD-1 which allowed cancer cells to resist T cell-mediated apoptosis (Azuma et al. 2008). These experiments involved engineered PD-1 and PD-L1 with normal binding but impaired ability to transmit signals to tumour cells or T cells.

Truncation of the intracellular domain of PD-L1 but not PD-1 suppressed lysis of cancer cells. Replacing the extracellular domain of PD-L1 with the corresponding region from PD-L2 did not affect the lysis of cancer cells (Azuma et al. 2008).

Three sequence motifs in the intracellular domain of PD-L1 were linked with tumour progression (Gato-Cañas et al. 2017). Expression of IFN-β was linked to lethality of murine melanoma cells (B16) when PD-L1 expression was silenced or the cytoplasmic domain was deleted. "RMLDVEKC" and "DTSSK" were identified to be associated with a posttranslational modification mechanism that leads to ubiquitination and destabilisation (Lim et al. 2016) through mutation of these sequences (Gato-Cañas et al. 2017). Moreover, a third sequence motif "QFEET" was found to protect against the effects of IFN-β-mediated cytotoxicity, whereas deletion of "RMLDVEKC" and "DTSSK" enhanced resistance to IFN-β toxicity. Silencing of PD-L1 using PD-L1 knockout B16 cells increased STAT3 phosphorylation (Y705), and caspase 7 after IFN-β stimulation. Moreover, mutation of the human homolog of the "DTSSK" motif also enhanced resistance to type I and type II IFN-induced toxicity (IFN-α, IFN-β and IFN-γ). These findings indicate that signalling motifs in the intracellular domain of PD-L1 confer resistance against IFN-induced cytotoxicity in order to protect cancer cells (Gato-Cañas et al. 2017).

A recent study highlighted a role of PD-L1 in promoting survival of LECs (Lucas et al. 2018). Type I IFN-α/β receptor signalling was demonstrated to induce PD-L1 expression in human and mouse LECs of the LN, particularly on the subcapsular sinus. This was observed during early time points following immunisation (polyI:C) and infection (vaccinia virus, and chikungunya). Of importance was the level of PD-L1 expression which was shown to negatively correlate with the division of LECs and the expression of caspase-3/7 in response to type I IFN-inducing stimuli. In response to an acute inflammatory response, there was more LEC division and apoptosis in PD-L1-low expressing mice during expansion and contraction of the LN. In addition, LECs with high PD-L1 expression had elevated levels of CXCL4, a known inhibitor of endothelial cell division. This report demonstrates that type I IFN stimulation leads to PD-L1 upregulation on LN-LECs, which could determine apoptosis of LECs and the growth of lymphatic vasculature (Lucas et al. 2018).

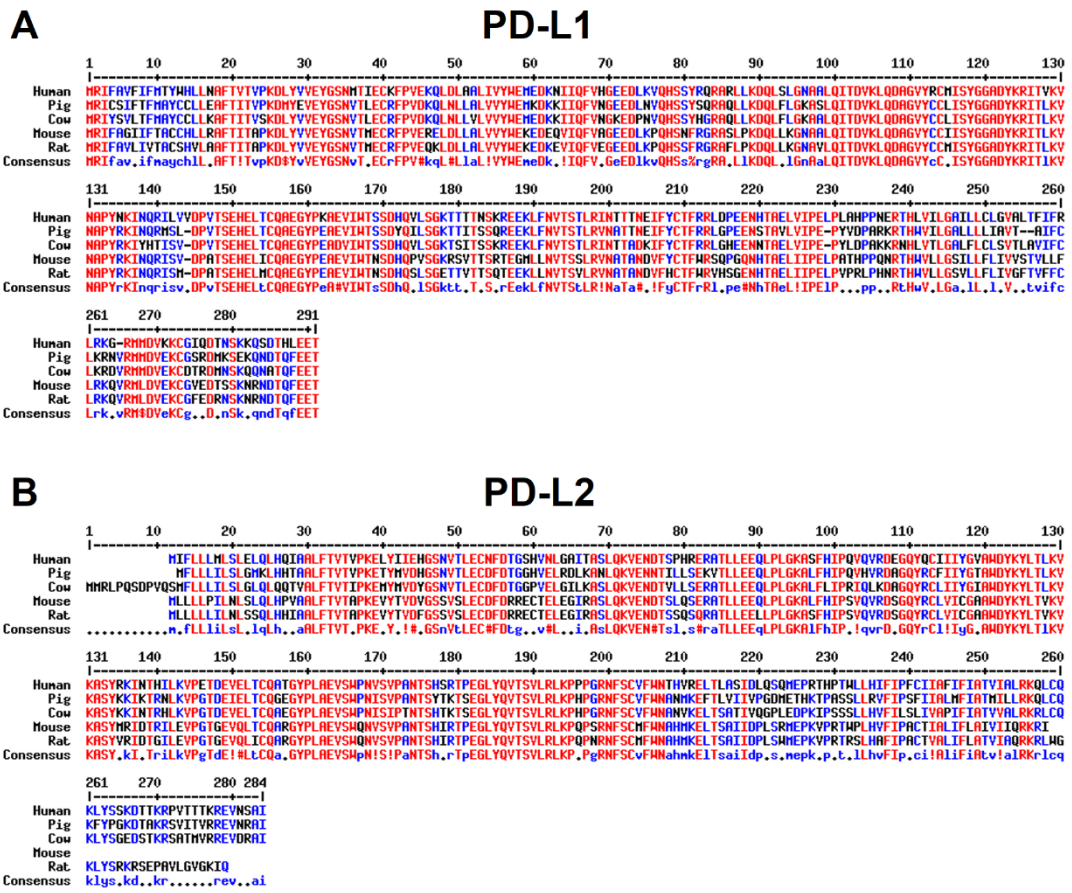

Figure 6.1. **Alignments of PD-L1 and PD-L2 protein sequences in mammals.** A) PD-L1 compared between human, pig, cow, mouse and rat. B) Similar for PD-L2. Red (90% consensus) and blue (50%) represent conserved residues. The consensus sequence is presented below the species. Note: "RM$DVEKC", "D.nsk", "qfEET" consensus sequences in the cytoplasmic tail of PD-L1 of which the mouse sequences ("RMLDVEKC", "DTSSK", "QFEET") have been characterised (Gato-Cañas et al. 2017).

6.2. Effects of PD-L1 knockdown on intracellular signalling and miRNAs

Since, I identified that miRNA-mediated regulation of PD-L1 occurs in HDLECs. I investigated whether PD-L1 expression could affect the expression of miRNAs or had any role on intrinsic signalling in HDLECs. I aimed to do this by transfecting siRNAs targeting PD-L1 and confirmed knockdown at the protein level by approximately 80% after 48 hours (Figure 6.2A). In IFN-γ and TNF-α-stimulated cells with PD-L1 knockdown, p-STAT3 levels were increased compared to the control at 8 and 24 h post-stimulation (Figure 6.2A and Figure 3.9A). In addition, p-STAT5 was increased in both IFN-γ, and IFN-γ and TNF-α-stimulated cells following PD-L1 knockdown (Figure 6.2B). No difference in p-STAT1 expression was observed. These results suggest that in activated cells, PD-L1 can affect specific components of the STAT pathway. However, the mechanism or any downstream

effects remain to be clarified. Moreover, there was a modest decrease in the phosphorylation of Akt (S473) in IFN-γ and TNF-α-stimulated cells with PD-L1 knockdown, compared to no knockdown.

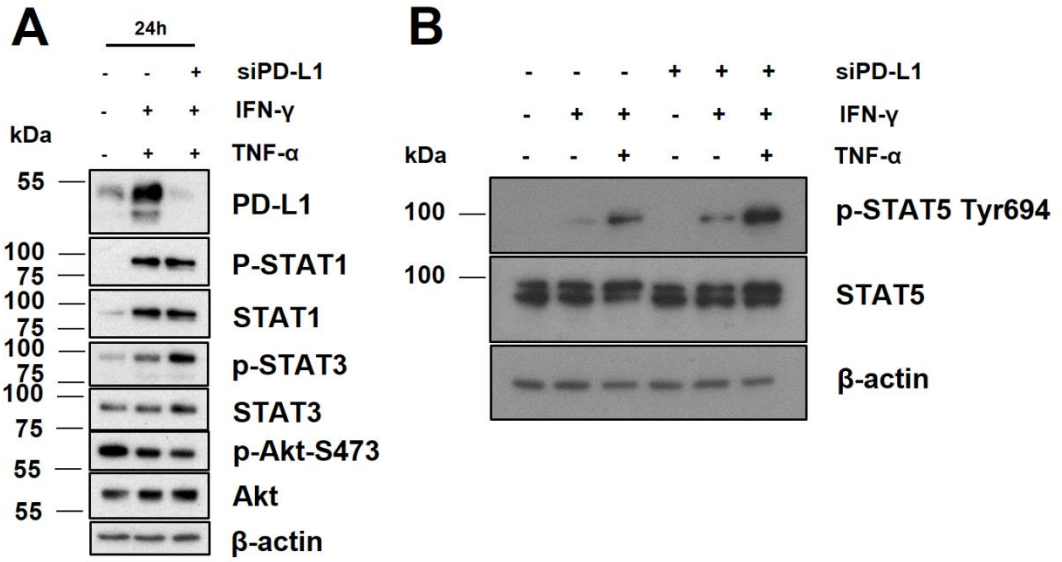

Figure 6.2. **PD-L1 knockdown has modest effects on the STAT and AKT pathway.** A and B) Protein expression in HDLECs transfected (48 h) with siRNAs targeting PD-L1 or non-targeting control and subsequently stimulated with IFN-γ and TNF-α (24 h). For (A) HDLEC experiments were run in parallel with the samples collected for small RNA sequencing and used for validation of knockdown. n = 2 independent experiments.

Next, I studied the effect of PD-L1 knockdown on mRNA expression in HDLECs. CD80 expression was induced by IFN-γ and TNF-α stimulation, although CD80 is lowly expressed in HDLECs determined by the cycle threshold value when analysed by qRT-PCR (Figure 6.3). This finding provides low signal to noise ratio and difficulty determining the results where CD80 is increased or decreased following PD-L1 knockdown. In addition, I detected very low levels of CD80 surface expression in HDLECs by flow cytometry analysis, compared to secondary antibody staining only, indicating that CD80 surface expression is under posttranscriptional control (Figure 6.4). The mRNA expression of angiogenic factors VEGFR1, VEGFR2, ANG1 and ANG2 were next analysed. I found that VEGFR1 expression was increased following PD-L1 knockdown in IFN-γ and TNF-α-activated cells but not with IFN-γ stimulation alone. VEGFR2 was suppressed regardless of knockdown in IFN-γ and TNF-α-activated cells. I also observed that VEGFR2 is upregulated only in untreated cells after inhibition of PD-L1 and not with stimulated cells. Moreover, IFN-γ and TNF-α-stimulated cells suppressed the expression of ANG2. PD-L1 did not affect the expression of ANG1 or ANG2. The addition of TNF-α to IFN-γ suppressed VEGFR2,

ANG1 and ANG2 but not VEGFR1. These data show that inflammatory signalling affect key angiogenic factors and suggest that PD-L1 may be associated with VEGFR1 and VEGFR2 expression.

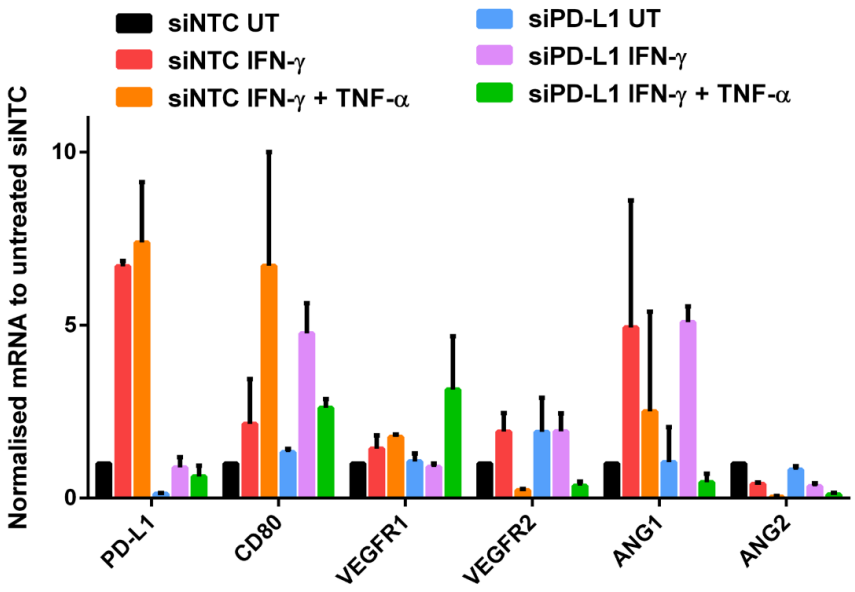

Figure 6.3. **The effect of PD-L1 knockdown on angiogenic factors and CD80.** HDLECs transfected with siRNAs targeting PD-L1 or non-targeting control (48 h) and stimulated with IFN-γ and TNF-α (24 h) were collected for RNA. mRNA expression of angiogenic factors and the co-stimulatory molecules CD80 was analysed by qRT-PCR.

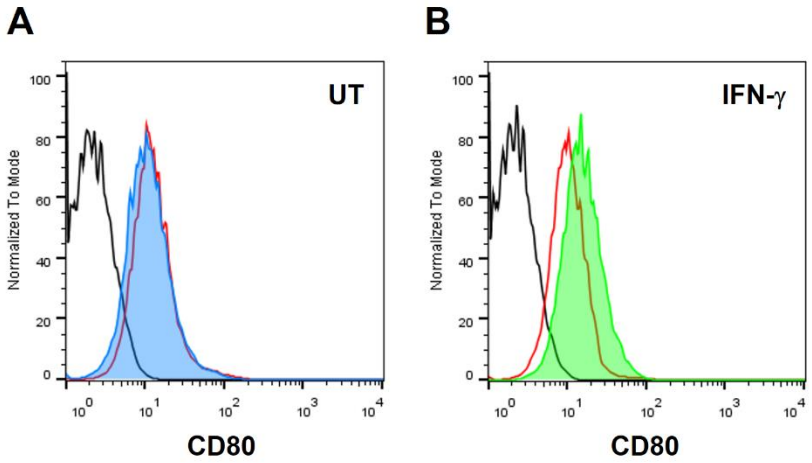

Figure 6.4. **CD80 surface expression in HDLECS.** Flow cytometric analysis showing CD80 surface expression (MFI) after stimulation (24 h) on live HDLECs. A) Untreated (UT) levels of CD80. B) IFN-γ stimulated (24 h) levels of CD80. MFI of CD80 staining: IFN-γ (green) = 15.4, UT (blue) = 11.0, secondary antibody only (red) = 10.2 and unstained = 1.90. n = 2 experiments.

As described in previous chapters (Chapter 3 and 4) that miRNAs including miR-155 can determine the expression of PD-L1 in inflammatory-activated cells, I determined whether PD-L1 may have any feedback mechanism that can affect miRNA expression (Figure 6.5). No difference was observed with miR-155 expression following PD-L1 knockdown suggesting a lack of negative feedback from miRNA modulation of PD-L1 expression. The other miRNAs studied were tested previously to determine the effect of IFN-γ and TNF-α (Chapter 3). I did not observe any changes due to PD-L1 knockdown on any of these miRNAs (Figure 6.5). However, this was a limited selection of miRNAs and to widely explore this I continued to investigate whether the expression of other miRNAs could be affected by PD-L1 using small RNA sequencing.

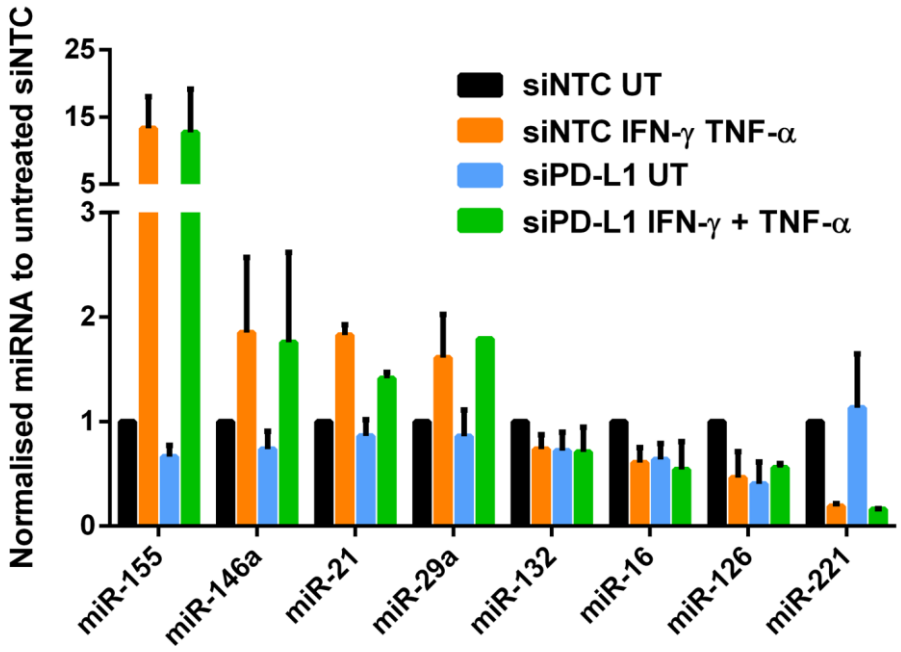

Figure 6.5. **The effect of PD-L1 knockdown on miRNA levels.** miRNA expression as analysed by qRT-PCR in HDLECs transfected (48 h) with siRNAs targeting PD-L1 or non-targeting control and subsequently stimulated with IFN-γ and TNF-α (24 h). n = 2 independent experiments.

6.3. Identification of potential miRNAs affected by PD-L1 using small RNA sequencing

To this aim, HDLECs with siRNAs targeting PD-L1 or non-targeting control were set up in parallel and treated with IFN-γ and TNF-α. No untreated sample was set up with PD-L1 knockdown because it was thought that there would be a greater effect due to the difference in expression in activated cells. Samples were set up alongside those shown (Figure 6.2) to confirm knockdown of PD-L1 expression. Sequencing of these samples were also performed

in parallel as those described and simultaneously statistically analysed (Chapter 3). Deletion of PD-L1 resulted in differentially expressed miRNAs (Figure 6.6) but less than those analysed with or without IFN-γ and TNF-α-stimulation (Chapter 3). Sequencing analysis identified that miRNAs that were significantly different between samples with PD-L1 knockdown compared to control were predicted by TargetScan to target PD-L1 including miR-20a-5p and miR-576-3p. There is no known resource like TargetScan to predict whether miRNA targets can affect the expression of miRNAs themselves. However, low stability of miRNAs can lead to changes in response to altered transcription or processing (Rüegger & Großhans 2012). It could be possible that upon miRNA-mRNA interaction that a feedback mechanism be applied on the miRNA as part of a miRNA-mRNA network, such that target mRNAs can modulate miRNA stability in a reciprocal regulation (Rüegger & Großhans 2012). Candidate miRNAs were selected for validation based on the following criteria: significant fold-change in expression ($p < 0.05$), known relevant targets in the literature, predicted site-binding on PD-L1 3'UTR and predicted targets using TargetScan (Agarwal et al. 2015) and Search Tool for the Retrieval of Interacting Genes/Proteins database (STRING) (Szklarczyk et al. 2015). For validation of sequencing, both the most upregulated (miR-223-3p) and downregulated miRNAs (miR-15b-5p) were selected. In addition, the miR-23-27-24 cluster was shown to be linked to the regulation of Th2 immunity (Cho et al. 2016). I used qRT-PCR to analyse the expression of these miRNAs following PD-L1 deletion in HDLECs (Figure 6.7). There were discrepancies between the sequencing and qRT-PCR analysis. Firstly, miR-223-3p was suggested to be very lowly expressed in activated cells but highly upregulated after knockdown of PD-L1. This was not observed with qRT-PCR where miR-223-3p is detectable in activated cells with no knockdown. Similarly, no downregulation of miR-15b-5p was found in qRT-PCR but an increase to levels of the miRNA following deletion of PD-L1. miR-20a-5p and miR-23b-3p were indicated by analysis of sequencing to increase by approximately ~2 fold after knockdown of PD-L1 of which only a modest increase was observed in qRT-PCR. Sequencing indicated that IFN-γ and TNF-α stimulation downregulates miR-576-3p (~0.5 fold decrease), seen with qRT-PCR, but there was no further downregulation of miR-576-3p in cells with PD-L1 knockdown that was suggested by sequencing. Additionally, the list of candidate miRNAs included miR-302c-3p and miR-6865-3p which were undetectable in qRT-PCR. Overall, I could not convincingly conclude any of the candidate miRNAs to be affected by PD-L1 knockdown using two different techniques to measure miRNA expression. This may be due to the sensitivity of each technique although previous miRNAs were validated using both techniques (Chapter 3).

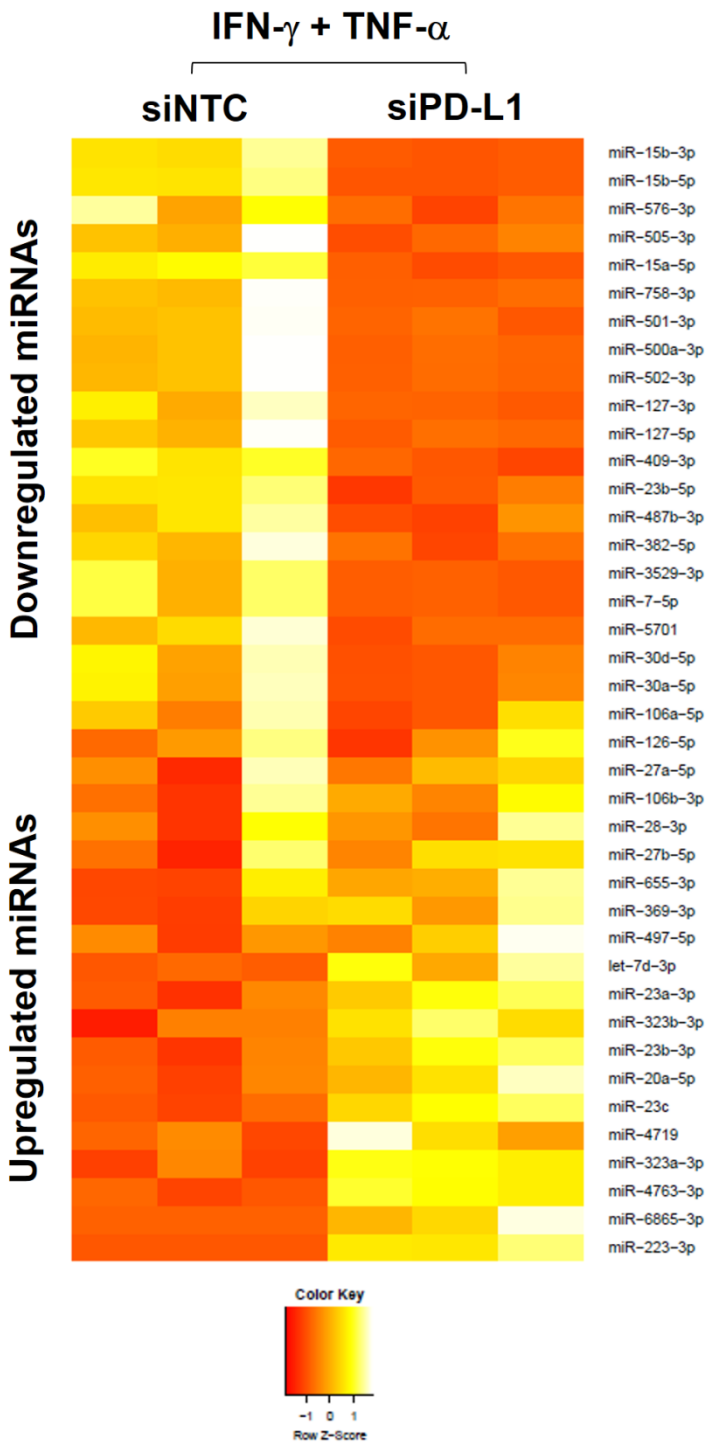

Figure 6.6. **The effect of PD-L1 deletion on miRNA expression.** Heat map showing fold-change in expression of miRNAs from small RNA sequencing (adjusted $p < 0.1$). HDLECs were transfected with PD-L1 siRNA or non-targeting control (48 h) and then stimulated with IFN-γ and TNF-α (24 h). Row Z-score represents mean ± S.D., n = 3 independent samples performed in triplicate.

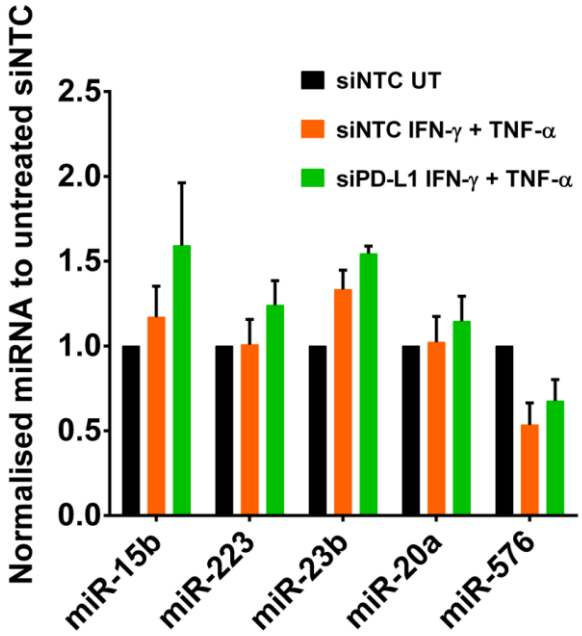

Figure 6.7. **Validation of miRNAs identified through small RNA sequencing.** HDLECs were transfected (48 h) with siRNAs targeting PD-L1 or non-targeting control and subsequently stimulated with IFN-γ and TNF-α (24 h). Total RNA was isolated from HDLECs and analysed by qRT-PCR for miRNA expression.

6.4. Chapter discussion

This chapter aimed to address the possibility that PD-L1 has intrinsic signalling in primary vascular cells. Previous studies using murine or tumour cells have highlighted that knockdown of PD-L1 affects cell proliferation, glycolytic metabolism, autophagy, angiogenesis as well as confer protection against IFN-β-mediated cytotoxicity or T cell-mediated apoptosis (Azuma et al. 2008; Jin et al. 2011; Chang et al. 2015; Clark et al. 2016; Gato-Cañas et al. 2017). Here, I describe preliminary findings following the effect of PD-L1 siRNA knockdown in primary HDLECs. I show that knockdown of PD-L1 in has a modest increase on phosphorylation of STAT3 and STAT5 in IFN-γ and TNF-α-activated cells (8 and 24 h). The period of stimulation of cells may be important since the kinetics of p-STAT3 activation are observed at 4 h and does not appear gradually increase at 8 or 24 h, compared to phosphorylation of STAT1 (Figure 3.9). An effect was similarly reported in IFN-β-stimulated PD-L1 knockout B16 cells where phosphorylation of STAT3 was increased after 10-20 min stimulation (Gato-Cañas et al. 2017). In addition, there was an increase in STAT3 levels after 24 h stimulation and there was no difference in upregulation of STAT1 or STAT2 compared to control B16 cells. These findings were linked to lethality of B16 cells caused by the combination of IFN-β/mutated PD-L1 as deletion of IFNAR1, JAK1, STAT3

and CASP7 reduced these effects (Gato-Cañas et al. 2017). Moreover, the blockade or deletion of PD-L1 sensitised murine and human cancer cells to IFN-β *in vitro* and affected tumour growth and survival *in vivo.* Overexpression of PD-L1 in B16 cells that were administered into mice significantly offset the inhibitory effects of intratumoural IFN-β and improved tumour progression (Gato-Cañas et al. 2017). This protective effect requires non-classical regulatory sequence motifs found in the cytoplasmic domain of PD-L1 (see introduction of this chapter) that are not similar to any classical signalling motif. Furthermore, this report could indicate that upregulation of PD-L1 expression on cancer cells acts as an additional protective response against IFNs in the tumour microenvironment upon PD-1 engagement. The production of IFN-β by fibroblasts, tissue resident macrophages and DCs, or IFN-γ secreted from Th1 $CD4^+$ cells and $CD8^+$ promote anti-tumour activity including inducing apoptosis (Parker et al. 2016). Additionally, cancer patients with JAK1/2 loss-of-function mutations can be resistant to IFN-induced toxicity (Shin et al. 2017). It would be interesting to investigate whether the IFN-induced anti-apoptotic effect observed in described reports (Gato-Cañas et al. 2017; Lucas et al. 2018) is similar in HDLECs. This includes overexpressing PD-L1 in IFN-γ and TNF-α activated HDLECs to determine whether the phosphorylation of STAT3 or STAT5 are as a consequence downregulated and further measuring the expression of apoptotic markers such as caspase-3 or 7 and membrane integrity via 4',6-diamidino-2-phenylindole (DAPI). Overexpression could be achieved through lentiviral transduction of a plasmid expressing PD-L1, generated using HEK293T cells.

My preliminary findings showed similar results to a previous report in mouse endothelial cells (Jin et al. 2011) that PD-L1 knockdown increases VEGFR2 mRNA expression in untreated HDLECs. In contrast, I detected very low levels of CD80 on the surface which suggests that PD-L1/CD80 interaction between HDLECs is unlikely. In addition, I observed upregulated VEGFR1 expression in IFN-γ and TNF-α-activated cells that had PD-L1 knockdown. VEGFR1/2 expression were dependent on the inflammatory stimulus, particularly TNF-α. Both VEGFR1 and VEGFR2 are similarly connected receptor tyrosine kinases with shared ligands (Rahimi 2006). TNF-α modulates the expression of both VEGFR1 and VEGFR2 in human endothelial cells (Patterson et al. 1996; Giraudo et al. 1998). In my study, the function of PD-L1 on VEGFR1/2 signalling pathways may lead to downstream effects towards development or angiogenesis in HDLECs. However, this requires further investigation including measuring proliferative levels of HDLECs. Overexpression of PD-L1 could determine whether the effects on VEGFR1 or VEGFR2 are dependent on PD-L1 regardless of inflammatory stimulus.

Target RNAs can stabilise or de-stabilise partially complementary miRNAs in different systems (Rüegger & Großhans 2012), suggesting a potential mechanism for negative feedback. In a situation where target RNAs can de-stabilise miRNAs, a study showed that high complementarity between target RNA (*egfp*) and the miRNA (miR-277) caused a significant decrease in the levels of the miRNA in drosophila (Ameres et al. 2010). This was shown to be effective against AGO1-bound miR-277 but not AGO2-associated miR-277. Small RNAs bound to AGO2 can be protected by the addition 2'-O-methyl groups mediated by Hen1 in the final step of AGO2 loading that prevents tailing or trimming of the miRNA. Moreover, there is also the mechanism of target-mediated miRNA protection that can be induced by the expression of mRNAs which correlates with the abundance of cognate miRNAs (Chatterjee et al. 2011; Haas et al. 2016). Here, I investigated whether there is a reverse mechanism by which PD-L1 expression regulates the abundance of certain miRNAs. There have been no reports that suggest PD-L1 signalling can affect miRNA expression. It is also not known to be linked to any miRNA degrading enzymes. Small RNA sequencing and qRT-PCR analysis did not coherently reveal any miRNAs from the candidate list that were affected by PD-L1 knockdown. Those miRNAs that have been reported or predicted to target PD-L1 and that were tested included miR-15b (Kao et al. 2017), miR-20a, miR-576 and miR-155. As described (Chapter 3), miR-155 targets PD-L1 but silencing of PD-L1 does not lead to any effect on the expression of miR-155. This suggests a lack of a regulatory feedback loop from PD-L1 back to miRNA expression and that PD-L1 does not modulate the regulatory effect of miR-155. The modest effect of PD-L1 knockdown on phospho-STAT3 or -STAT5 may have not generated any noticeable miRNA profile changes. However, the identification of miR-20a may be relevant since miR-20a has been demonstrated to regulate STAT3 mRNA expression during MDSC-mediated suppression (Zhang et al. 2011; Haghikia et al. 2012).

The effect on PD-L1 on miR-15b is left open and additional techniques would be required to determine a possible feedback loop. Such as validation of miR-15b targeting of PD-L1 in primary cells as well as overexpression of PD-L1 with and without the cytoplasmic domain to determine the effect on miRNAs in the opposite direction. Although as previously reported (Chapter 3) that I validated several miRNAs using both techniques, the discrepancy between small RNA sequencing and qRT-PCR analysis is not novel. Sequencing is used to generate a global outlook on the number of targets that could be complementary investigated by qRT-PCR (Costa et al. 2013). Both techniques assess gene expression in a different experiment setup which can introduce bias in the final analysis as well as the quality of the sample used. However, it is recommended to test whether both techniques determine a consistent and reproducible analysis of gene expression for further experimentation. Indeed,

I only investigated a small number of miRNAs from a larger list that were revealed to be significant from the sequencing analysis. In fact, a number of factors are needed to take into consideration (Git et al. 2010). Firstly, how strict the analysis and normalisation of the sequencing is performed such as the number mismatches that are tolerated which would not be the same with the TaqMan primers that are designed for qRT-PCR. In addition, the expression of the miRNA is important and both techniques use different values and normalisation for gene expression. This is the RPKM for sequencing which is using absolute values, as opposed to the relative expression of qRT-PCR products to the reference gene. The candidate list did take into consideration a range of miRNAs with differential expression above the arbitrary threshold to filter possible low expressing miRNAs. Some of these miRNAs from the list were not detectable with qRT-PCR suggesting a discrepancy in the sensitivity of these techniques and that the sequencing technique may be more affected by this. It also seems that normalised fold change from the sequencing analysis of ~2 fold is not picked up as strongly when using qRT-PCR in these results and that fold change should not be strictly expected to be the same for both methods. Also for genes that are identified in sequencing to be lowly expressed can exaggerate the fold change greatly. Overall, even though there was a lack of validation between small RNA sequencing and qRT-PCR analysis. There are still a lack of understanding of potential signalling mechanisms from PD-L1 which may suggest that the likelihood of PD-L1 affecting miRNA expression may be small. The next experimental setup would be to overexpress PD-L1 in HDLECs and to observe whether the JAK/STAT pathway or miRNA expression are affected to provide clarity on the above findings.

7. General discussion

7.1 Review of aims and summary of findings

This study aimed to address the significance of PD-L1 expression and function, and the miRNA mechanisms that regulate and fine-tune its expression in human stromal and endothelial cells. I used a variety of techniques including western blot, flow cytometry, qRT-PCR to address my aims. Here, I review the main outcomes of the study and revisit the list of aims, described in the introduction of this thesis (Chapter 1). I further reflect on the significance of miR-155-mediated posttranscriptional regulation of PD-L1, potential future research and the implications of this study on miR-155 therapeutic options and PD-1/PD-L1 immunotherapy.

Hypothesis: Expression and function of PD-L1 in stromal, vascular and cancer cells is posttranscriptionally regulated by inflammatory-driven microRNAs.

Aim 1: To characterise PD-L1 expression under inflammatory conditions, using inflammatory mediators IFN-γ and TNF-α (Chapter 3).

Here, I demonstrated why HDLECs/HFFs are a good model for investigating regulatory mechanisms behind PD-L1 expression in primary cells, partly due to their responsiveness to IFN-γ and TNF-α.

Main outcomes:

- Th1 cytokines IFN-γ and TNF-α synergistically induce high levels of PD-L1 in HDLECs and HFFs.
- The JAK/STAT pathway which is a primary target of IFN-γ signalling is activated as demonstrated by increased levels of STAT1 phosphorylation in correlation with PD-L1 expression.
- IFN-γ and TNF-α upregulate MHC class I and class II molecules on HDLECs.
- IFN-γ and TNF-α downregulate lineage commitment markers PROX1, VEGFR1, COUP-TFII and LYVE1 in HDLECs.

Aim 2: To determine the dynamics of the microRNA landscape in vascular and stromal cells exposed to inflammatory stimuli (Chapter 3).

The outcome from small RNA sequencing provided a mass of data that showed several dysregulated miRNAs under inflammatory conditions and led to a number of candidates to investigate miRNA regulation of PD-L1 expression.

Main outcomes:

- Small RNA sequencing of IFN-γ and TNF-α-stimulated HDLECs showed several up- (19) and downregulated (29) miRNAs ($p < 0.01$).
- Validated upregulated miRNAs: miR-155-5p, miR-4485-3p, miR-218-5p, miR-146a-5p
- Validated downregulated miRNAs: miR-582-5p, miR-582-3p, miR-93-5p, miR-217 and miR-125bp-5p
- Knockdown of Dicer did not affect PD-L1 protein expression in HDLECs.

Aim 3: To investigate the effect of dysregulated microRNAs on regulation of PD-L1 expression (Chapter 3).

I determined that IFN-γ and TNF-α induce both PD-L1 and miR-155 expression, in which a role of miR-155 is to regulate and fine-tune the levels of PD-L1 in stromal/vascular cells.

Main outcomes:

- 49 out of 631 miRNAs detected in HDLECs were predicted to target PD-L1.
- Determined that miR-155 binds directly to PD-L1 via two binding sites on the 3'-UTR.
- Overexpression and inhibition of miR-155 down- or upregulates PD-L1 protein expression, respectively, in IFN-γ and TNF-α-activated HDLECs/HFFs.
- Overexpression of miR-218 induces PD-L1 protein expression in untreated and IFN-γ and TNF-α-activated HDLECs/HFFs.

Aim 4: To compare microRNA-mediated mechanisms of PD-L1 expression between primary stromal cells and human cancer cell lines (Chapter 4).

Here, I showed that miR-155 regulation of PD-L1 expression is not limited to stromal/vascular cells and can be found in renal, breast and lung cancer cell lines. There was also evidence of differential miR-155 regulatory mechanisms of PD-L1 in a subset of cancer cell lines.

Main outcomes:

- In many tumour types analysed from TCGA data, miR-155 and/or PD-L1 expression are overexpressed. However, there is no obvious correlation in terms of expression.
- Demonstrated that miR-155 regulates PD-L1 protein expression in RCC4 and MDA-MB-231 cells.
- In a subset of lung cancer cells, miR-155 regulates PD-L1 protein expression. Differences in regulation may be accounted by accessibility to the 3'-UTR e.g. obstructed by other RNA-binding proteins or posttranslational regulation e.g. glycosylation.

- In cancer cell lines, overexpression of miR-218 has a subtle effect in A549s but there is no effect in RCC4 or MDA-MB-231.

Aim 5: To develop a co-culture model that can be used to functionally test the relevance of the above findings, particularly the mechanism of a miRNA/PD-L1 regulatory loop (Chapter 5).

I developed two co-culture models with an output of measuring T cell activation (IL-2 ELISA, NFAT luciferase) to understand the biological relevance of PD-L1 posttranscriptional regulation on stromal fibroblast/vascular cells on the activation of T cells. This work was met with some challenging aspects and would need to be followed up in the future. I could not suitably show that PD-1/PD-L1 interaction was a factor to the effects on T cell activation when HFFs/HDLECs were co-cultured with Jurkat T cells.

Main outcomes:

- Both assays showed some effect (activation/suppression) on T cell activation when HFFs/HDLECs were co-cultured with Jurkat cells.
- However, blockade of PD-1/PD-L1 with antibodies or siRNA knockdown of PD-L1 did not affect the activation of Jurkat cells, suggesting these assays were not suitable to test PD-1/PD-L1 interaction in the current state.

Aim 6: To determine whether PD-L1 expression or signalling affects miRNA regulatory loops (Chapter 6).

I showed that silencing of PD-L1 does not broadly affect miRNA expression in HDLECs, inclusive of miR-155. However there is some data that suggest deletion of PD-L1 may affect the JAK/STAT pathway.

Main outcomes:

- PD-L1 has a short cytoplasmic domain with no known signalling motifs, however, knockdown of PD-L1 increased the phosphorylation levels of STAT3 and STAT5.
- Small RNA sequencing indicated some miRNAs that were dsyregulated after deletion of PD-L1, although this could not be validated using qRT-PCR.
- Silencing of PD-L1 did not affect expression of miR-155 suggesting the IFN-γ/TNF-α/miR-155/PD-L1 mechanism is an incoherent feed-forward loop and not a negative feedback mechanism.

7.2 Reflections on miRNA-mediated regulation of PD-L1 expression

The PD-1/PD-L1 checkpoint is an important determinant of immune homeostasis and tolerance that regulates T cell activity (Sun et al. 2018). Our knowledge of PD-L1 regulation

has expanded to understand that the dynamic expression of PD-L1 is regulated at the transcriptional, posttranscriptional and posttranslational level, leading to heterogeneity in the clinical response to PD-1/PD-L1 immunotherapy (Sun et al. 2018). Posttranscriptional regulation of protein-coding genes by miRNAs is an important mechanism that controls a diverse number of cellular processes through the degradation of mRNA targets or inhibition of translation (Ha & Kim 2014). The 3'-UTR of PD-L1 is long and serves as a negative regulatory role (Kataoka et al. 2016; Mezzadra et al. 2017), facilitating an interface for posttranscriptional regulation by RNA-binding proteins (Coelho et al. 2017) and miRNAs (Sun et al. 2018).

Here in this thesis, I demonstrated that inflammation-induced miRNAs can be critical regulators of immune checkpoint (PD-L1) expression in HDLECs and that an IFN-γ/TNF-α-mediated incoherent feed-forward loop mechanism can also be found in HFFs and cancer cells *in vitro*. Overall, this study contributes towards to the systemic understanding of PD-L1 regulation in an inflammatory environment that would be of interest to other investigators (Table 7.1). The strength of these findings fills an important knowledge gap in primary human cell types (HDLECs/HFFs) and highlights the importance of PD-L1 expression on non-immune or non-transformed cells. The setup of co-culture assays to answer whether the effect of miR-155 regulation of PD-L1 expression alters the activation of T cells remains to be completed, and would inevitably support the significant findings of this study. It would also be important to further understand the physiological role of miR-155/PD-L1 interaction and the immunological significance of this interaction *in vivo*. Host-derived PD-L1 expression in DCs and macrophages can impact the effectiveness of PD-L1 blockade (Lin et al. 2018; Tang et al. 2018). It is unknown whether miR-155 can regulate PD-L1 expression in DCs or macrophages. However, there is wide-spread expression of miR-155 in myeloid cells, which can act as a critical regulator of cytokine production in DCs (O'Connell, Rao, et al. 2010; Smyth et al. 2015) and macrophages (O'Connell et al. 2007; Tili et al. 2007).

The role of miR-155/PD-L1 regulation is in line with the overarching miR-155 regulation of inflammatory responses in addition to its functions in the development and maintenance of the immune system (Table 7.2). The miR-155/PD-L1 mechanism demonstrates that inflammatory responses elevate high levels of miR-155 to regulate the induction of PD-L1, indicating that miR-155 acts as a pro-inflammatory mediator or amplifier of the immune response through the modulation of peripheral tolerance. Similarly, high levels of miR-155 found in atopic dermatitis can regulate the expression of the immune checkpoint CTLA-4 and enhance T cell proliferation (Sonkoly et al. 2010). These studies highlight that the activation of miRNAs such as miR-155 can facilitate the temporal release of the brakes of the immune system that adjust the balance between immune tolerance and autoimmunity.

NF-κB activity has been suggested to regulate the macrophage inflammatory response through controlling the kinetics and stability of miR-155 and miR-146a, which functions as a negative regulator (Mann et al. 2017). I identified in some lung cancer cell lines that miR-155 regulation of PD-L1 may not function in the same manner as HDLECs/HFFs suggesting there are different networks of PD-L1 regulation in place in these cells that may affect the inhibition of miRNA-mediated regulation or secondary effects such as posttranslational regulation that affect the stability or degradation.

I speculate that in the context of tumour immunity, miR-155 regulation of PD-L1 expression would span across tumour/stromal/vascular cells in the tumour microenvironment and the draining LNs and affect the activation of T cells in a tumour-specific manner. IFN-γ and TNF-α cytokines in the microenvironment, produced by T cells and NK cells, induce a defensive response from activated stromal/vascular cells to dampen the local immune response through PD-L1 expression. PD-L1 signalling can facilitate the survival of high PD-L1-expressing cells by regulating apoptosis (Lucas et al. 2018). The induction of miR-155 through IFN-γ and TNF-α fine-tunes (rather than abolishes) the level of PD-L1 immunosuppression in order to maintain pro-inflammatory Th1 and $CD8^+$ T cell responses in the local microenvironment as well as to preserve the survival of PD-L1-expressing cells.

Table 7.1. **A summary of PD-L1 regulation.** Modified from Chapter 1 and (Sun et al. 2018).

Regulation of PD-L1	**References**
Inflammatory signalling: IFN-α/β, IFN-γ, JAK/STAT/IRF TLR, NF-κB, TNF-α, LPS IL-6, IL-10, TGF-β	(Freeman et al. 2000; Dong et al. 2002; Loke & Allison 2003; Mazanet & Hughes 2002; Kondo et al. 2010; Wölfle et al. 2011; Mariathasan et al. 2018)
Oncogenic signalling: ALK/STAT3 MEK/ERK, RAS/ERK, PI3K/Akt/mTOR, EGFR, MYC, CDK5 HIF-1α, HIF-2α	(Marzec et al. 2008; Liu et al. 2007; Coelho et al. 2017; Akbay et al. 2013; Parsa et al. 2007; Casey et al. 2016; Dorand et al. 2016; Noman et al. 2014; Messai et al. 2016)
Genetic alteration: disruption of 3'-UTR, structural variations (amplification, insertion)	(Twa et al. 2014; Roemer et al. 2016; Ikeda et al. 2016; George et al. 2017; Bellone et al. 2018; Kataoka et al. 2016)
MicroRNAs: Non-transformed cells: miR-513, **miR-155** Cancer cells: miR-200, miR-34a, miR-138, miR-142-5p, miR-106b-5p/miR-93-5p, miR-570, miR-152, miR-217, miR-17-5p, miR-15a, miR-16, miR-193a, miR-20b/miR-21/miR-130b, miR-197	(Gong et al. 2009; Chen et al. 2014; Cortez et al. 2016; Zhao et al. 2016; Jia et al. 2017; Cioffi et al. 2017; Wang et al. 2012; Xie et al. 2017; Miao et al. 2017; Audrito et al. 2017; Kao et al. 2017; Zhu et al. 2014; Fujita et al. 2015)
Posttranslational regulation: Degradation: CSN5, CDK4, CMTM4/6 Glycosylation: GSK3β	(Lim et al. 2016; Zhang et al. 2018; Burr et al. 2017; Mezzadra et al. 2017; Li et al. 2016)

Table 7.2. **An overview of miR-155 function and regulation in physiological and pathological processes.**

miR-155	**References**
Stimuli: antigen receptor activation (TCR, BCR), inflammatory/TLR signalling (LPS, TNF-α, IFNs, KSHV), TGF-β/SMAD signalling, hypoxia	(Elton et al. 2013; Taganov et al. 2006; Tili et al. 2007; Gottwein et al. 2007; Kong et al. 2008; Stanczyk et al. 2008; Ceppi et al. 2009; Bruning et al. 2011)
Negative regulators: NF-κB, IL-10, TP53, BRCA1	(McCoy et al. 2010; Mann et al. 2017; Van Roosbroeck et al. 2017; Bayraktar & Van Roosbroeck 2018)
Key transcriptional activators: NF-κB, AP-1, IRFs, SMAD4, MYB, FOXP3	(Elton et al. 2013; Bayraktar & Van Roosbroeck 2018)
Cell types: Haematopoietic stem-progenitor cells Myeloid: NK cells, monocytes (macrophages, dendritic cells), granulocytes Lymphocytes: B cells, $CD4^+$ (Th1, Th17, T reg) and $CD8^+$ T cells **Fibroblasts, lymphatic endothelial cells**	(Elton et al. 2013; Taganov et al. 2006; Rodriguez et al. 2007; Vigorito et al. 2007; Lu et al. 2009; Lu et al. 2015)
Functions: haematopoiesis, inflammation (innate immunity, adaptive immunity), infection, autoimmunity	
Regulation of development, differentiation, maturation and apoptosis of T cells, B cells, monocytes: AID, C/EBPβ, PU.1, IFN-γRα, c-Maf	(Rodriguez et al. 2007; Thai et al. 2007; Banerjee et al. 2010; Teng et al. 2008; Dorsett et al. 2008; Lu et al. 2014)
Regulation of inflammatory responses: c-Maf, TAB2, SOCS1, STAT1, SHIP1, CTLA-4, **PD-L1**	(Ceppi et al. 2009; Androulidaki et al. 2009; Lu et al. 2009; O'Connell et al. 2009; Sonkoly et al. 2010; Gracias et al. 2013; Dudda et al. 2013; Lu et al. 2015)

Oncogenic miRNA: apoptotic resistance, proliferation, invasion, migration, resistance to chemo- and radiotherapy Haematological malignancies: diffuse large B cell lymphoma, Hodgkin lymphoma, acute myeloid leukaemia Solid tumours: melanoma, breast, colon, lung, kidney, head and neck, pancreas, stomach	(Eis et al. 2005; Volinia et al. 2006; Yanaihara et al. 2006; Vigorito et al. 2013; Bayraktar & Van Roosbroeck 2018)
Autoimmunity: generation of pathogenic self-reactive T and B cell responses, regulation of cytokine/chemokine production Multiple sclerosis, rheumatoid arthritis, systemic lupus erythematosus	(O'Connell, Kahn, et al. 2010; Blüml et al. 2011; Kurowska-Stolarska et al. 2011; Alivernini et al. 2016)

7.3 The modulation of stromal fibroblast/vascular cell function through IFN-γ and TNF-α activation

A critical role in the regulation of PD-L1 throughout the study was played by inflammatory cytokines IFN-γ and TNF-α that are typically produced by $CD4^+$ and $CD8^+$ T cells and NK cells, and induce PD-L1 expression on stromal/vascular cells. These seemingly quiescent-like cells become activated in response to cytokines and have an active role in the regulation of the inflammatory response. The synergy between IFN-γ and TNF-α has been reported to involve the interplay of both STAT1 and NF-κB in the induction of several inflammatory genes including IRF-1 and ICAM-1 (Ohmori et al. 1997). The promoter region of IRF-1 was found to have both a STAT binding element and a NF-κB sequence motif. Deletion of the STAT1 gene nearly ablated (90% reduction) the synergistic induction of IRF-1 promoter activity in fibroblasts. In addition, mutation of the STAT binding element and NF-κB site on IRF-1 abolished the response to IFN-γ and TNF-α. Since, IRF-1 has been reported to be involved in the induction of PD-L1 (Lee et al. 2006), it is likely the synergistic effect of IFN-γ and TNF-α in the upregulation of PD-L1 on HDLECs/HFFs occurred through activation of IRF-1.

Endothelial cells are characterised by two types of activation: type I refers to binding of G-protein-coupled receptors to ligands that can lead to an increase in intracellular Ca^{2+} where there is a role for leukocyte recruitment and neutrophil extravasation (Pober & Sessa 2007). Type I signals typically last for 10-20 min until the receptors are desensitised. Type II activation, where inflammatory signals provided by TNF, IL-1, LPS or IFN-γ can

persistently stimulate endothelial cells for a longer time. IFN-γ and TNF-α have been suggested to induce damage to the endothelial cell barrier which could affect the inflammatory response by increasing permeability to immune cells in inflammatory disorders such as psoriasis (Mehta et al. 2017). Acute inflammation of LECs in a mice model can affect the lymphatic propulsive flow and frequency, which could prevent the spread of pathogens or inflammatory mediators beyond LNs (Aldrich & M. 2013). In addition, high concentrations of IFN-γ and TNF-α have been shown to modulate LEC proliferation in mice and human models (Chaitanya et al. 2010).

IFN-γ and TNF-α produced by antigen-activated $CD8^+$ T cells were shown to be required for elimination of antigen loss variants (ALVs) in mouse tumours (Spiotto et al. 2004; Zhang et al. 2008). ALVs are a subpopulation of cancer cells that do not express antigens. These studies showed that for destruction of large solid tumours, $CD8^+$ T cells moved to destroy the host stroma to prevent outgrowth or escape of tumours in a so-called bystander effect. Expression of receptors for IFN-γ, TNF-α or MHC molecules on stroma were targeted by $CD8^+$ T cells to generate anti-tumour immunity. In addition, cross-presentation of tumour antigen (from antigen-positive cancer cells) by non-bone marrow-derived stromal cells facilitated the removal of ALVs (Spiotto et al. 2004; Zhang et al. 2008). These studies show the importance of IFN-γ and TNF-α and how responsive stromal cells are to these cytokines, which in turn influence the local microenvironment and inflammatory response. Although it was not investigated, PD-L1 expression on stromal/vascular cells in the tumour microenvironment may act as a defence mechanism against $CD8^+$ T cells to prevent their own destruction. These studies could suggest another reason that the tumour stroma could be targeted for PD-1/PD-L1 immunotherapy to prevent the escape and metastasis of cancer cells.

7.4 In perspective: PD-L1 expression on stromal fibroblasts and endothelial cells

The significance of PD-L1 expression on stromal fibroblasts/vascular may affect anti-tumour immunity. Although not the focus of the thesis, studies on the tumour microenvironment demonstrate the contribution of stromal fibroblasts or lymphatic vessel structure in the modulation of immune cells in their access, activation and function (Hendry et al. 2016). In the tumour microenvironment, there are a diverse number of interactions between malignant and non-transformed cells through the release of soluble factors (e.g. cytokines and chemokines) as well as cell-cell contacts that can be inflammatory, immunosuppressive or influence angiogenesis (Schaaf et al. 2018). The tumour microenvironment has been suggested to limit the effect of cancer immunotherapy due to a

shift towards an immunosuppressive phenotype, which has been acquired through cancer immunoediting (Adachi & Tamada 2015). This can occur off a combination of existing immunosuppressive populations (e.g.) T reg, MDSCs; cytokines or chemokines produced by stromal cells (e.g. TGF-β, IDO, IL-10) or expression of immune checkpoint molecules (e.g. CTLA-4, PD-L1) on stromal cells and infiltrating immune cells (Adachi & Tamada 2015).

Cancer immunoediting describes the dynamic anti-tumour response in order to protect the host and consists of three parts: elimination (cancer immunosurveillance), equilibrium and escape (Dunn et al. 2004; Vesely et al. 2011). Briefly, elimination represents the innate and adaptive immune responses to tumour cells due to the presentation of abnormal (tumour) antigens and destroys the tumour before it becomes clinically apparent. Equilibrium (dormancy) describes the period in which tumour cells escape the elimination phase after incomplete tumour destruction and co-exist with the immune system, particularly the adaptive arm. Escape is in reference to the outgrowth of tumours in an uncontrolled manner in which it becomes symptomatic and the failure of the immune system to control transformed cells (Dunn et al. 2004; Vesely et al. 2011). The latter part includes the immunosuppression of anti-tumour immunity where PD-L1 expression is a key mediator of peripheral tolerance (Vesely et al. 2011). In addition, the majority of experimental cancer cell lines are those that have escaped the control of the immune response.

Cancer immunosurveillance is driven primarily by effector T cells, which become activated by antigen-presenting DCs in peripheral LNs (Schaaf et al. 2018). Activated T cells egress from LNs and travel to the tumour site where they leave from the blood vessels to infiltrate the tumour. On speculation, expression of PD-L1 on LECs could inhibit T cell function within peripheral lymphatic vessels or in the LN. This could include where activated T cells move into the LN from afferent vessels and are challenged by LECs on the subcapsular sinus, or by preventing the priming of naïve T cells in the medullary sinus of the LN (Tewalt et al. 2012; Lucas et al. 2018). Lymphatic vessels (LVs) are more frequent, dilated and larger in the peritumoural region than intratumoural vessels, which were found to be small and collapsed (Ji et al. 2007; Zhang et al. 2009; Schaaf et al. 2018). Both types of tumoural LVs were significantly higher than those of normal cervix tissues (Zhang et al. 2009). Intratumoural LVs are in close contact with tumour cells and the collapse of these vessels may be due to mechanical stress caused by the outgrowth of tumour cells (Ji et al. 2007). Peritumoural LVs were filled with clusters of malignant cells which may preclude metastasis to regional LNs. Tumour-associated LVs were shown to upregulate PD-L1 in a similar manner to LN-resident LECs in both mice models of melanoma (B16F10-VEGFC) and breast cancer (4T1) (Dieterich et al. 2017). The expression of PD-L1 was significantly higher in intratumoural LVs, compared to normal mice. Peritumoural LVs expressed lower

amounts of PD-L1 than intratumoural LVs. Interestingly, there was a significant reduction in the expression of PD-L1 on BECs in the tumour microenvironment, compared to normal skin BECs. PD-L1 expression on immortalised mouse LECs was upregulated by IFN-γ (up to 40-fold after 24 h), whereas TNF-α had a minor effect (2-fold), and VEGF-A and VEGF-C had no effect. There was some evidence of interaction between T cells and tumour-associated LVs in both mouse tumour models shown by immunofluorescence staining. By using the ovalbumin-derived, MHC class I-restricted peptide SIINFEKL, immortalised mouse LECs reduced the activation of OT-1 $CD8^+$ T cells which could be restored upon blockade of PD-L1, resulting in elevated expression of CD25 and production of IFN-γ *in vitro* (Dieterich et al. 2017). This study in addition to the other studies (described in Chapter 1) provide support in demonstrating that the inhibition of $CD8^+$ T cell responses by PD-L1-expressing LECs in both peripheral tissues and the LN are significant in maintenance of peripheral tolerance (Tewalt et al. 2012; Hirosue et al. 2014; Rouhani et al. 2015). In addition, miR-155 is often overexpressed in lymphatic cancers (Higgs & Slack 2013), further investigation is required to understand the differential effect on PD-L1 expression and function in both physiological and pathological contexts of the lymphatic system.

CAFs (see Chapter 1), which are activated fibroblasts adjacent to a tumour, are the most common component of the cancer stroma and share similar characteristics to fibroblasts found in wounds and inflammatory sites (Mao et al. 2013). CAFs do not only arise from fibroblasts but also bone marrow-derived mesenchymal stems cells and epithelial cells (Bhome et al. 2016). CAFs express fibroblast activation protein (FAP) and are the only tumoural source of cancer-associated chemokine CXCL12, which is suggested to be involved in tumoural immunosuppression and evasion (Feig et al. 2013). The murine model of pancreatic ductal adenocarcinoma resembling a human disease lacks T cells in regions where cancer cells can be found in the tumour. Inhibition of CXCR4, a receptor for CXCL12, increased T cell accumulation and reduced tumour growth. In addition, the combination of the CXCR4 inhibitor with an anti-PD-L1 antibody showed significant decline in the relative volume of the tumour, whereas there was no augmentative effect with anti-CTLA-4 treatment. There was no effect with anti-PD-L1 treatment alone, indicating that targeting CAFs may be instrumental in the response to PD-1/PD-L1 therapy (Feig et al. 2013). Similarly, TGF-β signalling from peritumoural stromal fibroblasts can exclude CD8+ T cells from the tumour parenchyma, which leads to a lack of response from PD-L1 blockade in metastatic urothelial cancer (Mariathasan et al. 2018). As described in Chapter 1, CAFs also directly contribute to anti-tumour T cell responses by cross-presenting tumour antigen through MHC class I molecules and upregulate PD-L1 and PD-L2 to impair T cell suppression (Nazareth et al. 2007; Lakins et al. 2018). In human tumours, the exclusion of

infiltrating $CD8^+$ T cells was a characteristic observed in patients that were non-responders to anti-PD-L1 therapy, even though PD-L1 expression was identified in tumour-infiltrating immune cells at the tumour margin (Herbst et al. 2014). Overall, these studies demonstrate that the response to PD-1/PD-L1 immunotherapy are influenced by the expression of CAFs in the tumour stroma, either through the exclusion of T cells in the tumour or in direct contact with T cells. Moreover, miR-155 is significantly upregulated in CAFs which contributes to the migration and invasion of ovarian cancer cells as well as programming normal fibroblasts into CAFs through the suppression of tumour protein 53-inducible nuclear protein 1 (TP53INP1) (Mitra et al. 2012; Gascard & Tlsty 2016). This also presents an opportunity to investigate the significance of miR-155/PD-L1 regulation in CAFs.

In general, the microenvironment in which stromal/vascular cells are present in may determine the type of phenotype (immunoactivating/immunosuppressing) that these cells develop in responding to immune cells. In addition, there are multiple places of interaction that could potentially enable stromal/vascular cells to induce immunosuppression of T cells or facilitate miRNA regulation of immune checkpoints.

7.5 Future experiments

RNA-sequencing to study inflammation-induced transcriptional networks in HDLECs

The aim of this work will be to determine the mRNA transcriptome of inflamed HDLECs and integrate with previously acquired data on small RNA profiles. Particularly, to characterise further targets of miR-155 in HDLECs. First, to perform and analyse RNA sequencing in HDLECs treated with IFN-γ and TNF-α in the presence or absence of miR-155 inhibitors to test the effect of miR-155 expression on the HDLEC transcriptome. The following conditions for the setup would be: control (no treatment), + IFN-γ and TNF-α, + miR-155 inhibitors, and + IFN-γ and TNF-α and + miR-155 inhibitors. With sequencing, this would provide a core dataset to reveal novel microRNA/mRNA inflammation-driven networks in HDLECs. Further experiments can include qRT-PCR to validate mRNA expression changes and western blot analysis to characterise the effects on downstream signalling components. In addition, overexpression and inhibition of affected genes will provide further data to expand these novel regulatory networks.

Investigate the mechanism of miR-155 regulation of PD-L1 in NSCLC cell lines

In some NSCLC cell lines, different miR-155 regulation of PD-L1 was observed in which PD-L1 expression was either suppressed or did not change after overexpression of miR-155. Luciferase assays would determine whether miR-155 directly binds the 3'-UTR of PD-L1 via the two conserved binding sites. To address the differential regulation, one possibility may be due to RNA-binding proteins (Pumilio, DND1) or ARE-binding proteins (HuR, TTP)

that have been shown to affect miRNA-induced inhibition of mRNAs (Bhattacharyya et al. 2006; Kedde et al. 2007; Kedde et al. 2010), or the stability of PD-L1 mRNA driven by RAS-MEK signalling (Coelho et al. 2017). Interestingly, low expression of TTP (ZFP36, bottom 25%) correlated with a shift towards high expression of PD-L1 mRNA in TCGA analysis of LUAD tumour samples (Figure 4.16). Whereas, high expression of TTP has a broader expression profile of PD-L1, which may inhibit miR-155 regulation of PD-L1 expression. TargetScan software predicts that there is one poorly conserved miR-155 binding site on TTP. Overexpression of miR-155 with mimics was reported to reduce TTP protein abundance in airway smooth muscle cells (Comer et al. 2016: American Thoracic 2016 International Conference). In contrast, overexpression of TTP regulates miR-155 expression via miR-1 in cystic fibrosis lung epithelial cells (Bhattacharyya et al. 2013) Therefore, I propose to characterise expression of TTP, a negative regulator of PD-L1, in lung cancer cell lines at normal levels and after knockdown. In addition, to overexpress miR-155 in lung cancer cell lines that have TTP or non-targeting control knockdown and subsequently characterise PD-L1 expression.

Development of the PD-1/PD-L1 co-culture assay

The development of this assay aimed to investigate the functional relevance of the effects of miRNA regulation of PD-L1 protein expression that was studied in Chapter 3. PD-1 Jurkat cells with the NFAT luciferase system represented the better of the two models and was able to detect a reproducible response from HFFs and HDLECs to target Jurkat cells. The specific mechanism of this response was not clearly identified. A positive control that only expresses PD-L1 and not any of the other known immune checkpoints would help optimise the assay better when further using antibodies to block PD-1/PD-L1. The number of immune checkpoint molecules found on HFFs and HDLECs may have interfered with the PD-1/PD-L1 mechanism and therefore overshadowed the effects that I may have observed when investigating miRNA-mediated regulation of PD-L1 expression.

7.6 Implications of miR-155 regulation of PD-L1 expression in a therapeutic context

Therapeutic approaches that attempt to mimic or inhibit the miRNA function are one of the classes of RNA-based drugs that extend the number of ‘druggable’ targets to include nucleic acids (Lieberman 2018). The targeting of RNA is in its infancy but could likely revolutionise drug development in the future. The advantages in the use of RNA-based drugs over therapeutic antibodies are that RNAs can be chemically synthesised rather than using living cells, which reduce the costs of manufactured drugs as well as limit immunogenicity (Lieberman 2018). Identifying and utilising miRNAs to regulate PD-L1 expression may lead to additional avenues to regulate inflammatory responses. The miR-200/ZEB1 axis, which is

associated with metastasis, was demonstrated to target PD-L1 and contribute to immunosuppression in lung metastases (Chen et al. 2014). The effect of anti-PD-L1 blockade did not significantly differ from tumours in mice that had high miR-200 levels, both treatments had reduced tumour burden and metastasis. Furthermore, the tumour suppressor miR-34a was reported to have several oncogenic and immune-related targets including PD-L1 (Cortez et al. 2016). *In vivo* delivery of miR-34 mimics (MRX34) in a mouse model of lung cancer increased the number of tumour-infiltrating $CD8^+$ T cells and relieved exhausted PD-1-positive $CD8^+$ T cells, macrophages and T reg. This effect was further augmented in combination with radiotherapy (Cortez et al. 2016). MRX34 is the first miRNA therapy based on miR-34a-loaded liposomes and was in Phase I trials (NCT01829971) with 47 patients carrying various solid tumours (Beg et al. 2017). Despite showing preliminary evidence of anti-tumour activity, MRX34 was halted following multiple immune-related serious adverse events (Beg et al. 2017).

Using miRNA inhibitors can have a more acceptable safety profile compared to high doses of miRNA mimics but remains to be tested in future clinical trials (Bayraktar & Van Roosbroeck 2018). The use of therapeutics to overexpress or inhibit miR-155 expression could be a useful treatment but consideration needs to take into account the number of miR-155/mRNA targets that are essential for normal development and function of the immune response and the context of the disease (Rodriguez et al. 2007). Therefore specific targeting of a cell type (immune, stromal or cancer cell) would need to be carefully chosen. Therapeutics have been proposed to suppress the activity of miR-155 in the treatment of cancer (Bayraktar & Van Roosbroeck 2018). Anti-miR-155 therapeutics using nanoparticles or locked nuclei acids (LNAs) can be delivered to B cells to induce rapid tumour regression in mouse models of lymphoma (Babar et al. 2012; Zhang et al. 2012). The expression of miR-155 in murine lung cancer models can be reduced by treatment with 1,2-dioleoyl-sn-glycero-3-phosphocholine (DOPC) liposomal nanoparticle-loaded anti-miR-155 with low toxicity (Van Roosbroeck et al. 2017). In addition, the suppression of miR-155 re-sensitised chemoresistant tumours to the chemotherapeutic agent, cisplatin, suggesting that targeting of miRNAs can be used to overcome drug resistance. Currently, MRG-106 (miRagen Therapeutics Inc.) is in the drug pipeline (phase 1: NCT02580552) for treatment of certain lymphomas and leukaemias by inhibition of miR-155. Preliminary results have indicate that MRG-106 is well tolerated and phase 2 trials are forthcoming. Furthermore, miR-155 expression drives pathology in autoimmune diseases such as rheumatoid arthritis and inhibition of miR-155 in autoimmunity is a clear target for therapeutic intervention (Alivernini et al. 2018).

There is also an unmet need for a panel of biomarkers to evaluate the response to PD-1/PD-L1 immunotherapy on top of PD-L1 expression on host and tumour cells. miR-155 could serve as a biomarker in the serum for human cancer detection (Sun et al. 2012; J. Wang et al. 2016) and to determine the levels of T cell activation in viral and cancer contexts (Dudda et al. 2013; Lind et al. 2013). A study in HIV-1-infected patients found that there was positive correlation between PD-1^+ T cells and miR-155 levels in $CD4^+$ and $CD8^+$ T cells, although it is unclear the regulatory link between miR-155 and PD-1 (Jin et al. 2017). Would miR-155 serve as a biomarker to predict the response to PD-1/PD-L1 immunotherapy? Mice with T cell-specific deletion of miR-155 and bearing tumour cells (B16-F10-OVA) were treated with an immune checkpoint blockade cocktail (anti-PD-1, anti-PD-L1 and anti-CTLA-4), which resulted in the rescue of anti-tumour immunity (Huffaker et al. 2017). There was a reduction in the size of tumour, similar to that of control mice, and the production of IFN-γ by $CD4^+$ and $CD8^+$ T cells were increased, suggesting immune checkpoint blockade rescues defective miR-155 regulation of the anti-tumour response. This indicates that the function of miR-155 may overlap with the restorative effect generated by immune checkpoint blockade (Huffaker et al. 2017). Since the expression of miR-155 in tumour-infiltrating myeloid cells (tumour-associated macrophages) is also important for anti-tumour responses (Zonari et al. 2013). It would be interesting to investigate whether miR-155 deficiency in tumour-associated stromal/vascular cells affects the anti-tumour response and whether modulation of miR-155 expression can improve the efficacy of immune checkpoint blockade. Furthermore, anti-PD-1/PD-L1 agents are associated with immune-related adverse events which was indicated to have a global incidence of 26.82% for any grade and 6.10% for severe grades, respectively (P. F. Wang et al. 2017). These adverse events were organ-specific and associated with the drug and types of tumour treated, such that there is a need for miRNA biomarkers that can predict the risk of immune-related adverse events (Dragomir et al. 2018).

7.7 Concluding remarks

In summary, stromal fibroblasts and endothelial cells respond to cytokines and their activation can determine the inflammatory response through surface ligands or secreted products. PD-L1 expression on host stromal cells inside and outside of the tumour microenvironment have a significant role on the efficacy of PD-1/PD-L1 immunotherapy by regulating the activation of T cells. Posttranscriptional mechanisms such as miRNAs can fine-tune the expression of PD-L1 in stromal fibroblasts and endothelial cells to regulate the inflammatory response. In this thesis, I investigated that during inflammatory cytokine activation of human fibroblasts and endothelial cells, miR-155 is activated and can regulate the expression of PD-L1 protein. This may lead to alterations in the balance between autoimmunity and immunosuppression which remains to be studied in further functional

assays. Targeting of miRNAs as a biomarker or therapeutic agent could be used to predict or adjust inflammatory responses in conjunction with PD-1/PD-L1 immunotherapy.

8. Abbreviations

β-gal	β-galactosidase
β-TrCP	β-transducin repeats-containing protein
AGO	Argonaute
AID	Activation-induced deaminase
AIRE	Autoimmune regulator
ALK	Anaplastic lymphoma kinase
ALV	Antigen loss variant
ANG	Angiopoietin
AP-1	Activator protein-1
APC	Antigen-presenting cell
ARE	Adenylate-uridylate (AU)-rich element
B3GNT3	β-1,3-N-acetylglucosaminyl transferase
BCA	Bicinchoninic acid assay
BCR	B cell receptor
BEC	Blood endothelial cell
BMP	Bone morphogenetic protein
BSA	Bovine serum albumin
C/EBPβ	CCAAT/enhancer-binding protein beta
CAF	Cancer-associated fibroblast
CAT-1	Cationic amino acid transporter 1
CCL	Chemokine (C-C motif) ligand
CD	Cluster of differentiation
CDK	Cyclin-dependent kinase
ChIP	Chromatin immunoprecipitation
cHL	Classical Hodgkin lymphoma
CHO	Chinese hamster ovary
CKS1B	Cyclin-dependent kinases regulatory subunit 1
CLIP	Class II-associated invariant chain peptide
c-MAF	V-maf musculoaponeurotic fibrosarcoma oncogene homolog
CMTM6	CKLF-like MARVEL transmembrane domain containing protein 6
COUP-TFII	COUP transcription factor 2
COX-2	Cyclooxygenase-2
CRISPR	Clustered Regularly Interspaced Short Palindromic Repeats

CSN5	COP9 signalosome 5
CTL	Cytotoxic T lymphocytes
CTLA-4	Cytotoxic T lymphocyte antigen-4
CXCL	Chemokine (C-X-C motif) ligand
DAG	Diacylglycerol
DC	Dendritic cells
DGCR8	DiGeorge syndrome critical region 8
DMEM	Dulbecco's Modified Eagle Medium
dMMR	Mismatch repair deficient
DMSO	Dimethyl sulfoxide
DNC	Double-negative cells
DND1	Dead end 1
dsRBD	dsRNA-binding domains
ECM	Extracellular matrix
EDTA	Ethylenediaminetetraacetic acid
EGFR	Epidermal growth factor receptor
ELISA	Enzyme-linked immunosorbent assay
EMT	Epithelial-mesenchymal transition
ER	Endoplasmic reticulum
ERAP	ER aminopeptidase
ERK	Extracellular signal-regulated kinase
FACS	Fluorescence assisted cell sorting
FAP	Fibroblast activation protein
FasL	Fas ligand
FCS	Fetal calf serum
FOXC2	Forkhead box protein C2
FoxO1	Forkhead box protein O1
FOXP3	Forkhead box P3
FRC	Fibroblastic reticular cells
GAS	IFN-γ-activated sequence
GITR	Glucocorticoid-induced TNFR-related protein
GSK3β	Glycogen synthase kinase 3β
HDLECs	Human dermal lymphatic endothelial cells
HER2	Human epidermal growth factor receptor 2
HFFs	Human foreskin fibroblasts
HIF-1α	Hypoxia-inducible factor 1-alpha

HLA	Human leukocyte antigen
HRP	Horseradish peroxidase
HuR	Hu antigen R
HUVEC	Human umbilical vein endothelial cells
ICAM-1	Intercellular adhesion molecule 1
ICOS	Inducible T cell co-stimulator
IDO	Indoleamine 2,3-dioxygenase
IFN	Interferon
IFNGR	IFN-γ receptor
Ig	Immunoglobulin
IKK	Inhibitor of NF-κB kinase
IL	Interleukin
IP_3	Inositol-1,4,5-triphosphate
IRAK	IL-1 receptor-associated kinase 1
IRF	Interferon regulatory factor
ISG15	Interferon-stimulated gene 15
ITAM	Immunoreceptor tyrosine-based activation motifs
ITK	IL-2-inducible T cell kinase
ITSM	Immunoreceptor tyrosine-based switch motif
JAK	Janus kinase
KSHV	Kaposi's sarcoma-associated herpesvirus
LAG-3	Lymphocyte activation gene 3
LAT	Linker of activated T cells
LCK	Lymphocyte-specific protein tyrosine kinase
LCMV	Lymphocytic choriomeningitis virus
LEC	Lymphatic endothelial cell
LN	Lymph node
LNSC	Lymph node stromal cells
LPS	Lipopolysaccharide
LV	Lymphatic vessel
LYVE-1	Lymphatic vessel hyaluronan receptor-1
MAPK	Mitogen-activated protein kinase
MCP	Monocyte chemoattractant protein
MDSC	Myeloid-derived suppressor cell
MFI	Median fluorescence intensity
MHC	Major histocompatibility complex

MIIC	MHC class II-containing compartment
MIP	Macrophage inflammatory protein
miRNAs	MicroRNAs
MMP	Matrix metalloproteinase
MPN	Myeloproliferative neoplasms
MSCs	Mesenchymal stem cells
MSI	Microsatellite instability
mTOR	Mammalian target of rapamycin
mTORC	mTOR complex
MYD88	Myeloid differentiation primary response 88
NF-κB	Nuclear factor kappa-light-chain-enhancer of activated B cells
NFAT	Nuclear factor of activated T cells
NK	Natural killer
NOS2	Nitric oxide synthase 2
NRP2	Neuropilin 2
NSCLC	Non-small-cell lung cancer
NTC	Non-targeting control
ORF	Open reading frame
OVA	Ovalbumin
PACT	Protein activator of the interferon-induced protein kinase
PBS	Phosphate-buffered saline
PD-1	Programmed cell death protein 1
PD-L1	Programmed death ligand-1
PD-L2	Programmed death ligand-2
PGE-2	Prostaglandin E2
PHA	Phytohemagglutinin
PI3K	Phosphoinositide 3-kinase
PIP_2	Phosphatidylinositol-4,5-bisphosphate
PKCθ	Protein kinase C
PLC	Phospholipase C
PLGRKT	Plasminogen receptor, C-terminal lysine
PMA	Phorbol 12-myristate 13-acetate
PMBCL	Primary mediastinal large B cell lymphoma
PNGase F	Peptide: N-glycosidase F
PolyI:C	Polyinosinic:polycytidylic acid
PROX1	Prospero-related homeodomain protein 1

PTA	Peripheral tissue antigen
PTEN	Phosphatase and tensin homolog
PTPN2	Tyrosine-protein phosphatase non-receptor type 2
PUM	Pumilio
qRT-PCR	Quantitative real-time polymerase chain reaction
RA	Rheumatoid arthritis
RANTES	Regulated on activation, normal T cell expressed and secreted
RBP	RNA-binding protein
RCC	Renal clear cell carcinoma
RIP	Receptor interacting protein kinase
RIPA	Radioimmunoprecipitation assay
RISC	RNA-induced silencing complex
S1P	Sphingosine 1-phosphate
SEE	Staphylococcal enterotoxin E
SHIP1	SH2 domain-containing inositol 5'-phosphate 1
SHP2	Src homology phosphatase 2
siRNA	Small interfering RNA
SLP-76	Src homology 2 domain-containing leukocyte phosphoprotein of 76 kDa
SOCS1	Suppressor of cytokine signalling 1
SPRED-1	Sprout-related protein-1
STAT	Signal transducer and activator of transcription
STRING	Search Tool for the Retrieval of Interacting Genes/Proteins database
TAB2	TGF-β activated kinase 1
TAM	Tumour-associated macrophage
TAP	Transporter associated with antigen processing
TBST	Tris-buffered saline and Tween 20
TCGA	The Cancer Genome Atlas
TCR	T cell receptor
TGF	Transforming growth factor-β
Th	T helper
TIE	TEK tyrosine kinase
TIGIT	T cell immunoreceptor with Ig and ITIM domains
TIL	Tumour-infiltrating lymphocyte
TIM3	T cell immunoglobulin and mucin-domain containing-3

TLR	Toll-like receptor
TMB	3,3’,5,5’-tetramethylbenzidine
TNF-α	Tumour necrosis factor-α
TNFR	Tumour necrosis factor receptor
TP53INP1	Tumour protein 53-inducible nuclear protein 1
TRAF2	TNF receptor-associated factor 2
TRBP	Transactivating response RNA-binding protein
TTP	Tristetraprolin
UTR	Untranslated region
VCAM-1	Vascular cell adhesion molecule 1
VEGFR	Vascular endothelial growth factor receptor
VHL	Von Hippel-Lindau
VISTA	V-domain Ig suppressor of T cell activation
XPO5	Exportin-5
ZAP70	Zeta-chain-associated protein kinase 70
ZEB1	Zinc-finger E-box-binding homeobox 1

Abbreviations for tumour types can be found in Table 4.1.

9. References

Abraham, R.T. & Weiss, A., 2004. Jurkat T cells and development of the T-cell receptor signalling paradigm. *Nature Reviews Immunology*, 4(4), pp.301–308.

Adachi, K. & Tamada, K., 2015. Immune checkpoint blockade opens an avenue of cancer immunotherapy with a potent clinical efficacy. *Cancer Science*, 106(8), pp.945–950.

Agarwal, V. et al., 2015. Predicting effective microRNA target sites in mammalian mRNAs. *eLife*, 4(AUGUST2015), pp.1–38.

Agata, Y., Kawasaki, A. & Nishimura, H., 1996. Expression of the PD-1 antigen on the surface of stimulated mouse T and B lymphocytes. *International Immunology*, 8(5), pp.765–772.

Akbay, E.A. et al., 2013. Activation of the PD-1 pathway contributes to immune escape in EGFR-driven lung tumors. *Cancer Discovery*, 3(12), pp.1355–1363.

Aldrich, M.B. & M., S.-M.E., 2013. Cytokines are systemic effectors of lymphatic function in acute inflammation. *Cytokine*, 64(1), pp.362–369.

Alivernini, S. et al., 2018. MicroRNA-155-at the critical interface of innate and adaptive immunity in arthritis. *Frontiers in Immunology*, 8(JAN).

Alivernini, S. et al., 2016. MicroRNA-155 influences B-cell function through PU.1 in rheumatoid arthritis. *Nature Communications*, 7, pp.1–12.

Ameres, S.L. et al., 2010. Target RNA-directed trimming and tailing of small silencing RNAs. *Science*, 328(5985), pp.1534–1539.

Anand, S. et al., 2010. MicroRNA-132-mediated loss of p120RasGAP activates the endothelium to facilitate pathological angiogenesis. *Nature medicine*, 16(8), pp.909–914.

Anantharaman, A. et al., 2016. Programmed death-ligand 1 (PD-L1) characterization of circulating tumor cells (CTCs) in muscle invasive and metastatic bladder cancer patients. *BMC Cancer*, 16(1), pp.1–11.

Androulidaki, A. et al., 2009. The Kinase Akt1 Controls Macrophage Response to Lipopolysaccharide by Regulating MicroRNAs. *Immunity*, 31(2), pp.220–231.

Angeli, V.V. et al., 2006. B cell-driven lymphangiogenesis in inflamed lymph nodes enhances dendritic cell mobilization. *Immunity*, 24(2), pp.203–215.

Antón, O. et al., 2008. An essential role for the MAL protein in targeting Lck to the plasma membrane of human T lymphocytes. *The Journal of Experimental Medicine*, 205(13), pp.3201–3213.

Audrito, V. et al., 2017. PD-L1 up-regulation in melanoma increases disease aggressiveness and is mediated through miR-17-5p. *Oncotarget*, 8(9), pp.15894–15911.

Azuma, T. et al., 2008. B7-H1 is a ubiquitous antiapoptotic receptor on cancer cells. *Blood*, 111(7), pp.3635–3643.

Babar, I.A. et al., 2012. Nanoparticle-based therapy in an in vivo microRNA-155 (miR-155)-dependent mouse model of lymphoma. *Proceedings of the National Academy of Sciences*, 109(26), pp.E1695–E1704.

Backes, C. et al., 2016. miEAA: microRNA enrichment analysis and annotation. *Nucleic acids research*, 44(W1), pp.W110–W116.

Baek, D. et al., 2008. The impact of microRNAs on protein output. *Nature*, 455(7209), pp.64–71.

Baltimore, D. et al., 2008. MicroRNAs: new regulators of immune cell development and function. *Nature immunology*, 9(8), pp.839–45.

Baluk, P. et al., 2005. Pathogenesis of persistent lymphatic vessel hyperplasia in chronic airway inflammation. *Journal of Clinical Investigation*, 115(2), pp.247–257.

Banerjee, A. et al., 2010. Micro-RNA-155 inhibits IFN-gamma signaling in CD4+ T cells. *European journal of immunology*, 40(1), pp.225–231.

Banerji, S. et al., 1999. LYVE-1, a new homologue of the {CD}44 glycoprotein. *The Journal of Cell Biology*, 144(4), pp.789–801.

Baptista, A.P. et al., 2014. Lymph node stromal cells constrain immunity via MHC class II self-antigen presentation. *eLife*, 3(November), pp.1–18.

Barber, D.L. et al., 2006. Restoring function in exhausted CD8 T cells during chronic viral infection. *Nature*, 439(7077), pp.682–7.

Barnas, J.L. et al., 2010. T cells and stromal fibroblasts in human tumor microenvironments represent potential therapeutic targets. *Cancer Microenvironment*, 3(1), pp.29–47.

Barsoum, I.B. et al., 2014. A mechanism of hypoxia-mediated escape from adaptive immunity in cancer cells. *Cancer Research*, 74(3), pp.665–674.

Bartel, D.P., 2009. MicroRNAs: target recognition and regulatory functions. *Cell*, 136(2),

pp.215–33.

Bayraktar, R. & Van Roosbroeck, K., 2018. miR-155 in cancer drug resistance and as target for miRNA-based therapeutics. *Cancer and Metastasis Reviews*, 37(1), pp.33–44.

Bazigou, E. et al., 2009. Integrin-α9 Is Required for Fibronectin Matrix Assembly during Lymphatic Valve Morphogenesis. *Developmental Cell*, 17(2), pp.175–186.

Bazzini, A.A., Lee, M.T. & Giraldez, A.J., 2012. Ribosome Profiling Shows That miR-430 Reduces Translation Before Causing mRNA Decay in Zebrafish. *Science*, 336(April), pp.233–237.

Beg, M.S. et al., 2017. Phase I study of MRX34, a liposomal miR-34a mimic, administered twice weekly in patients with advanced solid tumors. *Investigational New Drugs*, 35(2), pp.180–188.

Bellone, S. et al., 2018. Exceptional response to pembrolizumab in a metastatic, chemotherapy/radiation resistant ovarian cancer patient harboring a CD274/PD-L1-genetic rearrangement. *Clinical Cancer Research*, (5), p.clincanres.1805.2017.

Bellucci, R. et al., 2015. Interferon-γ-induced activation of JAK1 and JAK2 suppresses tumor cell susceptibility to NK cells through upregulation of PD-L1 expression. *OncoImmunology*, 4(6), p.e1008824.

Bernstein, E. et al., 2003. Dicer is essential for mouse development. *Nature genetics*, 35(3), pp.215–217.

Berthon, C. et al., 2010. In acute myeloid leukemia, B7-H1 (PD-L1) protection of blasts from cytotoxic T cells is induced by TLR ligands and interferon-gamma and can be reversed using MEK inhibitors. *Cancer Immunology, Immunotherapy*, 59(12), pp.1839–1849.

Beswick, E.J. et al., 2014. TLR4 activation enhances the PD-L1-mediated tolerogenic capacity of colonic CD90+ stromal cells. *Journal of immunology (Baltimore, Md. : 1950)*, 193(5), pp.2218–29.

Bhattacharyya, S. et al., 2013. Regulation of miR-155 biogenesis in cystic fibrosis lung epithelial cells: Antagonistic role of two mRNA-destabilizing proteins, KSRP and TTP. *Biochemical and Biophysical Research Communications*, 433(4), pp.484–488.

Bhattacharyya, S.N. et al., 2006. Relief of microRNA-Mediated Translational Repression in Human Cells Subjected to Stress. *Cell*, 125(6), pp.1111–1124.

Bhome, R. et al., 2016. Translational aspects in targeting the stromal tumour

microenvironment: From bench to bedside. *New Horizons in Translational Medicine*, 3(1), pp.9–21.

Black, M. et al., 2016. Activation of the PD-1/PD-L1 immune checkpoint confers tumor cell chemoresistance associated with increased metastasis. *Oncotarget*, 7(9), pp.10557–67.

Blank, C.U. et al., 2016. The "cancer immunogram." *Science*, 352(6286), pp.658–660.

Blüml, S. et al., 2011. Essential role of microRNA-155 in the pathogenesis of autoimmune arthritis in mice. *Arthritis and Rheumatism*, 63(5), pp.1281–1288.

Boldin, M.P. et al., 2011. miR-146a is a significant brake on autoimmunity, myeloproliferation, and cancer in mice. *The Journal of experimental medicine*, 208(6), pp.1189–1201.

Boyman, O. & Sprent, J., 2012. The role of interleukin-2 during homeostasis and activation of the immune system. *Nature Reviews Immunology*, 12(3), pp.180–190.

Brahmer, J.R. et al., 2010. Phase I study of single-agent anti-programmed death-1 (MDX-1106) in refractory solid tumors: Safety, clinical activity, pharmacodynamics, and immunologic correlates. *Journal of Clinical Oncology*, 28(19), pp.3167–3175.

Brodaczewska, K.K. et al., 2016. Choosing the right cell line for renal cell cancer research. *Molecular Cancer*, 15(1), pp.1–15.

van den Broek, T., Borghans, J.A.M. & van Wijk, F., 2018. The full spectrum of human naive T cells. *Nature Reviews Immunology*, 18(June).

Brogan, P.A. et al., 2004. Vbeta-restricted T cell adherence to endothelial cells: A mechanism for superantigen-dependent vascular injury. *Arthritis & Rheumatism*, 50(2), pp.589–597.

Brown, J. a et al., 2003. Blockade of programmed death-1 ligands on dendritic cells enhances T cell activation and cytokine production. *Journal of immunology (Baltimore, Md. : 1950)*, 170(3), pp.1257–1266.

Bruning, U. et al., 2011. MicroRNA-155 Promotes Resolution of Hypoxia-Inducible Factor 1 Activity during Prolonged Hypoxia. *Molecular and Cellular Biology*, 31(19), pp.4087–4096.

Buchbinder, E.I. & Desai, A., 2016. CTLA-4 and PD-1 pathways similarities, differences, and implications of their inhibition. *American Journal of Clinical Oncology: Cancer Clinical Trials*, 39(1), pp.98–106.

Burr, M.L. et al., 2017. CMTM6 maintains the expression of PD-L1 and regulates anti-Tumour immunity. *Nature*, 549(7670), pp.101–105.

Bussard, K.M. et al., 2016. Tumor-associated stromal cells as key contributors to the tumor microenvironment. *Breast Cancer Research*, 18(1), pp.1–11.

Butte, M.J. et al., 2008. Interaction of human PD-L1 and B7-1. *Molecular immunology*, 45(13), pp.3567–72.

Butte, M.J. et al., 2007. Programmed death-1 ligand 1 interacts specifically with the B7-1 costimulatory molecule to inhibit T cell responses. *Immunity*, 27(1), pp.111–22.

Calabrese, L.H., Calabrese, C. & Cappelli, L.C., 2018. Rheumatic immune-related adverse events from cancer immunotherapy. *Nature Reviews Rheumatology*, 14(10), pp.569–579.

Cancian, L., Hansen, A. & Boshoff, C., 2013. Cellular origin of Kaposi's sarcoma and Kaposi's sarcoma-associated herpesvirus-induced cell reprogramming. *Trends in Cell Biology*, 23(9), pp.421–432.

Carbognin, L. et al., 2015. Differential activity of nivolumab, pembrolizumab and MPDL3280A according to the tumor expression of programmed death-ligand-1 (PD-L1): Sensitivity analysis of trials in melanoma, lung and genitourinary cancers. *PLoS ONE*, 10(6).

Casey, S.C. et al., 2016. MYC regulates the antitumor immune response through CD47 and PD-L1. *Science*, 352(6282), pp.227–231.

Ceppi, M. et al., 2009. MicroRNA-155 modulates the interleukin-1 signaling pathway in activated human monocyte-derived dendritic cells. *Proceedings of the National Academy of Sciences of the United States of America*, 106(8), pp.2735–40.

Chaitanya, G.V. et al., 2010. Differential Cytokine Responses in Human and Mouse Lymphatic Endothelial Cells to Cytokines *in Vitro*. *Lymphatic Research and Biology*, 8(3), pp.155–164.

Chakraborty, S. et al., 2015. MicroRNA Signature of Inflamed Lymphatic Endothelium and Role of miR-9 in Lymphangiogenesis and Inflammation. *American Journal of Physiology - Cell Physiology*, p.ajpcell.00122.2015.

Chang, C.H. et al., 2015. Metabolic Competition in the Tumor Microenvironment Is a Driver of Cancer Progression. *Cell*, 162(6), pp.1229–1241.

Chatterjee, S. et al., 2011. Target-Mediated Protection of Endogenous MicroRNAs in C.

elegans. *Developmental Cell*, 20(3), pp.388–396.

Chemnitz, J.M. et al., 2004. SHP-1 and SHP-2 associate with immunoreceptor tyrosine-based switch motif of programmed death 1 upon primary human T cell stimulation, but only receptor ligation prevents T cell activation. *Journal of immunology*, 173(2), pp.945–954.

Chen, L. et al., 2014. Metastasis is regulated via microRNA-200/ZEB1 axis control of tumour cell PD-L1 expression and intratumoral immunosuppression. *Nature Communications*, 5, p.5241.

Chen, N. et al., 2015. Up-regulation of PD-L1 by EGFR Activation Mediates the Immune Escape in EGFR-driven NSCLC. *Journal of Thoracic Oncology*, XX(Xx), p.1.

Cheng, H.H. et al., 2014. Quiescent and proliferative fibroblasts exhibit differential p300 HAT activation through control of 5-methoxytryptophan production. *PLoS ONE*, 9(2).

Cheng, X. et al., 2013. Structure and interactions of the human programmed cell death 1 receptor. *Journal of Biological Chemistry*, 288(17), pp.11771–11785.

Cho, S. et al., 2016. miR-23∼27∼24 clusters control effector T cell differentiation and function. *The Journal of Experimental Medicine*, p.jem.20150990.

Chong, M.M.W. et al., 2010. Canonical and alternate functions of the microRNA biogenesis machinery. *Genes and Development*, 24(17), pp.1951–1960.

Chong, M.M.W. et al., 2008. The RNAseIII enzyme Drosha is critical in T cells for preventing lethal inflammatory disease. *The Journal of Experimental Medicine*, 205(9), pp.2005–2017.

Chow, C.W., Rincón, M. & Davis, R.J., 1999. Requirement for transcription factor NFAT in interleukin-2 expression. *Molecular and cellular biology*, 19(3), pp.2300–2307.

Christiansen, A.J. et al., 2016. Lymphatic endothelial cells attenuate suppression of dendritic cell maturation inflammation via. *Oncotarget*, 7(26).

Chu, A. et al., 2016. Large-scale profiling of microRNAs for the Cancer Genome Atlas. *Nucleic Acids Research*, 44(1), p.e3.

Cimmino, A. et al., 2005. miR-15 and miR-16 induce apoptosis by targeting BCL2. *Proceedings of the National Academy of Sciences*, 103(7).

Cioffi, M. et al., 2017. The miR-25-93-106b cluster regulates tumor metastasis and immune evasion via modulation of CXCL12 and PD-L1. *Oncotarget*, 8(13), pp.21609–21625.

Clark, C.A. et al., 2016. Tumor-intrinsic PD-L1 signals regulate cell growth, pathogenesis, and autophagy in ovarian cancer and melanoma. *Cancer Research*, 76(23), pp.6964–6974.

Cobb, B.S. et al., 2006. A role for Dicer in immune regulation. *The Journal of Experimental Medicine*, 203(11), pp.2519–2527.

Cobb, B.S. et al., 2005. T cell lineage choice and differentiation in the absence of the RNase III enzyme Dicer. *The Journal of Experimental Medicine*, 201(9), pp.1367–1373.

Coelho, M.A. et al., 2017. Oncogenic RAS Signaling Promotes Tumor Immunoresistance by Stabilizing PD-L1 mRNA. *Immunity*, 47(6), p.1083–1099.e6.

Cohen, J.N. et al., 2010. Lymph node-resident lymphatic endothelial cells mediate peripheral tolerance via Aire-independent direct antigen presentation. *The Journal of experimental medicine*, 207(4), pp.681–8.

Cohen, J.N. et al., 2014. Tolerogenic properties of lymphatic endothelial cells are controlled by the lymph node microenvironment. *PloS one*, 9(2), p.e87740.

Comer, B.S., Halayko, A.J. & Gerthoffer, W., 2016. MicroRNA-155 targets tristetraprolin and enhances cytokine expression in airway smooth muscle. *Am J Respir Crit Care Med*, 193.

Concha-Benavente, F. et al., 2016. *Identification of the cell-intrinsic and -extrinsic pathways downstream of EGFR and IFNγ that induce PD-L1 expression in head and neck Cancer*,

Cortez, M.A. et al., 2016. PDL1 Regulation by p53 via miR-34. *Journal of the National Cancer Institute*, 108(1), pp.djv303-djv303.

Costa, C. et al., 2013. Comprehensive molecular screening: from the RT-PCR to the RNA-seq. *Translational lung cancer research*, 2(2), pp.87–91.

Crane, C.A. et al., 2009. PI(3) kinase is associated with a mechanism of immunoresistance in breast and prostate cancer. *Oncogene*, 28(2), pp.306–12.

Dang, C. V., 2012. MYC on the path to cancer. *Cell*, 149(1), pp.22–35.

Deng, R. et al., 2015. B7H1/CD80 interaction augments PD-1-dependent T cell apoptosis and ameliorates graft-versus-host disease. *Journal of immunology (Baltimore, Md. : 1950)*, 194(2), pp.560–74.

Dieterich, L.C. et al., 2017. Tumor-Associated Lymphatic Vessels Upregulate PDL1 to

Inhibit T-Cell Activation. *Frontiers in Immunology*, 8(February), pp.1–13.

Djuranovic, S., Nahvi, A. & Green, R., 2012. miRNA-Mediated Gene Silencing. *Science*, 336(April), pp.237–241.

Dong, H. et al., 2002. Tumor-associated B7-H1 promotes T-cell apoptosis: A potential mechanism of immune evasion. *Nature Medicine*, 8(4), pp.793–800.

Dorand, R.D. et al., 2016. Cdk5 disruption attenuates tumor PD-L1 expression and promotes antitumor immunity. *Science*, 353(6297), pp.399–403.

Dorsett, Y. et al., 2008. MicroRNA-155 Suppresses Activation-Induced Cytidine Deaminase-Mediated Myc-Igh Translocation. *Immunity*, 28(5), pp.630–638.

Dragomir, M. et al., 2018. Key questions about the checkpoint blockade-are microRNAs an answer? *Cancer Biology & Medicine*, 15(2), p.103.

Dubrot, J. et al., 2014. Lymph node stromal cells acquire peptide-MHCII complexes from dendritic cells and induce antigen-specific CD4+ T cell tolerance. *The Journal of experimental medicine*, 211(6), pp.1153–66.

Dudda, J.C. et al., 2013. MicroRNA-155 is required for effector CD8+ T cell responses to virus infection and cancer. *Immunity*, 38(4), pp.742–753.

Dunn, G.P., Old, L.J. & Schreiber, R.D., 2004. The immunobiology of cancer immunosurveillance and immunoediting. *Immunity*, 21(2), pp.137–148.

Dunworth, W.P. et al., 2014. Bone morphogenetic protein 2 signaling negatively modulates lymphatic development in vertebrate embryos. *Circulation Research*, 114(1), pp.56–66.

Dyck, L. & Mills, K.H.G., 2017. Immune checkpoints and their inhibition in cancer and infectious diseases. *European Journal of Immunology*, 47(5), pp.765–779.

Eichhorn, S.W.W. et al., 2014. mRNA Destabilization Is the Dominant Effect of Mammalian MicroRNAs by the Time Substantial Repression Ensues. *Molecular cell*, 56(1), pp.104–115.

Eis, P.S. et al., 2005. Accumulation of miR-155 and BIC RNA in human B cell lymphomas. *Proceedings of the National Academy of Sciences of the United States of America*, 102(10), pp.3627–32.

Elton, T.S. et al., 2013. Regulation of the MIR155 host gene in physiological and pathological processes. *Gene*, 532(1), pp.1–12.

Emuss, V. et al., 2009. KSHV manipulates Notch signaling by DLL4 and JAG1 to alter cell

cycle genes in lymphatic endothelia. *PLoS Pathogens*, 5(10).

English, K. et al., 2007. IFN-γ and TNF-α differentially regulate immunomodulation by murine mesenchymal stem cells. *Immunology Letters*, 110(2), pp.91–100.

Eppihimer, M.J. et al., 2002. Expression and regulation of the PD-L1 immunoinhibitory molecule on microvascular endothelial cells. *Microcirculation*, 9(2), pp.133–145.

Escors, D., 2014. Tumour Immunogenicity, Antigen Presentation, and Immunological Barriers in Cancer Immunotherapy. *New Journal of Science*, 2014, pp.1–25.

Eulalio, A. et al., 2007. Target-specific requirements for enhancers of decapping in miRNA-mediated gene silencing. *Genes and Development*, 21(20), pp.2558–2570.

Faraoni, I. et al., 2012. MiR-424 and miR-155 deregulated expression in cytogenetically normal acute myeloid leukaemia: Correlation with NPM1 and FLT3 mutation status. *Journal of Hematology and Oncology*, 5, pp.2–6.

Feig, C. et al., 2013. Targeting CXCL12 from FAP-expressing carcinoma- associated fibroblasts synergizes with anti – PD-L1 immunotherapy in pancreatic cancer. *Proc Natl Acad Sci U S A*, 110(50), pp.20212–20217.

Filipowicz, W., Bhattacharyya, S.N. & Sonenberg, N., 2008. Mechanisms of post-transcriptional regulation by microRNAs: are the answers in sight? *Nature reviews. Genetics*, 9(2), pp.102–114.

Fish, J.E. et al., 2008. miR-126 Regulates Angiogenic Signaling and Vascular Integrity. *Developmental Cell*, 15(2), pp.272–284.

Fletcher, A.L. et al., 2010. Lymph node fibroblastic reticular cells directly present peripheral tissue antigen under steady-state and inflammatory conditions. *The Journal of experimental medicine*, 207(4), pp.689–97.

Flister, M.J. et al., 2010. Inflammation induces lymphangiogenesis through up-regulation of VEGFR-3 mediated by NF-kB and Prox1. *Blood*, 115(2), pp.418–429.

Förster, R., Davalos-Misslitz, A.C. & Rot, A., 2008. CCR7 and its ligands: balancing immunity and tolerance. *Nature reviews. Immunology*, 8(5), pp.362–71.

Francois, M. et al., 2008. Sox18 induces development of the lymphatic vasculature in mice. *Nature*, 456(7222), pp.643–647.

Fraser, J.D., Newton, M.E. & Weiss, A., 1992. CD28 and T cell antigen receptor signal transduction coordinately regulate interleukin 2 gene expression in response to

superantigen stimulation. *J.Exp.Med.*, 175(April), pp.1131–1134.

Frebel, H. et al., 2012. Programmed death 1 protects from fatal circulatory failure during systemic virus infection of mice. *The Journal of experimental medicine*, 209(13), pp.2485–99.

Freeman, G.J. et al., 2000. Engagement of the PD-1 immunoinhibitory receptor by a novel B7 family member leads to negative regulation of lymphocyte activation. *The Journal of experimental medicine*, 192(7), pp.1027–34.

Fujita, Y. et al., 2015. The Clinical Relevance of the miR-197/CKS1B/STAT3-mediated PD-L1 Network in Chemoresistant Non-small-cell Lung Cancer. *Molecular Therapy*, 23(4), pp.717–727.

Gale, N.W. et al., 2002. Angiopoietin-2 is required for postnatal angiogenesis and lymphatic patterning, and only the latter role is rescued by angiopoietin-1. *Developmental Cell*, 3(3), pp.411–423.

Gale, N.W. et al., 2007. Normal lymphatic development and function in mice deficient for the lymphatic hyaluronan receptor LYVE-1. *Molecular and cellular biology*, 27(2), pp.595–604.

Garcia-Diaz, A. et al., 2017. Interferon Receptor Signaling Pathways Regulating PD-L1 and PD-L2 Expression. *Cell Reports*, 19(6), pp.1189–1201.

Gascard, P. & Tlsty, T.D., 2016. Carcinoma-associated fibroblasts: Orchestrating the composition of malignancy. *Genes and Development*, 30(9), pp.1002–1019.

Gato-Cañas, M. et al., 2017. PDL1 Signals through Conserved Sequence Motifs to Overcome Interferon-Mediated Cytotoxicity. *Cell Reports*, 20(8), pp.1818–1829.

George, J. et al., 2017. Genomic amplification of CD274 (PD-L1) in small-cell lung cancer. *Clinical Cancer Research*, 23(5), pp.1220–1226.

Gharaee-Kermani, M., Denholm, E.M. & Phan, S.H., 1996. Costimulation of Fibroblast Collagen and Transforming Growth Factor β_1 Gene Expression by Monocyte Chemoattractant Protein-1 via Specific Receptors. *Journal of Biological Chemistry*, 271(30), pp.17779–17784.

Giannoni, E. et al., 2010. Reciprocal activation of prostate cancer cells and cancer-associated fibroblasts stimulates epithelial-mesenchymal transition and cancer stemness. *Cancer Research*, 70(17), pp.6945–6956.

Gioia, L. et al., 2018. A genome-wide survey of mutations in the Jurkat cell line. *BMC*

Genomics, 19(1), pp.1–13.

Giraudo, E. et al., 1998. Tumor necrosis factor-alpha regulates expression of vascular endothelial growth factor receptor-2 and of its co-receptor neuropilin-1 in human vascular endothelial cells. *The Journal of biological chemistry*, 273(34), pp.22128–22135.

Git, A. et al., 2010. Systematic comparison of microarray profiling, real-time PCR, and next-generation sequencing technologies for measuring differential microRNA expression. *Rna*, 16(5), pp.991–1006.

Goers, L., Freemont, P. & Polizzi, K.M., 2014. Co-culture systems and technologies: taking synthetic biology to the next level. *Journal of The Royal Society Interface*, 11(96), pp.20140065–20140065.

Golubovskaya, V. & Wu, L., 2016. Different subsets of T cells, memory, effector functions, and CAR-T immunotherapy. *Cancers*, 8(3).

Gong, A. et al., 2009. MicroRNA-513 regulates B7-H1 translation and is involved in IFN-γ-induced B7-H1 expression in cholangiocytes. *The Journal of Immunology*, 182(3), pp.1325–1333.

Gong, J. et al., 2018. Development of PD-1 and PD-L1 inhibitors as a form of cancer immunotherapy: A comprehensive review of registration trials and future considerations. *Journal for ImmunoTherapy of Cancer*, 6(1), pp.1–18.

Gottwein, E. et al., 2007. A viral microRNA functions as an orthologue of cellular miR-155. *Nature*, 450(7172), pp.1096–9.

Gowrishankar, K. et al., 2015. Inducible but Not Constitutive Expression of PD-L1 in Human Melanoma Cells Is Dependent on Activation of NF-κB. *Plos One*, 10, p.e0123410.

Gracias, D.T. et al., 2013. The microRNA miR-155 controls CD8(+) T cell responses by regulating interferon signaling. *Nature immunology*, 14(6), pp.593–602.

Green, M.R. et al., 2010. Integrative analysis reveals selective 9p24.1 amplification, increased PD-1 ligand expression, and further induction via JAK2 in nodular sclerosing Hodgkin lymphoma and primary mediastinal large B-cell lymphoma. *Blood*, 116(17), pp.3268–3277.

Griffiths-Jones, S. et al., 2006. miRBase: microRNA sequences, targets and gene nomenclature. *Nucleic acids research*, 34(Database issue), pp.D140-4.

Gröger, M. et al., 2004. IL-3 induces expression of lymphatic markers Prox-1 and podoplanin in human endothelial cells. *Journal of immunology*, 173(12), pp.7161–9.

Guo, H. et al., 2010. Mammalian microRNAs predominantly act to decrease target mRNA levels. *Nature*, 466(7308), pp.835–840.

Ha, M. & Kim, V.N., 2014. Regulation of microRNA biogenesis. *Nature reviews. Molecular cell biology*, 15(8), pp.509–524.

Haas, G. et al., 2016. Identification of factors involved in target RNA-directed microRNA degradation. *Nucleic Acids Research*, 44(6), pp.2873–2887.

Haghikia, A. et al., 2012. STAT3 regulation of and by microRNAs in development and disease. *Jak-Stat*, 1(3), pp.143–50.

Haile, S.T., Horn, L.A. & Ostrand-rosenberg, S., 2014. A Soluble Form of CD80 Enhances Antitumor Immunity by Neutralizing Programmed Death Ligand-1 and Simultaneously Providing Costimulation. *Cancer Immunology Research*, 2(7), pp.610–615.

Hanahan, D. & Weinberg, R.A., 2011. Hallmarks of cancer: The next generation. *Cell*, 144(5), pp.646–674.

Haniffa, M.A. et al., 2007. Adult Human Fibroblasts Are Potent Immunoregulatory Cells and Functionally Equivalent to Mesenchymal Stem Cells. *The Journal of Immunology*, 179(3), pp.1595–1604.

Hansen, A. et al., 2010. KSHV-encoded miRNAs target MAF to induce endothelial cell reprogramming. *Genes & development*, 24(2), pp.195–205.

Harris, T.A. et al., 2008. MicroRNA-126 regulates endothelial expression of vascular cell adhesion molecule 1. *Pnas*, 105(5), pp.1516–21.

Hayes, J., Peruzzi, P.P. & Lawler, S., 2014. MicroRNAs in cancer: Biomarkers, functions and therapy. *Trends in Molecular Medicine*, 20(8), pp.460–469.

Hendry, S.A. et al., 2016. The role of the tumor vasculature in the host immune response: Implications for therapeutic strategies targeting the tumor microenvironment. *Frontiers in Immunology*, 7(DEC), pp.1–21.

Herbst, R.S. et al., 2016. Pembrolizumab versus docetaxel for previously treated, PD-L1-positive, advanced non-small-cell lung cancer (KEYNOTE-010): A randomised controlled trial. *The Lancet*, 387(10027), pp.1540–1550.

Herbst, R.S. et al., 2014. Predictive correlates of response to the anti-PD-L1 antibody

MPDL3280A in cancer patients. *Nature*, 515(7528), pp.563–567.

Higgs, G. & Slack, F., 2013. The multiple roles of microRNA-155 in oncogenesis. *Journal of Clinical Bioinformatics*, 3(1), pp.1–8.

Hirosue, S. et al., 2014. Steady-state antigen scavenging, cross-presentation, and CD8+ T cell priming: a new role for lymphatic endothelial cells. *Journal of immunology*, 192(11), pp.5002–11.

Hong, S. et al., 2016. Upregulation of PD-L1 by EML4-ALK fusion protein mediates the immune escape in ALK positive NSCLC: Implication for optional anti-PD-1/PD-L1 immune therapy for ALK-TKIs sensitive and resistant NSCLC patients. *OncoImmunology*, 5(3), pp.1–12.

Hong, Y.-K. et al., 2002. Prox1 is a master control gene in the program specifying lymphatic endothelial cell fate. *Developmental dynamics : an official publication of the American Association of Anatomists*, 225(3), pp.351–7.

Hong, Y.-K.K. et al., 2004. Lymphatic reprogramming of blood vascular endothelium by Kaposi sarcoma-associated herpesvirus. *Nat Genet*, 36(7), pp.683–685.

Hu, R. et al., 2014. MiR-155 Promotes T Follicular Helper Cell Accumulation during Chronic, Low-Grade Inflammation. *Immunity*, 41(4), pp.605–619.

Hu, W. & Coller, J., 2012. What comes first: Translational repression or mRNA degradation? the deepening mystery of microRNA function. *Cell Research*, 22(9), pp.1322–1324.

Huffaker, T.B. et al., 2017. Antitumor immunity is defective in T cell–specific microRNA-155– deficient mice and is rescued by immune checkpoint blockade. *Journal of Biological Chemistry*, 292(45), pp.18530–18541.

Huffaker, T.B. et al., 2012. Epistasis between MicroRNAs 155 and 146a during T Cell-Mediated Antitumor Immunity. *Cell Reports*, 2(6), pp.1697–1709.

Huggenberger, R. et al., 2011. An important role of lymphatic vessel activation in limiting acute inflammation An important role of lymphatic vessel activation in limiting acute inflammation. *Blood*, 117(17), pp.4667–4678.

Huggenberger, R. et al., 2010. Stimulation of lymphangiogenesis via VEGFR-3 inhibits chronic skin inflammation. *The Journal of experimental medicine*, 207(10), pp.2255–69.

Hui, E. et al., 2017. T cell costimulatory receptor CD28 is a primary target for PD-1–mediated inhibition. *Science*, 1292(March), p.eaaf1292.

Huntzinger, E. & Izaurralde, E., 2011. Gene silencing by microRNAs: contributions of translational repression and mRNA decay. *Nature reviews. Genetics*, 12(2), pp.99–110.

Ikeda, S. et al., 2016. PD-L1 Is Upregulated by Simultaneous Amplification of the PD-L1 and JAK2 Genes in Non–Small Cell Lung Cancer. *Journal of Thoracic Oncology*, 11(1), pp.62–71.

Ilangumaran, S. et al., 2002. A positive regulatory role for suppressor of cytokine signaling 1 in IFN-gamma-induced MHC class II expression in fibroblasts. *Journal of immunology (Baltimore, Md. : 1950)*, 169(9), pp.5010–20.

Iliopoulos, D., Hirsch, H.A. & Struhl, K., 2009. An Epigenetic Switch Involving NF-κB, Lin28, Let-7 MicroRNA, and IL6 Links Inflammation to Cell Transformation. *Cell*, 139(4), pp.693–706.

Imaizumi, T. et al., 2010. IFN-γ and TNF-α synergistically induce microRNA-155 which regulates TAB2/IP-10 expression in human mesangial cells. *American Journal of Nephrology*, 32(5), pp.462–468.

Iorio, M. V. & Croce, C.M., 2012. MicroRNA dysregulation in cancer: Diagnostics, monitoring and therapeutics. A comprehensive review. *EMBO Molecular Medicine*, 4(3), pp.143–159.

Ishida, Y. et al., 1992. Induced expression of PD-1 , a novel member of the immunoglobulin gene superfamily , upon programmed cell death. *The EMBO Journal*, 11(11), pp.3887–3895.

Iwakawa, H. oki & Tomari, Y., 2015. The Functions of MicroRNAs: mRNA Decay and Translational Repression. *Trends in Cell Biology*, 25(11), pp.651–665.

Jackson, D.G., 2004. Biology of the lymphatic marker LYVE-1 and applications in research into lymphatic trafficking and lymphangiogenesis. *Apmis*, 112(7–8), pp.526–538.

Jenkins, R.W., Barbie, D.A. & Flaherty, K.T., 2018. Mechanisms of resistance to immune checkpoint inhibitors. *British Journal of Cancer*, 118(1), pp.9–16.

Ji, R.C., Eshita, Y. & Kato, S., 2007. Investigation of intratumoural and peritumoural lymphatics expressed by podoplanin and LYVE-1 in the hybridoma-induced tumours. *International Journal of Experimental Pathology*, 88(4), pp.257–270.

Jia, L. et al., 2017. miR-142-5p regulates tumor cell PD-L1 expression and enhances anti-tumor immunity. *Biochemical and Biophysical Research Communications*, 488(2), pp.425–431.

Jiang, S. et al., 2010. MicroRNA-155 functions as an oncomiR in breast cancer by targeting the suppressor of cytokine signaling 1 gene. *Cancer Research*, 70(8), pp.3119–3127.

Jilaveanu, L.B. et al., 2014. PD-L1 expression in clear cell renal cell carcinoma: An analysis of nephrectomy and sites of metastases. *Journal of Cancer*, 5(3), pp.166–172.

Jin, C. et al., 2017. MicroRNA-155 is a biomarker of T-cell activation and immune dysfunction in HIV-1-infected patients. *HIV Medicine*, 18(5), pp.354–362.

Jin, Y. et al., 2011. A novel function for programmed death ligand-1 regulation of angiogenesis. *The American journal of pathology*, 178(4), pp.1922–9.

Jing, Q. et al., 2005. Involvement of MicroRNA in AU-Rich Element-Mediated mRNA Instability. *Cell*, 120(5), pp.623–634.

Johnson, L.A. et al., 2006. An inflammation-induced mechanism for leukocyte transmigration across lymphatic vessel endothelium. *Journal of Experimental Medicine*, 203(12), pp.2763–2777.

Johnson, L.A. et al., 2007. Inflammation-induced uptake and degradation of the lymphatic endothelial hyaluronan receptor LYVE-1. *Journal of Biological Chemistry*, 282(46), pp.33671–33680.

Johnson, N.C. et al., 2008. Lymphatic endothelial cell identity is reversible and its maintenance requires Prox1 activity. *Genes & development*, pp.3282–3291.

Jones, D. et al., 2012. Mirtron MicroRNA-1236 inhibits VEGFR-3 signaling during inflammatory lymphangiogenesis. *Arteriosclerosis, Thrombosis, and Vascular Biology*, 32(3), pp.633–642.

June, C.H., Warshauer, J.T. & Bluestone, J.A., 2017. Is autoimmunity the Achilles' heel of cancer immunotherapy? *Nature Medicine*, 23(5), pp.540–547.

Juneja, V.R. et al., 2017. PD-L1 on tumor cells is sufficient for immune evasion in immunogenic tumors and inhibits CD8 T cell cytotoxicity. *The Journal of Experimental Medicine*, 214(4), pp.895–904.

Kammerer-Jacquet, S.F. et al., 2017. Independent association of PD-L1 expression with noninactivated VHL clear cell renal cell carcinoma—A finding with therapeutic potential. *International Journal of Cancer*, 140(1), pp.142–148.

Kamphorst, A.O. et al., 2017. Rescue of exhausted CD8 T cells by PD-1 – targeted therapies is CD28-dependent. *Science*, 0683(March), pp.1–9.

Kang, J. et al., 2010. An exquisite cross-control mechanism among endothelial cell fate regulators directs the plasticity and heterogeneity of lymphatic endothelial cells. *Blood*, 116(1), pp.140–150.

Kao, S.C. et al., 2017. Tumor Suppressor microRNAs Contribute to the Regulation of PD-L1 Expression in Malignant Pleural Mesothelioma. *Journal of Thoracic Oncology*, 12(9), pp.1421–1433.

Kataoka, K. et al., 2016. Aberrant PD-L1 expression through 3′-UTR disruption in multiple cancers. *Nature*, 534(7607), pp.402–406.

Kataru, R.P. et al., 2009. Critical role of CD11b+ macrophages and VEGF in inflammatory lymphangiogenesis, antigen clearance, and inflammation resolution. *Blood*, 113(22), pp.5650–5659.

Kataru, R.P. et al., 2011. T Lymphocytes Negatively Regulate Lymph Node Lymphatic Vessel Formation. *Immunity*, 34(1), pp.96–107.

Kawasaki, T. & Kawai, T., 2014. Toll-like receptor signaling pathways. *Frontiers in Immunology*, 5(SEP), pp.1–8.

Kazenwadel, J. et al., 2015. GATA2 is required for lymphatic vessel valve development and maintenance. *Journal of Clinical Investigation*, 125(8), pp.2879–2994.

Kazenwadel, J. et al., 2010. Prox1 expression is negatively regulated by miR-181 in endothelial cells. *Blood*, 116(13), pp.2395–2401.

Kedde, M. et al., 2010. A Pumilio-induced RNA structure switch in p27-3′2 UTR controls miR-221 and miR-222 accessibility. *Nature Cell Biology*, 12(10), pp.1014–1020.

Kedde, M. et al., 2007. RNA-Binding Protein Dnd1 Inhibits MicroRNA Access to Target mRNA. *Cell*, 131(7), pp.1273–1286.

Keir, M.E. et al., 2008. PD-1 and its ligands in tolerance and immunity. *Annual review of immunology*, 26, pp.677–704.

Keir, M.E. et al., 2005. Programmed Death-1 (PD-1):PD-Ligand 1 Interactions Inhibit TCR-Mediated Positive Selection of Thymocytes. *The Journal of Immunology*, 175(11), pp.7372–7379.

Kendall, R.T. & Feghali-Bostwick, C.A., 2014. Fibroblasts in fibrosis: Novel roles and mediators. *Frontiers in Pharmacology*, 5 MAY(May), pp.1–13.

Kertesz, M. et al., 2007. The role of site accessibility in microRNA target recognition.

Nature Genetics, 39(10), pp.1278–1284.

Khunger, M. et al., 2017. Programmed Cell Death 1 (PD-1) Ligand (PD-L1) Expression in Solid Tumors As a Predictive Biomarker of Benefit From PD-1/PD-L1 Axis Inhibitors: A Systematic Review and Meta-Analysis. *JCO Precision Oncology*, 1(1), pp.1–15.

Kim, H., Kataru, R.P. & Koh, G.Y., 2014. Inflammation-associated lymphangiogenesis: a double-edged sword? *The Journal of clinical investigation*, 124(3), pp.936–942.

Kim, S. et al., 2017. Comparative analysis of PD-L1 expression between primary and metastatic pulmonary adenocarcinomas. *European Journal of Cancer*, 75, pp.141–149.

Kim, Y.-K., Kim, B. & Kim, V.N., 2016. Re-evaluation of the roles of DROSHA, Exportin 5, and DICER in microRNA biogenesis. *Proceedings of the National Academy of Sciences of the United States of America*, 113(13), pp.E1881-1889.

Kiyasu, J. et al., 2015. Expression of programmed cell death ligand 1 is associated with poor overall. *Blood*, 126(19), pp.2193–2201.

Kleffel, S. et al., 2015. Melanoma Cell-Intrinsic PD-1 Receptor Functions Promote Tumor Growth. *Cell*, 162(6), pp.1242–1256.

Kleinovink, J.W. et al., 2017. PD-L1 expression on malignant cells is no prerequisite for checkpoint therapy. *OncoImmunology*, 6(4), pp.1–7.

Kondo, A. et al., 2010. Interferon-γ and tumor necrosis factor-α induce an immunoinhibitory molecule, B7-H1, via nuclear factor-κB activation in blasts in myelodysplastic syndromes. *Blood*, 116(7), pp.1124–1131.

Kong, W. et al., 2008. MicroRNA-155 Is Regulated by the Transforming Growth Factor /Smad Pathway and Contributes to Epithelial Cell Plasticity by Targeting RhoA. *Molecular and Cellular Biology*, 28(22), pp.6773–6784.

Kong, W. et al., 2014. Upregulation of miRNA-155 promotes tumour angiogenesis by targeting VHL and is associated with poor prognosis and triple-negative breast cancer. *Oncogene*, 33(6), pp.679–689.

Koralov, S.B. et al., 2008. Dicer Ablation Affects Antibody Diversity and Cell Survival in the B Lymphocyte Lineage. *Cell*, 132(5), pp.860–874.

Korbie, D.J. & Mattick, J.S., 2008. Touchdown PCR for increased specificity and sensitivity in PCR amplification. *Nature Protocols*, 3(9), pp.1452–1456.

Krönig, H. et al., 2014. Interferon-induced programmed death-ligand 1 (PD-L1/B7-H1)

expression increases on human acute myeloid leukemia blast cells during treatment. *European Journal of Haematology*, 92(3), pp.195–203.

Kuehbacher, A. et al., 2007. Role of Dicer and Drosha for endothelial microRNA expression and angiogenesis. *Circulation Research*, 101, pp.59–68.

Kuehbacher, A., Urbich, C. & Dimmeler, S., 2008. Targeting microRNA expression to regulate angiogenesis. *Trends in Pharmacological Sciences*, 29(December), pp.12–15.

Kumar, B. V., Connors, T.J. & Farber, D.L., 2018. Human T Cell Development, Localization, and Function throughout Life. *Immunity*, 48(2), pp.202–213.

Kumarswamy, R., Volkmann, I. & Thum, T., 2011. Regulation and function of miRNA-21 in health and disease. *RNA Biology*, 8(5).

Kurowska-Stolarska, M. et al., 2011. MicroRNA-155 as a proinflammatory regulator in clinical and experimental arthritis. *Proceedings of the National Academy of Sciences*, 108(27), pp.11193–11198.

Kwon, S.C. et al., 2016. Structure of Human DROSHA. *Cell*, 164(1–2), pp.81–90.

Lagos-Quintana, M. et al., 2002. Identification of tissue-specific MicroRNAs from mouse. *Current Biology*, 12(9), pp.735–739.

Lagos, D. et al., 2010. miR-132 regulates antiviral innate immunity through suppression of the p300 transcriptional co-activator. *Nature cell biology*, 12(5), pp.513–9.

Lakins, M.A. et al., 2018. Cancer-associated fibroblasts induce antigen-specific deletion of CD8+ T Cells to protect tumour cells. *Nature Communications*, 9(1), p.948.

Larkin, J. et al., 2015. Combined Nivolumab and Ipilimumab or Monotherapy in Untreated Melanoma. *New England Journal of Medicine*, 373(1), pp.23–34.

Lastwika, K.J. et al., 2015. Control of PD-L1 expression by oncogenic activation of the AKT/mTOR pathway in non-small cell lung cancer. *Cancer Research*, 76(2), pp.227–238.

Latchman, Y. et al., 2001. PD-L2 is a second ligand for PD-1 and inhibits T cell activation. *Nature immunology*, 2(3), pp.261–268.

Lau, J. et al., 2017. Tumour and host cell PD-L1 is required to mediate suppression of anti-tumour immunity in mice. *Nature Communications*, 8, p.14572.

Lee, S.-J. et al., 2006. Interferon regulatory factor-1 is prerequisite to the constitutive expression and IFN-gamma-induced upregulation of B7-H1 (CD274). *FEBS letters*,

580(3), pp.755–62.

Lee, S.K. et al., 2005. IFN-gamma regulates the expression of B7-H1 in dermal fibroblast cells. *Journal of Dermatological Science*, 40(2), pp.95–103.

Lee, Y. et al., 2003. The nuclear RNase III Drosha initiates microRNA processing. *Nature*, 425(September), pp.1–5.

Leonov, G. et al., 2015. Suppression of AGO2 by miR-132 as a determinant of miRNA-mediated silencing in human primary endothelial cells. *International Journal of Biochemistry and Cell Biology*, 69, pp.75–84.

Li, C.-W. et al., 2016. Glycosylation and stabilization of programmed death ligand-1 suppresses T-cell activity. *Nature Communications*, 7, p.12632.

Li, C.W. et al., 2018. Eradication of Triple-Negative Breast Cancer Cells by Targeting Glycosylated PD-L1. *Cancer Cell*, 33(2), p.187–201.e10.

Li, M. et al., 2018. Heterogeneity of PD-L1 expression in primary tumors and paired lymph node metastases of triple negative breast cancer. *BMC Cancer*, 18(1), pp.1–9.

Lieberman, J., 2018. Tapping the RNA world for therapeutics. *Nature Structural and Molecular Biology*, 25(5), pp.357–364.

Lim, L.P. et al., 2005. Microarray analysis shows that some microRNAs downregulate large numbers of target mRNAs. *Nature*, 433(7027), pp.769–773.

Lim, S.-O. et al., 2016. Deubiquitination and Stabilization of PD-L1 by CSN5. *Cancer Cell*, 30(6), pp.925–939.

Lin, C.-C. et al., 2015. Regulation rewiring analysis reveals mutual regulation between STAT1 and miR-155-5p in tumor immunosurveillance in seven major cancers. *Scientific Reports*, 5(1), p.12063.

Lin, H. et al., 2018. Host expression of PD-L1 determines efficacy of PD-L1 pathway blockade – mediated tumor regression Find the latest version : Host expression of PD-L1 determines efficacy of PD-L1 pathway blockade – mediated tumor regression. *The Journal of Clinical Investigation*, 128(April), pp.805–815.

Linardou, H. & Gogas, H., 2016. Toxicity management of immunotherapy for patients with metastatic melanoma. *Annals of Translational Medicine*, 4(14), pp.272–272.

Lind, E.F., Elford, A.R. & Ohashi, P.S., 2013. Micro-RNA 155 Is Required for Optimal CD8+ T Cell Responses to Acute Viral and Intracellular Bacterial Challenges. *The*

Journal of Immunology, 190(3), pp.1210–1216.

Ling, H., Fabbri, M. & Calin, G.A., 2013. MicroRNAs and other non-coding RNAs as targets for anticancer drug development. *Nature Reviews Drug Discovery*, 12(11), pp.847–865.

Linsley, P.S. et al., 2007. Transcripts Targeted by the MicroRNA-16 Family Cooperatively Regulate Cell Cycle Progression. *Molecular and Cellular Biology*, 27(6), pp.2240–2252.

Van Linthout, S., Miteva, K. & Tschöpe, C., 2014. Crosstalk between fibroblasts and inflammatory cells. *Cardiovascular Research*, 102(2), pp.258–269.

Liston, A. et al., 2008. Dicer-dependent microRNA pathway safeguards regulatory T cell function. *The Journal of experimental medicine*, 205(9), pp.1993–2004.

Liu, J. et al., 2007. Plasma cells from multiple myeloma patients express B7-H1 (PD-L1) and increase expression after stimulation with IFN-gamma and TLR ligands via a MyD88-, TRAF6-, and MEK-dependent pathway. *Blood*, 110(1), pp.296–304.

Loke, P. & Allison, J.P., 2003. PD-L1 and PD-L2 are differentially regulated by Th1 and Th2 cells. *Proceedings of the National Academy of Sciences of the United States of America*, 100(9), pp.5336–41.

Louveau, A. et al., 2015. Structural and functional features of central nervous system lymphatic vessels. *Nature*, 523(7560), pp.337–41.

Lu, D. et al., 2014. The miR-155–PU.1 axis acts on Pax5 to enable efficient terminal B cell differentiation. *The Journal of Experimental Medicine*, 211(11), pp.2183–2198.

Lu, L.F. et al., 2015. A Single Mirna-Mrna Interaction Affects The Immune Response In A Context- And Cell-Type-Specific Manner. *Immunity*, 43(1), pp.52–64.

Lu, L.F. et al., 2009. Foxp3-Dependent MicroRNA155 Confers Competitive Fitness to Regulatory T Cells by Targeting SOCS1 Protein. *Immunity*, 30(1), pp.80–91.

Lucas, E.D. et al., 2018. Type 1 IFN and PD-L1 Coordinate Lymphatic Endothelial Cell Expansion and Contraction during an Inflammatory Immune Response. *Journal of immunology (Baltimore, Md. : 1950)*, p.ji1800271.

Lukacs-Kornek, V. et al., 2011. Regulated release of nitric oxide by nonhematopoietic stroma controls expansion of the activated T cell pool in lymph nodes. *Nature Immunology*, 12(11), pp.1096–1104.

Lund, A.W. et al., 2016. Lymphatic vessels regulate immune microenvironments in human and murine melanoma. *The Journal of clinical investigation*, 126(9), pp.1–14.

Lund, A.W.W. et al., 2012. VEGF-C promotes immune tolerance in B16 melanomas and cross-presentation of tumor antigen by lymph node lymphatics. *Cell reports*, 1(3), pp.191–9.

Ma, F. et al., 2011. The microRNA miR-29 controls innate and adaptive immune responses to intracellular bacterial infection by targeting interferon-γ. *Nature immunology*, 12(9), pp.861–869.

Malhotra, D. et al., 2012. Transcriptional profiling of stroma from inflamed and resting lymph nodes defines immunological hallmarks. *Nature Immunology*, 13(5), pp.499–510.

Malissen, B. et al., 2014. Integrative biology of T cell activation. *Nature Immunology*, 15(9), pp.790–797.

Manguso, R.T. et al., 2017. In vivo CRISPR screening identifies Ptpn2 as a cancer immunotherapy target. *Nature*, 547(7664), pp.413–418.

Mann, M. et al., 2017. An NF-κB-microRNA regulatory network tunes macrophage inflammatory responses. *Nature Communications*, 8(1).

Mao, Y. et al., 2013. Stromal cells in tumor microenvironment and breast cancer. *Cancer and Metastasis Reviews*, 32(1–2), pp.303–315.

Mariathasan, S. et al., 2018. TGFβ attenuates tumour response to PD-L1 blockade by contributing to exclusion of T cells. *Nature*, 554(7693), pp.544–548.

Marzec, M. et al., 2008. Oncogenic kinase NPM/ALK induces through STAT3 expression of immunosuppressive protein CD274 (PD-L1, B7-H1). *Proceedings of the National Academy of Sciences of the United States of America*, 274, pp.1–6.

Mason, R.J., 2006. Biology of alveolar type II cells. *Respirology (Carlton, Vic.)*, 11 Suppl, pp.S12-5.

Mathew, L.K. et al., 2014. miR-218 opposes a critical RTK-HIF pathway in mesenchymal glioblastoma. *Proceedings of the National Academy of Sciences of the United States of America*, 111(1), pp.291–6.

Mayr, C., 2017. Regulation by 3 -Untranslated Regions. *Annu. Rev. Genet*.

Mayr, C. & Bartel, D.P., 2009. Widespread Shortening of 3′UTRs by Alternative Cleavage

and Polyadenylation Activates Oncogenes in Cancer Cells. *Cell*, 138(4), pp.673–684.

Mazanet, M.M. & Hughes, C.C.W., 2002. B7-H1 Is Expressed by Human Endothelial Cells and Suppresses T Cell Cytokine Synthesis. *The Journal of Immunology*, 169(7), pp.3581–3588.

McCoy, C.E. et al., 2010. IL-10 inhibits miR-155 induction by toll-like receptors. *Journal of Biological Chemistry*, 285(27), pp.20492–20498.

McGettrick, H.M. et al., 2009. Fibroblasts from different sites may promote or inhibit recruitment of flowing lymphocytes by endothelial cells. *European Journal of Immunology*, 39(1), pp.113–125.

Mehta, A. & Baltimore, D., 2016. MicroRNAs as regulatory elements in immune system logic. *Nature Reviews Immunology*, 16(5), pp.279–294.

Mehta, N.N. et al., 2017. IFN-γ and TNF-α synergism may provide a link between psoriasis and inflammatory atherogenesis. *Scientific Reports*, 7(1), pp.1–11.

Messai, Y. et al., 2016. Renal Cell Carcinoma Programmed Death-ligand 1, a New Direct Target of Hypoxia-inducible Factor-2 Alpha, is Regulated by von Hippel–Lindau Gene Mutation Status. *European Urology*, 70(4), pp.623–632.

Mezzadra, R. et al., 2017. Identification of CMTM6 and CMTM4 as PD-L1 protein regulators. *Nature*, 549(7670), pp.106–110.

Miao, S. et al., 2017. miR-217 inhibits laryngeal cancer metastasis by repressing AEG-1 and PD-L1 expression. , 8(37), pp.62143–62153.

Michonneau, D. et al., 2016. The PD-1 Axis Enforces an Anatomical Segregation of CTL Activity that Creates Tumor Niches after Allogeneic Hematopoietic Stem Cell Transplantation. *Immunity*, 44(1), pp.143–154.

Minet, E. et al., 2000. ERK activation upon hypoxia: Involvement in HIF-1 activation. *FEBS Letters*, 468(1), pp.53–58.

Minguet, S. et al., 2007. Full Activation of the T Cell Receptor Requires Both Clustering and Conformational Changes at CD3. *Immunity*, 26(1), pp.43–54.

Miranda-Carus, M.-E. et al., 2004. IL-15 and the Initiation of Cell Contact-Dependent Synovial Fibroblast-T Lymphocyte Cross-Talk in Rheumatoid Arthritis: Effect of Methotrexate. *The Journal of Immunology*, 173(2), pp.1463–1476.

Mishima, K. et al., 2007. Prox1 Induces Lymphatic Endothelial Differentiation via Integrin

α9 and Other Signaling Cascades □. *Molecular Biology of the Cell*, 18(April), pp.1421–1429.

Mitra, A.K. et al., 2012. MicroRNAs reprogram normal fibroblasts into cancer-associated fibroblasts in ovarian cancer. *Cancer Discovery*, 2(12), pp.1100–1108.

Mittendorf, E. a. et al., 2014. PD-L1 Expression in Triple-Negative Breast Cancer. *Cancer Immunology Research*, 2(4), pp.361–370.

Morisada, T. et al., 2005. Angiopoietin-1 promotes LYVE-1 – positive lymphatic vessel formation. *Blood*, 105(12), pp.4649–4656.

Mueller, S.N. et al., 2010. PD-L1 has distinct functions in hematopoietic and nonhematopoietic cells in regulating T cell responses during chronic infection in mice. *The Journal of clinical investigation*, 120(7), pp.11–13.

Mukherji, D. et al., 2016. Programmed Death-Ligand 1 Expression in Muscle-Invasive Bladder Cancer Cystectomy Specimens and Lymph Node Metastasis: A Reliable Treatment Selection Biomarker? *Clinical Genitourinary Cancer*, 14(2), pp.183–187.

Muljo, S.A. et al., 2005. Aberrant T cell differentiation in the absence of Dicer. *The Journal of Experimental Medicine*, 202(2), pp.261–269.

Narayan, N., Bracken, C.P. & Ekert, P.G., 2018. MicroRNA-155 expression and function in AML: An evolving paradigm. *Experimental Hematology*, 62, pp.1–6.

Nazareth, M.R. et al., 2007. Characterization of Human Lung Tumor-Associated Fibroblasts and Their Ability to Modulate the Activation of Tumor-Associated T Cells. *The Journal of Immunology*, 178(9), pp.5552–5562.

Neal, C.S. et al., 2010. The VHL-dependent regulation of microRNAs in renal cancer. *BMC Medicine*, 8, pp.1–17.

Network, T.C.G.A.R. et al., 2013. The Cancer Genome Atlas Pan-Cancer analysis project. *Nature Genetics*, 45(10), pp.1113–1120.

Nichols, L.A. et al., 2007. Deletional Self-Tolerance to a Melanocyte / Melanoma Antigen Cell in Peripheral and Mesenteric Lymph Nodes 1. *The Journal of Immunology*, 179(16), pp.993–1003.

Nicoli, S. et al., 2012. MiR-221 Is Required for Endothelial Tip Cell Behaviors during Vascular Development. *Developmental Cell*, 22(2), pp.418–429.

Ning, B.I. & Mamrack, M.D., 1994. PMA inhibits the growth of human fibroblasts after the

induction of immediate-early genes. *Experimental Cell Research*, 212(1), pp.105–112.

Nishimura, H. et al., 2001. Autoimmune dilated cardiomyopathy in PD-1 receptor-deficient mice. *Science (New York, N.Y.)*, 291(5502), pp.319–22.

Nishimura, H. et al., 1999. Development of lupus-like autoimmune diseases by disruption of the PD-1 gene encoding an ITIM motif-carrying immunoreceptor. *Immunity*, 11(2), pp.141–51.

Noguchi, T. et al., 2017. Temporally Distinct PD-L1 Expression by Tumor and Host Cells Contributes to Immune Escape. *Cancer Immunology Research*, 5(2), pp.106–117.

Noman, M.Z. et al., 2014. PD-L1 is a novel direct target of HIF-1α, and its blockade under hypoxia enhanced MDSC-mediated T cell activation. *The Journal of experimental medicine*, 211(5), pp.781–90.

Nörder, M. et al., 2012. Lymph node-derived lymphatic endothelial cells express functional costimulatory molecules and impair dendritic cell-induced allogenic T-cell proliferation. *FASEB journal : official publication of the Federation of American Societies for Experimental Biology*, 26(7), pp.2835–46.

Norrmen, C. et al., 2009. FOXC2 controls formation and maturation of lymphatic collecting vessels through cooperation with NFATc1. *Journal of Cell Biology*, 185(3), pp.439–457.

O'Connell, R.M. et al., 2009. Inositol phosphatase SHIP1 is a primary target of miR-155. *Proceedings of the National Academy of Sciences of the United States of America*, 106(17), pp.7113–8.

O'Connell, R.M. et al., 2007. MicroRNA-155 is induced during the macrophage inflammatory response. *Proceedings of the National Academy of Sciences of the United States of America*, 104(5), pp.1604–1609.

O'Connell, R.M., Kahn, D., et al., 2010. MicroRNA-155 promotes autoimmune inflammation by enhancing inflammatory T cell development. *Immunity*, 33(4), pp.607–619.

O'Connell, R.M., Rao, D.S., et al., 2010. Physiological and pathological roles for microRNAs in the immune system. *Nature reviews. Immunology*, 10(2), pp.111–22.

O'Connell, R.M., Rao, D.S. & Baltimore, D., 2012. microRNA Regulation of Inflammatory Responses. *Annual Review of Immunology*, 30(1), pp.295–312.

Ohmori, Y., Schreiber, R.D. & Hamilton, T.A., 1997. Synergy between interferon-γ and

tumor necrosis factor-α in transcriptional activation is mediated by cooperation between signal transducer and activator of transcription 1 and nuclear factor κB. *Journal of Biological Chemistry*, 272(23), pp.14899–14907.

Oka, M. et al., 2008. Inhibition of endogenous TGF-2 signaling enhances lymphangiogenesis. *Blood*, 111(9), pp.4571–4579.

Oliver, G., 2004. Lymphatic vasculature development. *Nature reviews. Immunology*, 4(1), pp.35–45.

Onder, L. et al., 2012. IL-7 – producing stromal cells are critical for lymph node remodeling. *Blood*, 120(24), pp.4675–4683.

Paladini, L. et al., 2016. Targeting microRNAs as key modulators of tumor immune response. *Journal of Experimental & Clinical Cancer Research*.

Pang, W. et al., 2015. Pancreatic cancer-secreted miR-155 implicates in the conversion from normal fibroblasts to cancer-associated fibroblasts. *Cancer Science*, 106(10), pp.1362–1369.

Pardoll, D.M., 2012. The blockade of immune checkpoints in cancer immunotherapy. *Nature reviews. Cancer*, 12(4), pp.252–64.

Park, J.-J.J. et al., 2010. B7-H1/CD80 interaction is required for the induction and maintenance of peripheral T-cell tolerance. *Blood*, 116(8), pp.1291–8.

Park, S.Y. et al., 2009. miR-29 miRNAs activate p53 by targeting p85α and CDC42. *Nature Structural and Molecular Biology*, 16(1), pp.23–29.

Parker, B.S., Rautela, J. & Hertzog, P.J., 2016. Antitumour actions of interferons: implications for cancer therapy. *Nature Reviews Cancer*, 16(3), pp.131–144.

Parry, R. V et al., 2005. CTLA-4 and PD-1 Receptors Inhibit T-Cell Activation by Distinct Mechanisms CTLA-4 and PD-1 Receptors Inhibit T-Cell Activation by Distinct Mechanisms †. *Molecular and Cellular Biology*, 25(21), pp.9543–9553.

Parsa, A.T. et al., 2007. Loss of tumor suppressor PTEN function increases B7-H1 expression and immunoresistance in glioma. *Nature medicine*, 13(1), pp.84–8.

Patterson, C. et al., 1996. Downregulation of vascular endothelial growth factor receptors by tumor necrosis factor-alpha in cultured human vascular endothelial cells. *The Journal of clinical investigation*, 98(2), pp.490–6.

Pazdur, R., 2008. Endpoints for Assessing Drug Activity in Clinical Trials. *The Oncologist*,

13(Supplement 2), pp.19–21.

Pedrioli, D.M.L. et al., 2010. miR-31 functions as a negative regulator of lymphatic vascular lineage-specific differentiation in vitro and vascular development in vivo. *Molecular and cellular biology*, 30(14), pp.3620–34.

Pentcheva-Hoang, T. et al., 2007. Programmed death-1 concentration at the immunological synapse is determined by ligand affinity and availability. *Proceedings of the National Academy of Sciences of the United States of America*, 104(45), pp.17765–70.

Petrova, T. V. et al., 2002. Lymphatic endothelial reprogramming of vascular endothelial cells by the Prox-1 homeobox transcription factor. *EMBO Journal*, 21(17), pp.4593–4599.

Petrova, T. V et al., 2004. Defective valves and abnormal mural cell recruitment underlie lymphatic vascular failure in lymphedema distichiasis. *Nature medicine*, 10(9), pp.974–81.

Pinchuk, I. V. et al., 2008. PD-1 Ligand Expression by Human Colonic Myofibroblasts/Fibroblasts Regulates CD4+ T-Cell Activity. *Gastroenterology*, 135(4), pp.1228–1237.

Pober, J.S. & Sessa, W.C., 2007. Evolving functions of endothelial cells in inflammation. *Nature reviews. Immunology*, 7(10), pp.803–15.

Podgrabinska, S. et al., 2009. Inflamed Lymphatic Endothelium Suppresses Dendritic Cell Maturation and Function via Mac-1/ICAM-1-Dependent Mechanism. *The Journal of Immunology*, 183(3), pp.1767–1779.

Postow, M.A. et al., 2015. Nivolumab and Ipilimumab versus Ipilimumab in Untreated Melanoma. *New England Journal of Medicine*, 372(21), pp.2006–2017.

Powles, T. et al., 2017. Efficacy and Safety of Durvalumab in Locally Advanced or Metastatic Urothelial Carcinoma. *JAMA Oncology*, p.e172411.

Prestipino, A. et al., 2018. Oncogenic JAK2 ^{V617F} causes PD-L1 expression, mediating immune escape in myeloproliferative neoplasms. *Science Translational Medicine*, 10(429), p.eaam7729.

Quan, L. et al., 2015. PD-1 Blockade can restore functions of tcells in Epstein-Barr virus-positive diffuse large b-cell lymphoma in vitro. *PLoS ONE*, 10(9), pp.1–19.

Rahimi, N., 2006. VEGFR-1 and VEGFR-2: two non-identical twins with a unique physiognomy. *Frontiers in bioscience : a journal and virtual library*, 11, pp.818–29.

Randolph, G.J. et al., 2017. The Lymphatic System: Integral Roles in Immunity. *Annual Review of Immunology*, 35(1), pp.31–52.

Rappl, G. et al., 2001. Dermal fibroblasts sustain proliferation of activated T cells via membrane-bound interleukin-15 upon long-term stimulation with tumor necrosis factor-α. *Journal of Investigative Dermatology*, 116(1), pp.102–109.

Rasmussen, T.K. et al., 2015. Overexpression of microRNA-155 increases IL-21 mediated STAT3 signaling and IL-21 production in systemic lupus erythematosus. *Arthritis research & therapy*, 17, p.154.

Rather, M.I. et al., 2013. Oncogenic microRNA-155 down-regulates tumor suppressor CDC73 and promotes oral squamous cell carcinoma cell proliferation: Implications for cancer therapeutics. *Journal of Biological Chemistry*, 288(1), pp.608–618.

Ribas, A. & Hu-Lieskovan, S., 2016. What does PD-L1 positive or negative mean? *The Journal of experimental medicine*, p.jem.20161462-.

Robert, C. et al., 2014. Nivolumab in Previously Untreated Melanoma without BRAF Mutation. *New England Journal of Medicine*, 372(4), p.141116004513004.

Rock, K.L., Reits, E. & Neefjes, J., 2016. Present Yourself! By MHC Class I and MHC Class II Molecules. *Trends in Immunology*, 37(11), pp.724–737.

Rodig, N. et al., 2003. Endothelial expression of PD-L1 and PD-L2 down-regulates CD8+ T cell activation and cytolysis. *European journal of immunology*, 33(11), pp.3117–26.

Rodriguez, A. et al., 2007. Requirement of bic/microRNA-155 for Normal Immune Function. *Science*, 316(5824), pp.608–611.

Roemer, M.G.M. et al., 2016. PD-L1 and PD-L2 genetic alterations define classical hodgkin lymphoma and predict outcome. *Journal of Clinical Oncology*, 34(23), pp.2690–2697.

Van Roosbroeck, K. et al., 2017. Combining anti-miR-155 with chemotherapy for the treatment of lung cancers. *Clinical Cancer Research*, 23(11), pp.2891–2904.

Rosenberg, J.E. et al., 2016. Atezolizumab in patients with locally advanced and metastatic urothelial carcinoma who have progressed following treatment with platinum-based chemotherapy: A single-arm, multicentre, phase 2 trial. *The Lancet*, 387(10031), pp.1909–1920.

Rota, G. et al., 2018. Shp-2 Is Dispensable for Establishing T Cell Exhaustion and for PD-1 Signaling In Vivo. *Cell Reports*, 23(1), pp.39–49.

Rouhani, S.J. et al., 2015. Roles of lymphatic endothelial cells expressing peripheral tissue antigens in CD4 T-cell tolerance induction. *Nature Communications*, 6, p.6771.

Rüegger, S. & Großhans, H., 2012. MicroRNA turnover: When, how, and why. *Trends in Biochemical Sciences*, 37(10), pp.436–446.

Ryan, B., Joilin, G. & Williams, J.M., 2015. Plasticity-related microRNA and their potential contribution to the maintenance of long-term potentiation. *Frontiers in Molecular Neuroscience*, 8(February), pp.1–17.

Sabin, F.R., 1902. On the origin of the lymphatic system from the veins and the development of the lymph hearts and thoracic duct in the pig. *American Journal of Anatomy*, 1(3), pp.367–389.

Sancho, D., Gómez, M. & Sánchez-Madrid, F., 2005. CD69 is an immunoregulatory molecule induced following activation. *Trends in Immunology*, 26(3), pp.136–140.

Schaaf, M.B., Garg, A.D. & Agostinis, P., 2018. Defining the role of the tumor vasculature in antitumor immunity and immunotherapy. *Cell Death & Disease*, 9(2), p.115.

Schaer, D.A. et al., 2018. The CDK4/6 Inhibitor Abemaciclib Induces a T Cell Inflamed Tumor Microenvironment and Enhances the Efficacy of PD-L1 Checkpoint Blockade. *Cell Reports*, 22(11), pp.2978–2994.

Schmitter, D. et al., 2006. Effects of Dicer and Argonaute down-regulation on mRNA levels in human HEK293 cells. *Nucleic Acids Research*, 34(17), pp.4801–4815.

Schroder, K. et al., 2004. Interferon-gamma: an overview of signals, mechanisms and functions. *Journal of leukocyte biology*, 75(February), pp.163–189.

Sedger, L.M. & McDermott, M.F., 2014. TNF and TNF-receptors: From mediators of cell death and inflammation to therapeutic giants - past, present and future. *Cytokine and Growth Factor Reviews*, 25(4), pp.453–472.

Selbach, M. et al., 2008. Widespread changes in protein synthesis induced by microRNAs. *Nature*, 455(7209), pp.58–63.

Seo, M. et al., 2015. MicroRNA miR-466 inhibits Lymphangiogenesis by targeting prospero-related homeobox 1 in the alkali burn corneal injury model. *Journal of biomedical science*, 22(1), p.3.

Shaked, I. et al., 2009. MicroRNA-132 Potentiates Cholinergic Anti-Inflammatory Signaling by Targeting Acetylcholinesterase. *Immunity*, 31(6), pp.965–973.

Sharpe, A.H. et al., 2007. The function of programmed cell death 1 and its ligands in regulating autoimmunity and infection. *Nature immunology*, 8(3), pp.239–45.

Sheedy, F.J. et al., 2010. Negative regulation of TLR4 via targeting of the proinflammatory tumor suppressor PDCD4 by the microRNA miR-21. *Nature Immunology*, 11(2), pp.141–147.

Shen, X. & Zhao, B., 2018. Efficacy of PD-1 or PD-L1 inhibitors and PD-L1 expression status in cancer: meta-analysis. *Bmj*, p.k3529.

Sheppard, K.A. et al., 2004. PD-1 inhibits T-cell receptor induced phosphorylation of the ZAP70/CD3 signalosome and downstream signaling to PKC. *FEBS Letters*, 574(1–3), pp.37–41.

Shin, D.S. et al., 2017. Primary resistance to PD-1 blockade mediated by JAK1/2 mutations. *Cancer Discovery*, 7(2), pp.188–201.

Sica, A. & Mantovani, A., 2012. Macrophage plasticity and polarization: in vivo veritas Antonio. *Journal of Clinical Investigation*, 122(3), pp.787–795.

Skalniak, L. et al., 2017. Small-molecule inhibitors of PD-1/PD-L1 immune checkpoint alleviate the PD-L1-induced exhaustion of T-cells. *Oncotarget*, 8(42), pp.72167–72181.

Small, E.M. et al., 2010. Microrna-218 regulates vascular patterning by modulation of slit-robo signaling. *Circulation Research*, 107(11), pp.1336–1344.

Smith-Garvin, J.E., Koretzky, G.A. & Jordan, M.S., 2009. T Cell Activation. *Annual Review of Immunology*, 27(1), pp.591–619.

Smyth, L.A. et al., 2015. MicroRNAs affect dendritic cell function and phenotype. *Immunology*, 144(2), pp.197–205.

Sonkoly, E. et al., 2010. MiR-155 is overexpressed in patients with atopic dermatitis and modulates T-cell proliferative responses by targeting cytotoxic T lymphocyte-associated antigen 4. *Journal of Allergy and Clinical Immunology*, 126(3).

Sood, P. et al., 2006. Cell-type-specific signatures of microRNAs on target mRNA expression. *Proceedings of the National Academy of Sciences*, 103(8), pp.2746–2751.

Spiotto, M.T., Rowley, D.A. & Schreiber, H., 2004. Bystander elimination of antigen loss variants in established tumors. *Nature Medicine*, 10(3), pp.294–298.

Srinivasan, R.S. et al., 2007. Lineage tracing demonstrates the venous origin of the mammalian lymphatic vasculature. *Genes and Development*, 21(19), pp.2422–2432.

Srinivasan, R.S. et al., 2010. The nuclear hormone receptor Coup-TFII is required for the initiation and early maintenance of Prox1 expression in lymphatic endothelial cells. *Genes and Development*, 24, pp.696–707.

Srinivasan, R.S. et al., 2014. The Prox1 – Vegfr3 feedback loop maintains the identity and the number of lymphatic endothelial cell progenitors. *Genes & development*, 28, pp.2175–2187.

Stanczyk, J. et al., 2008. Altered expression of microRNA in synovial fibroblasts and synovial tissue in rheumatoid arthritis. *Arthritis and Rheumatism*, 58(4), pp.1001–1009.

Staron, M.M. et al., 2014. The Transcription Factor FoxO1 Sustains Expression of the Inhibitory Receptor PD-1 and Survival of Antiviral CD8+ T Cells during Chronic Infection. *Immunity*, 41(5), pp.802–814.

Stelekati, E. et al., 2018. Long-Term Persistence of Exhausted CD8 T Cells in Chronic Infection Is Regulated by MicroRNA-155. *Cell Reports*, 23(7), pp.2142–2156.

Suárez, Y. et al., 2007. Dicer dependent microRNAs regulate gene expression and functions in human endothelial cells. *Circulation Research*, 100(8), pp.1164–1173.

Subtelny, A.O. et al., 2014. Poly(A)-tail profiling reveals an embryonic switch in translational control. *Nature*, 508(7494), pp.66–71.

Sullivan, D.E. et al., 2009. TNF-α induces TGF-β1expression in lung fibroblasts at the transcriptional level via AP-1 activation. *Journal of Cellular and Molecular Medicine*, 13(8 B), pp.1866–1876.

Sun, C., Mezzadra, R. & Schumacher, T.N., 2018. Regulation and Function of the PD-L1 Checkpoint. *Immunity*, 48(3), pp.434–452.

Sun, Y. et al., 2012. Serum MicroRNA-155 as a Potential Biomarker to Track Disease in Breast Cancer. *PLoS ONE*, 7(10), pp.1–8.

Sunshine, J. & Taube, J.M., 2015. PD-1/PD-L1 inhibitors. *Current Opinion in Pharmacology*, 23, pp.32–38.

Swaika, A., Hammond, W.A. & Joseph, R.W., 2015. Current state of anti-PD-L1 and anti-PD-1 agents in cancer therapy. *Molecular Immunology*, 67(2), pp.4–17.

Swartz, M.A., 2001. The physiology of the lymphatic system. *Advanced Drug Delivery Reviews*, 50(1–2), pp.3–20.

Szklarczyk, D. et al., 2015. STRING v10: Protein-protein interaction networks, integrated

over the tree of life. *Nucleic Acids Research*, 43(D1), pp.D447–D452.

Taganov, K.D. et al., 2006. NF-kappaB-dependent induction of microRNA miR-146, an inhibitor targeted to signaling proteins of innate immune responses. *Proceedings of the National Academy of Sciences of the United States of America*, 103(33), pp.12481–6.

Tam, W., Ben-Yehuda, D. & Hayward, W.S., 1997. bic, a novel gene activated by proviral insertions in avian leukosis virus-induced lymphomas, is likely to function through its noncoding RNA. *Molecular and cellular biology*, 17(3), pp.1490–502.

Tamburini, B.A., Burchill, M.A. & Kedl, R.M., 2014. Antigen capture and archiving by lymphatic endothelial cells following vaccination or viral infection. *Nature communications*, 5, p.3989.

Tammela, T. & Alitalo, K., 2010. Lymphangiogenesis: Molecular Mechanisms and Future Promise. *Cell*, 140(4), pp.460–476.

Tang, F. & Zheng, P., 2018. Tumor cells versus host immune cells: Whose PD-L1 contributes to PD-1/PD-L1 blockade mediated cancer immunotherapy? *Cell and Bioscience*, 8(1), pp.1–8.

Tang, H. et al., 2018. PD-L1 on host cells is essential for PD-L1 blockade – mediated tumor regression. *The Journal of Clinical Investigation*, 128(2), pp.580–588.

Taube, J.M. et al., 2012. Colocalization of Inflammatory Response with B7-H1 Expression in Human Melanocytic Lesions Supports an Adaptive Resistance Mechanism of Immune Escape. *Science Translation Medicine*, 4(127), pp.1–22.

Teng, G. et al., 2008. MicroRNA-155 Is a Negative Regulator of Activation-Induced Cytidine Deaminase. *Immunity*, 28(5), pp.621–629.

Tewalt, E.F., Cohen, J.N., Rouhani, S.J. & Engelhard, V.H., 2012. Lymphatic endothelial cells - key players in regulation of tolerance and immunity. *Frontiers in immunology*, 3(September), p.305.

Tewalt, E.F., Cohen, J.N., Rouhani, S.J., Guidi, C.J., et al., 2012. Lymphatic endothelial cells induce tolerance via PD-L1 and lack of costimulation leading to high-level PD-1 expression on CD8 T cells. *Blood*, 120(24), pp.4772–82.

Thai, T. et al., 2007. Regulation of the Germinal Center. *Science*, 316(April), pp.604–609.

Tian, R. et al., 2015. Combinatorial proteomic analysis of intercellular signaling applied to the CD28 T-cell costimulatory receptor. *Proceedings of the National Academy of Sciences*, 112(13), pp.E1594–E1603.

Tili, E. et al., 2007. Modulation of miR-155 and miR-125b levels following lipopolysaccharide/TNF-alpha stimulation and their possible roles in regulating the response to endotoxin shock. *Journal of immunology (Baltimore, Md. : 1950)*, 179(8), pp.5082–9.

Tili, E. et al., 2011. Mutator activity induced by microRNA-155 (miR-155) links inflammation and cancer. *Proceedings of the National Academy of Sciences*, 108(12), pp.4908–4913.

Toki, M.I. et al., 2016. EGFR-GRB2 protein colocalization is a prognostic factor unrelated to overall EGFR expression or EGFR mutation in lung adenocarcinoma. *Journal of Thoracic Oncology*, 11(11), pp.1901–1911.

Trickett, A. & Kwan, Y.L., 2003. T cell stimulation and expansion using anti-CD3/CD28 beads. *Journal of Immunological Methods*, 275(1–2), pp.251–255.

Tumeh, P.C. et al., 2014. PD-1 blockade induces responses by inhibiting adaptive immune resistance. *Nature*, 515(7528), pp.568–571.

Turley, S.J., Cremasco, V. & Astarita, J.L., 2015. Immunological hallmarks of stromal cells in the tumour microenvironment. *Nature Reviews Immunology*, 15(11), pp.669–682.

Twa, D.D.W. et al., 2014. Genomic rearrangements involving programmed death ligands are recurrent in primary mediastinal large B-cell lymphoma. *Blood*, 123(13), pp.2062–2066.

Ulvmar, M.H. et al., 2014. The atypical chemokine receptor CCRL1 shapes functional CCL21 gradients in lymph nodes. *Nature immunology*, 15(7), pp.623–30.

Ulvmar, M.H. & Mäkinen, T., 2016. Heterogeneity in the lymphatic vascular system and its origin. *Cardiovascular Research*, 111(4), pp.310–321.

Vaiana, C.A., Kurcon, T. & Mahal, L.K., 2016. MicroRNA-424 predicts a role for β-1,4 branched glycosylation in cell cycle progression. *Journal of Biological Chemistry*, 291(3), pp.1529–1537.

Vasudevan, S., 2012. Posttranscriptional Upregulation by MicroRNAs. *Wiley Interdisciplinary Reviews: RNA*, 3(3), pp.311–330.

Venkataraman, S. et al., 2013. MicroRNA 218 acts as a tumor suppressor by targeting multiple cancer phenotype-associated genes in medulloblastoma. *Journal of Biological Chemistry*, 288(3), pp.1918–1928.

Vesely, M.D. et al., 2011. Natural Innate and Adaptive Immunity to Cancer. *Annual Review*

of Immunology, 29(1), pp.235–271.

Vigl, B. et al., 2011. Tissue inflammation modulates gene expression of lymphatic endothelial cells and dendritic cell migration in a stimulus-dependent manner. *Blood*, 118(1), pp.205–215.

Vigorito, E. et al., 2007. microRNA-155 Regulates the Generation of Immunoglobulin Class-Switched Plasma Cells. *Immunity*, 27(6), pp.847–859.

Vigorito, E. et al., 2013. miR-155: An ancient regulator of the immune system. *Immunological Reviews*, 253(1), pp.146–157.

Villarino, A. V, Kanno, Y. & O'Shea, J.J., 2017. Mechanisms and consequences of Jak–STAT signaling in the immune system. *Nature Immunology*, 18(4), pp.374–384.

Volinia, S. et al., 2006. A microRNA expression signature of human solid tumors defines cancer gene targets. *Proceedings of the National Academy of Sciences of the United States of America*, 103(7), pp.2257–2261.

Voong, K.R. et al., 2017. Beyond PD-L1 testing-emerging biomarkers for immunotherapy in non-small cell lung cancer. *Annals of Translational Medicine*, 5(18), pp.376–376.

Wang, H. et al., 2004. Kaposi sarcoma herpesvirus–induced cellular reprogramming contributes to the lymphatic endothelial gene expression in Kaposi sarcoma. *Nature Genetics*, 36(7), pp.687–693.

Wang, J., Chen, J. & Sen, S., 2016. MicroRNA as Biomarkers and Diagnostics. *Journal of Cellular Physiology*, 231(1), pp.25–30.

Wang, L. et al., 2017. Development of a robust reporter gene assay to measure the bioactivity of anti-PD-1/anti-PD-L1 therapeutic antibodies. *Journal of Pharmaceutical and Biomedical Analysis*, 145, pp.447–453.

Wang, L. et al., 2018. EMT- and stroma-related gene expression and resistance to PD-1 blockade in urothelial cancer. *Nature Communications*, 9(1), p.3503.

Wang, P. et al., 2010. Inducible microRNA-155 feedback promotes type I IFN signaling in antiviral innate immunity by targeting suppressor of cytokine signaling 1. *Journal of immunology (Baltimore, Md. : 1950)*, 185(10), pp.6226–6233.

Wang, P.F. et al., 2017. Immune-related adverse events associated with anti-PD-1/PD-L1 treatment for malignancies: A meta-analysis. *Frontiers in Pharmacology*, 8(OCT), pp.1–12.

Wang, S. et al., 2008. The Endothelial-Specific MicroRNA miR-126 Governs Vascular Integrity and Angiogenesis. *Developmental Cell*, 15(2), pp.261–271.

Wang, W. et al., 2012. A frequent somatic mutation in CD274 3'-UTR leads to protein over-expression in gastric cancer by disrupting miR-570 binding. *Human mutation*, 33(3), pp.480–4.

Wang, W. et al., 2013. A miR-570 binding site polymorphism in the B7-H1 gene is associated with the risk of gastric adenocarcinoma. *Human Genetics*, 132(6), pp.641–648.

Wang, X. et al., 2016. PD-L1 expression in human cancers and its association with clinical outcomes. *OncoTargets and Therapy*, 9, pp.5023–5039.

Wang, X. et al., 2015. Tumor suppressor miR-34a targets PD-L1 and functions as a potential immunotherapeutic target in acute myeloid leukemia. *Cellular Signalling*, 27(3), pp.443–452.

Wang, Y. et al., 2007. DGCR8 is essential for microRNA biogenesis and silencing of embryonic stem cell self-renewal. *Nature Genetics*, 39(3), pp.380–385.

Watanabe, R. et al., 2017. Pyruvate controls the checkpoint inhibitor PD-L1 and suppresses T cell immunity. *Journal of Clinical Investigation*, 127(7), pp.2725–2738.

Wei, S.C., Duffy, C.R. & Allison, J.P., 2018. Fundamental mechanisms of immune checkpoint blockade therapy. *Cancer Discovery*, 8(9), pp.1069–1086.

Wigle, J.T. & Oliver, G., 1999. Prox1 function is required for the development of the murine lymphatic system. *Cell*, 98, pp.769–778.

Wolchok, J.D. et al., 2013. Nivolumab plus ipilimumab in advanced melanoma. *The New England journal of medicine*, 369(2), pp.122–33.

Wölfle, S.J. et al., 2011. PD-L1 expression on tolerogenic APCs is controlled by STAT-3. *European journal of immunology*, 41(2), pp.413–24.

Wu, Y.H. et al., 2011. The manipulation of miRNA-gene regulatory networks by KSHV induces endothelial cell motility. *Blood*, 118(10), pp.2896–2905.

Xie, G. et al., 2017. Helicobacter pylori promote B7-H1 expression by suppressing miR-152 and miR-200b in gastric cancer cells. *PLoS ONE*, 12(1), pp.1–13.

Xu-Monette, Z.Y. et al., 2017. PD-1/PD-L1 blockade: Have we found the key to unleash the antitumor immune response? *Frontiers in Immunology*, 8(DEC).

Xu, Y. et al., 2010. Neuropilin-2 mediates VEGF-C-induced lymphatic sprouting together with VEGFR3. *Journal of Cell Biology*, 188(1), pp.115–130.

Yanaihara, N. et al., 2006. Unique microRNA molecular profiles in lung cancer diagnosis and prognosis. *Cancer Cell*, 9(3), pp.189–198.

Yang, W. et al., 2008. PD-L1: PD-1 Interaction Contributes to the Functional Suppression of T-Cell Responses to Human Uveal Melanoma Cells In Vitro. *Invest Ophthalmol Vis. Sci.*, 49(6), pp.2518–2525.

Yang, W.J. et al., 2005. Dicer is required for embryonic angiogenesis during mouse development. *Journal of Biological Chemistry*, 280(10), pp.9330–9335.

Yellin, M.J. et al., 1995. Ligation of CD40 on fibroblasts induces CD54 (ICAM-1) and CD106 (VCAM-1) up-regulation and IL-6 production and proliferation. *Journal of Leukocyte Biology*, 58(2), pp.209–216.

Yokosuka, T. et al., 2012. Programmed cell death 1 forms negative costimulatory microclusters that directly inhibit T cell receptor signaling by recruiting phosphatase SHP2. *The Journal of experimental medicine*, 209(6), pp.1201–17.

Yoo, J. et al., 2010. Kaposin-B enhances the PROX1 mRNA stability during lymphatic reprogramming of vascular endothelial cells by Kaposi's sarcoma herpes virus. *PLoS Pathogens*, 6(8), pp.37–38.

You, L.R. et al., 2005. Suppression of Notch signalling by the COUP-TFII transcription factor regulates vein identity. *Nature*, 435(7038), pp.98–104.

Yuan, L. et al., 2002. Abnormal lymphatic vessel development in neuropilin 2 mutant mice. *Development*, 129(20), pp.4797–4806.

Zang, Y.S. et al., 2012. MiR-155 inhibits the sensitivity of lung cancer cells to cisplatin via negative regulation of Apaf-1 expression. *Cancer Gene Therapy*, 19(11), pp.773–778.

Zhang, B. et al., 2008. IFN-γ- and TNF-dependent bystander eradication of antigen-loss variants in established mouse cancers. *Journal of Clinical Investigation*, 118(4), pp.1398–1404.

Zhang, J. et al., 2018. Cyclin D-CDK4 kinase destabilizes PD-L1 via cullin 3-SPOP to control cancer immune surveillance. *Nature*, 553(7686), pp.91–95.

Zhang, M. et al., 2011. Both miR-17-5p and miR-20a Alleviate Suppressive Potential of Myeloid-Derived Suppressor Cells by Modulating STAT3 Expression. *The Journal of Immunology*, 186(8), pp.4716–4724.

Zhang, M. et al., 2017. Transmembrane TNF-α promotes activation-induced cell death by forward and reverse signaling. *Oncotarget*, 8(38), pp.63799–63812.

Zhang, N. & Bevan, M.J., 2011. CD8+ T Cells: Foot Soldiers of the Immune System. *Immunity*, 35(2), pp.161–168.

Zhang, S.Q., Yu, H. & Zhang, L.L., 2009. Clinical implications of increased lymph vessel density in the lymphatic metastasis of early-stage invasive cervical carcinoma: A clinical immunohistochemical method study. *BMC Cancer*, 9, pp.1–6.

Zhang, X. et al., 2004. Structural and functional analysis of the costimulatory receptor programmed death-1. *Immunity*, 20(3), pp.337–347.

Zhang, Y. et al., 2012. LNA-mediated anti – miR-155 silencing in low-grade B-cell lymphomas. *Blood*, 120(8), pp.1678–1687.

Zhao, H., Anand, A.R. & Ganju, R.K., 2014. Slit2-Robo4 Pathway Modulates Lipopolysaccharide-Induced Endothelial Inflammation and Its Expression Is Dysregulated during Endotoxemia. *The Journal of Immunology*, 192(1), pp.385–393.

Zhao, J. et al., 2014. β-arrestin2/miR-155/GSK3β regulates transition of 5'-azacytizine-induced Sca-1-positive cells to cardiomyocytes. *Journal of Cellular and Molecular Medicine*, 18(8), pp.1562–1570.

Zhao, L. et al., 2016. The tumor suppressor miR-138-5p targets PD-L1 in colorectal cancer. *Oncotarget*, 7(29), pp.45370–45384.

Zhao, X. dong et al., 2013. Overexpression of miR -155 Promotes Proliferation and Invasion of Human Laryngeal Squamous Cell Carcinoma via Targeting SOCS1 and STAT3. *PLoS ONE*, 8(2), pp.1–11.

Zhao, Y. et al., 2018. Antigen-Presenting Cell-Intrinsic PD-1 Neutralizes PD-L1 in cis to Attenuate PD-1 Signaling in T Cells. *Cell Reports*, 24(2), p.379–390.e6.

Zhou, X. et al., 2008. Selective miRNA disruption in T reg cells leads to uncontrolled autoimmunity. *The Journal of Experimental Medicine*, 205(9), pp.1983–1991.

Zhu, J. et al., 2014. MiR-20b, -21, and -130b inhibit PTEN expression resulting in B7-H1 over-expression in advanced colorectal cancer. *Human immunology*, 75(4), pp.348–53.

Zhu, J., Yamane, H. & Paul, W.E., 2010. Differentiation of Effector CD4 T Cell Populations. *Annual Review of Immunology*, 28(1), pp.445–489.

Zonari, E. et al., 2013. A role for miR-155 in enabling tumor-infiltrating innate immune cells

to mount effective anti-tumor responses A role for miR-155 in enabling tumor-infiltrating innate immune cells to mount effective anti-tumor responses. , 122(2), pp.243–253.